PUSHING THE BOUNDARIES OF CONCENTRATED DISPERSIONS

High Solids Content Bimodal Latex for Paper Coating Applications

by

RAUL PACHECO DE MORAES

A thesis submitted to the Department of Chemical Engineering

In conformity with the requirements for

the degree of Doctor of Philosophy

Queen's University

Kingston, Ontario, Canada

(May, 2011)

Abstract

New processes for the production of polymeric dispersions with high solids content and low viscosity were developed, investigated and characterized. The specifications required for the desired application of paper coating, which constitutes one of the major innovative aspects of this thesis, requires in average particle sizes smaller than 200 nm. This particle size is significantly smaller than obtained in previous work in this area. The main objective of this project was to increase the solids content of existing products from ~50 to ~60 wt% while keeping the viscosity at low levels (< 1200 mPa•s at 20 s^{-1}).

In order to produce high solids content latexes with low viscosity, bimodal particle size distributions were resorted to. To obtain highest packing fraction, the small particle size population should be about 7 times smaller than the large particles, bringing the size of the small particles to less than 30 nm.

Modified (micro)emulsion processes were developed in order to produce small particle size latex with reduced surfactant concentration and increased solids content. The large particle population was developed using a semi-batch emulsion polymerization process, simulating a product that is commercially available (~52 wt% solids content and viscosity of ~500 mPa•s at 20 s^{-1}). To increase the solids content of this product up to 60 wt%, a second population of small particles was created using two approaches.

In the first approach, the small particles were generated *in situ* using the modified (micro)emulsion approaches developed previously. This process resulted in latexes of ~ 60% solids content and viscosities lower than 500 mPa•s at 20 s^{-1}.

In the second approach, the second population of particles was created by the addition of seeds by using small cross-linked particles as pseudo inert-fillers. This process resulted in products with ~58% solids and viscosities lower than 1400 mPa•s at 20 s^{-1}. The slightly decreased solids content and increased viscosity relative to the previous approaches is due to the difficulty in producing cross-linked seeds with particle sizes smaller than 30 nm at an acceptable concentration, causing deviations from ideal conditions.

Co-Authorship

The bulk of the research was carried out by me, under the supervision of Dr. Timothy F.L. McKenna and Dr. Robin A. Hutchinson. The material presented in Chapter 3 has been accepted in *Journal of Polymer Science A: Polymer Chemistry*. Philippe Lauvernier, an undergraduate student, performed some experiments under my supervision, for the work presented in Chapter 4 (phase diagrams and some preliminary polymerizations). Dr. Niels M.B. Smeets assisted with the SEC characterization and discussion of the results presented in Chapter 4. Isabelle C. Zavecz, an undergraduate student, performed most part of the experiments presented in Chapter 5, in addition to some experiments during the development of the semi-batch growth of the large particles for Chapter 6, under my supervision. Dr. Juergen Schmidt-Thummes provided technical guidance for the work presented in Chapters 6 and 7. The preparation and editing of the aforementioned manuscript and of this thesis was conducted by me under the supervision of Dr. Timothy F.L. McKenna and Dr. Robin A. Hutchinson.

Acknowledgements

Table of Contents

List of Figures

xi

List of Tables

Nomenclature

Acronyms

AA	Acrylic acid
AIBN	2,2-azobisisobutyronitrile
APS	Ammonium persulphate
Asc. Ac.	Ascorbic acid
BET	Methodology to determine the SSA of materials
CCT	Catalytic chain transfer
CMC	Critical micelle concentration
Cos.	Cosurfactant
CTAB	Cetyl trimethylammonium bromide
CSSC	Critical saturation surface coverage
DBSA	Dodecylbenzene sulphonic acid
DDAB	Didodecyl diethylammonium bromide
DLS	Dynamic light scattering
DTAB	Dodecyl trimethylammonium bromide
DSC	Differential scanning calorimetry
DVB	Divinylbenzene
DWF2A1	Dowfax 2A1
EDL	Electric double layer
EVB	Ethylvinylbenzene
FA	Fumaric acid
FCC	Face Centered Cubic array
FES77	Disponil FES77
HPLC	High performance liquid chromatography
HPO	Hydrogen peroxide
HSC	High solids content
HSC/LV	High solids content/low viscosity
I	Ionic strength
IA	Itaconic acid
IPD	Interparticle distance
KBr	Potassium bromide
KCl	Potassium chloride
K_2SO_4	Potassium sulphate
KPS	Potassium persulphate
$_L$	Variable subscript indicating relation to large particles
LALS	Low angle light scattering
O/W	Oil in water emulsion
MWD	Molecular weight distribution
MA	Methyl Acrylate
MAA	Methacrylic acid
MADQUAT	2-(Methacryloyloxy) ethyltrimethylammonium chloride
MMA	Methyl Methacrylate
NaCl	Sodium Chloride
NaPS	Sodium persulphate
PBA	Poly(butylacrylate)

P(C$_6$MA)	Poly(hexylmethylacrylate)
PdI	Polydispersity index from Malvern instruments software
PDI	Polydispersity index of MWD (M_w/M_n)
PAA	Poly(acrylic acid)
PMA	Poly(methylacrylate)
PMMA	Poly(methylmethacrylate)
PE	Preemulsion
PS	Poly(styrene)
PSD	Particle size distribution
PVAc	Poly(vinyl acetate)
QELS	Quasi-elastic light scattering
PE	Preemulsion
RAFT	Reversible addition-fragmentation chain transfer
RALS	Right angle light scattering
RHS	Right hand side
RI	Refractive index
RT	Room temperature (25°C)
s	Variable subscript indicating relation to small particles
SDS	Sodium dodecyl sulphate
SEC	Size exclusion chromatography
SC	Solids content
SSA	Specific surface area (m^2/g)
Sty	Styrene
TEM	Transmission electron microscopy
THF	Tetrahydrofuran
UV	Ultraviolet light
VOC	volatile organic compound
wt	Weight

Greek

δ	Debye Length corresponding to the thickness of electric double layer
ρ_2	Polymer density
ϕ	Solids fraction
ϕ$_L$	Volume fraction of large mode
ϕ$_{max}$	Maximum solids fraction
ϕ$_{rlp}$	Volume fraction referent to random loose packing array
ϕ$_{scp}$	Volume fraction referent to simple cubic packing array
ϕ_1	Volume fraction of the monomer
ϕ_2	Volume fraction of the polymer
η	Viscosity [mPa•s]
χ	Monomer-polymer interaction parameter
γ	Interfacial tension between the particle and dispersion medium [mN/m]
ε	Dielectric constant

λ	Average number of repeated units between cross-links
Θ	Contact angle between the tangent at the wetting line and the plate surface in the tensiometer apparatus

Variables

$\Delta \overline{G}*$	Partial molar free energy or chemical potential
$\Delta \overline{G}_m$	Variation in monomer-polymer mixing force
$\Delta \overline{G}_t$	Variation in particle-water interfacial tension force
$\Delta \overline{G}_{el}$	Variation in polymer network elastic-retractile force
ΔVp	Variation of volume of particle
Δt	Variation of time
Dp	Diameter of particle
Dp_L	Diameter of particles of the family of large particles
Dp_S	Diameter of particles of the family of small particles
Dp_L/Dp_S	Diameter of large to small particles ratio
Dp/Dp_0	Diameter of swollen particle to original diameter of particles ratio
F	Force [kg·m/s]
[HPO]	Hydrogen peroxide concentration [Mol/L]
[I]	Initiator concentration [Mol/L]
j	Ratio of equivalent number of molecular segments between the polymer and monomer
k	Constant
k_B	Boltzmann constant
k_p	Propagation rate constant
[KPS]	Potassium persulphate concentration
k_{tr}	Rate coefficient transfer constant to monomer
κ^{-1}	Debye Length corresponding to the thickness of electric double layer
$\overline{M}_C$	Average molecular weight between two cross-links in the network
M_n	Number-average molecular weight
M_0	(Mean) molecular weight per monomer
$[M]_p$	Monomer concentration in the particles
M_w	Weight-average molecular weight
M_z	Critical degree of polymerization of oligoradicals
Np	Number of particles
Np_L	Number of particles of the family of large particles
Np_S	Number of particles of the family of small particles
$\overline{n}$	Average number of radicals per particles
N_A	Avogrado's number (1/mol)
P	Wetted length of the platinum plate used for interfacial tension measurement [m]

pK$_a$	Acid dissociation constant
[P•]	Concentration of active particles
q	Cross-link density
r	Mole fraction of DVB
r_p	Radius of particle
R	Universal constant of gases
R$_p$	Rate of polymerization
Rp$_V$	Rate of volumetric particle growth
Rp$_{V,L}$	Rate of volumetric particle growth in the family of large particles
Rp$_{V,S}$	Rate of volumetric particle growth in the family of small particles
[SDS]	Sodium dodecyl sulphate concentration
t	Time [hour, minute]
T	(Absolute) temperature
T$_g$	Glass transition temperature
V_1	Molar volume of the monomer

Chapter 1

Introduction

1.1 Overview

Nanoscience and nanotechnology cover the investigation, control and exploration of the properties of nanometric size objects, 1-100nm, and their utilization in environments of these dimensions. The diameter of an atom is about 0.25 nm while the typical size of a protein is 50 nm. Therefore, it is in this regime that the capacity to work in the molecular level to create greater structures with a molecular organization that is fundamentally new becomes apparent. Nano scales structures can exhibit physical, chemical and biologic properties and phenomenon that are significantly new and/or modified.

Emulsion polymerization and related techniques are unique chemical processes that result in a dispersion of colloidally stable polymer particles in water that range from 5 to 1000 nm size. The main advantages responsible for the continued industrial and academic interest in these products rely on: i) the environmentally friendly aspect of using of water as solvent instead of volatile organic compounds, considered an example of applied green chemistry; ii) because of the highly exothermic nature of polymerization processes, oil-in-water emulsion polymerization presents better thermal control compared to other polymerization techniques because water acts as a heat sink (low viscosity and high heat capacity) and iii) it enables higher rate of polymerization and yet high molecular weights compared to homogeneous polymerization techniques, due to the segregation of the radicals in the huge number of particles composing the disperse phase, leading to a higher overall concentration and longer kinetic lifetime of radicals.

The product of an emulsion polymerization is called a latex and it finds applications in a wide range of commodities such as adhesives, binders, printing inks, synthetic rubber, additives, coatings and paints among others. The world demand for emulsion polymers is estimated at 7 - 20 million tons, with an annual growth rate of 3.6%.[1-3] Some specialty applications include drug delivery carriers, immunoassays and diagnostic tests products, based on the extremely well tailored responsive capacity and functional chemical groups incorporated to these particles. A valuable degree of sophistication to the commodity products mentioned above is the production of high solids content, low viscosity latexes for the production of (not exclusively) high performance coatings. These products offer economical advantage for being significantly more concentrated (lower costs for storage and transportation, higher productivity per unit volume) but they also show better results in terms of application performance (shorter drying time and improved film properties).[4-6]

1.2 Research objectives and original contribution

The solids content is the concentration of solids (polymer + additives) in the latex. There is a physical limitation that one can pack identical spherical particles into a given space, which is 74%. This corresponds to the face centered cubic (FCC) array where the particles are in contact and this implies that the viscosity of the FCC assembly is infinite. In the case of latexes, this upper limit is severely decreased since the particles cannot stay in an ordered state because of agitation and additionally the stabilization layer that surrounds each particle and prevents their coalescence. Therefore, in practice, latexes with particles of approximately same size have a maximum solids content of 55-60% solids. The higher the solids content in a monodisperse, the higher the viscosity. Higher solids content are obtainable by the production of latexes with more than one, usually two, populations of different particle sizes with the objective of filling the gaps (void spaces) of the large particles with small particles. In order to keep viscosity low, one has to

2

control the particle sizes and the volume fraction of each population adequately. This way it is possible to achieve solids contents on the order of 75%.[7, 8] However, these values correspond to particle sizes in the order of 1000 nm for the large particles.

This project is different from previous high solids content latex researches in the sense that the particle size specifications are much more restrictive. Due to the final application requirements of this latex in paper coatings, the size of the particles have to be smaller than 200 nm to provide the desired properties. This means that out of the two populations, in order to fit in the voids of the larger particles and to enable us to concentrate this product without significant increase on its viscosity, the second population of particles has to be smaller than 30 nm. Figure 1-1 illustrates the difference in particle size relative to the latexes described above. The production of such small particles (in the nanometric range), the control of their particle size distribution (PSD) and their stability are among the challenges faced in this project.

When the average particle size of a latex is decreased the upper limit of solids content achievable is decreased as well. This is due to the fact that the thickness of the stabilizing layer is constant and independent of the particle size, thus the volumetric fraction that it occupies becomes more and more important as the particle size is decreased, as shown in Figure 1-1. The solids content is reduced because these layers of hydrated ions account for the particle diameter but not for the solids content of the latex. As the volume fraction of this layer becomes more important, the correspondent loss in solids content capacity become more appreciable.

Figure 1-2 presents a more quantitative analysis of the loss in solids contents capacity with decreasing the particle size in a latex. The average distance between two particles, assuming a latex composed of perfectly identical spheres and hexagonal packing (same packing fraction of random close packing, ϕ_{rcp}=0.64), is shown to decrease as the volume fraction of solids is

increased and the particle size is decreased. As the solids fraction of a latex with a certain average particle size is increased, the distance between two particles decreases and viscosity increases due to interaction between particles. When the interparticle distance is as small as the value of two times the stabilizing layer thickness (2δ), the particles are literally touching each other and this is defined as the maximum solids fraction of that latex. At this point viscosity is virtually infinite. In fact, viscosity increases exponentially as the solids content approaches the value of maximum solids fraction.
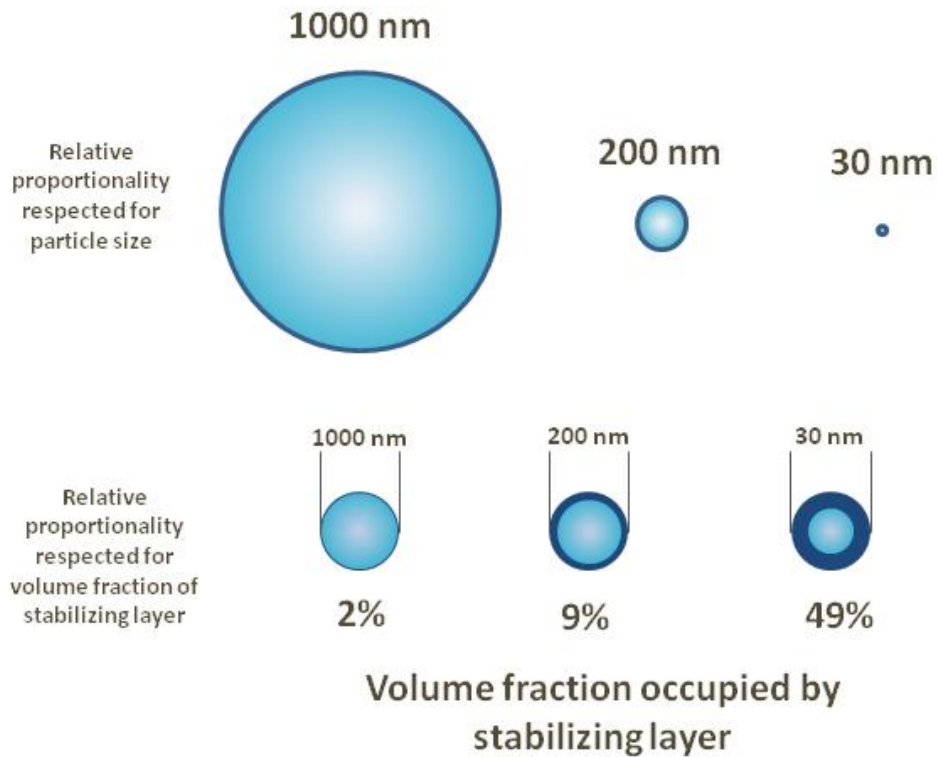
Figure 1-1. Relative size and volume fraction difference between spherical particles and their stabilizing layer. The proportionality between the drawings was respected for comparison purposes and the relative volume fraction corresponds to a 3 nm thick stabilizing layer (δ).

The objective is to develop higher solids content formulations than is currently possible (~50 wt%) for paper coating. Because of the reduction in the value of maximum solids fraction when working with smaller particles, our target for HSC latex in this work is to bring the concentration from 50 wt% to ~60 wt% while keeping viscosity low. Obviously a bimodal process is a good way of doing this. Our industrial sponsor, BASF, has shown that bimodal latexes can be achieved by mixing colloidal silica with a monodisperse coating. The problem is that silica is too expensive, so we will be the first to try to do an *in-situ* process where small, dense polymer particles are generated and used as pseudo (inert) nanofillers. We therefore need to be able to control the particle size distribution (PSD) for viscosity reasons at high solids content. This implies that we need to create a small particle population that will have a diameter on the order of 30 nm (preferably) at the end of the production run. Different strategies for doing so will be presented in Chapters 3-5.
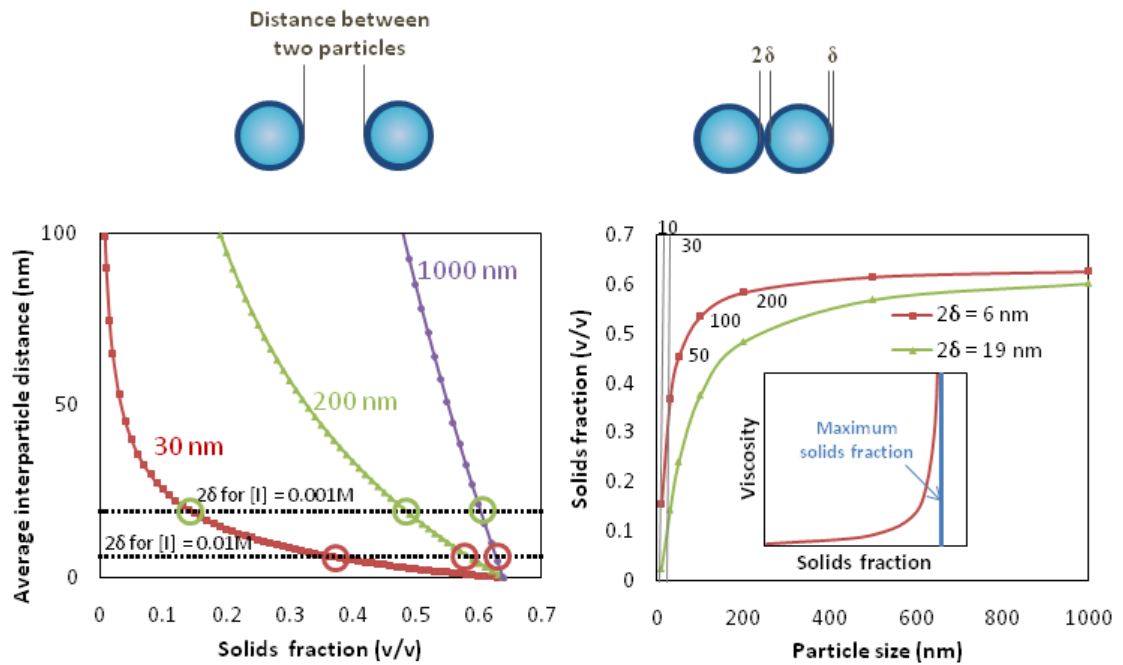
Figure 1-2. Average interparticle distance and maximum solids content of monomodal latexes as a function of particle size, assuming stabilizing layer thickness (δ) of 3 and 9.5 nm.

More specifically, the objective of this project is to produce a latex of polystyrene with 3-5 wt% of acrylic acid in its composition (the styrene phase can eventually include a fraction of divinylbenzene – or other – as reticulating agent) with a final solids content of around 60 wt%. The latex will have a bimodal PSD with a maximum particle size of 160-200 nm (preferably 160), and a viscosity less than 1200 mPa·s at a shear rate of 20 s^{-1} at pH 6.5.

Another innovative aspect of this project is the approach or strategy that will be taken for the production of this latex. As will be discussed in the literature review in Chapter 2, all works published so far have used one of the following generalized strategies: (i) a shot of surfactant to nucleate the small family of particles in the presence of the large particles (unseeded approach), (ii) adding small seeds during the synthesis of the large particles (seeded approach), (iii) preparing two families of monomer stable droplets sizes separately using appropriate recipes and miniemulsification processes, mixing them together and polymerizing to create a bimodal latex (miniemulsion approach). All of these approaches are followed by growth of both families in parallel until reaching the desired latex concentration. More details about each of these approaches and some possible variations are presented in Chapter 2.

In this work we studied the generation and growth of the larger particle size population in the presence of the small mode of particles. The small particles were cross-linked to avoid their swelling and growth during the nucleation and growth of the large particles. Figure 1-3 presents the schematics of this approach. The fact that the two families of particles have different properties is something that has never been reported before and this represents a great challenge; for the first time the small particles will have to be created before the large particles if the unseeded approach is desired, inverting the order of the particle families' creation.

6

It is worth mentioning that the commercial formulation intended for this product is composed of styrene-butadiene copolymer; however throughout this development project, butadiene has not been employed for practical reasons, since it requires pressurized reactors as a gas-phase monomer.

1.3 Thesis outline

To achieve the requirements stated in the objectives, we will examine different processes and formulations through disperse phase polymerization techniques, such as emulsion polymerization and microemulsion polymerization. In Chapter 2 we provide a brief literature review on important theoretical aspects with implications to this project. This literature review elucidates the challenges involved in each step of the project and examines contributions from previous works that could enhance the understanding of several parameters related to our processes.

Creation of small x-linked particles → Creation of large particles → Growth of large particles
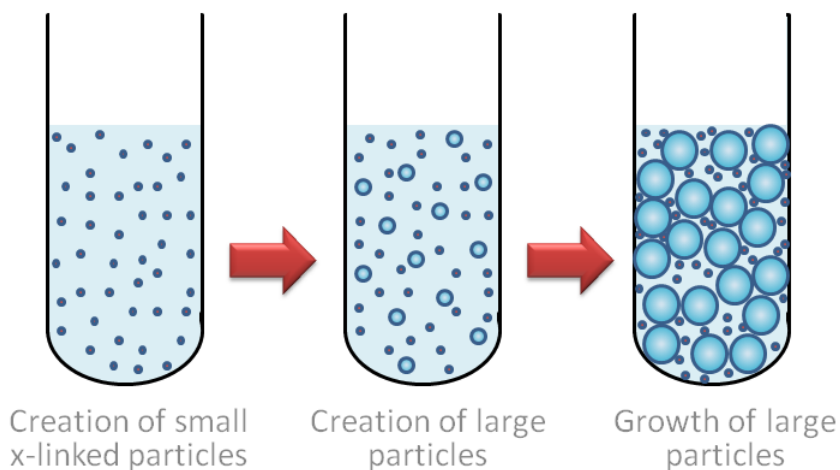
Figure 1-3. Scheme to describe the innovative pseudo inert fillers approach to produce high solids content with low viscosity (bimodal) latexes.

Since small particles have a much higher surface to volume ratio than larger ones, their production typically requires the use of large quantities of surfactant. In general this is not desired for industrial products for a number of reasons including excessive foaming and poor end use properties. In Chapters 3-5 we will therefore explore ways to create very small particles (< 50 nm) using as little surfactant as possible.

In Chapter 6 we report the production of the large particles population, which requires precise control over the number of particles during their generation and growth as they are concentrated. In addition, we will also explore the production of the second population (small particles) in the presence of the large particles, using techniques developed in Chapters 3 and 5.

Chapter 7 brings the study of the cross-linking of the small particles population in order to enable their use as pseudo-filler during the generation and growth of the large particles, and the application of these cross-linked particles to achieve high solids content latexes, growing the large particles in the presence of the cross-linked small particles to produce a concentrated the latex with low viscosity.

Finally, Chapter 8 presents an overall conclusion for the work, with reflections about the questions answered and questions raised by this thesis, and an outlook for future works.

References

1. De La Cal, J.; Leiza, J. R.; Asua, J. M.; Butte, A.; Storti, G.; Morbidelli, M. Emulsion Polymerization. In *Handbook of Polymer Reaction Engineering;* Meyer, T., Keurentjes, J., Eds.; Wiley-VCH: Weinheim, 2005; Vol. 1.

2. Schmidt-Thummes, J.; Schwarzenbach, E.; Lee, D. I. Applications in the Paper Industry. In *Polymer dispersions and their industrial applications;* Urban, D., Takamura, K., Eds.; Wiley-VCH: Weinheim, 2002.

3.   *http://www.chemanager-online.com/en/topics/chemicals-distribution/surfing-global-megatrends* (accessed 03/07, 2011).

4. Guyot, A.; Chu, F.; Schneider, M.; Graillat, C.; McKenna, T. F. *Prog.Polym.Sci.* **2002***, 8,* 1573-1615.

5. Ai, Z.; Deng, R.; Zhou, Q.; Liao, S.; Zhang, H. *Adv. Colloid Interface Sci.* **2010***, 1,* 45-59.

6. Mariz, I. d. F. A.; Millichamp, I. S.; de la Cal, J. C.; Leiza, J. R. *Prog. Org. Coat.* **2010***, 3,* 225-233.

7. Boutti, S.; Graillat, C.; McKenna, T. F. *Polymer* **2005***, 4,* 1211-1222.

8. Schneider, M.; Claverie, J.; Graillat, C.; McKenna, T. F. *J Appl Polym Sci* **2002***, 10,* 1878-1896.

Chapter 2

Literature Review

2.1 Coating Technology and Development

Basic aspects of coating technology

Coating is the process whereby a thin layer of material is deposited on a substrate. It is primarily used for surfaces protection and as such provides a defence against chemical, mechanical and environmental threats by preventing water, oil or air penetration, chemical corrosion, UV penetration and electrical conduction. Coatings also have decorative functions, such as colourful decorating for buildings, printing materials, and various utensils.

Generally, the components in a coating recipe are classified in two groups; one includes volatile components, such as solvents, coalescing agents and condensation products, another includes non-volatile component, consisting of film-forming substances, resins, plasticizers, additives, dyes and pigments.[1] Film-forming substances, resins and plasticizers are generally called binders and are the materials that form the continuous phase film binding on the surface of a substrate. Resins must be soluble (and/or dispersed) either in water or an organic solvent and they are applied to increase the performance such as gloss, softness or hardness and adhesion. The glass transition temperature (T_g) of the coating is controlled by its polymeric composition and the addition of plasticizers, which are oily organic components with a low molecular weight used to decrease T_g of film-forming components.[2]

Volatile components are present in large volumes in all coating formulas. They evaporate during the film forming stage. Previously, almost all volatile components were organic solvents with a low molecular weight. Currently, many coatings have been developed, such as high-solids

coatings and waterborne coatings, based on their advantages in terms of environmental concerns, volatile organic compound (VOC) emissions and energy savings.[3] The most significant development in the protective coating field occurred in the middle of nineteenth century with the development of water-based paints. The new synthetic latex made the rapid growth of water-based coatings possible. The driving force of waterborne coating is increased legislative restrictions on the emission of organic materials to the atmosphere (VOC emissions), leading to an increasing trend to replace the organic solvents by environmental friendly solution, water.[4] In addition, water-based latex coatings have been widely used in many areas for many years because they offer other numerous advantages such as rapid drying, low solvent odour, easy clean-up, reduced fire hazard, good durability and better long-term retention of mechanical properties. Moreover, macroscopic viscosity is independent of the molecular weight, which means that we can control the mechanical properties without paying a penalty in terms of post-reactor handling.[3]

Paper coating

Paper is coated primarily to improve its appearance and its printability. The magnitude of improvement that can be realized through coating is dependent upon the base sheet characteristics, the coating formulation, and the process for applying the coating. Typical applications of water-based paper coating are shown in Table 2-1 and these products demand about 23% of the global emulsion polymer market.[5]

The finished paper contains numerous voids and it is the light scattering from these that gives the coating its whiteness. Fine particle size latexes are more efficient binders owing to the increased number of contacts in the coating; however excess surfactant will lead to poor wet pick values, implying that as the surfactant concentration increases, more ink/coating becomes removable from the surface, which gives lower ink density readings. High levels of surfactant would render the coating unsuitable for printing.[6]

Table 2-1. Typical application for water-based paper coatings. Adapted from Vaha-Nissi 2001.[7]

Food packaging	Non-food packaging
Frozen/chilled food cartons	Ream & reel wrap
Pet food packaging	Poster and wallpaper
Candy boxes and wraps	Release paper
Fast food packaging	Building material wrap
Fish and vegetable boxes	Paper sacks
Cake/cookie packaging	Detergent cartons
Disposables	Corrugated board

Gloss levels rise with increasing stiffness of the resin. The strength of the coating is also dependent on the gel content of the polymer: the strength of the coating rises with the amount of gel until cross-linking inhibits film formation, which results in rapid strength decline. A certain amount of acrylic acid is also used to improve mechanical properties and compatibility with pigments. Medium-stiffness carboxylated styrene-butadiene latexes dominate the market on account of their good binding properties and moderate raw material costs.[6]

Waterborne polymer coatings

There are different methods of obtaining polymer dispersed in an aqueous phase and they are summarized in Table 2-2 as a function of the particle size obtained in each technique.[8, 9]

For reasons associated with constrains on particle size of this project (< 200 nm), we will not consider suspension, dispersion or solution polymerization. The product of an emulsion polymerization and related techniques is a colloidally stable polymer dispersion (called a latex) and below we present concepts involved in the production of such polymer dispersions.

Table 2-2. Size range of polymer particles produced by techniques of polymerization in presence of water.

Polymerization in presence of water	Range of particle size
Suspension Polymerization	0.01-2mm
Aqueous solution Polymerization	Soluble
Dispersion Polymerization	0.1-10μm
Emulsion Polymerization	50-1000nm
Miniemulsion Polymerization	50-500nm
Microemulsion Polymerization	5-100nm

2.2 Latex production

Emulsion polymerization is certainly the most widely used process to prepare polymer colloids.[5, 10] The particle size of emulsion latexes usually ranges between 50 to 1000 nm and the mechanism and kinetics of the reaction have been extensively studied since the 1930's.[11, 12] Miniemulsion and microemulsion products have particles size in the order of 50 to 500 nm and 5 to 100 nm (often less than 50 nm) respectively and both been extensively studied starting around 1980.[13, 14] These two relatively new techniques have experienced great number of developments since its beginning and recently they have attracted a great deal of attention. Miniemulsion because of its mechanism of particle nucleation and the absence of monomer transport through the water phase which opens the doors to a new set of applications, such as the incorporation of extremely hydrophobic materials and inorganic species into the latex. Microemulsion because of the small particle size that implies in an enhanced internal surface area, which can originate highly functionalized particles or microgels that find diverse applications.

The concepts of miniemulsion polymerization was not considered in this literature review because there was no necessity of incorporation of extremely hydrophobic components and the particle size obtained with this technique is obtainable with conventional emulsion

polymerization, eliminating the high energy consumption normally required for the miniemulsification step.[15-17] Therefore, the techniques that will be involved in this project are emulsion and microemulsion polymerization, for the production of the large and small families of particles respectively.

2.2.1 Emulsion polymerization

Emulsion polymerization is predominantly used for the commercial production of vinyl acetate, vinyl chloride, acrylamide, various acrylate copolymerizations, and copolymerizations of butadiene with styrene and acrylonitrile.[18] In general, emulsion polymerizations have been widely used in many industries such as synthetic rubbers, high-impact polymers, latex foams, latex paints, adhesives, binders, paper coating, textile and construction.

Below we provide a brief description of the process. For more comprehensive literature the reader is recommended to refer to textbooks and papers cited in this section. For general principles of emulsion polymerization the reader is referred to Lovell and El-Aasser, 1997[11] and Chern, 2008[19]; for emulsion polymerization kinetics: Gilbert 1995.[12]

2.2.1.1 Process description

An emulsion polymerization starts with water, surfactant, a water-insoluble (or scarcely soluble) monomer and initiator in an oil/water or water/oil system (we only consider the former in this thesis as the industrial process being studied is an oil-in-water system). The emulsion is formed by agitation with the aid of surfactant. The initiator is generally soluble in the continuous medium rather than in the monomer in a conventional emulsion polymerization. In emulsion polymerization, large monomer droplets (1-10 μm) coexist with pure surfactant or monomer-swollen surfactant micelles (5-20 nm) before polymerization and during the early stages of the reaction. During polymerization, the monomer diffuses from the larger monomer particles

through the medium to micelles or newly-initiated polymer particles. The micelle is the primary nucleation loci and the latex particle is not the primary emulsion droplet.

The rate of polymerization (R_p) depends on the propagation rate constant (k_p), the monomer concentration in the particle ($[M]_p$) and the concentration of active particles ($[P\bullet]$), according to Equation 1.

$$R_p = k_p[M]_p[P\bullet] \tag{1}$$

the concentration of active particles $[P\bullet]$ is expressed by

$$[P\bullet] = \frac{\bar{n}Np}{N_A} \tag{2}$$

where Np is the number of particles per volume, $\bar{n}$ is the average number of radicals per particles, and N_A is the Avogadro's number. When the two above equations are combined together, the resulting equation is expressed by

$$R_p = k_p[M]_p\frac{\bar{n}Np}{N_A} \tag{3}$$

Changes in R_p during a batch reaction can be roughly placed in one of three intervals as presented in Figure 2-1. In Interval I particle nucleation occurs and R_p builds up with increasing Np. The end of the nucleation, and therefore Interval I, is characterized by the absence of free micelles. The system is composed of growing polymer particles and monomer droplets, all of them stabilized by surfactants localized at their surfaces. In Interval II, polymerization proceeds in the polymer particles. R_p remains almost constant, when no new nucleation or coagulation takes place, or can increase slightly with conversion in consequence of the gel or Trommsdorf effect[i]. Another major factor that keeps R_p approximately constant is that the $[M]_p$ is maintained

---

[i] The Trommsdorff effect occurs when the rate of termination inside the polymer particle is reduced due to the increase in viscosity as conversion is increased causing the polymer chains to have a lower mobility.

at equilibrium (saturation) level by diffusion of monomers from the monomer droplets through the continuous media. Equilibrium $[M]_p$ is characteristic for each monomer and is related to thermodynamics considerations. A discussion about polymer swelling and concentration of monomer in the polymer particles is given in Appendix A. More information about this topic will also be presented in section 2.5. Interval II ends when the monomer in the droplets is consumed by the reaction. In Interval III, the monomer concentration inside the particles decreases as a function of time in a batch reactor, since monomer droplets are no longer present to feed the particles. However, Rp might continue to increase for a certain amount of time due to the Trommsdorff effect which essentially leads to the reduction of the termination rate inside the particles (i.e. $\bar{n}$ can increase). Nevertheless, as the monomer supply decreases continuously, the rate will eventually tend to zero.

The value of $\bar{n}$ during Intervals II and III is critical to the determination of R_p. Three cases can be distinguished, known as Smith-Ewart theory cases.[12, 18-20]

Case 1: $\bar{n} < 0.5$. The average number of radicals per particle can drop below 0.5 if radical desorption from particles and termination in the aqueous phase are not negligible. The decrease in $\bar{n}$ is larger for small particle sizes and low initiation rates.

Case 3: $\bar{n} > 0.5$. Applies to systems with large particle size or with low termination rate constant, and is typical of the kinetics during the initial stages of interval III.

Case 2: $\bar{n} = 0.5$. This is the classical case most described in the literature. It requires that the rate of desorption of radicals is negligible compared to that of absorption and that termination is essentially instantaneous upon entry of a second radical into a particle.

16
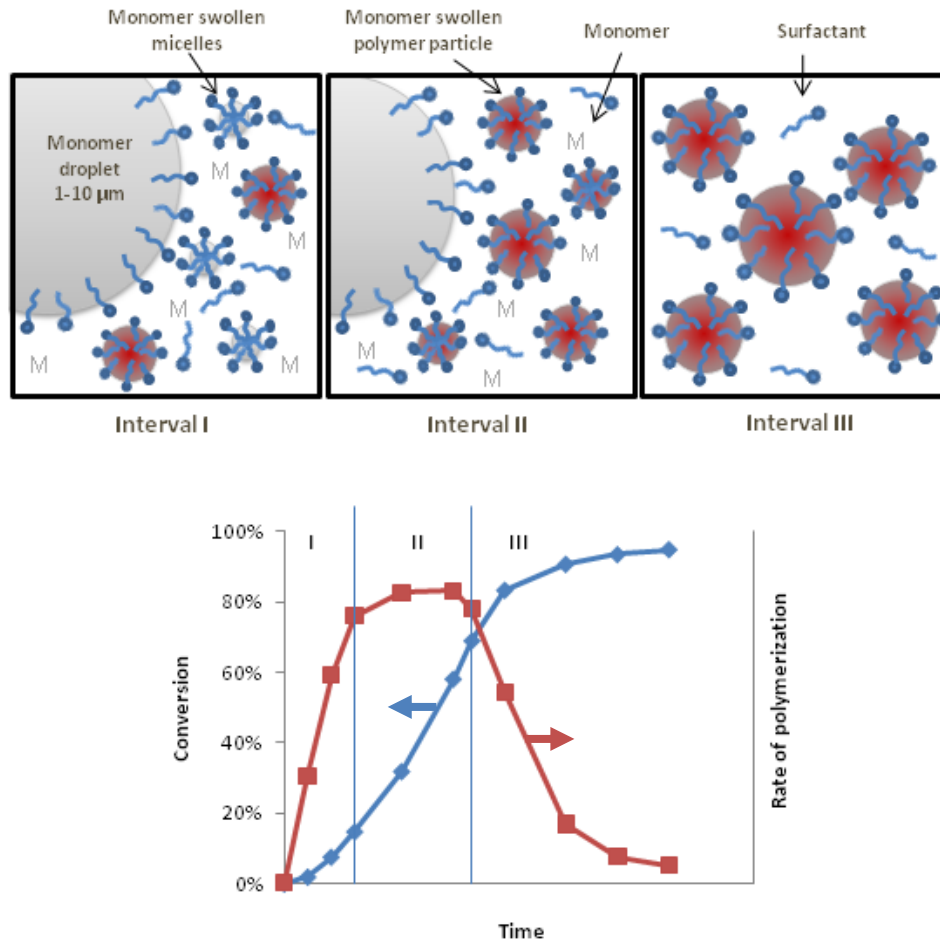
Figure 2-1. Scheme of the evolution of an emulsion polymerization.

2.2.1.2 Particle nucleation mechanisms

Particle nucleation may occur through heterogeneous nucleation, homogeneous nucleation and coagulative nucleation (Figure 2-2). As will be discussed later, the homogeneous-coagulative nucleation is a direct extension of the homogeneous nucleation, thus in the literature, two major nucleation mechanisms are frequently considered: homogeneous and heterogeneous nucleation. Droplet nucleation is commonly neglected in emulsion polymerization because the surface area of

the monomer droplets is 100-1000 times lower than that of the micelles and particles. However it

is the main nucleation mechanism for miniemulsion and microemulsion polymerization.
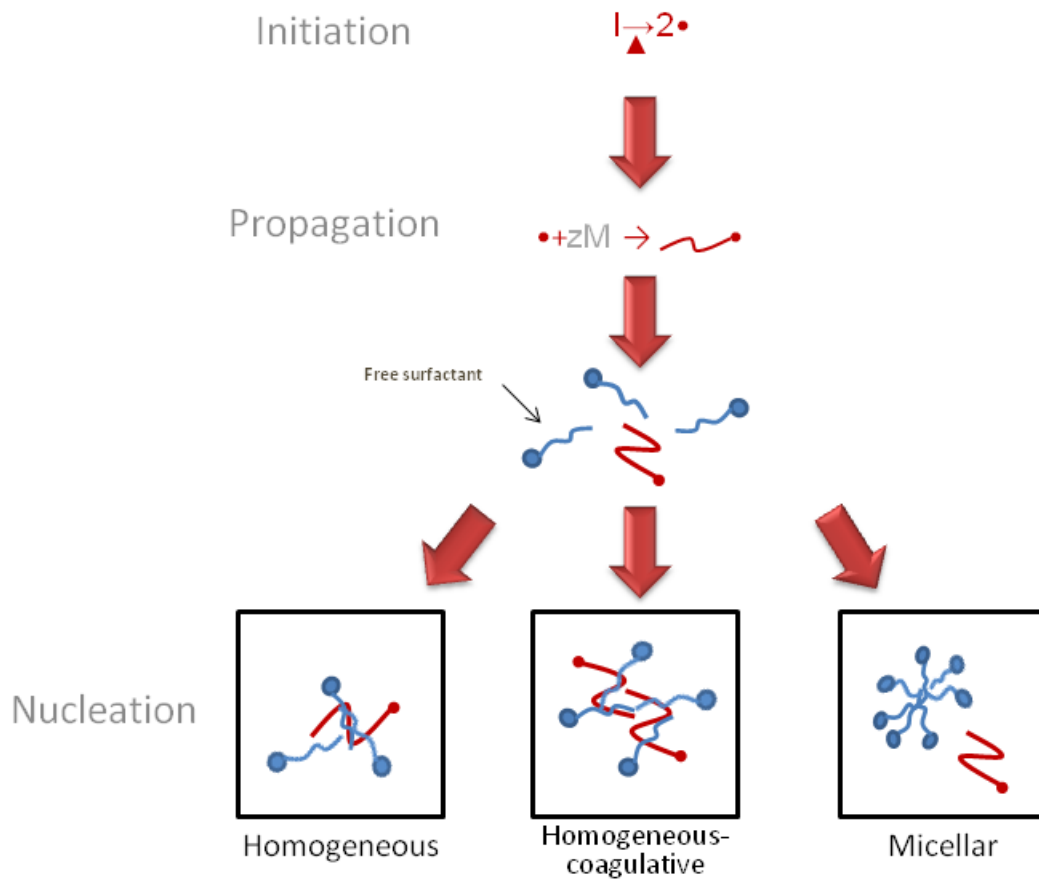
Figure 2-2. Particle nucleation mechanisms.

Homogeneous nucleation theory. According to this theory the polymer particles are generated

by the precipitation of oligoradicals of critical degree of polymerization (M_z), formed in the

aqueous phase. In other words, according to this theory, the homogeneous nucleation is related to

the formation of a surface-active molecule (which has a hydrophilic and a hydrophobic part) with

similar properties to that of a surfactant, and present a critical degree of polymerization

responsible for its precipitation. This means of particle formation is potentially important when one uses partially (or totally) water-soluble monomers such as methyl methacrylate or carboxylic acids, and water soluble initiators in the form of ionisable salts (e.g. persulphates).

Homogeneous-coagulative nucleation theory. The homogeneous-coagulative nucleation theory is a direct extension of the homogeneous nucleation theory. The quantitative analysis of this theory was proposed by Feeney *et al.* in 1987.[21] In this mechanism, the species formed by entry of radicals into micelles and by self-precipitation of radicals are considered non-stable precursor particles. The actual particles are formed by coagulation of two or more precursor particles and polymerization growth.

Micellar nucleation theory. When the surfactant concentration exceeds the critical micelle concentration (CMC), the excess surfactant molecules join together and form a small colloidal grouping called micelles (more information about micelles formation provided in Appendix B). The monomer swollen micelles capture the free radical from the aqueous phase and provide the radical propagation to the formation of the particle.

The micelle nucleation is favoured by low water solubility monomers and high surfactant concentration, whereas high water solubility monomers and surfactant concentrations below CMC favour homogeneous nucleation. It is believed that homogeneous nucleation, micellar nucleation and homogeneous-coagulative nucleation coexist in emulsion polymerization, with one of them being of more or less importance depending on the system characteristics. For most emulsion systems, micellar nucleation dominates and other nucleation mechanisms are considered secondary.[12]

19

2.2.2 Microemulsion polymerization

Microemulsions (also referred to as monomer swollen micellar solution, micellar emulsions, or spontaneous transparent emulsion) are transparent liquid systems consisting of at least ternary mixtures of oil, water and surfactant.[22]

The concept of polymerization in microemulsions appeared only around 1980.[23, 24] However, it has developed to a rapidly growing field of research. There are some recent reviews that summarize much of the work done to date.[14, 25-27] A primary goal of investigators that study microemulsion polymerization has been to produce thermodynamically stable latexes in the range of particle diameter (Dp) < 50 nm not attainable with classical emulsion polymerization process. The interesting features of microemulsion polymerization include large interface area, optical transparency, thermodynamic stability, spontaneous formation, small domain length scales and great variety of structures that result in unique microenvironments. Such microemulsions can be used to produce novel materials with interesting morphologies and polymers with specific properties.[14] The size range of microemulsion latexes is appropriate for the population of small particles that we want to make.

Oil in water microemulsions described in the literature usually require a high surfactant concentration (7-15 wt%) for solubilizing only a relatively low monomer content, generally of less than 10 wt%. This means that the amount of surfactant used is very high, with a surfactant/monomer weight ratio of at least unity.[22, 25, 26, 28]

The mechanics of forming microemulsions differ somewhat from those used in making (macro)emulsions. The most significant difference is the fact that increasing emulsifier content or putting work into a macroemulsion usually improves its stability. However, this is not true for microemulsions, as these systems appear to be dependent upon specific interactions among molecules of oil, emulsifiers, and water in their formulations. If the specific interactions are not

realizable, no amount of work input nor excess emulsifier will produce the desired product. Ultrasonication, high speed or high shear homogenization will not work if the chemistry is not right. On the other hand, when the composition is right, microemulsification occurs (almost) spontaneously.[22]

Sometimes a cosurfactant is needed for the formation of a thermodynamically-stable microemulsion. It was observed that the titration of a coarse emulsion by a coemulsifier leads in some cases to the formation of a transparent microemulsion. During addition of a coemulsifier to a coarse emulsion, excess coemulsifier accumulates at the o/w interface. The transition from opaque emulsion to transparent solution is spontaneous and well defined. Zero or very low interfacial tension obtained during redistribution of the coemulsifier plays a major role in the spontaneous formation of microemulsion.[29]

Long chain normal aliphatic alcohols are normally used as cosurfactant in microemulsion formulations. Other cosurfactants like cholesterol or long chain amines, which are used with ionic surfactants, serve to lower interfacial tension between the two mutually insoluble liquids.[22] However, when dealing with microemulsion polymerization, the use of alcohols may have some drawbacks, such as lack of compatibility with the polymer, because alcohols are non-solvents for some polymers. In addition, they may act as chain-transfer agents, thus lowering the polymer molecular weight, reaction rate and conversion.[25, 30-32]

2.2.2.1 Process description

The rate of polymerization in microemulsion can be analyzed in terms of Equation 3 with some differences[33, 34] when compared to emulsion polymerization. It is generally accepted that an o/w microemulsion polymerization proceeds via a continuous particle nucleation mechanism.[35] The particle nucleation is generally postulated to occur in microemulsion droplets (micellar

21

nucleation mechanism) for less water-soluble monomers, such as styrene and butyl acrylate. Even for more water-soluble monomers, homogeneous nucleation may be insignificant because of an extremely large number of microemulsion droplets ($\sim 10^{16}$-10^{17} L^{-1}) that can effectively capture the free radicals generated.[25, 26]

Similarly to miniemulsion polymerization, the reaction kinetics of microemulsion polymerization is characterized by two polymerization rate intervals;[36] the Interval II of constant rate characteristic of emulsion polymerization is missing as shown in Figure 2-3. The continuous nucleation of polymer particles during polymerization results from the very high number of monomer-swollen micelles or microdroplets and therefore, the rate of polymerization increases with the number of particles in Interval I. On the other hand, monomer concentration at the reaction loci decreases with increasing conversion describing Interval III. These two opposing effects result in the appearance of a maximal rate at ~ 20-25% conversion.[26, 29]

In a typical microemulsion polymerization, the concentration of micelles is approximately 1000 times greater than the concentration of particles that ultimately form, so the probability of a radical entering a particle is negligible. Thus, the probability of biradical termination is also negligible in a typical microemulsion polymerization. Figure 2-4 shows a scheme of the evolution of a microemulsion polymerization. Propagation continues in the surfactant-stabilized polymer particle with monomer diffusing from the surrounding uninitiated micelles to the locus of polymerization until the monomer is completely consumed. If transfer of the radical from the polymer to monomer occurs during the polymerization, then the monomeric radical may either continue propagating in the particle or exit the particle and enter a micelle to initiate a new particle. However, the amount of radical transfer is generally quite small. The final latex consists of surfactant-stabilized polymer particles that typically contain a single polymer chain and empty micelles formed by the excess surfactant.[27]

22
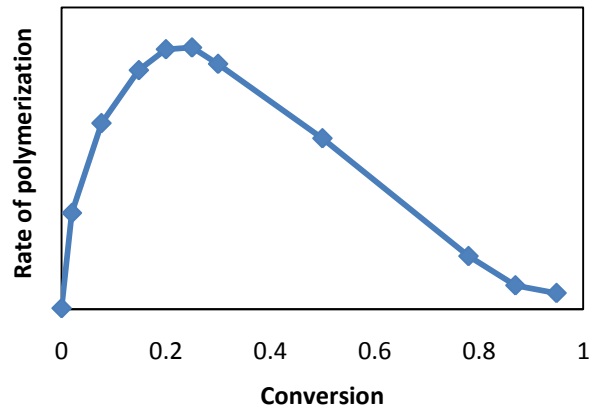
Figure 2-3. Rate of polymerization versus conversion profile for a typical microemulsion polymerization.
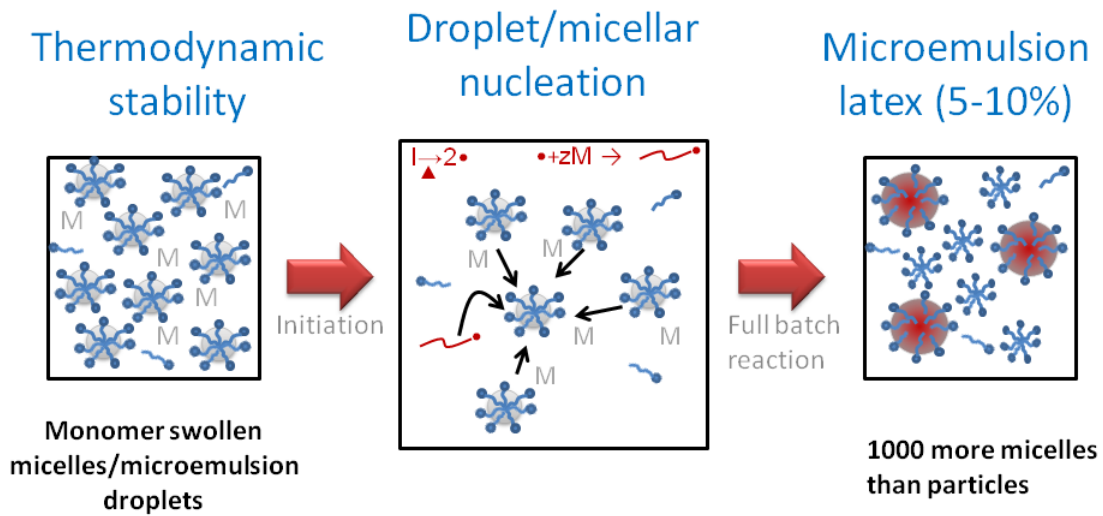
Figure 2-4. Scheme of the evolution of a microemulsion polymerization.

2.2.2.2 High polymer-to-surfactant ratios in microemulsion polymerization

In microemulsion polymerization large amounts of surfactants are essential to the spontaneous formation of microemulsion droplets, fast nucleation of latex particles, and stabilization of latex particles during the course of polymerization and storage. The major difference between emulsions and microemulsions comes from the amount of surfactant needed to stabilize the

23

respective systems. Much more surfactant is needed for microemulsions. Conventional oil in water (O/W) batch microemulsion polymerization recipes call for the use of at least an equal amount of surfactant and monomer, which makes polymerization and surfactant removal processes unreasonably expensive. In addition, the presence of excessive surfactants in film-forming polymers can confer water sensitivity on the film, which is a drawback for protective coatings. Therefore, the high ratio of surfactant to monomer required to form the initial, thermodynamically stable microemulsions is a significant disadvantage to the commercial implementation of microemulsion polymerization. For this reason, the synthesis of polymer latexes with high ratios of polymer to surfactant by microemulsion polymerization is an emerging research topic. Moreover, as mentioned in section 2.1, high levels of surfactant in paper coating formulations make the coating unsuitable for printing applications, reason why improved formulations have to be pursued in this project.

Several approaches to reduce the level of surfactant used in microemulsions have been proposed. A recent review of these methods is provided by Xu and Gan.[37] The amount of surfactant in batch microemulsion polymerization can be decreased through the use of reactive or polymerizable surfactants. In addition, new surfactant molecules that are able to solubilize large amounts of monomer can be employed, although such molecules are not always available commercially. Nevertheless, semi-continuous microemulsion polymerization process is the most successful method to increase the amount of polymer produced for a given amount of surfactant. Table 2-3 presents the works reported on this area of research. The results are shown in terms of formulation, final particle size and solids content (SC), and it classifies the recipes in terms of the amount of surfactant used relative to the monomer mass. All works employ semi-continuous microemulsion polymerization, where (at least the beginning of the process) the monomer has very low concentration in the system, known as starved-feed conditions. In this way high

surfactant/monomer weight ratio as well as excess initiator free radicals is assured. The starved-feed conditions provide great efficiency in the nucleation of polymer particles in microemulsion polymerization. The monomer added by a differential manner can dissolve and quickly diffuse in the water phase, and be continuously consumed, which significantly enhances probability of homogeneous nucleation.[38]

Dan et al.[39] synthesized PMMA latex using SDS as surfactant and achieved an average particle size of 33 nm for 30 wt% solids content with 2.3 wt% SDS with respect to the monomer mass, the lowest level of surfactant among the works reported. When they increased the SC to 40 wt%, the particle size was less than 40 nm and the amount of SDS was less the 5 wt% with respect to the monomer mass.

Table 2-3. Works published in the area of high polymer-to-surfactant ratios and high solids content (SC) latexes by semi-continuous microemulsion polymerization process.

Author	Ref	Polymer	Surfactant			Cosurfactant			Dp (nm)	SC (%)
			Type	wt% (total)	wt% (mon.)	Type	wt% (total)	wt% (mon.)		
Dan, Y. et al. 2002	39	PMMA	SDS	0.7	2.3	-	-	-	33	30
		PMMA	SDS	<3	<5	-	-	-	<40	40
Ming, W. et al. 1998	40	PMMA	DTAB	0.8	3.2	-	-	-	47	25
Ming, W. et al. 1998	41	PMA	SDS	1	3.3	1-Pentanol	0.2	0.67	15	30
		PS	SDS	1.5	15	1-Pentanol	0.2	2	15	10
He G. et al., 2003	42	PMMA	SDS	1.9	5.3	1-Pentanol	0.44	1.22	40	36
Xu, X. et al. 1999	43	PS	CTAB	1	7.6	-	-	-	52	13
He G.; Pan Q. 2004	44	PMMA-PS	SDS	3.1	8.9	1-Pentanol	0.36	1.05	32	38
Barrere, M. et al. 2002	45	PDMS	DBSA/BRIJ35	7.1	9.0	-	-	-	43	30.2
Roy S.; Devi S. 1997	46	PMMA-PBA	DWF2A1	3.7	9.2	-	-	-	39	41
		PMMA-PBA	DWF2A1	3.7	9.2	Acrylamide	0.4	1	35	42
		PMMA-PBA	DWF2A1	3.7	9.2	1-Pentanol	0.4	1	50	38
Aguiar, A. et al. 1999	47	PS-PBA (IA)	DTAB	1.7	14	-	-	-	60	14 (15)
Kong, X. et al. 2006	38	PS	SDS	2.9	20	n-Butanol	0.3	2	28	18
Rabelero, M. et al. 1997	48	PS	DTAB	8.8	21	-	-	-	45	38
Hermanson, K. D.; Kaler E. W. 2003	49	P(C$_6$MA)	DTAB/DDAB	4.1	24	-	-	-	53	17

We will not describe every work, as Table 2-3 provides all important information, but we will rather describe general characteristics and trends of this collection of works. For instance, it is clear that hydrophilic monomers provide smaller particle size and higher polymer-to-surfactant ratios. This can be realized when looking at the works which use the same surfactant, i.e. SDS, for hydrophilic[2] monomers such as methyl methacrylate (MMA) and methyl acrylate (MA) versus hydrophobic monomers such as styrene (Sty). This result is believed to be due to a combination of factors. (i) Homogeneous nucleation generates smaller particles compared to monomer-swollen micellar nucleation, since the size of a monomer-swollen micelle is relatively large, about to 2.5 to 5 nm.[50] Moreover, in microemulsion swollen micelles usually act as monomer reservoir. That will make the free radicals propagate very quickly and therefore the particle size is larger than that from homogeneous nucleation. (ii) The surface tension of hydrophilic monomers/water is lower which decreases surface energy and favours the generation of smaller particles. (iii) Since the probability of biradical termination in microemulsion polymerization is negligible due to the large concentration of micelles, if transfer to monomer occurs, the more hydrophilic the monomer is, the higher the exit rate, which favours the nucleation of new particles.

Another point that can be made is about the use of cosurfactants. As can be inferred from semi-continuous starved-feed conditions for microemulsion polymerization, at the beginning of the polymerization, this system is at a high concentration of surfactant and very low concentration of monomers. Thus, the increased ratio of surfactant-to-polymer in the beginning of the process allows for the fast nucleation of particles. Because of the process conditions, the concentration of monomers is maintained at low levels throughout which tends to minimize the solubilization of monomer into micelles, and as a consequence the formation of microdroplets should not take

---

[2] Water solubility @ 20°C (mg/L): MA = 50000; MMA = 15000; Sty = 310

place. Therefore, cosurfactant is not always required. Roy and Devi[46] used Dowfax2A1 as surfactant to polymerize PMMA and PBA (1:1) applying starved-feed semi-continuous microemulsion polymerization. Among other studies, they verified the influence of using acrylamide and 1-pentanol as cosurfactants. Acrylamide provided smaller particle sizes than pentanol. The authors justify this by the non-solvency of the polymer by pentanol, which created coagulum and instability. However, acrylamide is also much more hydrophilic than pentanol (water solubility of 204 and 2.7 g/100mL respectively) and could provide better cosurfactant properties, i.e. further decrease the interfacial tension between oil and water and enhance the flexibility of the interfacial film.[13, 26, 51] The authors reached 42% solids content in a latex with average particle size of 35 nm when using 3.7% of Dowfax2A1 and 0.4% acrylamide.

Kong et al.[38] synthesized PS latexes using SDS as surfactant and n-butanol as cosurfactant. They obtained an average particle size of 28 nm with 2% butanol and 20 wt% SDS with respect to the monomer mass in an 18% SC latex. Although not the best polymer-to-surfactant ratio, their study raised an interesting point. They compared the starved-feed process with the batch process and introduced a novel feeding method "first dropwise, and then in one portion". They realized that the effect of differential feeding on increasing the nucleation number is only pronounced at low amounts of styrene fed in the starving mode, until it reaches a proper value. The subsequent supply of monomer in differential manner is no longer beneficial for increasing the nucleation number, which implies that the dropwise addition is meaningless at the late stage of polymerization. This way, the "addition in one portion" at the late stage simplifies the experiment procedure without negative effect on the particle size as well as monodispersity. Their results suggest that about 30 wt% of the monomer charge should be fed in a differential manner, thus reducing the process time.

The literature review allowed us to set a start point and parameters for this project. We will see in Chapter 3 that we were able to improve the current results of polymer to surfactant ratio of styrene-SDS microlatexes, and to increase the concentration of latexes with reasonable surfactant levels.

2.3 Rheology of Monodisperse and Bimodal Latexes

Viscosity is one of the most important properties of a latex in terms of its final application, i.e. in paints, adhesives and coatings. In an industrial setting, these products are typically applied using high speed machines, therefore the latex must have well controlled uniform viscosity to avoid changes in process parameters reflected in down time and related costs. Viscosity is also a limiting factor from a polymerization processing point of view, due to generation of problems such as mixing and heat removal. In addition, during the manipulation of latexes in an industrial context, it becomes more efficient if the product has good flowing properties. This means that high viscosities must be avoided.

In this project we will apply a strategy based on the use of bimodal latexes. We will present a brief literature review of the processes used to make high solids content, low viscosity (HSC/LV) latexes and discuss the major points that influence our work. For a more in-depth treatment of the subject the reader is referred to recent reviews by Guyot et al.[52] and Ai et al.[53]

If we assume that a latex is composed of identical spherical particles, there is an upper limit on the amount of polymer that can be packed into a given space. The volume fraction of particles packed in a Face Centered Cubic (FCC) array, is 74%. Randomly packed, identical spheres will have an average volume fraction of 64%.[53] In either case, all of the spheres would be in contact at the maximum packing fraction, and the apparent viscosity of the system would be infinite. In a real latex, one must also take into consideration the space occupied by the stabilizers situated on

the surface of the particles, and must also avoid excessively high viscosities. In fact, the solids content of industrial latexes rarely exceeds 55 to 60 wt% when the products have a monomodal PSD.[54-56] The reason for this was illustrated by Figure 1-2, where the graph shows the average interparticle distance as a function of the solids volume fraction for three different particle diameters. The graph also shows the quantity 2δ, which is two times the thickness of the stabilizing layer around ionically stabilized particles, at two different ionic strengths. The interparticle distance (IPD) can be described by Equation 4,[54, 57]

$$IPD = Dp\left[\left(\frac{\phi_{max}}{\phi}\right)^{\frac{1}{3}} - 1\right] \tag{4}$$

where Dp is the average diameter of particle (nm), ϕ_{max} and ϕ are the maximum solids fraction (0.64) and the simulated solids fraction for monodisperse latexes respectively.

The thickness (δ) of the electric double layer (EDL) is often correlated with the Debye Length denoted as the Debye-Hückel parameter (κ^{-1}), which can be calculated using Equation 5,[11, 19, 58]

$$\delta = \frac{1}{\kappa} = \sqrt{\frac{\varepsilon k_B T}{8\pi e^2 N_A I}} \tag{5}$$

where ε is dielectric constant of continuous medium (water), k_B the Boltzmann's constant, T the absolute temperature, I the ionic strength (mol•L^{-1}), e the charge of a single electron, and N_A Avogadro's number. At room temperature (25°C) and in water Equation 5 reduces to Equation 6.[58]

$$\delta(nm) = \frac{0.304}{\sqrt{I}} \tag{6}$$

Equation 6 shows that, at constant temperature, the thickness of the EDL is inversely proportional to the ionic strength of the medium.

The intersection of the curves with the straight line in Figure 1-2 represents the maximum volume fraction of solids possible in a monodisperse emulsion. As the particle size is reduced, the maximum volume fraction of solids is decreased, as the effective particle volume is the sum of the polymer volume plus the volume occupied by the stabilizing layer. When working with larger particles, the volume fraction occupied by the EDL of the disperse phase is negligible, since the surface area of larger particles is smaller than for small particles at same solids concentration. In fact, increasing particle size is an efficient way to increase solids content of a latex.[53]

An increase in ionic strength implies in a decrease of δ, and thus, a decrease in the effective volume fraction of the particles, increasing the limiting volume fraction of solids for a determined average particle size. The increase in ionic strength can be achieved by using a buffer or working at high pH,[59, 60] however with decreasing the size of the EDL, the colloidal stability of the particles are also reduced and they will be more vulnerable to suffer coalescence and aggregation, compromising the entire latex stability.[11, 19]

Above about 50% (v/v) solids, a solid-liquid mixture with bimodal PSD can have a much lower viscosity than a mixture with monodisperse distribution, if the PSD is well controlled.[52, 53, 61] This could be understood by the idea that the small particles can fit in the available spaces between big particles as illustrated in Figure 2-5. The critical diameter ratio of large to small particles (Dp_L/Dp_S) that permits small particles to fit into the triangular pores between large particles is 6.46.[62]

Therefore, in order to reduce the viscosity of HSC emulsion polymerization products, one needs to work with PSD that is not monodisperse. Farris,[63] Sadler and Sim[61] and Schneider et al.[55, 56] showed that reduction in viscosity at a certain level of solids fraction, or the increase in the value of maximum volume fraction for a determined solid-liquid mixture is progressively less significant as the modality of the disperse phase increases. Furthermore, since Schneider[55] also

showed that there is very little to be gained in terms of increasing solids content with tri- and quadrimodal latexes, we chose to limit our study to more manageable bimodal systems. Further discussion about having a third mode of particle size related to the incremental contribution to the volume fraction of solids relative to the task of producing 4 nm particles and the volume fraction occupied by the EDL in these particles is discussed in Chapter 6.
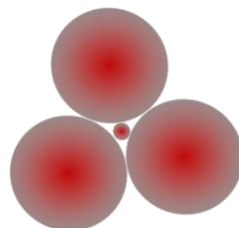
Figure 2-5. Insertion of a small particle in the interstices of three large particles in a two dimensional illustration.

Schneider et al.[55, 56] combined simulation and experimental work to study the viscosity of bimodal latexes. The simulations revealed, among other things, that the presence of a large fraction of fines is detrimental to particle packing, and thus to the viscosity of a dispersion made from these same particles. In addition, they concluded that the most adequate PSD to reach HSC/LV latexes, is a bimodal PSD composed of 15 to 20 vol% of small particles. In fact, for a fixed ratio of the large particle diameter to the small particle diameter, more than 25 vol% of small particles implies an increase of viscosity for a given solids content.[64]

Indeed, many authors[52, 65, 66] agree that the best way to obtain low viscosity at HSC is to aim for a latex composed of 80-85 vol% of large particles with ratio of large to small particles between 6 and 8. Moreover, because viscosity is sensitive to the presence of fines, it is necessary to limit the fraction of small particles. That is, it appears better to have 10 than 25 vol% of them, and it appears better to have a diameter ratio of large to small particles of 10 than 4.

In Chapter 6 we will demonstrate the approach we used to theoretically determine the optimal volume fraction of the small particles, considering particle size and EDL effects, in order to achieve maximum volume fraction of solids, or lowest latex viscosity, in the production of our HSC/LV bimodal latex.

2.4 Production of High Solids Content Multimodal Latexes

There are many ways of obtaining such bimodal PSDs latex:[54]

1) Blends of seeds,

2) Batch processes,

3) Semi-continuous processes using miniemulsions,

4) Semi-continuous emulsion processes.

2.4.1 Blend of seeds and batch processes

Since we are physically limited in the maximum solids content of a monomodal PSD latex, we cannot hope to reach HSC by simply blending monomodal latexes with the same solids content. This option would require the latex to be concentrated after the blending step, however evaporation is not an efficient technique to concentrate a latex since it requires a great deal of energy. Thus, blends of seeds must be concentrated by a semi-batch polymerization stage to get high solids. It is difficult to reach HSC using unseeded batch processes because of the low reproducibility of PSD when nucleating 50% v/v solids content emulsions due to stability issues. Heat transfer is also a problem, however some industrial processes are known to use semi-adiabatic reactors that could handle the heat released and pressure associated. In this project, we will concern ourselves essentially with the last two methods. We will discuss briefly the most important points of each process in this text. For more in depth details, the reader is referred to recent review articles in the subject.[52, 53]

2.4.2 Semi-continuous miniemulsion processes

The use of miniemulsions as the starting point can provide new routes for the synthesis of HSC/LV latexes. Since the nucleation occurs in the droplets, the PSD can be fixed from the beginning of the polymerization and the blend of two miniemulsions with different initial sizes allows the production of bimodal PSD latexes.[52, 53] As an example, a latex with a viscosity of 650 mPa•s at a shear rate of 20 s^{-1} and 70 wt% solids content was obtained by Ouzineb et al.,[67] with particles ranging from 100 to 900 nm with a broad PSD rather than a well-defined bimodal PSD. Despite the potential, miniemulsification will not be considered in this thesis since it is not yet a viable alternative on a commercial scale. For more on this topic see Guyot et al.[52] and Ai et al.[53]

2.4.3 Semi-continuous emulsion processes

This is the most studied category of processes for the production of HSC/LV latexes in the literature. From the works available we can highlight some common characteristics. Most of the latexes have large particle modes with particles sizes well above 500 nm (typically around 800 nm). The second population is either created in-situ, using a shot of surfactant or a polar monomer, or by the addition of a seed latex at an intermediate point. Then both modes are grown together to reach the desired solids content.

The highest solids content (with low viscosity) obtained so far are reported to be ~73 wt% [68] with a bimodal PSD consisting of 900 and 110 nm particles, using the addition of seeds to create the smaller population, with a viscosity of 300 mPa•s at a shear rate of 20 s^{-1}, and ~77 wt%[69] with PSD of 1400 nm and 200 nm, using a shot of surfactant to create the smaller population, showing a viscosity of 1.5 Pa•s at a shear rate of 20 s^{-1}.

We should call attention here to an innovative strategy that was taken by Schneider et al.[68] to control the relative rate of polymerization in the large particles versus the small particles. These authors used a mixture of monomer and oil soluble initiator at one stage of the process to swell

the large particles before the seed addition to create the small particles. Having the large particles containing oil soluble initiator allowed for the control of the rate at which the large particles grow compared to the small particles. This method provided good control over the PSD by enabling the growth of the large population while keeping the small particles at a constant size for a while. This could be viewed as a tentative to render the small population populations inert while the other polymerizes. After this individual growth step, the process returned to its conventional operation mode where a semi-continuous addition of pre emulsion and water soluble initiator was fed into the reactor and both families of particles would undergo parallel polymerization and growth until the desired solids content was reached.

More recently, Mariz et al.[70] reported the production of HSC latexes with relatively small particles. They obtained 65 wt% with a bimodal PSD consisting of 350 nm and 50 nm particles, using addition of seeds to create the smaller population, with a viscosity of ~250 mPa·s at a shear rate of 20 s^{-1}. In their approach they report an iterative strategy to determine the optimal point in time at which the small seeds should be added to the reactor. In order to use this iterative method, the authors relied on a value determined experimentally corresponding to the ratio of volumetric particle growth rates between the large and the small mode ($k = Rp_{V,L}/Rp_{V,S}$) when polymerized in parallel. These authors claimed a value of $k = 21.36$ and attributed this difference in volumetric growth rate between the large and small particles to the difference in the value of average radicals per particle ($\bar{n}$) in the large and small particles.

These works represent the only two elaborated attempts to have a more precise control of the PSD by controlling the individual rates of polymerization of the distinct population of particles.

2.5 Incorporation of divinylbenzene as cross-linking agent

Following particle nucleation, the growing polymer particles continue to absorb monomer, which is continuously converted into polymer. This happens because most monomers are good

solvents for their own polymer, however the polymer particles dispersed in water are not fully dissolved by the monomer due to the thermodynamic equilibrium that is established between the surface energy of the particle (which increases as the particle absorbs monomer), and the entropy of mixing of small monomer molecules with long chain polymers (which decreases with the concentration of monomer). As a result the term "swelling of particles" is used to describe this phenomenon.

In cross-linked polymer structures, the polymer networks function as elastic forces acting against swelling. The partial molar free energy, $\Delta \overline{G}^*$, of a monomer in the cross-linked polymer particles during swelling is composed of following three contributions:

$$\Delta \overline{G}^* = \Delta \overline{G}_m + \Delta \overline{G}_t + \Delta \overline{G}_{el} \tag{7}$$

where $\Delta \overline{G}_m$, $\Delta \overline{G}_t$ and $\Delta \overline{G}_{el}$ are contributions of monomer-polymer mixing force (osmotic contribution), particle–water interfacial tension force (surface energy contribution), and polymer network elastic-retractile force, respectively.[71]

The partial molar free energy change by the absorption of the monomer by polymer particles developed by Morton et al.[72] accounts for the entropy of mixing (first two terms in brackets on the right hand side-RHS), the enthalpy of mixing (second term in brackets on the RHS) and the interfacial free energy contribution (last term in brackets on the RHS), given as follows:

$$\Delta \overline{G}_{m+t} = RT \left[\ln \phi_1 + \left(1 - \frac{1}{j}\right)\phi_2 + \phi_2^2 \chi + \frac{2V_1\gamma}{r_p RT} \right] \tag{8}$$

where R is the universal constant of gases, T is temperature, ϕ_1 is the volume fraction of the monomer, ϕ_2 is the volume fraction of the polymer, j is the ratio of equivalent number of

molecular segments between the polymer and monomer, χ the monomer-polymer interaction parameter, γ the interfacial tension between the particle and dispersion medium, r_p the radius of the particles and V_1 the molar volume of the monomer.

The elastic free energy change, $\Delta \overline{G}_{el}$ is an entropy term associated with the change in the configuration of the polymer network,[73] and described as follows:

$$\Delta \overline{G}_{el} = RT \frac{V_1 \rho_2}{\overline{Mc}} \left(\phi_2^{1/3} - \frac{\phi_2}{2} \right) \qquad (9)$$

In Equation 9 ρ_2 is the polymer density, $\overline{M}_C$ is the average molecular weight between two cross-links in the network and can be expressed as:

$$\overline{M}_C = M_0 \lambda \qquad (10)$$

where M_0 is equal to the (mean) molecular weight per structural unit, and λ is defined in as the average number of repeated units in the backbone of the polystyrene segments between cross-link junctions is the inverse of the cross-link density q:

$$\lambda = \frac{1}{q} \qquad (11)$$

where the cross-link density, q is defined as the ratio of the number of atoms that may form cross-linking junctions to the total number of atoms in the backbone of the segments that constitute the cross-linked network, given by:

$$q = \frac{r}{(1+r)} \qquad (12)$$

where r is the mole fraction of DVB in the polymer. It can be inferred that for low values of DVB mole fraction (r) the cross-link density (q) has a value very close to r.

Substituting Equations (8) and (9) into (7) yields a general expression to calculate the change in chemical potential during swelling of latex particles as follows:[71]

$$\Delta\overline{G}^* = RT\left[\ln\phi_1 + \left(1 - \frac{1}{j}\right)\phi_2 + \phi_2^2\chi + \frac{2V_1\gamma}{r_p RT} + \frac{V_1\rho_2}{\overline{M}c}\left(\phi_2^{1/3} - \frac{\phi_2}{2}\right)\right] \tag{13}$$

If the latex particle is not cross-linked ($\overline{M}_C \Rightarrow \infty$), Equation (13) is identical to the Morton-Kaizerman-Altier equation (Equation 8). The last term on the RHS of the Equation (13) originates from the elastic free energy. As more and more solvent is absorbed (dissolved) by the polymer, the network is progressively expanded. The chains connecting multifunctional network junction points are forced to assume more elongated, less probable, configurations. Consequently, a decrease in chain configurational entropy is produced by swelling.[73] Hence, as crosslink density increases (decrease of $\overline{M}_C$) or as the polymer swells (decrease of ϕ_2), $\Delta\overline{G}_{el}$ increases (positively), which enhances the energy barrier against swelling.

One of the most important structural parameters characterizing cross-linked polymers is the average molecular weight between cross-links, which is directly related to the cross-link density. Errede[74] studied the swelling of poly(styrene-co-divinylbenzene) in terms of the cross-link density for diverse liquids. The critical cross-link density of the polymer, at or above which the volume of liquid absorbed is nil, for all solvents studied converged statistically to the value of 0.18 ± 0.04 that is to say a molar ratio of DVB of 0.22. This value corresponds to solid hard spheres of polymer that theoretically won't swell in the presence of any solvent. Lowering the

level of the molar ratio of DVB will allow proportionally higher swelling degrees, up to the maximum swelling degree corresponding to that of pure styrene (when no DVB is used).

A very important term to discuss is the particle-water interfacial tension force. As predicted from Morton's Equation 8 and shown by Tauer,[71] the degree of swelling of polymer particles is influenced by the particle size and by the interfacial tension between the oil and water phases. Figure 2-6 illustrates these two points in the obtaining of swelling equilibrium. It should be pointed out that these simulations are for non-cross-linked particles.

The fact that latex particles, with same composition, swell less and less as they get smaller is a fact that will benefit our attempt to decrease the rate of volumetric growth of the small particles in this project. This fact, together with the fact that $\bar{n}$ is also lower for smaller particles and the cross-linking of the particles should make a significant contribution to limit the growth of our small particles. It is also important to note that the lower the level of surfactant, the higher is the interfacial tension and lower will be the degree of swelling of the particles.
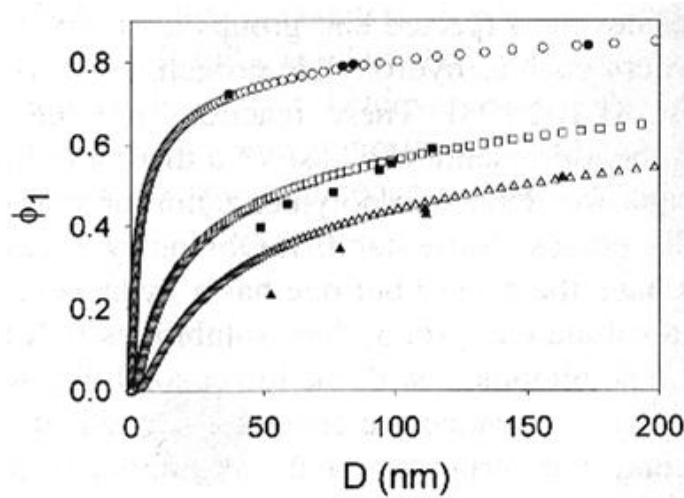
Figure 2-6. Styrene volume fraction (ϕ_1) inside polystyrene swollen particle size (D) at equilibrium swelling. The open symbols are calculated data according to Equation (8) with $\chi = 0.45$, 25°C and $\gamma = 3$ mN m^{-1} for ($\circ$), $\gamma = 30$ mN m^{-1} for ($\square$) and $\gamma = 70$ mN m^{-1} for ($\triangle$). Solid symbols are experimental results. Reproduced from Tauer 2001[71] with permission. Copyright Marcel Dekker 2001.

39

2.6 Incorporation of carboxylic monomers in emulsion polymerization

Carboxylic monomers are typically incorporated in emulsion polymerization formulations to improve colloidal stability of latexes used for instance as bonding agents in latex-based paper coating and surface treatments for paper products. Additionally, carboxylic monomers enhance the adhesive characteristics of the latexes on different substrates, improve mechanical properties of the films formed from polymer latexes, improve compatibility with pigments and provide pendant functional groups which impart more chemical reactivity and/or colloidal reactivity to the latex polymer particle.[75-77]

Among the functional carboxylic monomers used in latex production, acrylic acid (AA), methacrylic acid (MA), itaconic acid (IA) and fumaric acid (FA) are the most common. Numerous studies have been performed in the incorporation of acids, especially concerning the use of AA,[78-80] and MAA,[79, 81-83] and fewer fundamental studies have been done concerning the behaviour of IA,[75, 84-88] and FA [88, 89] in emulsion polymerization.

Common carboxylic acids are partially or totally soluble in water, and their partitioning between the organic phase and the continuous phase depends on the degree of ionization of the functional monomer, which is in turn a function of pH. There are three possible locations these carboxylic groups can be found: buried in the particle, on the surface of the particle or in the serum as hydrosolubles. It is evident that for the incorporation of functional monomers to be more effective (as a means to improve latexes' stabilization, as well as to enhance the improvements provided to the polymer material), they should be present mostly on the surface of the particles. The way the carboxylic acids distribute among these three locations during the polymer synthesis will depend to some extent on their water solubility, on the medium pH and the way these monomers are added during the emulsion polymerization.

One of the main difficulties of working with such functional monomers is related to controlling the incorporation of these monomers at the desired location in the particles. It has been shown that the partitioning coefficient between oil and water (o/w) of carboxylic monomers decreases considerably as the pH is increased.[81, 90, 91] At high pHs the carboxylic acid is dissociated and has a negative charge which increases its relative polarity and therefore its interaction with water, while decreasing its attraction for non-polar species such as styrene. AA is incorporated more efficiently when all carboxylic groups are protonated, that is, at pH below its pKa (4.25 in the case of AA).[78, 79, 81, 91] In addition, when working with anionic surfactants, the low pH reduces the electrostatic repulsion between charged (anionic) AA oligoradicals and the particle's surfaces, which facilitates the entry of AA-containing oligomer radicals into particles.[92] However, it is at higher pHs that the stabilization provided by carboxylic acids located at the surface of the particles is more effective, because the repulsion of charges between different particles prevents their aggregation and coalescence.[93, 94] Thus, the pH of the latex should be brought up to neutrality after the reaction is completed for best stability results.

According to Sarobe et al.,[95] and Slawinski et al.,[79, 96] the seed process or two step process, with the addition of carboxylic monomers either semi-continuously or in shots in the later stages of the process is preferred to obtain latexes functionalized with a high density of carboxylic groups at the particles' surface. In a recent study, Yuan et al.[97-99] showed that water-soluble oligomers formed during the emulsion polymerization of styrene-butadiene-acrylic acid have different roles during the course of the synthesis. During the particle nucleation period, they contribute to the generation of more particles, thus increasing the rate of polymerization. During the particle growth, watersoluble oligomers will stabilize the particles by radical entry enhancing the adsorption before the critical saturation surface coverage (CSSC) is reached. At surface coverages above the CSSC, the oligomers will contribute to the formation of water-soluble

polymers with high AA content. Yuan et al.[99] also proposed that these water-phase oligomers might cause the flocculation of the latex particles by the formation of hydrogen bonds between the particles. Therefore, the incorporation of AA may be a delicate process, especially when dealing with high solid content latexes and extremely small particles.

2.7 Overview

As discussed above, no one has tried bimodal latexes with such small particles, but we saw that the smaller the particles, the harder it is to achieve high solids at low viscosity. As was presented in Chapter 1 and discussed in section 2.5, we propose here an innovative approach to produce these latexes, by the inertization the family of small particles and grow the family large particles to increase solids content and achieve the desired Dp_L/Dp_S ratio.

An important and challenging aspect of this thesis is the production of extremely small particle size latex with reasonable surfactant concentrations and high solids content. This is an important step for this project since we have to learn how to efficiently make polymer particles smaller than 30 nm to be able to produce the bimodal latex with these PSD constraints. The characterization of the small particles, including their swelling behaviour at different levels of cross-linking agent in their composition is also another fundamental aspect to understand how these particles respond to the inertization process.

The production of the bimodal latex will require the development of a process to produce the large particles latex and then introduce the small particles generation step to it. The addition of the small particles will likely influence the production of the large particles and therefore actions will have to be taken to account adjust the process to accommodate both populations of particles.

Finally, as was presented, the incorporation of AA to the bimodal latex is better during the late stages of polymerization, so this will be done once the latex preparation procedure has been

understood and will then be added to the latest steps in the process. This process development will be tested in this sequence in the Chapters that follow.

References

1. Gooch, J. W. *Lead-Based Paint Handbook;* Plenum Press: New York, 1993.

2. Tsavalas, J. G. A molecular level investigation of hybrid miniemulsion polymerization, Georgia Institute of Technology, 2001.

3. Wicks, Z. W.; Jones, F. N.; Pappas, S. P.; Wicks, D. A. *Organic Coatings: Science and Technology;* Wiley Interscience: Toronto, 2007.

4. Ruhlmann, D. *Double Liaison--Phys., Chim.Econ.Peint.Adhes.* **1999**, 56-63.

5. Schmidt-Thummes, J.; Schwarzenbach, E.; Lee, D. I. Applications in the Paper Industry. In *Polymer dispersions and their industrial applications;* Urban, D., Takamura, K., Eds.; Wiley-VCH: Weinheim, 2002.

6. Dodgson, D. V. Surfactants and emulsion polymerization: an industrial perspective. In *Surfactants in Polymers, Coatings, Inks and Adhesives;* Karsa, D. R., Ed.; Blackwell Publishing & CRC Press LLC: Boca Raton, 2003.

7. Vaha-Nissi, M.; Lahti, J.; Savolainen, A.; Rissa, K.; Lepisto, T. *Appita J.* **2001**, *2,* 106-115.

8. Arshady, R. *Colloid Polym. Sci.* **1992**, *8,* 717-732.

9. Padget, J. C. *J.Coat.Technol.* **1994**, *839,* 89-105.

10. De La Cal, J.; Leiza, J. R.; Asua, J. M.; Butte, A.; Storti, G.; Morbidelli, M. Emulsion Polymerization. In *Handbook of Polymer Reaction Engineering;* Meyer, T., Keurentjes, J., Eds.; Wiley-VCH: Weinheim, 2005; Vol. 1.

11. Lovell, P. A.; El-Aasser, M. S. In *Emulsion Polymerization and Emulsion Polymers.* John Wiley & Sons: Chichester, 1997.

12. Gilbert, R. G. *Emulsion Polymerization, a mechanistic approach;* Academic Press: London, 1995.

13. Candau, F. Polymerization in Microemulsions. In *Polymerization in organized media;* Paleos, C. M., Ed.; Gordon and Breach Science Publishers: Philadelphia, 1992.

14. Antonietti, M.; Basten, R.; Lohmann, S. *Macromol. Chem. Phys.* **1995**, *2,* 441-466.

15. Landfester, K. *Annu.Rev.Mater.Res.* **2006**, 231-279.

16. Mittal, V. In *Miniemulsion Polymerization Technology.* Section Title: Chemistry of Synthetic High Polymers; 2010; pp 311.

17. Schork, F. J.; Luo, Y.; Smulders, W.; Russum, J. P.; Butte, A.; Fontenot, K. *Adv.Polym.Sci.* **2005***, Polymer Particles,* 129-255.

18. Odian, G. *Principles of Polymerization;* Wiley-Interscience: 2004.

19. Chern, C. *Principles and applications of emulsion polymerization;* Wiley: Hoboken, N.J., 2008.

20. Dunn, A. S. Harkins, Smith-Ewart and Related Theories. In *Emulsion Polymerization and Emulsion Polmyers;* Lovell, P. A., El-Aasser, M. S., Eds.; John Wiley and Sons: 1997.

21. Feeney, P. J.; Napper, D. H.; Gilbert, R. G. *Macromolecules* **1987***, 11,* 2922-2930.

22. Prince, L. M. In *Microemulsions, Theory and Practice.* Academic Press, Inc.: New York, 1977.

23. Stoffer, J. O.; Bone, T. *Journal of Dispersion Science and Technology* **1980***, 1,* 37-54.

24. Stoffer, J. O.; Bone, T. *J. Polym. Sci. Polym. Chem. Ed.* **1980***, 8,* 2641-2648.

25. Pavel, F. M. *Journal of Dispersion Science and Technology* **2004***, 1,* 1-16.

26. Chow, P. Y.; Gan, L. M. *Advances in Polymer Science* **2005**, 257-298.

27. O'Donnell, J.; Kaler, E. W. *Macromol. Rapid Commun.* **2007**, *14,* 1445-1454.

28. Candau, F.; Pabon, M.; Anquetil, J. *Colloids Surf., A* **1999**, *1-3,* 47-59.

29. Capek, I. *Nanocomposite Structures and Dispersions. Science and Nanotechnology - Fundamental Principles and Colloidal Particles.* Elsevier: Amsterdan, 2006; Vol. 23.

30. Puig, J. E.; Mendizábal, E.; Delgado, S.; Arellano, J.; López-Serrano, F. *Comptes Rendus Chimie* **2003**, *11-12,* 1267-1273.

31. Gan, L. M.; Chew, C. H.; Friberg, S. E. *J.Macromol.Sci., Chem.* **1983**, *5,* 739-756.

32. Gan, L. M.; Chew, C. H.; Lye, I.; Ma, L.; Li, G. *Polymer* **1993**, *18,* 3860-3864.

33. Morgan, J. D.; Lusvardi, K. M.; Kaler, E. W. *Macromolecules* **1997**, *7,* 1897-1905.

34. Morgan, J. D.; Kaler, E. W. *Macromolecules* **1998**, *10,* 3197-3202.

35. Candau, F.; Leong, Y. S.; Fitch, R. M. *J. Polym. Sci. Polym. Chem. Ed.* **1985**, *1,* 193-214.

36. de Vries, R.; Co, C. C.; Kaler, E. W. *Macromolecules* **2001**, *10,* 3233-3244.

37. Xu, X. J.; Gan, L. M. *Current Opinion in Colloid & Interface Science* **2005**, *5-6,* 239-244.

38. Kong, X.; Wu, Q.; Hu, W.; Wang, Z. *J.Polym.Sci., Part A: Polym.Chem.* **2008**, *13,* 4522-4528.

39. Dan, Y.; Yang, Y.; Chen, S. *J Appl Polym Sci* **2002**, *14,* 2839-2844.

40. Ming, W.; Jones, F. N.; Fu, S. *Polym.Bull.(Berlin)* **1998**, *6,* 749-756.

41. Ming, W.; Jones, F. N.; Fu, S. K. *Macromol.Chem.Phys.* **1998**, *6,* 1075-1079.

42. He, G.; Pan, Q.; Rempel, G. L. *Macromol.Rapid Commun.* **2003**, *9,* 585-588.

43. Xu, X. J.; Chew, C. H.; Siow, K. S.; Wong, M. K.; Gan, L. M. *Langmuir* **1999**, *23,* 8067-8071.

44. He, G.; Pan, Q. *Macromol.Rapid Commun.* **2004**, *17,* 1545-1548.

45. Barrere, M.; Capitao da Silva, S.; Balic, R.; Ganachaud, F. *Langmuir* **2002**, *3,* 941-944.

46. Roy, S.; Devi, S. *Polymer* **1997**, *13,* 3325-3331.

47. Aguiar, A.; Gonzalez-Villegas, S.; Rabelero, M.; Mendizabal, E.; Puig, J. E.; Dominguez, J. M.; Katime, I. *Macromolecules* **1999**, *20,* 6767-6771.

48. Rabelero, M.; Zacarias, M.; Mendizabal, E.; Puig, J. E.; Dominguez, J. M.; Katime, I. *Polym.Bull.(Berlin)* **1997**, *6,* 695-700.

49. Hermanson, K. D.; Kaler, E. W. *Macromolecules* **2003**, *6,* 1836-1842.

50. Gao, J.; Penlidis, A. *Prog.Polym.Sci.* **2002**, *3,* 403-535.

51. Ruckenstein, E. *J. Dispersion Sci. Technol.* **1981**, *1,* 1-25.

52. Guyot, A.; Chu, F.; Schneider, M.; Graillat, C.; McKenna, T. F. *Prog.Polym.Sci.* **2002**, *8,* 1573-1615.

53. Ai, Z.; Deng, R.; Zhou, Q.; Liao, S.; Zhang, H. *Adv. Colloid Interface Sci.* **2010**, *1,* 45-59.

54. Boutti, S. Synthesis of High Solid Content Latexes, Universite Claude Bernard - Lyon 1, Lyon, France, 2002.

55. Schneider, M. Etude de procedes de synthese de latex multipopules a haut extratit sec, Universite Claude Bernard Lyon I, France, 2000.

56. Schneider, M.; Claverie, J.; Graillat, C.; McKenna, T. F. *J Appl Polym Sci* **2002**, *10,* 1878-1896.

57. Hao, T.; Riman, R. E. *J Colloid Interface Sci* **2006**, *1,* 374-377.

58. Evans, D. F.; Wennerström, H. *The colloidal domain : where physics, chemistry, biology, and technology meet;* Wiley-VCH: New York, 1999.

59. Schneider, M.; Graillat, C.; Guyot, A.; McKenna, T. F. *J Appl Polym Sci* **2002***, 10,* 1897-1915.

60. Lopez, A.; Chemtob, A.; Milton, J. L.; Manea, M.; Paulis, M.; Barandiaran, M. J.; Theisinger, S.; Landfester, K.; Hergeth, W. D.; Udagama, R.; McKenna, T.; Simal, F.; Asua, J. M. *Ind Eng Chem Res* **2008***, 16,* 6289-6297.

61. Sadler, Y. L.; Sim, K. G. *Chemical Engineering Progress* **1991***, 3,* 68-71.

62. Greenwood, R.; Luckham, P. F.; Gregory, T. *J. Colloid Interface Sci.* **1997***, 1,* 11-21.

63. Farris, R. J. *Trans. Soc. Rheol.* **1968***, 2,* 281-301.

64. Boutti, S.; Graillat, C.; McKenna, T. F. *Polymer* **2005***, 4,* 1223-1234.

65. Chong, J. S.; Christiansen, E. B.; Baer, A. D. *J Appl Polym Sci* **1971***, 8,* 2007-2021.

66. Peters, A. C. I. A.; Overbeek, G. C.; Buckmann, A. J. P.; Padget, J. C.; Annable, T. *Progress in Organic Coatings* **1996***, 1-4,* 183-194.

67. Ouzineb, K.; Graillat, C.; McKenna, T. F. *J Appl Polym Sci* **2005***, 3,* 745-752.

68. Schneider, M.; Graillat, C.; Guyot, A.; Betremieux, I.; McKenna, T. F. *J Appl Polym Sci* **2002***, 10,* 1935-1948.

69. Boutti, S.; Graillat, C.; McKenna, T. F. *Polymer* **2005***, 4,* 1211-1222.

70. Mariz, I. d. F. A.; Millichamp, I. S.; de la Cal, J. C.; Leiza, J. R. *Prog. Org. Coat.* **2010***, 3,* 225-233.

71. Tauer, K. Emulsion Polymerization. In *Reactions and synthesis in surfactant systems;* Texter, J., Ed.; Marcel Dekker: New York, 2001; pp 429-453.

72. Morton, M.; Kaizerman, S.; Altier, M. W. *J. Colloid Sci.* **1954**, 300-312.

73. Flory, P. J. *Principles of polymer chemistry.* Cornell University Press: Ithaca, 1953.

74. Errede, L. A. *J Appl Polym Sci* **1986***, 6,* 1749-1761.

75. Ceska, G. W. *J Appl Polym Sci* **1974***, 8,* 2493-2499.

76. Blackley, D. C. *Polymer latices : science and technology;* Chapman & Hall: London; New York, 1997.

77. Sakota, K.; Okaya, T. *J Appl Polym Sci* **1977***, 4,* 1035-1043.

78. Vorwerg, L.; Gilbert, R. G. *Macromolecules* **2000***, 18,* 6693-6703.

79. Slawinski, M.; Schellekens, M. A. J.; Meuldijk, J.; Van Herk, A. M.; German, A. L. *J Appl Polym Sci* **2000***, 7,* 1186-1196.

80. Shoaf, G. L.; Poehlein, G. W. *J Appl Polym Sci* **1991***, 5,* 1213-1237.

81. Santos, A. M. D.; Mckenna, T. F.; Guillot, J. *J Appl Polym Sci* **1997***, 12,* 2343-2355.

82. Tang, J.; Dimonie, V. L.; Daniels, E. S.; Klein, A.; El-Aasser, M. S. *J Appl Polym Sci* **2000***, 3,* 644-659.

83. Guillaume, J. L.; Pichot, C.; Guillot, J. *J.Polym.Sci., Part A: Polym.Chem.* **1988***, 7,* 1937-1959.

84. Fordyce, R. G.; Ham, G. E. *J. Am. Chem. Soc.* **1947**, 695-696.

85. Vijayendran, B. R. *J Appl Polym Sci* **1979***, 3,* 893-901.

86. Lock, M. R.; El-Aasser, M. S.; Klein, A.; Vanderhoff, J. W. *J Appl Polym Sci* **1991***, 4,* 1065-1072.

87. Vaclavova, E.; Hrivik, A.; Chrastova, V. *Makromol. Chem.* **1992***, 9,* 2243-2250.

88. Oliveira, M. P.; Giordani, D. S.; Santos, A. M. *Eur.Polym.J.* **2006***, 5,* 1196-1205.

89. Sakota, K.; Okaya, T. *J Appl Polym Sci* **1976***, 7,* 1745-1752.

90. Santos, A. M.; Guillot, J.; Mckenna, T. F. *Chem. Eng. Sci.* **1998**, *12,* 2143-2151.

91. Greene, B. W. *J. Colloid Interface Sci.* **1973**, *2,* 449-461.

92. Coen, E. M.; Lyons, R. A.; Gilbert, R. G. *Macromolecules* **1996**, *15,* 5128-5135.

93. Reynhout, X. E. E.; Hoekstra, L.; Meuldijk, J.; Drinkenburg, A. A. H. *J.Polym.Sci., Part A: Polym.Chem.* **2003**, *19,* 2985-2995.

94. Reynhout, X. E. E.; Beckers, M.; Meuldijk, J.; Drinkenburg, B. A. H. *J.Polym.Sci., Part A: Polym.Chem.* **2005**, *4,* 726-732.

95. Sarobe, J.; Forcada, J. *Colloid Polym. Sci.* **1996**, *1,* 8-13.

96. Slawinski, M.; Meuldijk, J.; Van Herk, A. M.; German, A. L. *J. Appl. Polym. Sci.* **2000**, *4,* 875-885.

97. Yuan, X.; Dimonie, V. L.; Sudol, E. D.; El-Aasser, M. S. *Macromolecules* **2002**, *22,* 8346-8355.

98. Yuan, X.; Dimonie, V. L.; Sudol, E. D.; Roberts, J. E.; El-Aasser, M. S. *Macromolecules* **2002**, *22,* 8356-8370.

99. Yuan, X.; Dimonie, V. L.; Sudol, E. D.; El-Aasser, M. S. *J. Appl. Polym. Sci.* **2003**, *8,* 1988-1999.

Chapter 3

Small particles population – Starved-feed microemulsion

polymerization

3.1 Abstract

Starved feed semi-continuous microemulsion polymerization of styrene was investigated. The influence of the type (SDS or Dowfax 2A1) and concentration of anionic surfactant on the final particle size of latex made by the polymerization of microemulsions of styrene was studied. In addition, the influence of 1-pentanol and acrylic acid as cosurfactants was examined. Latexes with 20% solids content and polymer to surfactant ratio of 22 were produced, with a particle diameter of 42 nm and very low polydispersity indexes. Smaller particles are produced using SDS than Dowfax 2A1 for the same weight fraction of surfactant; however, similar particle sizes were obtained with the same molar concentrations of SDS and Dowfax 2A1. Further shot additions of monomer increased solids level as high as 40 wt% and polymer to surfactant ratios greater than 40, with particles remaining monodisperse with average diameter smaller than 60 nm.
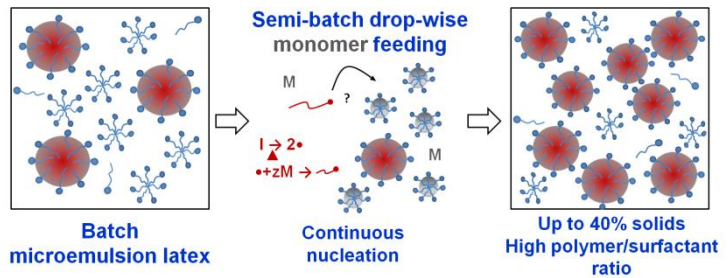
3.2 Introduction

In this Chapter we investigate the production of small particle size latexes using a modified microemulsion approach to increase the solids content of the latex. In addition, the need for low surfactant concentrations is a constraint imposed by the final product end use criteria; therefore the objective is to use the lowest surfactant concentration as possible.

Unlike conventional emulsion or miniemulsion polymerization, microemulsions form spontaneously without the need for intense mixing upon combining surfactant with water and

monomer. The system can be polymerized to produce small latex particles (typically less than 50 nm) with high molecular weight. However, microemulsions require much greater amounts of surfactant to stabilize the system than emulsions; typically 7-15 wt% surfactant is required to solubilise a monomer content of less than 10 wt%.[1-4] This high surfactant to monomer ratio is a significant disadvantage for commercial implementation. Semi-continuous starved-feed microemulsion polymerization processes have been successfully used to increase the amount of polymer produced for a given amount of surfactant.[2, 5, 6]

Table 3-1 summarized results found in the literature that report on the synthesis of polystyrene (PS) nanoparticles by microemulsion polymerization. The highest polymer to surfactant ratio (this ratio is defined as the mass of polymer per unit mass of surfactant) reported in the literature for styrene microemulsion formulations to date is 15. This result was reported by Xu and coworkers,[7] who synthesized 16% solids content (SC) PS latex with 78 nm particle size using a mixture of cetyltrimethylammonium bromide (CTAB) and a polymerizable nonionic surfactant. In a previous work, Xu et al.[8] synthesized a PS latex with 13% solids content using different alkyltrimetylammonium bromide cationic surfactants The highest polymer-to-surfactant ratio obtained in their report was 13 yielding particles with diameter of 52 nm. Ming et al.[9] synthesized PS microlatexes with sodium dodecyl sulfate (SDS) and obtained a polymer to surfactant ratio of 6.7 using 2% 1-pentanol with respect to the monomer mass as cosurfactant and reported a particle size of 15 nm in a 10% solids content latex. Kong et al.[10] reported a PS latex with SDS and 2 wt% n-butanol cosurfactant with respect to the mass of monomer. They obtained 18 wt% solids content latex with 28 nm particles and a polymer to surfactant ratio of 5.1. Rabelero et al.[11] produced PS microlatex using dodecyltrimethylammonium bromide (DTAB) as surfactant, obtaining a polymer to surfactant ratio of 4.7 with a particle size of 45 nm and solids content of 38 wt%.

51

Table 3-1. Works found in the literature reporting semi-continuous microemulsion polymerization of styrene.

| Author | Surfactant | | | | Cosurfactant | | | Dp (nm)[d] | SC (%)[e] |
	Type	wt% (total)[a]	wt% (mon.)[b]	Pol/Sur[c]	Type	wt% (total)[a]	wt% (mon.)[b]		
Xu et al.[7]	CTAB/PEO-R-MA-40	1	6.6	15.2	-	-	-	78	16
Xu et al.[8]	CTAB	1	7.6	13.2	-	-	-	52	13
Ming et al.[9]	SDS	1.5	15	6.7	1-Pentanol	0.2	2	15	10
Kong et al.[10]	SDS	2.9	20	5.0	n-Butanol	0.3	2	28	18
Rabelero et al.[11]	DTAB	8.8	21	4.8	-	-	-	45	38

[a] Weight percent relative to the total formulation mass; [b] Weight percent relative to monomer mass; [c] Polymer to surfactant ratio, defined as the mass of polymer per unit mass of surfactant; [d] Z-average diameter of particle; [e] Mass fraction of solids.

As described above, cosurfactants (weakly amphiphilic molecules, commonly short-chain alcohols) are sometimes used in microemulsion formulations. Incorporation of cosurfactants into the adsorbed layer of an anionic surfactant (i.e. SDS) around an oil droplet greatly reduces the electrostatic repulsion force between two anionic molecules, minimizes the oil-water interfacial tension, and enhances flexibility of interfacial membrane, which is greatly beneficial for the formation and stabilization of microemulsions.[3, 12, 13]

In this work we present the synthesis and characterization of PS latexes by multiple additions/drop-wise semi-continuous microemulsion polymerization. The anionic surfactants used were SDS and sodium (branched) dodecyl diphenyl oxide disulfonate (Dowfax 2A1 or Calfax DB-45). The objectives of this work were: (a) to produce microemulsions with high polymer to surfactant ratios and particle sizes as small as possible; (b) to develop an efficient procedure for doing so; (c) to compare SDS and Dowfax 2A1 as surfactants; and (d) to explore any possible benefits of using cosurfactants. A range of surfactant concentration was studied to determine its influence on the final particle size of PS latexes. In addition, the influence of pentanol and acrylic acid as cosurfactants to reduce the amount of surfactant required was studied.

3.3 Experimental

Materials. Styrene (ReagentPlus, ≥99%) and acrylic acid (99% pure) from Sigma-Aldrich, 1-pentanol (99%, extra pure), potassium persulfate (KPS, 99+%), sodium dodecyl sulphate (SDS, solid powder 99% grade) from Acros Organics, and sodium (branched) dodecyl diphenyl oxide disulfonate (Dowfax 2A1 or Calfax DB-45) solution surfactant with 45.7 wt.% actives from Pilot Chemical Company (USA), were used as received. All water was deionized using a Millipore - Synergy Ultrapure Water System.

Polymerizations. Polymerizations were carried out in a 3-L jacketed glass reactor equipped with a reflux condenser, nitrogen inlet, anchor stirrer and valve in the bottom for sampling. All

polymerizations were carried out at 80°C. The initial formulations used are provided in Table 3-2, with a total initial mass of 750g before semi-continuous addition of monomer.

Table 3-2. Initial formulations for experiments.

Components	wt.%
Monomer mixture	0.5
SDS or Dowfax 2A1	1-7.5
KPS	0.1
DI water	91.9-98.4

For the experiments where cosurfactants were used, the monomer mixture has a composition of 98 wt% styrene and 2 wt% cosurfactant, either 1-pentanol or acrylic acid. The water, surfactant and monomer mixture were added to the reactor under nitrogen atmosphere, and left under agitation while the temperature was raised using a controlled temperature water bath. The required mass of initiator was dissolved in a small aliquot of water (25 mL) and the initiator solution was added to the reactor when temperature reached 80°C. At this moment the reaction was considered started. A small nitrogen flux was used throughout the entire experiment. For *Stage 1* reactions, additional monomer mixture (160 g) was fed into the reactor in two different fashions: (i) multiple addition mode in which 43 separate shots were injected every 7.5 minutes, with the mass of monomer added calculated to keep the ratio of unreacted styrene to water at approximately 0.005 to prevent formation of monomer droplets; or (ii) infusion pump addition at a rate of approximately 0.5 ml/min. Very similar results were obtained using the two methods. The polymerization was carried out under starved feed conditions, with instantaneous conversion verified to be above 90% during the semi-batch process. These formulations have a final solids content of about 20 wt%. For higher solids content *Stage 2* experiments, two extra monomer mixture aliquots were added to the reactor. The first monomer shot was made 7.5 minutes after

54

the end of *Stage 1* and the second 30 minutes after.

Samples were withdrawn every 30 minutes, beginning 7.5 minutes after the start of the reaction, for conversion and particle size determinations. In the last 30 minutes of reaction the temperature was raised to 85°C as an attempt to minimize residual monomer.

Characterizations. A K12 Kruss tensiometer was used for the interfacial tension measurement (Wilhelmy plate method). Interfacial tension values were determined from the measured force as follows:

$$\gamma = \frac{F}{P \cdot \cos \Theta} \tag{14}$$

where γ is the interfacial tension, F is the measured force, P is the wetted length of the plate, and Θ is the contact angle between the tangent at the wetting line and the plate surface. To use Equation (14) for the determination of interfacial tension, the contact angle has to be zero so that $\cos \Theta = 1$ (total wetting). The roughened and cleaned platinum plate of known geometry hung vertically is used to fulfill this requirement, since the contact angle is zero for most liquids against platinum. The sample vessel was filled with the oil phase and the plate was immersed completely. The oil phase was removed, the aqueous phase was inserted and the plate was dipped automatically by the equipment. When the equipment was ready, the oil phase was then carefully inserted back to cover the plate. The average and standard deviation were obtained from a series of 10 measurements for each determination.

Gravimetry was employed to determine the conversion of the polymerization. The samples were dried in a forced convection oven at 85°C for 4 hours. Conversion was calculated by the ratio of the solids content at time t and the theoretical solids content, as calculated for total monomer added up to time t. Particle size distribution was determined using Dynamic Light

Scattering (DLS) in a Malvern Zeta-Sizer Nano-ZS instrument. Samples were diluted with a water solution of the surfactants just below the critical micelle concentration (CMC) in order to avoid particle coalescence. The Z-Average particle size and Polydispersity Index (PdI) were obtained from a series of 3 measurements with 5 runs, giving in total 15 runs for each sample at 25°C. According to the instrument manufacturer, the accuracy and precision from this technique, considering a stable and well prepared sample, is expected to be less than 2% deviation. The results obtained from the 3 measurements were observed to have precision within this range. PdI is used to describe the width of the particle size distribution around the average. This parameter is calculated from a Cumulants analysis[14] of the DLS measured intensity autocorrelation function. Indices ≤ 0.100 correspond to reasonably narrow monomodal distribution latexes. The number of particles (Np) is calculated from the average diameter of particles, conversion and the mass of monomer added to the reactor.

3.4 Results and discussions

The evolution of particle size and number of particles for the experiments conducted in *Stage 1* at different surfactant concentrations are shown in Figure 3-1 for Dowfax 2A1 and Figure 3-2 for SDS. The nucleation of new particles occurs throughout the polymerization for all experiments (increasing Np with time), but to a lesser extent as the weight fraction of surfactant is reduced. It can be seen that for the same weight fraction of surfactant, more particles are nucleated with SDS as compared to Dowfax 2A1; correspondingly, the particle size is smaller for the SDS system. The final latexes have conversions above 95%, with low polydispersity indices (PdI), between 0.01 and 0.09, indicating that the latexes are monodisperse.
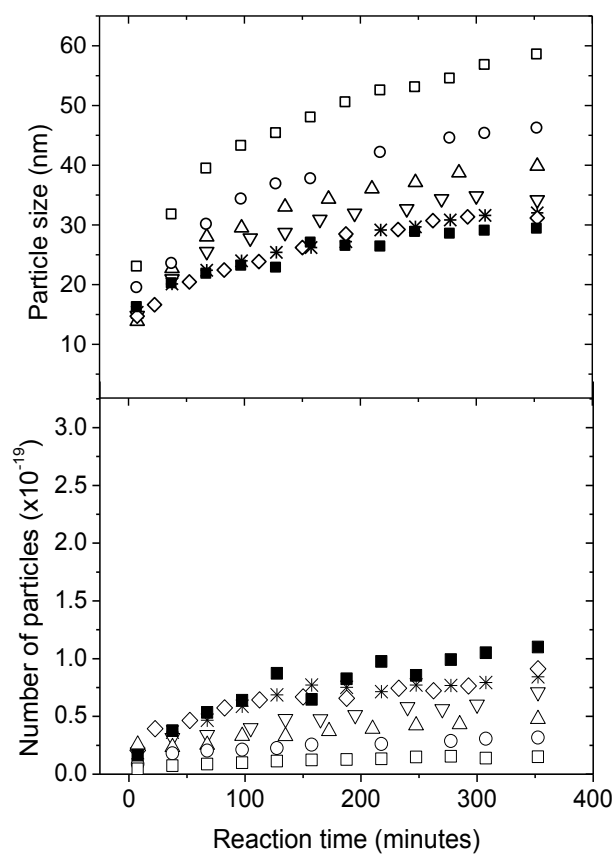
Figure 3-1. Evolution of particle size and number of particles with reaction time for styrene microemulsion experiments using Dowfax 2A1 as surfactant. The weight % concentration corresponds to the initial formulation of the reactor heel: (□) 1 wt%, (○) 2 wt%, (△) 3 wt%, (▽) 4 wt%, (◇) 5 wt%, (✳) 7.5 wt%, (■) 10.4 wt%.
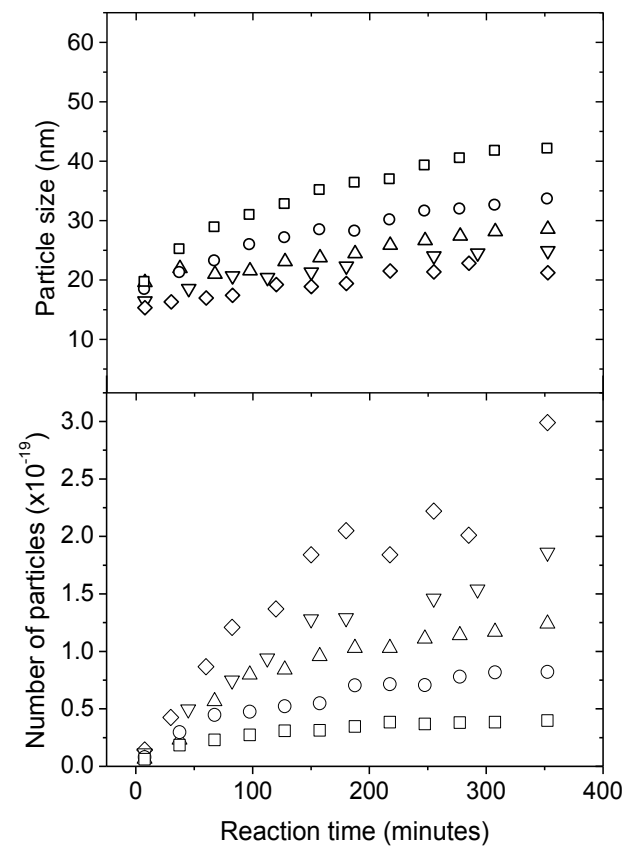
Figure 3-2. Evolution of particle size and number of particles with reaction time for styrene microemulsion experiments using SDS as surfactant. The weight % concentration corresponds to the initial formulation of the reactor heel: (□) 1 wt%, (○) 2 wt%, (△) 3 wt%, (▽) 4 wt%, (◇) 5 wt%.

57

The final particle size as a function of the mass fraction of surfactant is summarized in Figure 3-3 (a). Bearing in mind that these latexes have the same polymer content (ranging from 16 to 18 wt%), the polymer-to-surfactant ratio increases as the concentration of surfactant in the formulation is reduced. With 5 wt% surfactant (final polymer to surfactant ratio of 4.2), particles of 21 nm are produced using SDS, while with 1 wt% surfactant (final polymer to surfactant ratio of 22), particles are 42 nm. For the corresponding Dowfax 2A1 experiments, particle sizes are 30 and 58 nm respectively. The difference in particle sizes with surfactant type could be attributed to the higher availability of SDS molecules for the same weight fraction of surfactant. SDS has a molar mass of 288 g/mol, compared to 576 g/mol for Dowfax 2A1. Thus, for the same weight fraction of surfactant, there are about twice the number of molecules of SDS as compared to Dowfax 2A1, which promotes better stabilization of new nucleated particles and therefore smaller particles. Results are generally presented in terms of mass fraction of surfactant, even though the chemistry and thermodynamics should be considered on a molar basis. When plotted in terms of surfactant molar concentration, the curves of particle size overlap as shown in Figure 3-3 (b). This agreement was also found in the study carried by Vanderhoff et al.[15] that describes the synthesis of 60:40 styrene:butadiene latexes using Dowfax 2A1 and SDS in conventional emulsion polymerization; even though their surfactant concentrations were 2 order of magnitude lower than the present work, the similar (overlapping) curves of particle size as a function of molar concentration were obtained.

However, above a certain concentration of Dowfax 2A1 (above approximately 5 wt% or 0.1 M) particle sizes remain relatively constant at 30 nm, with no further decrease observed with increasing surfactant level. This behaviour is possibly related to the formation of rod-like shaped micelles. At higher concentrations the micelles often grow from spherical to long rod- or thread-like micelles,[16] limiting the number of micelles and reducing the surface area per volume ratio of

the micelle. Further investigation should be performed to determine the exact cause of this behaviour, nonetheless these results show that SDS is a more effective surfactant (per g added) for controlling particle size during styrene microemulsion polymerization.
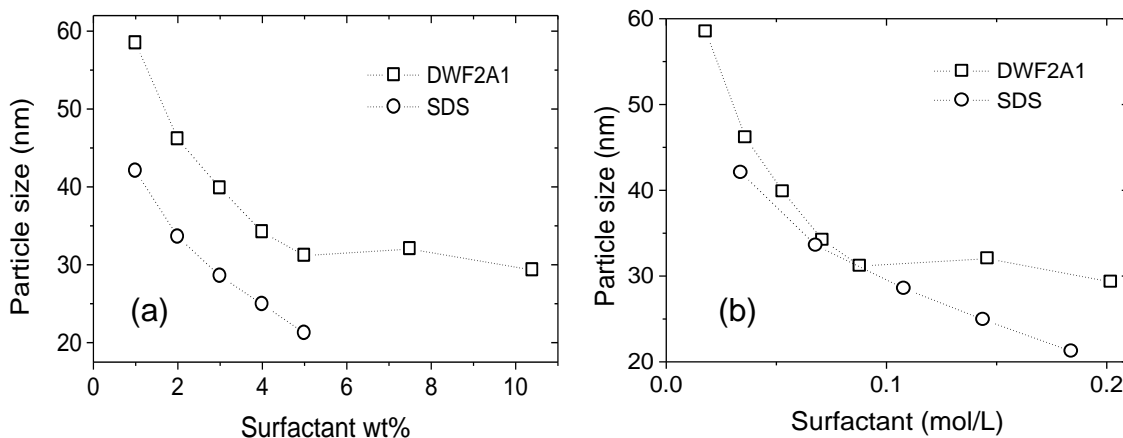
Figure 3-3. Final particle size at the end of polymerization for different concentrations of surfactants. Comparison of SDS and Dowfax 2A1 in terms of (a) weight fraction and (b) molar concentration of surfactant in the initial formulation.

The results presented so far were obtained without cosurfactant. Addition of cosurfactant can contribute to a further increase in polymer to surfactant ratio while keeping particle size small. Figure 3-4 presents the reduction of styrene/water interfacial tension by the addition of 1-pentanol or AA. It can be seen that AA reduces styrene/water interfacial tension as effectively as pentanol does. In addition AA is a more suitable cosurfactant agent than pentanol, in the sense that it is incorporated into the final product.

Figure 3-5 and Figure 3-6 present the evolution of particle size and number of particles with reaction time for experiments with SDS (Figure 3-5) and Dowfax 2A1 (Figure 3-6) at concentration of 1 wt% of the initial formulation using pentanol and AA as cosurfactants at concentration of 2 wt% of the monomer mass. When pentanol is used as cosurfactant with SDS,

there is a slight increase in particle size, and therefore a decrease in number of particles (Figure 3-5) compared to use of AA as cosurfactant. This result could be related to a low solubility of polystyrene in pentanol as observed by Gan and co-workers.[17] These authors verified the regions of styrene and polystyrene water in oil microemulsions stabilized with SDS and compared pentanol to butyl cellosolve (ethylene glycol monobutyl ether) as cosurfactants. The higher solubility of polystyrene in butyl cellosolve provided enhanced stability to the microemulsions compared to the use of pentanol as cosurfactant.
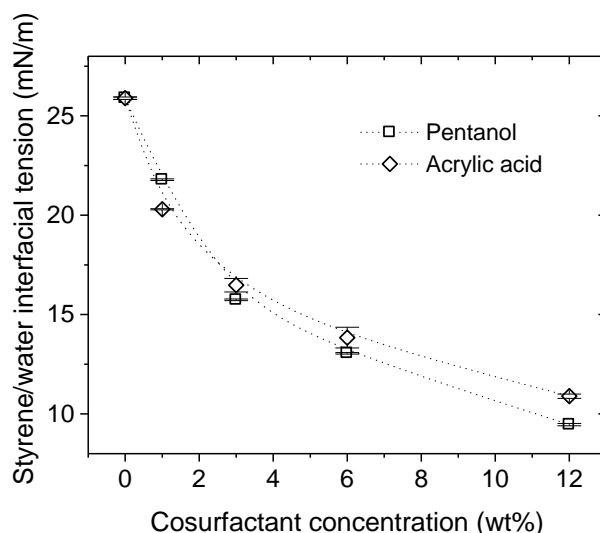
Figure 3-4. Styrene/water interfacial tension reduction as a function of the concentration of 1-pentanol and acrylic acid at 25°C. The concentration is in terms of weight % of the styrene mass. The error bar is the standard deviation calculated from ten measurements.

When pentanol is used as cosurfactant with Dowfax 2A1 (Figure 3-6), some particle destabilization is seen at 50-100 minutes; however, the system seems to recover stability as the semi-batch reaction continues. At the concentration of 2 wt % of the monomer phase, AA does not appear to play a significant role in the reaction kinetics or particle stabilization, for either SDS or Dowfax 2A1. Thus, one should be able to include low levels of AA in the microemulsion

formulation without any detriment.
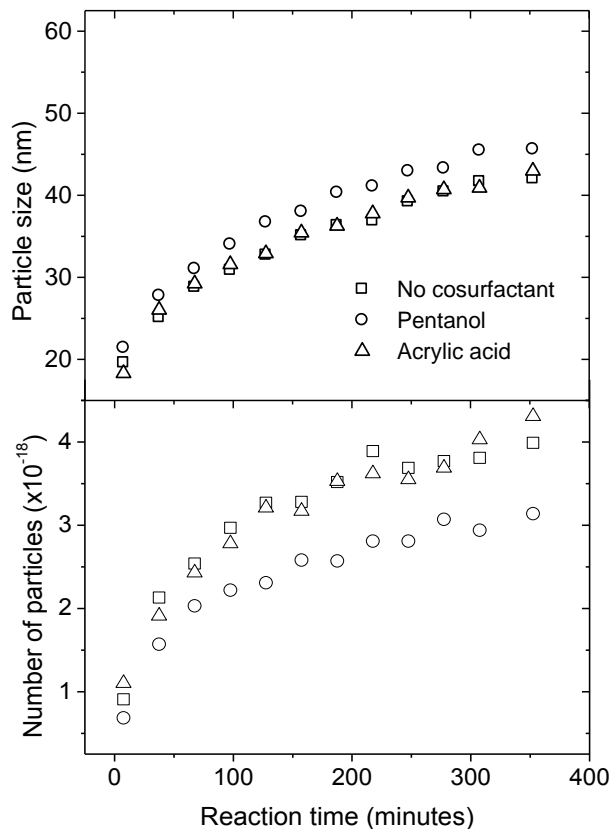
Figure 3-5. Evolution of particle size and number of particles with reaction time for styrene microemulsion experiments with SDS: influence of the cosurfactant type. SDS concentration: 1 wt% of the initial formulation; Cosurfactant concentration: 2 wt% of the monomer mass.

The experiments carried out with cosurfactants were brought to higher solids content during *Stage 2* of the semi-batch polymerization. For these experiments, additional monomer mixture was added at 330 and 360 minutes to bring total solids content from 20 wt% to 30 and 40 wt%, respectively (except for the system SDS/pentanol, which had a solids content of 35 wt%, see Table 3-3). The monomer mixture was added in shots rather than via slow feed, inspired by the observations reported by Kong et al.[10] who determined that the effect of differential feeding on

61

increasing the nucleation of new particles is most pronounced in the initial stage of polymerization under starved-feed addition (*Stage 1*), such that the latter supply of monomer can be added in differential manner or as a one-time addition without greatly affecting nucleation. The "shot addition" at the late stage simplifies the experiment procedure without negative effect on the particle size or polydispersity. The results of Kong et al.[10] suggest that about 30 wt% of the monomer charge should be fed in a differential manner, thus reducing the process time.

Table 3-3 presents formulation parameters and latex characterization for *Stage 2* of these experiments. Instantaneous conversions are higher than 93% for all intermediate samples. For Dowfax 2A1 experiments, final conversions were higher than 99%, however for SDS experiments the final conversions were above 90 and 87% for the systems SDS/AA and SDS/Pentanol respectively, because the experiments were stopped earlier as explained below.

With Dowfax 2A1 the starting diameter of particles (59 nm) was larger than with SDS (~45 nm). Thus, larger particles are produced in the *Stage 2* reaction and solids content (SC) could be increased up to 40% at still fluid viscosities. The final polymer/surfactant ratio obtained for the experiments using Dowfax 2A1 is greater than 60. With SDS, we were able to bring the solids content up to about 30 wt% and a polymer to surfactant ratio of about 40; these latter experiments were stopped due to the increased viscosity. It should be noted that viscosity is the limiting factor with regard to increasing solids content, especially for such small particles. The maximum solids volume fraction of a latex is decreased as the particle size is reduced, due to the increase in volume fraction of the stabilizing layer surrounding the particles.[18] Thus, for the same solids content, the viscosity of a latex increases as the particle sizes decreases.
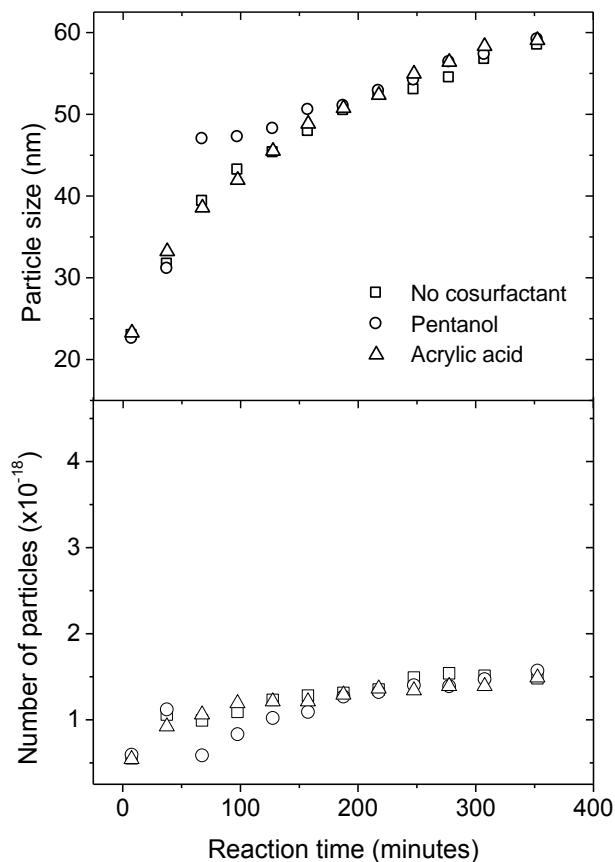
Figure 3-6. Evolution of particle size and number of particles with reaction time for styrene microemulsion experiments with Dowfax 2A1: influence of the cosurfactant type. Dowfax 2A1 concentration: 1 wt% of the initial formulation; Cosurfactant concentration: 2 wt% of the monomer mass.

The final solids content (as high as 40 wt%) and polymer to surfactant ratios (as high as 60) are much higher than those found in previous literature. These results were obtained with cosurfactant in the formulation; however, as the results indicate that cosurfactant does not greatly affect particle stabilization under our reaction conditions, we believe that these results should be achievable in cosurfactant-free systems as well.

Table 3-3. Formulation parameters and latex characterization: *Stage 2* – increase in solids content.

Initial formulation[a]	Monomer mixture addition		Latex characterization[d]				
	Period	Mass (g)	Dp (nm)[e,*]	PdI[f,*]	pol/surf	Np[g]	SC[h]
Dowfax/AA	End of *Stage 1*[b]	162	59.0	0.012	22	1.49	0.19
	After 1st shot[c]	162	70.0	0.046	43	2.97	0.31
	After 2nd shot	-	76.0	0.089	65	2.02	0.40
Dowfax/ Pentanol	End of *Stage 1*[b]	162	59.2	0.020	21	1.57	0.18
	After 1st shot[c]	162	62.5	0.014	39	3.13	0.28
	After 2nd shot	-	75.1	0.043	64	2.09	0.40
SDS/AA	End of *Stage 1*[b]	162	43.0	0.014	22	4.31	0.19
	After 1st shot[c]	162	52.7	0.018	40	8.62	0.28
	After 2nd shot	-	Not fluid				
SDS/Pentanol	End of *Stage 1*[b]	162	45.6	0.037	22	3.14	0.17
	After 1st shot[c]	81	54.5	0.034	38	6.28	0.28
	After 2nd shot	-	58.4	0.085	47	4.44	0.31

[a] surfactant/cosurfactant: surfactant added at 1 wt% of the initial formulation, with 2 wt% cosurfactant relative to monomer; [b] 330 min.; [c] 360 min.; [d] samples were withdrawn in the period indicated, before monomer shots; [e] Z-Average diameter of particles; [f] polydispersity index; [g] number of particles (x10^{18}); [h] mass fraction of solids.

Although, high solids content latexes are achievable, the shot addition of monomer has some minor effects on number of particles and system stabilization. From Table 3-3 it is possible to see that a spike in number of particles is observed when the first shot of monomer is added at about 20% solids content, both for SDS or Dowfax 2A1. This indicates that, even though the particle size increases with solids content, new particles are still being generated. However, with another shot of monomer, the particles seem to experience coalescence in a controlled manner and the number of particles decreases. It is likely that, as the solids content increases, the surface area for stabilization increases and that all free surfactant in the system is used. Thus, collision between particles leads to some coalescence and a decrease in number of particles.
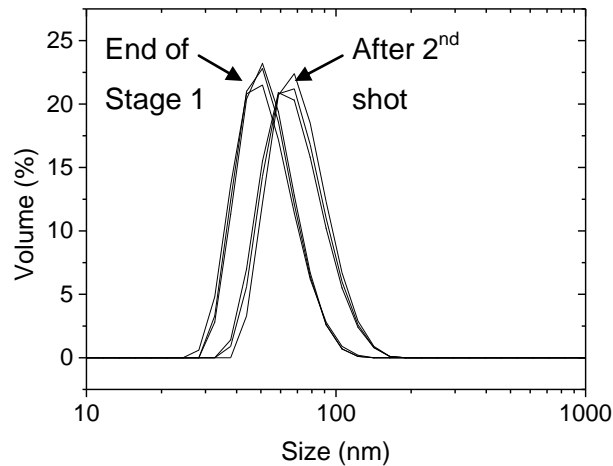
Figure 3-7. Size distribution by volume for samples referent to experiment Dowfax/AA at end of Stage 1 and after the 2nd monomer shot addition. Series of 3 measurements per sample.

Figure 3-7 shows particle size distribution (PSD) curves obtained for samples from the experiment with Dowfax/AA. After 2 shots of monomer the PSD curves shift towards higher values of particle size, without formation of a significant shoulder or tailing of the distribution. This observation is in agreement with the PdI of these latexes, which remain below 0.1 (Table

3-3). Since new particles are being nucleated during the process, Puig et al.[19] suggest a higher PdI should be expected. The results presented here demonstrated that it is possible to have continuous nucleation of particles and narrow monomodal PSD. From the principles of coagulative nucleation[12] it is accepted that when a particle is nucleated it is not necessarily stable, especially true for the small ones. So the fact that new particles are made does not preclude the fact that they can coagulate, among them and among pre-existing particles.

3.5 Conclusions

Polystyrene latexes with 20% solids content and polymer to surfactant ratio up to 22 were produced via drop-wise addition semi-continuous microemulsion polymerization, with particle size of 42 nm and very low polydispersity indices. Smaller particles are produced using SDS compared to Dowfax 2A1 for the same weight fraction of surfactant; however, both surfactants provide similar particle sizes for the same molar concentration.

Solids content were further increased with shot additions of monomer, to produce latexes with 40% solids content using Dowfax 2A1, with average particle sizes of 76 nm and polymer to surfactant ratio higher than 60. With SDS, 30% solids content latexes were produced with particle size smaller than 60 nm and polymer to surfactant ratio higher than 40.

Acrylic acid can be used as cosurfactant in place of 1-pentanol providing equivalent (or slightly improved) particle stabilization and polymerization kinetics. In addition, acrylic acid is commonly used as comonomer in emulsions to improve applications properties, such as for paper coating. More experiments were performed with increased ratio of cosurfactant to monomer to better understand the effect of these molecules on the process and the results will be discussed in Chapter 4.

This Chapter has demonstrated an efficient way of producing stable concentrated latexes

containing small particle sizes and narrow distributions using reduced surfactant concentration. The principle behind this methodology is the fact that the starved feed condition reduces the monomer concentration inside the existing particles, so in the case of a radical entering an existing particle, this particles will not grow significantly because there are few monomers available to be converted. On the other hand, the water phase is constantly saturated with monomer so are the water soluble radicals being decomposed. The combination of these two species and the availability of free micelles in the system enable the continuous nucleation of particles during the process and therefore the production of concentrated latexes with small particle size. This methodology was used to produce the small family of particles as will be presented in Chapters 6 and 7.

References

1. Pavel, F. M. *Journal of Dispersion Science and Technology* **2004**, *1,* 1-16.

2. Hentze, H.; Kaler, E. W. *Curr.Opin.Colloid Interface Sci.; Current Opinion in Colloid & Interface Science* **2003**, *2,* 164-178.

3. Candau, F. Polymerization in Microemulsions. In *Polymerization in organized media;* Paleos, C. M., Ed.; Gordon and Breach Science Publishers: Philadelphia, 1992.

4. Chow, P. Y.; Gan, L. M. *Advances in Polymer Science* **2005**, 257-298.

5. Xu, X. J.; Gan, L. M. *Current Opinion in Colloid & Interface Science* **2005**, *5-6,* 239-244.

6. O'Donnell, J.; Kaler, E. W. *Macromol. Rapid Commun.* **2007**, *14,* 1445-1454.

7. Xu, X. J.; Siow, K. S.; Wong, M. K.; Gan, L. M. *Colloid Polym. Sci.* **2001**, *9,* 879-886.

8. Xu, X. J.; Chew, C. H.; Siow, K. S.; Wong, M. K.; Gan, L. M. *Langmuir* **1999**, *23,* 8067-8071.

9. Ming, W.; Jones, F. N.; Fu, S. K. *Macromol.Chem.Phys.* **1998**, *6,* 1075-1079.

10. Kong, X.; Wu, Q.; Hu, W.; Wang, Z. *J.Polym.Sci., Part A: Polym.Chem.* **2008***, 13,* 4522-4528.

11. Rabelero, M.; Zacarias, M.; Mendizabal, E.; Puig, J. E.; Dominguez, J. M.; Katime, I. *Polym.Bull.(Berlin)* **1997***, 6,* 695-700.

12. Chern, C. *Principles and applications of emulsion polymerization;* Wiley: Hoboken, N.J., 2008.

13. Capek, I. *Adv. Colloid Interface Sci.* **1999***, 1-3,* 253-273.

14. Xu, R. *Particle characterization: light scattering methods;* Kluwer Academic: New York, 2002.

15. Vanderhoff, J. W.; Dimonie, V. L.; El-Aasser, M. S.; Settlemeyer, L. A. *J Appl Polym Sci* **1990***, 7-8,* 1549-1568.

16. Jonsson, B.; Lidman, B.; Holmberg, K.; Kronberg, B. *Surfactants and polymers in aqueous solution;* John Wiley & Sons: New York, 1998.

17. Gan, L. M.; Chew, C. H.; Friberg, S. E. *J.Macromol.Sci., Chem.* **1983***, 5,* 739-756.

18. Schneider, M.; Claverie, J.; Graillat, C.; McKenna, T. F. *J Appl Polym Sci* **2002***, 10,* 1878-1896.

19. Puig, J. E.; Corona-Galvan, S.; Maldonado, A.; Schulz, P. C.; Rodriguez, B. E.; Kaler, E. W. *J. Colloid Interface Sci.* **1990***, 1,* 308-310.

Chapter 4

Small particles population - Microemulsion polymerization

4.1 Abstract

Acrylic acid and pentanol were compared as cosurfactants in oil-in-water microemulsion formulations of styrene using sodium dodecyl sulphate as surfactant. Ternary phase diagrams were mapped out to identify the stability region of formulations containing both components. In addition, the influence of varying the temperature (25 and 70°C) and the ratios of cosurfactant/monomer and monomer/surfactant on the formation of microemulsion were investigated. A larger microemulsion stability region was observed for pentanol compared to acrylic acid for the same molar concentration at room temperature; however, at 70°C the difference was less significant. Latexes with particle diameters ranging from 25 to 35 nm and polymer weight-average molecular weights of the order of 10^6-10^7 g·mol^{-1} were produced upon polymerization of the stable microemulsions. The flux of free radicals influenced the way acrylic acid units were incorporated to the polymer backbone and the homogeneity of the polymer chains. Pentanol also influenced the molecular weight of PS latexes, but this effect was observed to be dependent on the initiator system used.
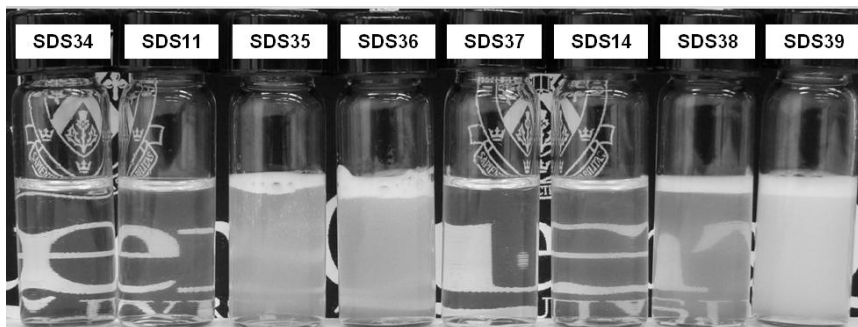
4.2 Introduction

Like in Chapter 3, in this Chapter we investigate the production of small particle size latexes. Here we investigate the role of acrylic acid (AA) and pentanol as cosurfactants in conventional microemulsion polymerization with the objective of increasing the solids content of the latex while keeping particle size as low as possible. The overall objective is to increase the polymer to

surfactant ratio of microemulsion systems while producing extremely small particle size latex.

Microemulsions are thermodynamically stable, optically transparent, isotropic, microheterogeneous dispersions of low viscosity composed of water, oil and surfactant. Microemulsions of vinyl monomers can be polymerized to produce stable polymer particles in the range of 10-50 nm in diameter.[1-4] The first report of microemulsion polymerization dates from 1980.[5] Since then, this new unique microenvironment has received a great deal of attention because of the potential to produce novel materials with different morphologies and polymers with specific properties.[1, 2] Optical transparency, large internal interface area, small size domain and variety of structures are amongst the key features of this technique. These extremely small particles produced via microemulsion polymerization find emerging applications in different areas of technology, such as biomedical materials,[6-8] drug delivery carriers[9, 10] and high performance coatings.[11, 12]

In order to increase the fraction of oil that can be solubilized by the system or reduce the amount of surfactant required for microemulsion formation, cosurfactants are sometimes employed.[13, 14] The role of the cosurfactant is to further decrease interfacial tension between oil and water and enhance flexibility of the interfacial film to promote spontaneous emulsification and provide thermodynamic stability.[2, 3, 15]

Oil-in-water (O/W) microemulsion formulations of styrene (Sty) with anionic surfactants, such as sodium dodecyl sulphate (SDS), have been studied previously using different cosurfactants, such as short chain alcohols (e.g., butanol, pentanol and octanol).[16-18] Nevertheless, apart from the fact that the alcohol has to be stripped out of the final product after synthesis, it is reasonably well accepted that using an alcohol in this manner presents some drawbacks.[1, 3] Incompatibility between the polymer and alcoholic cosurfactants has been shown by Gan and coworkers to limit the stability of microemulsions containing polymers.[19, 20] Discussions on the influence of alcohols

on polymerization rates and final conversions have also been presented. Lower reaction rates and lower conversions were observed with a cationic surfactant when alcohols were present,[21] while with an anionic surfactant no effects were observed.[22] In addition, conflicting results concerning the impact of alcoholic cosurfactants on the molecular weight distribution (MWD) have been reported. Chern and Wu[23] and Johnson and Gulari[24] suggested that pentanol could be acting as a chain transfer agent, decreasing the weight-average molecular weight (M_w) of poly(styrene) (PS) synthesized in microemulsion polymerization; however their results were not conclusive. Puig et al.[21] noticed an increase in the M_w of PS in the presence of alcohols, while Chern and Liu[25] and Herrera et al.[22] observed that increasing the concentration of alcohols reduced the M_w of PS and poly(vinyl acetate) (PVAc) microemulsion polymers respectively.

In order to avoid some of the potential effects of alcohols, alternative cosurfactants have been proposed in the literature. In particular, water soluble monomers (e.g.; acrylamide,[26-29] 2-(methacryloyloxy) ethyltrimethylammonium chloride (MADQUAT),[30-32] hydroxyalkyl methacrylate,[33] acrylic acid (AA)[20, 34-37] and methacrylic acid (MAA)[38] have been used as cosurfactants in microemulsion polymerization formulations. It is well known that the incorporation of carboxylic acids in the polymer particles can be beneficial to products such as dispersions for coating applications;[39-41] moreover, it improves colloidal stabilization[42-44] and provides functionality at the latex particle surface that can be used as sites for specific post synthesis reactions and tailored applications.[45-47] AA has been used as cosurfactant in different microemulsion systems. In fact, when polar monomers such as MMA[36, 37] and vinyl acetate (VAc)[34] were used, homogeneous systems using AA (water-in-oil (W/O), bicontinuous, O/W) were obtained even in absence of surfactant. Gan and Chew[20] reported the use of both AA and pentanol as cosurfactants in methyl methacrylate (MMA)-SDS W/O microemulsion systems, and studied the system stability in the presence of poly(methyl methacrylate) (PMMA) oligomers.

These authors reported that the stability of MMA microemulsions containing a low concentration of PMMA chains was improved by using AA as cosurfactant instead of pentanol and explained this observation by the fact that PMMA is partially soluble in AA and insoluble in pentanol. Puig et al.[48] co-polymerized Sty and AA in O/W microemulsions using the cationic surfactant dodecyltrimethylammonium bromide (DTAB) and verified that a random Sty-AA copolymer was formed. They produced stable latexes containing spherical particles of 21 nm in diameter.

The present work assesses the role of AA and pentanol as cosurfactants in Sty-SDS O/W microemulsion formulations. The study includes the determination of ternary phase diagrams [(Sty+cosurfactant)-SDS-water] using a titration of (Sty+cosurfactant) mixture, the influence of temperature (25 and 70°C) and variation in cosurfactant/monomer ratios on microemulsion stability. To the best of our knowledge, this is the first time O/W phase diagrams are reported using AA as cosurfactant. Moreover, this is the first time AA is directly compared in an O/W microemulsion system to a commonly used alcohol cosurfactant, such as pentanol. Stable microemulsions were polymerized using both cosurfactants, as well as no cosurfactant, to verify of the influence of these species on the microemulsion polymerization of Sty and the products obtained.

4.3 Experimental

Materials. Sty (≥99%), AA (99%), hydrogen peroxide (HPO, 30 wt% solution in water) and ascorbic acid (Asc. Ac., 97+%) were obtained from Sigma-Aldrich, 1-pentanol (99%) and potassium persulphate (KPS, 99+%) from Acros Organics, SDS from MP Biomedical (99.7%), and HPLC grade tetrahydrofuran (THF) was obtained from Fisher Scientific. All chemicals were used as received. Water was deionized using a Millipore – Synergy Ultrapure Water System.

Microemulsion formulations. The effect of the concentration of surfactant and cosurfactant was studied by preparing two series of formulations. The first had constant

surfactant/(monomer+cosurfactant) weight ratio and increasing cosurfactant concentration, according to Table 4-1. The second set of experiments had constant cosurfactant/Sty ratio and the surfactant/(Sty+cosurfactant) weight ratio was varied, according to Table 4-2.

Table 4-1. Compositions of the microemulsion formulations - Variation of the cosurfactant/(monomer+cosurfactant) weight ratio

Sample	SDS[a]	Monomer+cosurf.[a]	Pentanol[b]	AA[b]	Water[a]
SDS8	15	8	-	-	77
SDS9	15	8	2	-	77
SDS10	15	8	4	-	77
SDS11	15	8	8	-	77
SDS15	15	8	12	-	77
SDS12	15	8	-	2	77
SDS13	15	8	-	4	77
SDS14	15	8	-	8	77
SDS16	15	8	-	12	77

[a] wt% of total solution; [b] wt% of monomer+cosurfactant mixture

Formulations were prepared in 50 mL beakers. The cosurfactant (when used), Sty, SDS and water were added and stirred with a magnetic bar. An aliquot of each formulation was poured into 10 mL vials and kept sealed for monitoring. Monitoring consisted of letting the sample vials sit without agitation and observing aspects such as naked eye transparency and number of phases. It is worth mentioning that samples using AA may turn white (latex aspect) after some hours due to spontaneous polymerization caused by the highly reactive AA monomer. This conclusion was made after noticing that the solids content of these samples were higher than expected considering only SDS as non-volatile, indicating that the monomer content had partially converted to polymer or oligomers. Therefore, extremely small amounts of hydroquinone (~20

ppm relative to monomer) were added to all formulations to prevent monomers from polymerizing. No effect on the microemulsion stability is expected from the addition of hydroquinone due to its negligible concentration.

Table 4-2. Compositions of the microemulsion formulations - Variation of the surfactant/(monomer+cosurfactant) weight ratio

Sample	SDS[a]	Monomer+cosurf.[a]	Pentanol[b]	AA[b]	Water[a]
SDS34	15	6	8	-	79
SDS11	15	8	8	-	77
SDS35	15	10	8	-	75
SDS36	15	12	8	-	73
SDS37	15	6	-	8	79
SDS14	15	8	-	8	77
SDS38	15	10	-	8	75
SDS39	15	12	-	8	73

[a] wt% of total solution; [b] wt% of monomer+cosurfactant mixture

Phase diagrams. To construct the phase diagram, initial mixtures of water-SDS at different ratios were titrated with a monomer-cosurfactant mixture at room temperature. The monomer-cosurfactant mixture composition was Sty:cosurfactant in an 86:14 molar ratio for both cosurfactants, which corresponds to 90:10 and 88:12 w/w for Sty:AA and Sty:pentanol respectively. The molar ratio was chosen for the construction of the phase diagram to enable a more accurate comparison of the two cosurfactants since the system thermodynamics is governed in terms of molar concentrations.[15, 49-51] In order to prevent monomers from polymerizing, ~20 ppm of hydroquinone relative to monomer were added to these mixtures as well. Water-SDS mixtures were prepared in a 600 mL beaker. The components were left under mild mechanical stirring while the oil mixture was added from a burette. High temperature titrations, starting from

80:20 water:SDS mixtures, were carried out by placing the beaker in an oil bath at 70°C. On these occasions the beaker was partially covered with Parafilm to reduce losses by evaporation. The mixture was allowed to stand under mild agitation after the addition of the Sty-cosurfactant mixture (or pure monomer) until transparent, implying the absence of visible monomer droplets or crystalline phase aggregates formed from the previous addition. If the visual aspect of the mixture was transparent/translucent, but visible monomer droplets or crystalline phase aggregates could still be identified, the mixture was left mixing for a longer period, but not more than 1 hour. A phase transition was considered to have occurred if, one hour after the last addition, the following characteristics could be identified: (i) significant phase separation in the top layer of the mixture (creaming) or (ii) significant amount/volume of crystalline aggregates.

Batch polymerizations. Formulations (240 g) prepared from Table 4-3 were polymerized in a 500 mL round bottom flask with a reflux condenser, nitrogen atmosphere and a magnetic stirrer. When cosurfactant (1-pentanol or AA) was used, the Sty:cosurfactant ratio was 92:8 on a weight basis (from formulations SDS34 and SDS37 in Table 4-2). For the reference batch no cosurfactant was present and pure Sty was used.

Table 4-3. Microemulsion formulation – Batch polymerizations[a]

Components	wt%
Sty-cosurfactant mixture[b]	6
SDS	15
DI water	79

[a]Polymerizations were initiated using 0.81 mMol of KPS or HPO. When HPO was used, the redox pair Asc. Ac. was used in a ratio of 2:1 (Asc. Ac.:HPO).
[b]Composition: Sty:pentanol or Sty:AA on 92:8 weight ratio basis

Each formulation was prepared a day before polymerization and left under magnetic stirring in a closed container overnight. Three sets of polymerizations were carried out using the following initiator/temperature conditions: Asc. Ac./HPO redox pair at (i) room temperature and (ii) at 70°C and (iii) KPS at 70°C, at same molar concentration of initiator (0.81 mMol). The round bottom flasks were heated in an oil bath under magnetic stirring (500 rpm) and nitrogen flow. The solutions were observed to be clear to the naked eye at room temperature and at 70°C. The initiator (KPS or HPO) dissolved in a small amount (2 g) of water (included in the 240 g from the formulation) was then added. When Asc. Ac./HPO redox pair was used, the Asc. Ac. was inserted to the microemulsion formulation previously. The ratio of 2:1 Asc. Ac.:HPO in a weight basis was used.[52] The reactions were carried out for 1 hour and samples were periodically taken during the course of the reaction for conversion and average particle size analysis. The reaction in the sample vials was stopped by adding hydroquinone (approximately 30 ppm relative to monomer).

Characterizations. Conversions were determined by gravimetry. The samples were dried in an air-circulation oven at 85°C for 4 hours. Conversions were calculated by the ratio of polymer content at a given time of the reaction and the monomer content of the batch. In cases of monomer with added cosurfactant, AA was considered as part of the monomer content but not 1-pentanol. Average particle sizes were determined by Dynamic Light Scattering (DLS) in a Malvern Zeta-Sizer Nano-ZS. Samples were diluted in a water solution of SDS at critical micellar concentration (CMC) (2.36g/L)[53] to reduce dilution effects on the latex stability. For each sample, 3 measurements of 5 runs each were performed at 25°C to obtain the Z-average particle size and polydispersity index (PdI). The PdI is a value provided by the Malvern instrument and is used to describe the width of the particle size distribution around the average.[54] Indices ≤ 0.100 are assumed to correspond to reasonably narrow monomodal distribution latexes. Size exclusion chromatography (SEC) was performed using a Viscotek 270max separation module and a

refractive index (RI), viscosity (IV) and light scattering (low angle LALS and right angle RALS) triple detector setup. A set of two Polyanalytik SuperRes columns with an exclusion limit molecular weight of $20 \cdot 10^6$ g·mol^{-1} were used in series at 40°C. Distilled THF was used as the eluent at a flow rate of 1 mL·min^{-1}. A calibration curve based on the RI detector was constructed using narrow molecular weight polystyrene standards ranging from 6910 to 3.125.000 g·mol^{-1}. Dried samples from each batch polymerization were washed at least five times with water to remove excess of surfactant. Approximately 100 mg of each sample was solubilized in 10 mL of THF and filtered in 0.2 μm nylon filter. If surfactant was still present after filtration (precipitated at the bottom or as a cloudy solution), it was separated via centrifugation and the supernatant was filtered once again prior to injection into the instrument.

4.4 Results and Discussion

Microemulsion formulations. Photographs of the series of microemulsions formulated according to the recipes in Table 4-1 and Table 4-2 are shown in Figure 4-1 and Figure 4-2, respectively. Immediately after the components are mixed the formulations may be turbid or clear depending on the composition (Figure 4-1 (a) and Figure 4-2 (a)). After mixing is complete, the turbid formulations showed a creaming layer on the top; the thickness of which increases as the cosurfactant:(Sty+cosurfactant) and the surfactant:(Sty+cosurfactant) ratios were reduced. A stable microemulsion formulation was considered to have been obtained when no top creaming layer was found by visual inspection after 2 hours. In the first experiment (Figure 4-1), stable microemulsions formed at higher cosurfactant/(Sty+cosurfactant) ratios, when the cosurfactant concentrations were 8 and 12 wt% of the mixture Sty+cosurfactant.
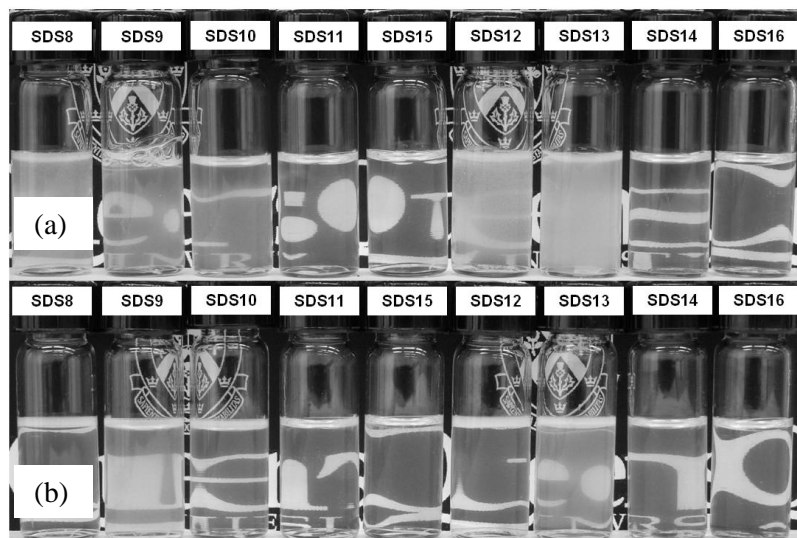
Figure 4-1. Microemulsion formulations with 15/8 SDS/Sty-cosurf. mixture wt. ratio and increasing cosurf./Sty wt. ratio according to Table 4-1: from left to right: no cosurf.; 2, 4, 8 and 12 wt% pentanol to Sty+cosurf. mixture; 2, 4, 8 and 12 wt% AA to Sty+cosurf. Mixture: (a) Immediately after mixing and (b) after repose.
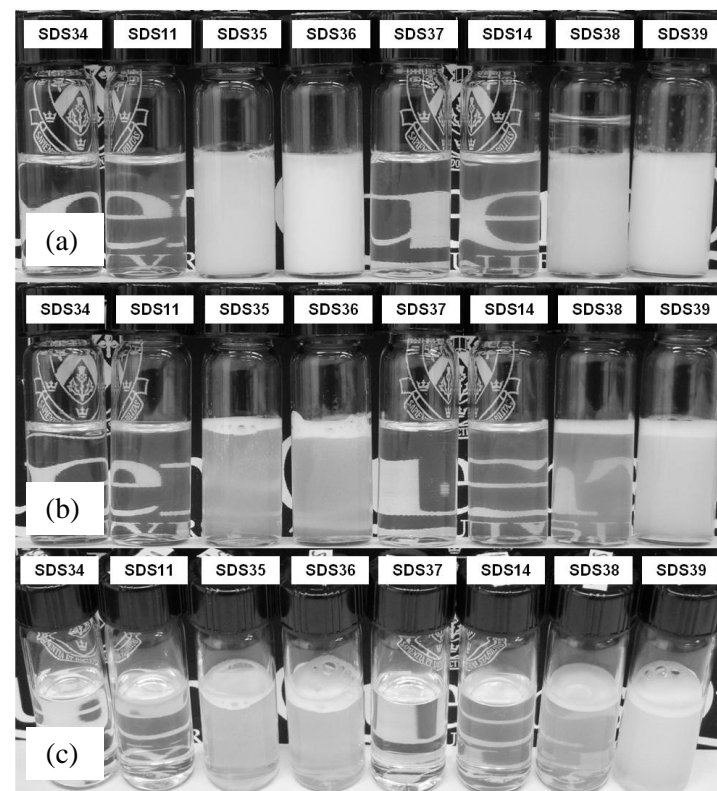
Figure 4-2. Microemulsion formulations with increasing Sty+cosurf mixture/surfactant wt. ratio according to Table 4-2: from left to right: 6, 8, 10 and 12 wt% of the Sty+cosurf. mixture with pentanol as cosurf.; 6, 8, 10 and 12 wt% Sty+cosurf. mixture with AA as cosurf.: (a) Immediately after mixing, (b) and (c) after repose.

78

In the second experiment (Figure 4-2), formulations become clear and without creaming when Sty+cosurfactant concentrations were 6 wt% and 8 wt%. At higher monomer concentrations (10 wt% and 12 wt%), a stable microemulsion could not be obtained; instead, a two phase system was observed, known as a Winsor I system, which consists of an O/W microemulsion that is in equilibrium with an oil phase.[55, 56] The formulations with 6 wt% of Sty+cosurfactant mixture at 8 % weight ratio of cosurfactant/(Sty+cosurfactant) were selected for the batch polymerization experiments.

Phase diagrams. The Sty-SDS-water O/W phase diagrams using pentanol and AA as cosurfactants at room temperature can be seen, respectively, in Figure 4-3 (a) and (b).
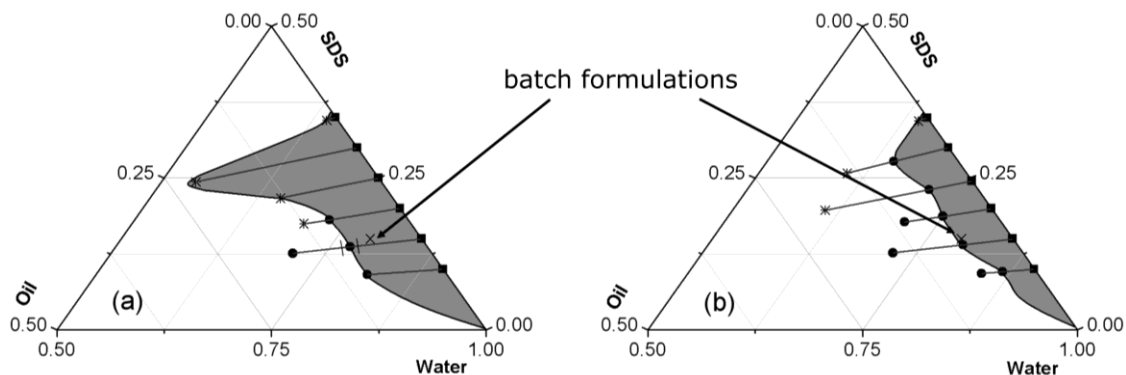
Figure 4-3. Phase diagram of formulations using (a) pentanol and (b) acrylic acid as cosurfactant at room temperature. Axis gives the weight fraction of each phase. The oil fraction is styrene:cosurfactant 86:14 on a molar basis. The shaded area is stable transparent microemulsion. Straight lines indicate the titration paths and the symbols indicate: (■) initial water-SDS mixtures composition, transition from stable transparent microemulsion to (●) 2 phases and (*) crystalline phase system. The composition of the batch formulation is also shown (×). The error bar is the deviation from 6 experiments.

Reproducibility studies were carried out to determine the variability of the results obtained from the titrations. From a series of 6 titrations using the same initial water-SDS composition, the maximum variability at room temperature was approximately plus or minus 10% of the average

fraction of oil in the composition at the phase change, as shown by the error bar in Figure 4-3(a). At 70°C, the variability is expected to be slightly higher due to eventual losses through evaporation. On the phase diagrams, the shaded area indicates stable microemulsion formulations. In most cases, the microemulsion was initially clear and became more and more translucent as the titration continued until the next transition was reached. The straight lines in Figure 4-3 symbolize the path of the titration of the SDS-water mixture by the Sty+cosurfactant mixture. They start on the water/SDS line with a single clear phase (no oil added). There is no change in the phase of the formulation (nature or number) until the next point on the line which is when the transition was observed. The transition to a two phase system indicates a clear phase with a creaming layer on the top, characteristic of Winsor I system.[2, 55] The crystalline phase transition occurs with the formation of a highly viscous phase (gel) similar to a solid-crystalline structure, which is observed for many surfactants, surfactant mixtures and microemulsion formulations[56-58] and arises from the organization of the surfactant micelles in a liquid crystalline structure to allow a better packing at high concentration. As can be seen from Figure 4-3, pentanol as a cosurfactant tends to form a liquid crystalline phase at lower SDS concentration compared to AA. At room temperature, the stable microemulsion region is smaller with AA as cosurfactant. Similar diagrams were obtained by Chern and Liu[25] by the titration of Sty-SDS-water conventional emulsion formulations with different short chain alcohols as cosurfactants and by Puig et al.[59] by the titration of DTAB-water solutions with Sty at different temperatures. In the case of pentanol, they also observed a small one phase microemulsion area followed by a lamellar gel transition for cosurfactant weight ratios higher than 10%.

Titrations with and without cosurfactants were carried out to verify the effect of AA and pentanol as cosurfactants. The results, summarized in Table 4-4, show that the boundary transition from the one phase clear microemulsion to a two phase Winsor I system occurs at

higher oil fractions when either cosurfactant is used, compared to the system with pure Sty. These results, and also the results from Figure 4-1, confirm their effectiveness as cosurfactants to increase the oil fraction that can be solubilized in the microemulsion formulation. These results suggest that the area of stable microemulsion formation for Sty without any cosurfactant would be smaller than the ones observed for pentanol and AA in Figure 4-3.

Table 4-4. Styrene-SDS-water microemulsion phase transitions – Influence of cosurfactant type and temperature

Cosurfactant[a]	Temperature	Phase transition to Winsor I[b]			
		H_2O	SDS	Sty.	Cos.
None	room	76.1	19	4.9	-
Pentanol	room	72.7	18.1	8.1	1.1
Acrylic acid	room	75.0	18.7	5.7	0.6
None	70°C	70.9	17.8	11.4	-
Pentanol	70°C	70.1	17.5	10.9	1.5
Acrylic acid	70°C	69.3	17.3	12	1.4

All titrations started from a mixture water:SDS at 80:20 weight ratio; [a] oil phase composition when cosurfactants were used: styrene:cosurfactant ratio of 86:14 molar; [b] composition of the systems at phase transition (wt%).

Titrations were carried out at 70°C to examine the effect of temperature on the microemulsion stability, for which results are also presented in Table 4-4. The mass fraction of Sty+cosurfactant mixture that can be solubilized forming a microemulsion at 70°C is significantly higher compared to the same titration at room temperature. This observation is in agreement with the results reported by Puig et al.[59] where the stable Sty-DTAB O/W microemulsion region was expanded by increasing the temperature from 25 to 60°C. Using pentanol as cosurfactant, the weight fraction

of Sty solubilized in the system shifted from 8.1 to 10.9 and for AA it shifted from 5.7 to 12; i.e., the increase in temperature largely eliminated the difference in stability observed at room temperature. In addition, it is noteworthy to see the increase in the Sty uptake capacity, from 4.9 to 11.4 wt% for the microemulsion formulation with no cosurfactant. This result indicates that at 70°C the two cosurfactants have a significantly less pronounced effect on the stability of the O/W Sty-SDS microemulsions. However, AA as a copolymerizable cosurfactant also increases the theoretical polymer content of the formulation, when the sum of (Sty+AA) content is considered.

The increase in the volume fraction of oil that can be solubilized in isotropic microemulsions at higher temperature is in agreement with the theory of microemulsion stability.[60, 61] The entropic term, which is responsible for the spontaneity of emulsification and thermodynamic stability of the system, is directly proportional to the absolute temperature. Physically, part of the enhancement of monomer mass uptake at higher temperature for the same SDS/water ratio could be attributed to the decrease of the interfacial tension between the monomer and the water phase[62, 63] and, to a lesser extent, the higher monomer solubility in water.[64]

Batch polymerizations. The batch reaction recipes used, presented in Table 4-3, fall in the stable region of microemulsion formulation for both cosurfactants at room temperature and at 70°C (see Figure 4-3 and Table 4-4). The evolution of monomer conversion with reaction time for the batch polymerizations with KPS at 70°C are shown in Figure 4-4 (a).

High conversions are reached within a few minutes of reaction due to the large number of particles and subsequently high rates of polymerization due to radical segregation.[2, 65] No significant effects could be observed in the reaction kinetics for either of the cosurfactant systems compared to the Sty control. The evolution of average particle size with reaction time is presented in Figure 4-4(b). The formulation containing AA resulted in a latex with smaller average particle size, however the difference is considered too small (aprox. 1.3 nm) to be significant.
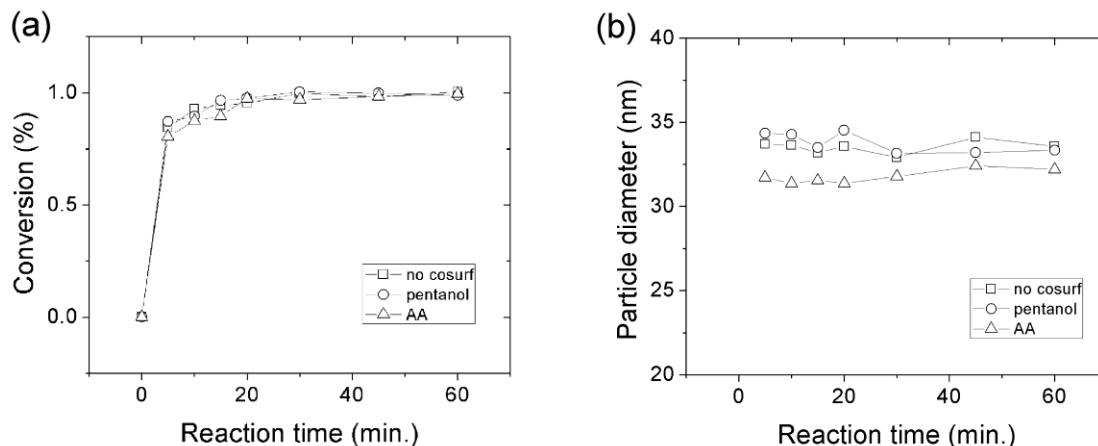
Figure 4-4. Evolution of (a) conversion and (b) average particle size with time for styrene microemulsion batch polymerizations at 70ºC with no cosurfactant (□), with pentanol (○) and with acrylic acid (△) as cosurfactants, at a styrene:cosurfactant weight ratio of 92:8.

Additional polymerizations were carried out using the HPO/Asc. Ac. redox pair initiator system. The average particle size results obtained after polymerization for all experiments are presented in Table 4-5. For the same molar concentration of initiator, smaller average particle sizes were obtained for Asc. Ac./HPO at 25°C and 70°C when compared to KPS. The use of Asc. Ac./HPO decreases the average particle size due to the higher availability of radicals, which are generated virtually instantaneously[52, 66] as compared to the thermal decomposition exponential profile obtained by persulphate initiators (1/2 life of 273 minutes at 70°C).[67, 68] A study by Uhniat et al.[69] showed that as AA lowered the pH of the medium, the oxidation of Asc. Ac. was reduced, slowing down the initiation process. The pHs of the latexes containing AA in this study were found all to be in the range of 3-4, so as might be expected, no changes in the rate of polymerization were observed. In conclusion, having a higher flux of radicals at the beginning of the synthesis, as a consequence of the use of redox pair Asc. Ac./HPO, resulted in the nucleation of more monomer microdroplets, thereby increasing the number of particles and decreasing the average particle size.[60]

Table 4-5. Final latex and polymer properties – Influence of the cosurfactant, initiator type and temperature

Initiator	Cosurf.	Temp.	Dp	PdI	M_w ($g \cdot mol^{-1} \times 10^{-5}$)	M_n ($g \cdot mol^{-1} \times 10^{-5}$)	PDI M_w/M_n
KPS	None	70°C	33.57	0.092	44.3	2.69	16.4
	Pentanol	70°C	33.34	0.067	34.9	2.57	13.6
	AA[a]	70°C	32.20	0.046	49.1	1.58	31.0
Asc. Ac./HPO	None	Room	27.73	0.047	37.4	2.13	17.5
	Pentanol	Room	29.34	0.021	44.5	2.02	22.0
	AA[a]	Room	30.01	0.087	77.6	0.52	150
	None	70°C	26.60	0.047	40.0	1.54	25.9
	Pentanol	70°C	26.92	0.073	48.2	1.80	26.8
	AA[a]	70°C	26.99	0.059	64.9	0.68	95.2

Experiments performed according to recipe presented in Table 4-3.

[a]Samples presented gel formation in THF, indicating the presence of polymers rich in acrylic acid units in their composition. The results presented correspond to the molecular weight of the soluble fraction of the sample, presented simply for comparison purposes.

The increase in temperature from 25 to 70°C also led to a decrease in the average particle size even more due to the higher Sty solubility in the water phase[64] and a higher propagation rate coefficient.[70] These two parameters resulted in faster polymerization in the water phase, thus increasing the radical entry frequency[71] increasing nucleation rate and lowering the average particle size. This result is in agreement with previous work available in the literature.[59, 72, 73]

The microemulsions turn from transparent to more translucent as soon as the initiator solution is added to the reaction vessel, and the turbidity increases with conversion due to the scattering of visible light by the polymer particles formed.[74, 75] This phenomenon is called the Tyndal Effect and it correlates to the Rayleigh scattering.[76] The transition in the visual aspect can be predominantly attributed to an increase in size and width of the distribution during the transition from monomer microdroplets/swollen micelles to polymer particles and, to a lesser extent, the change in the relative refractive index particle/water (because of the transition from monomer[77] (1.544) to polymer[54] (1.589)).

The molecular weight distributions (MWD) for the microemulsion polymerizations are presented in Figure 4-5 and the corresponding number-average (M_n) and weight-average (M_w) molecular weights and polydispersity index (PDI = M_w/M_n) are reported in Table 4-5. It should be noted that all polymerizations of the microemulsions co-stabilized by AA resulted in significant gel formation when the polymer was dried and suspended in THF. Consequently, the M_n and M_w values reported in Table 4-5 are obtained from the THF soluble fraction only, and are reported for comparative purposes, even though we are aware that both the average molecular weights as well as the shape of the MWD change upon fractionation of the sample in these cases.

All the MWDs display high average molecular weights and broad distributions with a long, low molecular weight tail (Figure 4-5). The polydispersity values (M_w/M_n) were very high, much higher than normally observed from conventional free-radical microemulsion[59, 73] polymerization systems. It is believed that these high values of PDI could be related to the fact of being operating outside the range of calibration of the equipment. These high molecular weights component extends to 10^8 g/mol, well outside the range of PS calibration used to calculate molecular weight averages. Thus, the numbers in Table 4-5 cannot be considered absolute, but are still useful for comparative purposes. Previous work reporting the addition of cosurfactants in microemulsion polymerization has resulted to ambiguous results. Both increase[21, 78] and decrease[25] in the M_w of PS in the presence of short chain alcohols has been reported prior to the current investigation. Here, no significant and reproducible shifts in the MWDs to lower or higher average molecular weights were observed upon the addition of pentanol to the microemulsion (Table 4-5).

Figure 4-5. Molecular weight distributions for microemulsion polymerization runs from recipe in Table 4-3. (a) KPS as initiator at 70 ºC, (b) AA as cosurfactant, (c) No cosurfactant.

When KPS was used as initiator there was a slight decrease in M_w value and the MWD (Figure 4-5). However, when HPO/Asc. Ac. initiator was used the shift in M_w values with pentanol were

towards higher molar masses. The rate coefficients of transfer to low molecular weight alcohols $(C_4 - C_6)$ (k_{tr}) at 70°C was determined at $8.9 \cdot 10^{-6}$.[25] A comparison with the rate coefficient of transfer constant to monomer in a styrene polymerization ($k_{tr} = 6\text{-}9 \cdot 10^{-5}$ at 70°C)[70, 79] illustrates that little effect of chain transfer to pentanol can be expected under the specific polymerization conditions. These effects could be less significant than interactions among the species constituents of the formulation. For instance, Puig et al.[21] noticed that by changing the counter ion of the surfactant used, the effects of several short-chain alcohols cosurfactants observed on kinetics and M_w practically disappeared.

The soluble molecular weight fraction of the MWD in the polymerizations where AA was used as cosurfactant differ significantly from the cases where either no co-surfactant or pentanol was used (Figure 4-5). The average molecular weights shift to higher average molecular weights and the PDI increases (Table 4-5). Moreover, a significant population of low molecular weight polymer can be observed in the MWDs, especially for the microemulsion polymerizations initiated by HPO/Asc. Ac. and although to a lesser extent, for the microemulsion polymerizations initiated by KPS. The major differences between the HPO/Asc Ac redox couple and KPS are the rate of radical generation and the charge of the radicals formed: negative (sulfate anion) for KPS and neutral (hydroxyl) for HPO. For HPO/Asc. Ac. radical generation is nearly instantaneous upon addition of HPO, whereas for KPS an exponential decay in the rate of radical generation is observed. This difference in initiator decomposition rates results in different aqueous phase polymerization kinetics and radical fluxes throughout the polymerization which are reflected in the MWD.

The AA cosurfactant has a high water-solubility and partitions between the monomer swollen micelles and the aqueous phase.[80] Upon the instantaneous decomposition of the HPO/Asc. Ac. redox couple it is likely that the majority of the available AA in the aqueous phase, which is

significantly higher than Sty (unlimited solubility from AA[80] versus 320 mg/L for Sty[64] at 25 °C), is homopolymerized due to high molar fraction in the water and its high reactivity, forming polymer chains rich in AA of lower molecular weight.[81] In addition, the high concentration of radicals and the increased solubility of oligomeric radicals in the continuous phase may result in higher termination rates in the water phase, generating water soluble polymers. Poly(acrylic acid) (PAA) is not THF soluble. This explains why significant amounts of gel are obtained upon suspending the dried polymers in THF. When KPS was used the gel formation was observed to a lesser (close to negligible) extent. KPS decomposition is slower and consequently it is likely that it results in less termination in the water phase resulting in a more even distribution of AA over the overall polymer chains, because of the tendency to form alternated copolymers of the couple AA and Sty.[70, 79].

For the cosurfactant-free polymerizations (Figure 4-5c) it can be observed that the MWDs are very similar according to Table 4-5.

4.5 Conclusions

AA and pentanol were compared as cosurfactants in the production of O/W Sty-SDS microemulsions and their polymerization. Ternary diagrams mapped out the region of stable O/W Sty-SDS microemulsion formation. For the monomer/cosurfactant ratio studied (86/14 molar), at room temperature this region was smaller in the case of AA when compared to pentanol. When no cosurfactant was used the stability of the microemulsion was decreased, indicating the effective role of both species, pentanol and AA, as cosurfactants increasing the oil solubility in the system. At 70°C, the mass fraction of Sty that could be solubilized was significantly increased for all systems and no significant cosurfactant effects were observed in terms of mass fraction of styrene that could be solubilized in the microemulsion formulations. The use of AA as a copolymerizable cosurfactant was shown to be advantageous in the sense that one can increase

the theoretical polymer contents of the microemulsion in an additional 0.6-1.4 wt%, however the solids content of the final latexes was still low (<10 wt%) and low polymer to surfactant ratios (<1) compared to the modified microemulsion method developed in Chapter 3.

Under the conditions studied, the batch polymerizations indicated no significant difference in the rate of polymerization among pure styrene, styrene/pentanol and styrene/AA systems. In addition, the cosurfactant, whether pentanol or AA, did not significantly influence the average particle sizes, which were observed to decrease for higher flux of free radicals and higher temperatures. Microlatexes with average particle sizes ranging from 26 to 34 nm were obtained. Molecular weights of the order of 10^6-10^7g·mol^{-1} were achieved. The results indicated that the incorporation of acrylic acid units in the polymer backbone is sensitive to the flux of radicals. When the HPO/Asc. Ac. redox pair was used, major gel formation occurred during the preparation of samples containing acrylic acid for SEC analysis, indicating the formation of acrylic acid rich polymer chains. When KPS was used the gel formation was observed to be less important indicating a more effective incorporation of AA. This information can be helpful when developing a method for the incorporation of AA to the formulation of the bimodal latexes.

In terms of the overall project objectives, this Chapter have shown that the use of conventional microemulsion polymerization to produce the smaller particles population is not attractive because of the high level of surfactant which is necessary to stabilize a small amount of monomer. Thus, even thought the particle size is found to be in the range of interest, the concentration of the microemulsion latex is very low and so is the polymer to surfactant ratio of the formulations. The use of cosurfactants provided limited improvement to the polymer to surfactant ratio, however the results obtained are still not interesting taking into account that the methodologies studied in Chapters 3 and 5 provided much better results. Finally, the use of acrylic acid in the formulation has shown that the incorporation of this monomer to the polymer

particles is sensitive to process parameters such as the flux of radicals.

References

1. Pavel, F. M. *Journal of Dispersion Science and Technology* **2004**, *1,* 1-16.

2. Chow, P. Y.; Gan, L. M. *Advances in Polymer Science* **2005**, 257-298.

3. Candau, F. Polymerization in Microemulsions. In *Polymerization in organized media;* Paleos, C. M., Ed.; Gordon and Breach Science Publishers: Philadelphia, 1992.

4. O'Donnell, J.; Kaler, E. W. *Macromol. Rapid Commun.* **2007**, *14,* 1445-1454.

5. Stoffer, J. O.; Bone, T. *J. Polym. Sci. Polym. Chem. Ed.* **1980**, *8,* 2641-2648.

6. Xie, C.; Yang, L.; Gao, Q. *Xiandai Huagong* **2004**, *9,* 62-65.

7. Shen, Y.; Zhang, X.; Lu, J.; Zhang, A.; Chen, K.; Li, X. *Colloids Surf. , A* **2009**, *1-3,* 87-90.

8. Wan, T.; Zang, T. S.; Wang, Y. C.; Zhang, R.; Sun, X. C. *Polym. Bull. (Heidelberg, Ger.)* **2010**, *6,* 565-576.

9. Gupta, A. K.; Wells, S. *IEEE Trans Nanobioscience* **2004**, *1,* 66-73.

10. Sanghvi, P.; Devi, S. *Int. J. Polym. Mater.* **2005**, *4,* 293-303.

11. Reddy, K. R.; Sin, B. C.; Yoo, C. H.; Sohn, D.; Lee, Y. *J. Colloid Interface Sci.* **2009**, *2,* 160-165.

12. Wu, H. S.; Hegenbarth, J.; Chen, X. K.; Chen, J. G. Patent Application Country: Application: US; Patent Country: US; Priority Application Country: US Patent 6046271, 2000.

13. Mendonca, C. R. B.; Silva, Y. P.; Bockel, W. J.; Simo-Alfonso, E. F.; Ramis-Ramos, G.; Piatnicki, C. M. S.; Bica, C. I. D. *J. Colloid Interface Sci.* **2009**, *2,* 579-585.

14. Hu, A.; Yao, Z.; Yu, X. *J. Appl. Polym. Sci.* **2009**, *4,* 2202-2208.

15. Ruckenstein, E. *J. Dispersion Sci. Technol.* **1981**, *1,* 1-25.

16. Gan, L. M.; Chew, C. H.; Friberg, S. E. *J.Macromol.Sci., Chem.* **1983**, *5,* 739-756.

17. Guo, J. S.; El-Aasser, M. S.; Sudol, E. D.; Yue, H. J.; Vanderhoff, J. W. *J. Colloid Interface Sci.* **1990**, *1,* 175-184.

18. Chern, C. -.; Wu, L. -. *J. Polym. Sci. Part A* **2001**, *19,* 3199-3210.

19. Gan, L. M.; Chew, C. H.; Friberg, S. E.; Higashimura, T. *J.Polym.Sci., Polym.Chem.Ed.; Journal of Polymer Science, Polymer Chemistry Edition* **1981**, *6,* 1585-1587.

20. Gan, L. M.; Chew, C. H. *J. Dispersion Sci. Technol.* **1983**, *3,* 291-312.

21. Puig, J. E.; Mendizábal, E.; Delgado, S.; Arellano, J.; López-Serrano, F. *Comptes Rendus Chimie* **2003**, *11-12,* 1267-1273.

22. Herrera, J. R.; Peralta, R. D.; Lopez, R. G.; Cesteros, L. C.; Mendizabal, E.; Puig, J. E. *Polymer* **2003**, *6,* 1795-1802.

23. Chern, C.; Wu, L. *J. Polym. Sci. A Polym. Chem.* **2001**, *6,* 898-912.

24. Johnson, P. L.; Gulari, E. *J.Polym.Sci., Polym.Chem.Ed.; Journal of Polymer Science, Polymer Chemistry Edition* **1984**, *12,* 3967-3982.

25. Chern, C. S.; Liu, C. W. *Colloid Polym. Sci.* **2000**, *4,* 329-336.

26. Gan, L. M.; Chew, C. H.; Lye, I.; Ma, L.; Li, G. *Polymer* **1993**, *18,* 3860-3864.

27. Holtzscherer, C.; Candau, F. *J. Colloid Interface Sci.* **1988**, *1,* 97-110.

28. Holtscherer, C.; Candau, F. *Colloids and Surfaces* **1988**, *4,* 411-423.

29. Roy, S.; Devi, S. *Polymer* **1997**, *13,* 3325-3331.

30. Buchert, P.; Candau, F. *J. Colloid Interface Sci.* **1990**, *2,* 527-540.

31. Candau, F.; Buchert, P. *Colloids and Surfaces* **1990***, 1-3,* 107-122.

32. Corpart, J. M.; Candau, F. *Colloid Polym. Sci.* **1993***, 11,* 1055-1067.

33. Larpent, C.; Bernard, E.; Richard, J.; Vaslin, S. *Macromolecules* **1997***, 3,* 354-362.

34. Donescu, D.; Fusulan, L.; Petcu, C. *Colloid Polym. Sci.* **1999***, 2-3,* 203-209.

35. Chew, C. H.; Gan, L. M. *J. Polym. Sci. , Polym. Chem. Ed.* **1985***, 8,* 2225-2232.

36. Raj, W. R. P.; Sasthav, M.; Cheung, H. M. *Langmuir* **1991***, 11,* 2586-2591.

37. Raj, W. R. P.; Sasthav, M.; Cheung, H. M. *J. Appl. Polym. Sci.* **1993***, 3,* 499-511.

38. Raj, W. R. P.; Sasthav, M.; Cheung, H. M. *Polymer* **1995***, 13,* 2637-2646.

39. Ceska, G. W. *J Appl Polym Sci* **1974***, 2,* 427-437.

40. Blackley, D. C. *Polymer latices : science and technology;* Chapman & Hall: London; New York, 1997.

41. Sakota, K.; Okaya, T. *J Appl Polym Sci* **1976***, 9,* 2583-2587.

42. Vesaratchanon, J. S.; Takamura, K.; Willenbacher, N. *J. Colloid Interface Sci.* **2010***, 2,* 214-221.

43. Reynhout, X. E. E.; Beckers, M.; Meuldijk, J.; Drinkenburg, B. A. H. *J.Polym.Sci., Part A: Polym.Chem.* **2005***, 4,* 726-732.

44. Woodward, R. T.; Chen, L.; Adams, D. J.; Weaver, J. V. M. *J. Mater. Chem.* **2010***, 25,* 5228-5234.

45. Gonzalez, V. D. G.; Gugliotta, L. M.; Meira, G. R. *J. Mater. Sci. : Mater. Med.* **2008***, 2,* 777-788.

46. Gonzalez, V. D. G.; Gugliotta, L. M.; Giacomelli, C. E.; Meira, G. R. *J. Mater. Sci. : Mater. Med.* **2008***, 2,* 789-795.

47. Agrawal, M.; Gupta, S.; Stamm, M. *J. Mater. Chem.* **2011***, 3,* 615-627.

48. Puig, J. E.; Corona-Galvan, S.; Maldonado, A.; Schulz, P. C.; Rodriguez, B. E.; Kaler, E. W. *J. Colloid Interface Sci.* **1990***, 1,* 308-310.

49. Ruckenstein, E. *J. Colloid Interface Sci.* **1978***, 2,* 369-371.

50. Ruckenstein, E. *Chem.Phys.Lett.* **1978***, 4,* 517-521.

51. Overbeek, J. T. G. *Faraday Discuss. Chem. Soc.* **1978***, Colloid Stabil.,* 7-19.

52. Boutti, S.; Zafra, R. D.; Graillat, C.; McKenna, T. F. *Macromol. Chem. Phys.* **2005***, 14,* 1355-1372.

53. Bales, B. L.; Messina, L.; Vidal, A.; Peric, M.; Nascimento, O. R. *J Phys Chem B* **1998***, 50,* 10347-10358.

54. Xu, R. *Particle characterization: light scattering methods;* Kluwer Academic: New York, 2002.

55. Winsor, P. A. *Trans.Faraday Soc.* **1948**, 376-382.

56. Winsor, P. A. *Solvent properties of amphiphilic compounds.* Butterworths Scientific Publications: London, 1954.

57. Rodrigues, C.; Kunieda, H. Phase Behavior and Microstructure of Liquid Crystals in Mixed Surfactant Systems. In *Mixed surfactant systems.* Abe, M., Scamehorn, J. F., Eds.; Marcel Dekker: New York, 2005.

58. Alany, R. G.; El Marghraby, G. M.; Krauel-Goellner, K.; Graf, A. Microemulsion Systems and Their Potential as Drug Carriers. In *Microemulsions properties and applications;* Fanun, M., Ed.; Taylor & Francis: Boca Raton, Fla., 2008.

59. Puig, J. E.; Perez-Luna, V. H.; Perez-Gonzalez, M.; Macias, E. R.; Rodriguez, B. E.; Kaler, E. W. *Colloid Polym. Sci.* **1993***, 2,* 114-123.

60. Antonietti, M.; Basten, R.; Lohmann, S. *Macromol. Chem. Phys.* **1995**, *2,* 441-466.

61. Miller, C. A.; Scriven, L. E. *J. Colloid Interface Sci.* **1970**, *3,* 361-371.

62. Lavelle, J. A. *J. Phys. Chem.* **1968**, *6,* 2283-2284.

63. Olayo, R.; Garcia, E.; Garcia-Corichi, B.; Sanchez-Vazquez, L.; Alvarez, J. *J. Appl. Polym. Sci.* **1998**, *1,* 71-77.

64. Lane, W. H. *Ind. Eng. Chem. , Anal. Ed.* **1946**, 295-296.

65. de Vries, R.; Co, C. C.; Kaler, E. W. *Macromolecules* **2001**, *10,* 3233-3244.

66. Kohut-Svelko, N.; Pirri, R.; Asua, J. M.; Leiza, J. R. *J. Polym. Sci. , Part A: Polym. Chem.* **2009**, *11,* 2917-2927.

67. Beylerian, N. M.; Vardanyan, L. R.; Harutyunyan, R. S.; Vardanyan, R. L. *Macromol. Chem. Phys.* **2002**, *1,* 212-218.

68. Santos, A. M.; Vindevoghel, P.; Graillat, C.; Guyot, A.; Guillot, J. *J.Polym.Sci., Part A: Polym.Chem.* **1996**, *7,* 1271-1281.

69. Uhniat, M.; Sikorski, R.; Woroszilo, L. *Polymer Science U.S.S.R.* **1981**, *11,* 2622-2627.

70. Brandrup, J.; Immergut, E. H.; Grulke, E. A. *Polymer Handbook;* John Wiley&Sons: New York, 2003, pp. II-88.

71. Gilbert, R. G. *Emulsion Polymerization, a mechanistic approach;* Academic Press: London, 1995.

72. Sanghvi, P. G.; Pokhriyal, N. K.; Devi, S. *Polym. Int.* **2002**, *8,* 721-728.

73. Guo, J. S.; El-Aasser, M. S.; Vanderhoff, J. W. *J. Polym. Sci. A Polym. Chem.* **1989**, *2,* 691-710.

74. Chen, W.; Liu, X.; Liu, Y.; Bang, Y.; Kim, H. *Colloids Surf. , A* **2010**, *1-3,* 145-150.

75. Smeets, N. M. B.; Moraes, R. P.; Wood, J. A.; McKenna, T. F. L. *Langmuir* **2011***, 2,* 575-581.

76. Hulst, H. C. v. d. *Light scattering by small particles;* Dover: New York, 1981.

77. Aminabhavi, T. M.; Patil, V. B.; Banerjee, K. *J. Chem. Eng. Data* **1999***, 6,* 1291-1297.

78. Chern, C.; Yu, T.; Hu, L. *J Appl Polym Sci* **2006***, 6,* 4406-4411.

79. Odian, G. *Principles of Polymerization;* Wiley-Interscience: 2004.

80. Shoaf, G. L.; Poehlein, G. W. *J Appl Polym Sci* **1991***, 5,* 1213-1237.

81. Slawinski, M.; Meuldijk, J.; Van Herk, A. M.; German, A. L. *J. Appl. Polym. Sci.* **2000***, 4,* 875-885.

Chapter 5

Small particles population – High flux of radicals micellar

polymerizations

5.1 Abstract

In this Chapter we present an emulsion polymerization approach that was designed to maximize the number of particles nucleated during the initial stages of the reaction using a higher than normal flux of water soluble free radicals. PS and PMMA nano-latexes with low surfactant (SDS) concentrations were obtained using three initiator systems: KPS, APS and HPO/ascorbic acid redox pair. Particle size was decreased by increasing SDS and initiator concentrations up to limit values at which point a further increase in SDS concentration did not decrease particle size. Optimized conditions for minimum particle size with highest polymer to surfactant ratio were determined by studying the influence of SDS and initiator in a wide range of concentrations, temperature and ionic strength. Stable nano-latexes with 19 wt% polymer content and particles <30 nm were achieved with a polymer to surfactant ratio of 3.6 in batch. These results correspond to an improvement compared to conventional microemulsion polymerization in the sense that the last generally requires a polymer to surfactant ratio of 1 or lower and the maximum solids content achievable is normally < 10 wt%. Finally, a comparison between this the starved-feed technique previously reported (Moraes et al. J. Polym. Sci. A: Polym. Chem. 2010, 48, 48; described in Chapter 3) was made and the process developed in Chapter 3 was shown to produce latexes with slightly smaller particle sizes for the same surfactant concentration by increasing the initiator concentration.

5.2 Introduction

The objective of this Chapter is to explore and develop an approach alternative to Chapter 3 to

produce small particle size latex particles using reduced concentrations of surfactants. The great disadvantage of the approach developed in Chapter 3 is that the starved-feed methodology requires long periods of time to synthesize the latexes. In this Chapter, we attempt to produce latexes as concentrated as possible, with particles as small as possible, using as little surfactant as possible by increasing the initiator concentration to increase the number of micelles nucleated in the early stages of the polymerization. This process is intended to be extremely fast with the objective of avoid monomer transfer from non-nucleated droplets/micelles to nucleated particles by nucleating a large fraction of them to keep their size small.

As we have mentioned in the previous Chapter, microemulsions are systems in which particles resulting from polymerization are very small (less than 50 nm) and typically contain only a few polymer chains. These products are also called nano-latexes and find diverse applications such as biomedical, coatings, and others.[1-5] Microemulsion systems usually require much greater amounts of surfactant than emulsions, which is a significant disadvantage and often a limiting factor for industrial applications. Therefore, many efforts have been made towards the production of nano-latexes using fewer quantities of surfactants recently. The principle means used to increase polymer to surfactant ratios consist mainly of drop-wise/starved-feed or differential semi-batch process,[6, 7] including vapour monomer feeding.[8] Such processes exploit the low monomer concentration inside the particles under starved-feed to limit their growth. In addition, the continuous saturation of the water phase with monomer combined with the high availability of micelles increase the probability that micelles will be converted to new particles. However, the use of controlled polymerization processes have also being successful, including catalytic chain transfer (CCT) polymerization,[9] and reversible addition-fragmentation chain transfer (RAFT) polymerization,[10] which exploit the radical transfer to the catalyst and the higher exit rate of these radicals to limit particle growth and nucleate new particles.

In microemulsion polymerization (as in conventional emulsion polymerization processes) increasing the initiator concentration has been shown to decrease the particle size for a specific surfactant concentration. Antonietti et al.[11] analyzed a series of works available in the literature[12-14] with regard to the dependency of the particle size on the initiator concentration in microemulsion polymerization. They pointed out that there is a change in the thermodynamic properties of microemulsions during the transition from oil droplets to polymer particles, described by the common growth of particles size observed during polymerization. This transition in the thermodynamic properties of the system during the polymerization process characterizes an apparently kinetically controlled process, probably related to the gain in the enthalpy and entropy of mixing after a particle is nucleated. This dynamic change in the thermodynamics of the system results in growth (swelling followed by polymerization) during synthesis by the absorption of monomer from non-nucleated swollen micelles or microdroplets.

Guo et al.[12] investigated the microemulsion polymerization of Sty using an oil-soluble (2,2'-azobis-(2-methyl butyronitrile)) and water-soluble (potassium persulfate, KPS) initiators. They verified that the polymer microemulsion latexes obtained were less translucent than the original microemulsions. For both initiators the latex particle and molecular weight decreased by increasing initiator concentration. In another work, Guo et al.[13] studied the microemulsion polymerization of Sty using KPS and concluded that the nucleation process was continuous throughout the course of the polymerization and most of the monomer resides in the polymer particles during the polymerization. By increasing KPS concentration from 0.14 to 0.69 mM, the latex particle size decreased from 27 to 22 nm and the molecular weight also showed a tendency to decrease with [I]. Puig et al.[14] compared the use of oil-soluble (2,2-azobisisobutyronitrile, AIBN) versus water soluble KPS initiators in the microemulsion polymerization of Sty and found that for both initiators the molecular weight and the latex particle size decrease with $[I]^{-0.4}$ and $[I]^{-}$

[0.2], respectively. They concluded that not all microemulsion droplets are nucleated and particles grow by recruiting monomer and surfactant from uninitiated swollen micelles. Sanghvi et al.,[15] compared KPS and HPO/ascorbic acid (Asc. Ac.) in the microemulsion copolymerization of Sty and 2-hydroxyethyl methacrylate. They observed that upon increasing the initiator concentration, smaller particle sizes were obtained for both initiator systems. In addition, they concluded that, due to the anionic nature of KPS radicals, the oligomeric radicals experienced more resistance to enter particles from the SDS molecules as compared to the neutral radicals generated from the decomposition of the HPO. They obtained particle sizes in the range of 22-38 nm. Irradiation (pulsed electron beam/UV/gamma) initiated polymerization systems,[16-18] have also been used to explore the high flux of free radicals formed to nucleate a large number of small particles. However, in this work we have focused on the chemical production of radicals only.

In the works mentioned above the surfactant concentration was very high, normally at a surfactant:monomer ratio of 1:1. In this work we present an modified (micro)emulsion polymerization approach for the production of nano-latexes in batch reaction with enhanced polymer to surfactant ratio. The approach is based on maximizing of particle nucleation by the generation of a high flux of free radicals to nucleate a higher fraction of the available micelles in a very short time, reducing the number of un-nucleated micelles and the time for monomer transfer to growing particles. This fast reaction minimizes the kinetic instability experienced during the transition from monomer to polymer microemulsions. This process also provides similar results for formulations which do not originate from thermodynamically stable microemulsions (conventional kinetic stable emulsions) allowing the achievement of nano-latexes at reduced surfactant concentrations. We further explore different conditions such as the influence of temperature, ionic strength, monomer composition, batch versus semi-continuous process and polymer content on the production of these nano-latexes. In contrast to the previous work, we

explore low surfactant (SDS) concentrations and use high initiator concentrations, applying KPS, NaPS or Asc. Ac./HPO redox pair to obtain very small particles with a high polymer to surfactant ratio.

5.3 Experimental

Materials. Styrene (Sty, ≥99%), methyl methacrylate (MMA, 99%), hydrogen peroxide (HPO, 30 wt% solution in water), Ascorbic Acid (Asc. Ac., ≥97%) and ammonium persulphate (APS, 98%) from Sigma-Aldrich, potassium persulphate (KPS, 99%) from Acros Organics, sodium chloride (NaCl, 95%), tetrahydrofuran (THF) (Certified) from Fisher Scientific, sodium dodecyl sulphate (SDS, solid powder 99.8%) from MP Biomedicals were used as received. All water was deionized using a Millipore-Synergy Ultrapure Water System.

Polymerizations. Reactions were carried out in a jacketed glass reactor of 250 mL equipped with a reflux condenser, nitrogen inlet, connected to a heated water bath for temperature control. The parameters investigated were: the influence of initiator concentration, the effect of surfactant concentration, the effect of increasing the formulations' polymer content, the influence of temperature, the influence of the ionic strength and the effect of different monomer compositions.

Influence of initiator concentration. The initiators systems studied were KPS, APS and Asc. Ac./HPO, in the range of concentration from 0.6-30.5 mol%, relative to monomer. Polymerizations were carried out in batch, according to the formulation presented in Table 5-1**Error! Reference source not found.**. The redox system components were used in the ratio Asc. Ac.:HPO of 2:1 (on a weight basis).[19]

The formulation components; water, SDS and Sty (and Asc. Ac. in the case of redox systems) were added to the reactor under N_2 atmosphere, and left under agitation while the temperature was raised. The reactor jacket temperature was heated up to 80°C prior to initiator addition and

kept constant over the length time of the reaction. Temperature inside the reactor was monitored using a datalogging thermometer (Sper Scientific, model 800005) coupled to a computer. The HPO, KPS or APS were dissolved in a small aliquot of water (40 g) and added to the reactor when desired temperature was reached, at this moment the reaction was considered started. Reactions were carried out for one hour. This procedure will be termed the "standard batch process", in the rest of the Chapter

Table 5-1. Formulations used for studying the influence of initiator concentration

Component	Quantity
Water	179 g
SDS	2.5 or 10 mol%[a]
Styrene	41 g
Initiator	0.6-30.5 mol%[a]

[a] relative to monomer

Effect of surfactant concentration. The polymerizations to investigate the effect of surfactant concentration were carried out according to the formulations presented in Table 5-2 using two different processes, batch and starved-feed semi-batch. The range of SDS concentration studied was from 2.5 to 35 mol% relative to monomer.

Table 5-2. Formulations used for studying the effect of surfactant concentration

Component	Quantity
Water	179 g
SDS	1.5-35 mol%[a]
Sty or MMA	41 g
Initiator	Variable, see Figure 5-4 and Figure 5-9

[a] relative to monomer

For reactions performed in batch, the procedure follows the standard batch process. Starved-feed semi-batch polymerizations were performed according to the procedure extracted from Chapter 3 and Moraes et al.,[6] with a few modifications to accommodate the use of HPO/Asc. Ac. initiator redox pair as described below. In addition, the initiator concentration used was 7.5 mol% relative to monomer, much higher than the 0.2 mol% KPS used in Chapter 3.

The corresponding mass of SDS (2.5, 5 or 10 mol%) solubilized in 154 g of water and 0.8 g of monomer were added to the reactor and degassed with N_2 during the heating to 80°C. To start the reaction, a solution of KPS in 10 g of water was added. When the HPO/Asc. Ac. initiatior redox pair was used, the corresponding mass of HPO was added to the reactor followed by a continuous addition of a solution of the corresponding mass of Asc. Ac. in 25 g of water, over 100 minutes using a low flow rate pump. The continuous addition of 40 g of monomer was started 7.5 minutes after the start of the reaction using a syringe pump, with a total infusion time of 80 minutes. The reactions were carried out for 100 minutes.

Influence of temperature. Polymerizations to investigate the effect of temperature were carried out according to the formulations presented in Table 5-1 using 1.8 mol% of HPO (with the redox pair Asc. Ac.) and 10 mol% of SDS in a batch process. The experimental procedure follows the standard batch process.

Effect of increasing polymer content. The polymerizations to investigate the effect of increasing polymer content were carried out in a batch process according to the formulations presented in Table 5-3. The experimental procedure follows the standard batch process, with the mass of Sty varied to study the effect of increasing polymer content under different conditions. The polymer content is defined as the ratio of the monomer mass (times the reaction conversion) to the total formulation mass.

102

Table 5-3. Formulations used for studying the effect of increasing polymer content

Component	Quantity
Water	179 g
SDS	5, or 15 wt%[a)]
Styrene	6-22 wt%[a)]
Initiator	1.8 or 4.8 mol%[b)]

[a)] relative to total mass of formulation; [b)] relative to monomer

Influence of the ionic strength. NaCl was used to increase the ionic strength of the formulations. The range of NaCl concentration studied using the standard batch process was from 0 to 2.0 wt% relative to water.

Effect of monomer composition. The effect of using the more hydrophilic monomer MMA (water solubility of 1500 mg/L at 20°C)[20] in place of Sty (solubility of 310 mg/L at 20°C),[21] was investigated using the formulations provided in Table 5-2, replacing Sty for MMA. Both batch and starved-feed semi-batch processes were studied, according to the procedures described above.

Characterizations. Conversion was measured by gravimetry. The Z-average particle size and Polydispersity Index (PdI) were measured by quasi-elastic light scattering (QELS) with Malvern Nanosizer ZS. The number of particles (Np) was calculated using the Z-average diameter of particles, the mass of monomer and instantaneous conversion. Surface coverage values are based on the surfactant concentration in the formulation and the total surface area of the particles in the latex, using a value of 0.5 nm^2/molecule of SDS.[22-24] Interfacial tension measurements follow the same procedure described in Chapter 3. Size exclusion chromatography (SEC) was performed to determine the molecular weight of the polymers using the same procedure described in Chapter 4.

5.4 Results and discussion

Influence of initiator concentration. Figure 5-1 presents the results of final average size of the polymer particles as a function of initiator concentration using the formulations presented in Table 5-1. The results show a decreasing trend in particle size with increasing initiator concentration all different initiator systems. For the same level of surfactant (10 mol%), the different initiators resulted in similar final particle sizes. No apparent effect was observed as a function of the radicals being negatively ($SO_4^{-\bullet}$) charged upon dissociation (the case for APS and KPS),[25, 26] or neutral ($OH^\bullet$) (the case for HPO).[19, 27] This is in agreement with the conclusions drawn by Boutti et al.[19] during a study comparing the interactions of APS and HPO with anionic and non-ionic surfactants in butyl acrylate and methyl methacrylate emulsion polymerizations.
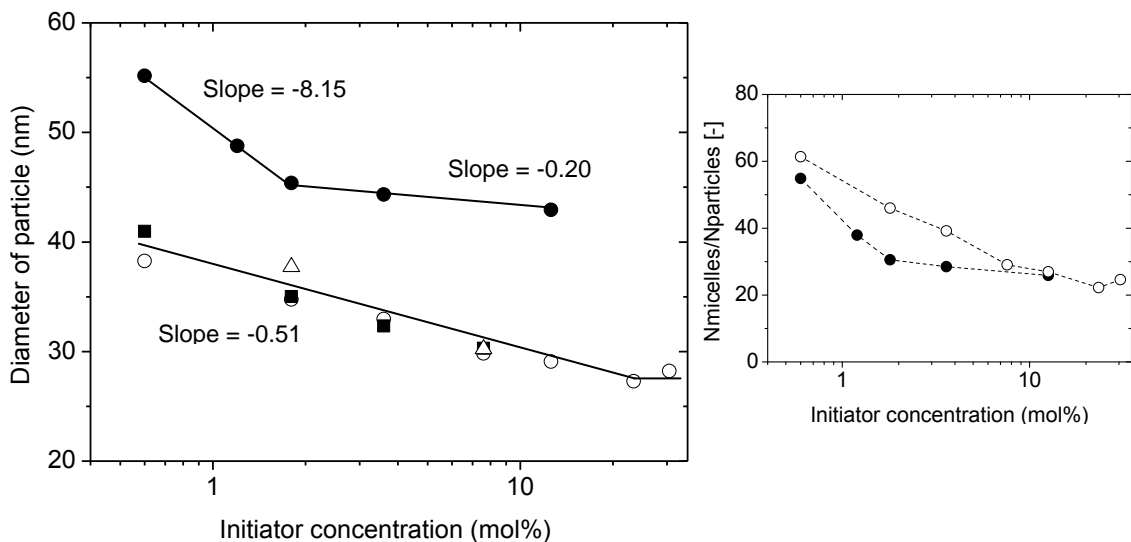
Figure 5-1. Influence of the initiator concentration on particle size of PS nano-latexes and the ratio of number of micelles to number of particles. Conditions are (●) HPO/ascorbic acid - [SDS] = 2.5 mol% to mon.; (○) HPO/ascorbic acid - [SDS] = 10 mol% to mon.; (■) KPS - [SDS] = 10 mol% to mon.; (Δ) APS - [SDS] = 10 mol% to mon.; the number of micelles was calculated assuming an aggregation number of 50.[28]

At the surfactant level of 2.5 mol%, the particle size reduction slope changes from -8.15 to -0.2 for [HPO] > 1.8 mol%. For the surfactant concentration of 10 mol%, the slope of -0.51 seems to change at [HPO] = 22 mol. The change in slopes occurs when the nucleation of particles approaches the number of micelles available at that particular surfactant concentration. As expected, the more surfactant present in the system, the higher the capacity of nucleating particles and, for the same solids content, the smaller the particle size. For the formulations using 2.5 mol% SDS, the results also show that the hydroxyl chain ends formed when using HPO as initiator have little or no surfactant properties. This is observed by the slope of decrease in particle size for HPO concentrations higher than 1.8 mol%, which is very low. Similar results were also observed by Hu et al.[17] in the study of the polymerization of styrene in emulsion using a UV light sensitive initiator, observing no significant increase in the stabilizing power of the formulations by the radicals generated from the decomposition of HPO.
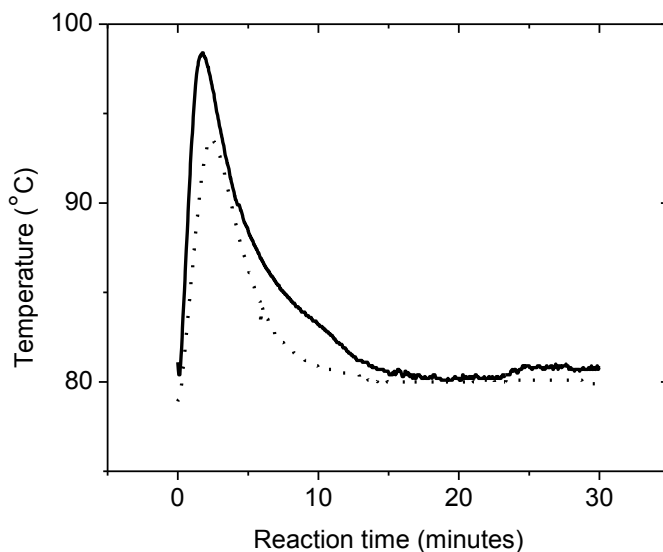
Figure 5-2. Temperature profiles of batch polymerization processes. Conditions: [SDS] = 10 mol% and [initiator] = 7.5 mol%; (——) HPO; (········) APS.

The temperature profile during the exothermic polymerization reaction[29] is monitored inside the reactor using a thermometer coupled to a computer. Figure 5-2 presents the temperature profile for the same reaction conditions, but two different initiators. The reaction initiated with HPO shows a slightly higher temperature peak compared to the KPS initiated reaction. This difference in the temperature profiles is attributed to the different mechanisms of initiator decomposition. Due to the redox reaction with Asc. Ac., HPO has practically instantaneous decomposition,[19, 27] versus a lower decomposition rate for KPS, which is a function of the temperature.[25, 26] The instantaneous high flux of radicals provided by the redox pair HPO/Asc. Ac. generated a higher rate of polymerization and therefore a higher heat release in the reactor compared to the slightly slower reaction that took place when using persulfate initiators. Nonetheless, the KPS decomposition becomes also quite fast because of an auto-catalytic effect, since the heat of reaction increases the temperature in the reactor and that increases the rate of initiator decomposition, causing a loop effect while there is still monomer left in the system. Thus, the slight difference between the two initiation systems is not noticeable in the final particle size obtained from these reactions, as shown in Figure 5-1. The temperature could be controlled and kept below boiling point of water in this small scale experiment as shown in Figure 5-2. For larger scale processes, it is believed that the temperature could be controlled by starting the reaction at lower temperatures and by the use of pressurized reactors. Since the monomer content of the formulations is relatively low (~17 wt%), the heat of reaction could be calculated to guarantee safe operation.

Figure 5-3 presents the molecular weight distributions of PS obtained using different HPO concentrations. As expected, increasing initiator concentration decreased the overall molecular weight of the final polymers.[30-32] Table 5-4, presents both the weight average molecular weight (M_w) and the number-average molecular weight (M_n) of the polymers obtained. Increasing [HPO]

from 0.6 mol% to 7.6 mol% decreased M_w one order of magnitude (factor >10). However, increasing [HPO] from 7.6 mol% to 30.6 mol% decreased M_w less significantly (factor of 4), probably due to a higher number of particles nucleated, increasing the segregation of the radicals in the system, even though a larger fraction of smaller polymer chains in the MWDs is seen in Figure 5-3. These high molecular weights component extends to 10^8 g/mol, outside the range of PS calibration used to calculate molecular weight averages. Thus, the numbers in Table 5-5 cannot be considered absolute, but are still useful for comparative purposes. As observed in Chapter 4, again the polydispersity values (M_w/M_n) were very high, much higher than normally observed from conventional free-radical emulsion[33] or microemulsion[12, 14] polymerization systems. It is believed that these high values of PDI could be related to the fact of being operating outside the range of calibration of the equipment. However, a significant reduction was observed as [HPO] was increased, indicating more narrow MWDs for higher initiator concentrations.
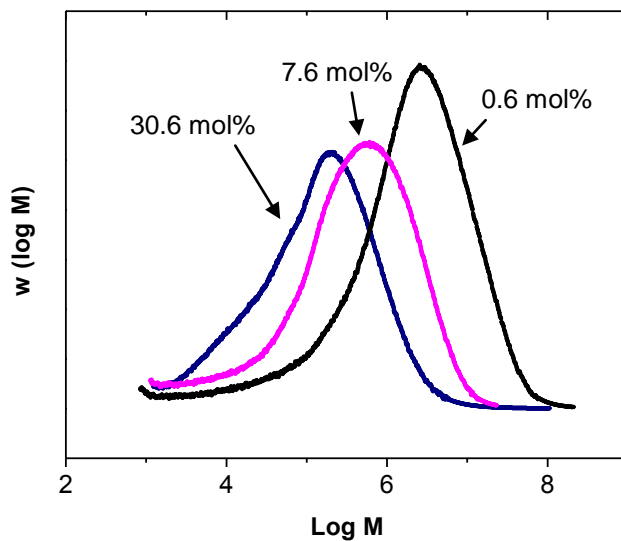
Figure 5-3. Molecular weight distribution of polymers synthesized using different initiator (HPO) concentrations. [SDS] kept constant at 10 mol%.

107

Table 5-4. Effect of increasing HPO concentration on the molecular weight of PS.

[HPO]	M_w	M_n	M_w/M_n
mol% to monomer	(g·mol^{-1} × 10^{-5})	(g·mol^{-1} × 10^{-5})	
0.6	43.4	0.6	72.3
7.6	8.7	0.4	21.8
30.6	3.6	0.3	12.0

The increase in initiator concentration reduces the particle size effectively and the nano-latexes are obtained much faster compared to the starved-feed process described in Chapter 3. The drawbacks of the approach described in this Chapter are the heat release and the reduction in the average molecular weight of the polymer. As we discussed, the heat release can be calculated and pressurized reactors (semi-adiabatic) can guarantee safe operations. The reduction in average molecular weight could be a constraint depending on the application. In our case it is not, but we decided to characterize for sake of completeness.

Effect of surfactant concentration. The influence of SDS concentration on the average particle size of the nano-latexes obtained is shown Figure 5-4 for batch and starved-feed processes. For batch processes, using the same initiator concentration, two distinct effects could be observed as the SDS concentration was increased. For relatively low SDS concentrations, more particles were nucleated as the surfactant concentration was increased and as a consequence smaller particles were obtained. At high SDS concentrations, the opposite effect was observed. These opposing effects can be explained by the fact that at relatively low SDS concentrations, as the surfactant concentration is increased more micelles are generated and therefore the probability of particles nucleation is increased. At higher surfactant concentration however, the micelles are believed to decrease in number and grow in size, from spherical aggregates to long rod- or thread-

like micelles.[28, 34] Therefore, as the micelles increase in size, they decrease in number, leading to the opposite effect from the one described before.
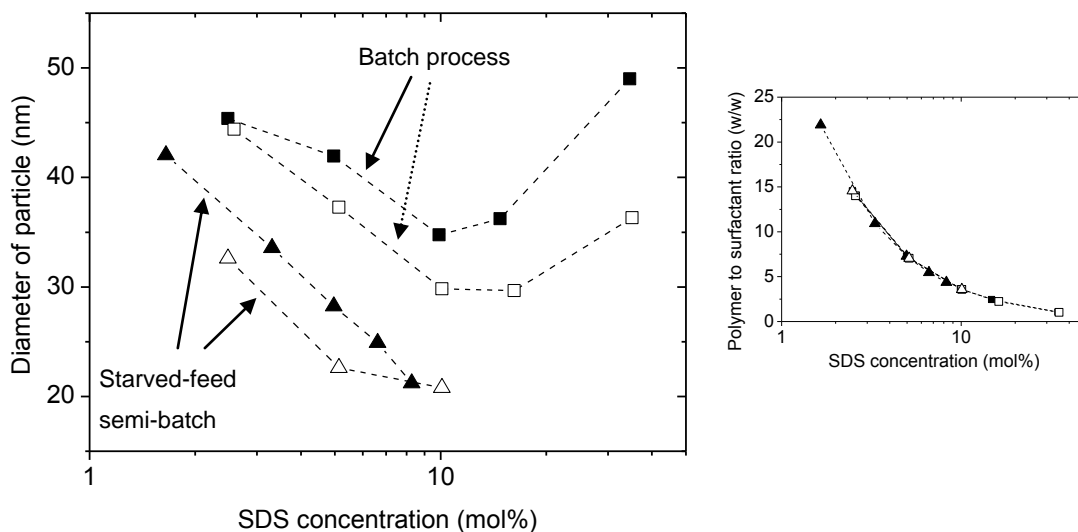
Figure 5-4. Effect of surfactant concentration on the average diameter of PS particles and polymer to surfactant ratio: (■) [HPO] = 1.8 mol%; (□) [HPO] = 7.1 mol%; (▲) [KPS] = 0.2 mol% (results presented in Chapter 3 and in Moraes et al.[6]); (△) [HPO] = 7.1 mol%.

Regarding the starved-feed process, for a fixed initiator concentration, average particle size diminishes as the SDS concentration is increased, as shown in Figure 5-4. In addition, at a fixed SDS concentration, a higher initiator concentration provides smaller particles, however the particle size difference seems to be less significant at high SDS concentrations, i.e. around 10 mol%. These results indicate that the process developed in Chapter 3 could be improved, producing smaller particles for the same level of surfactant, by increasing the initiator concentration.

In both processes, batch and starved-feed, the increase in initiator concentration has a noticeable influence on the particle size at the same SDS concentration. Smaller particle sizes are a consequence of higher nucleation efficiency resulting from a higher flux of radicals. Under

these conditions, PS particles with diameter < 30 nm were obtained with polymer to surfactant ratio of 3.6 and 7 for batch and starved-feed processes respectively.

For styrene polymerization it is believed that the nucleation occurs mainly via micellar entry because of its low water-solubility and high availability of micelles.[33] Figure 5-5 presents the ratio of the number of micelles in the initial formulation to the number of particles obtained at the end of the polymerization. The number of micelles was calculated assuming an aggregation number of 50.[28, 35] This is a reasonable assumption considering the high temperatures inside the reactor and how aggregation number of SDS responds to the increase in temperature.
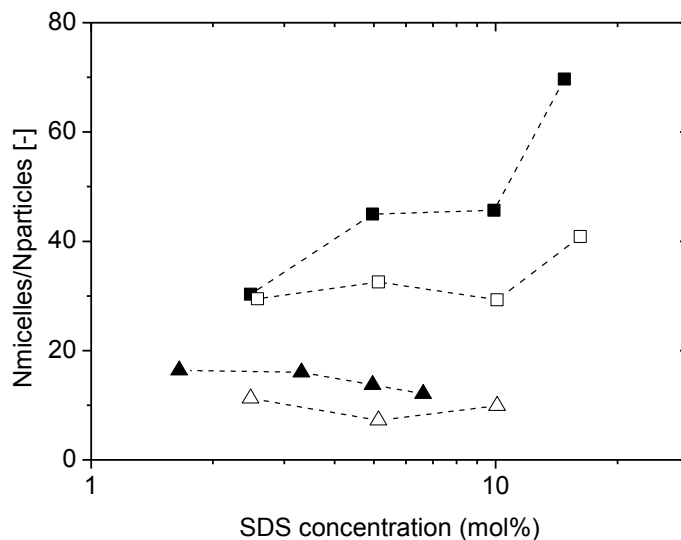
Figure 5-5. Effect of surfactant concentration on the number of micelles nucleated: (■) [HPO] = 1.8 mol%; (□) [HPO] = 7.1 mol%; (▲) [KPS] = 0.18 mol%; (Δ) [HPO] = 7.1 mol%; (square) batch process; (triangle) starved-feed semi-batch process.

In starved-feed process, one particle was nucleated for every 15-20 micelles, and for batch process, one particle was nucleated for every 35-40 micelles in the system. This shows that the

nucleation efficiency is still relatively low with respect to the number of micelles available and free surfactant exists at the end of the process.

Figure 5-6 presents the partial surface coverage of the particles by SDS. Surface coverage values are based on the surfactant concentration in the formulation and the total surface area of the particles in the latex, using a specific surface area coverage value of 0.5 nm^2/molecule of SDS.[22-24] Surface coverage values increase practically linearly with increasing [SDS] from 1.5 to 10 mol%, with different slopes for batch and starved-feed process. The lower slope of the starved-feed process confirms its higher efficiency in nucleating more particles for the same SDS concentration relative to the batch process. Coverage values above one (100%) obtained for high flux of radicals batch polymerization indicate the existence of excess of surfactant at the end of the synthesis.
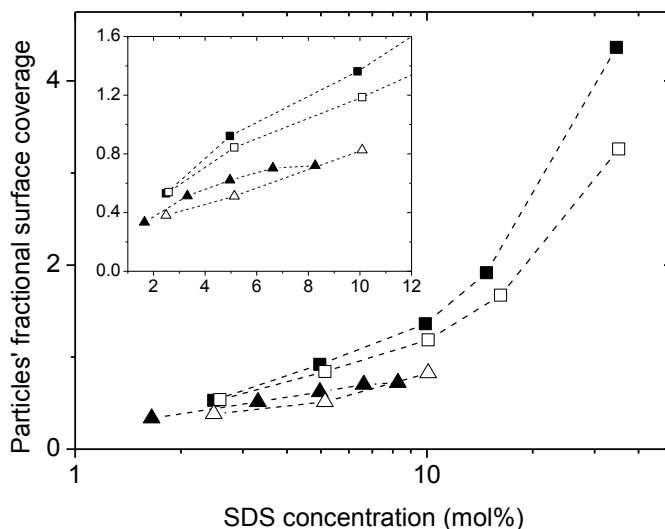
Figure 5-6. Effect of surfactant concentration on particles' fractional surface coverage: (■) [HPO] = 1.8 mol%; (□) [HPO] = 7.1 mol%; (▲) [KPS] = 0.18 mol%; (Δ) [HPO] = 7.1 mol%; (square) batch process; (triangle) starved-feed semi-batch process.

111

Effect of increasing polymer content. The effect of increasing monomer concentration on the particle size obtained at the end of the polymerizations is presented in Figure 5-7. Formulations with 15 mol% of SDS and 1.8 mol% HPO showed non-significant increments in particle size when the polymer content was increased from 6 wt% to 15 wt%. This enabled the increase in polymer to surfactant ratio from ~ 0.5 to 1.2 with no significant increase in particle size. The polymer to surfactant ratio for this formulation could not be increased any further because the formulations using this SDS concentration turned into a gel when the monomer content was increased. The gel formation is due to an organization of the surfactant micelles in a liquid crystalline structure to allow a better packing at high concentration[36-38] and it is observed for many surfactants, surfactant mixtures and microemulsion formulations, as was shown in Chapter 4.
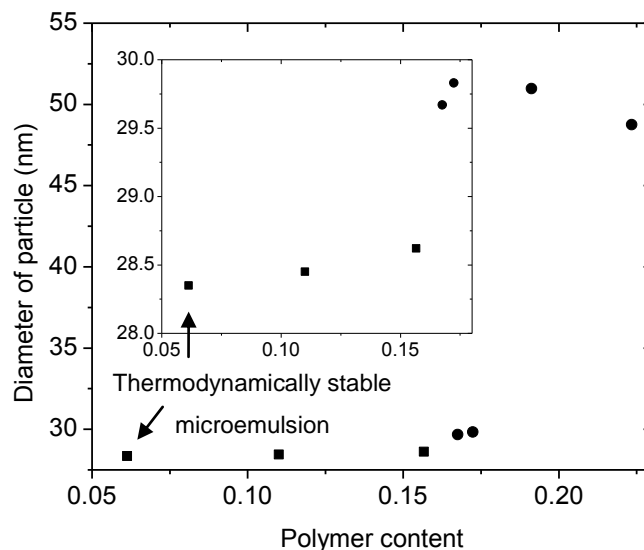
Figure 5-7. Effect of increasing polymer content: (■) [HPO] = 1.8 mol% and [SDS] = 15 wt% to total formulation; (●) [HPO] = 7.5 mol% and [SDS] = 4.8 wt% to total formulation.

In order to increase the polymer content, lower SDS concentrations (5 wt%) were used. Increasing polymer content from 16 wt% to 17 wt% increased particle size only by 1 nm, while

the polymer to surfactant ratio was increased from 1.2 to 2.2. However, increasing polymer content from 17 wt% to 18 wt% increased particle size an additional 20 nm, showing a strong sensitivity of the system to polymer contents above 17 wt% under these conditions.

Influence of temperature. The influence of the initial temperature on the particle size of the latexes obtained was studied at 50, 65 and 80°C, in a series of three experiments for each condition. Even though the temperature inside the reactor increases during polymerization (see Figure 5-2, the initial temperature will affect the extent to which the spike is observed. As shown in Table 5-5, average particle sizes decreased approximately 6 nm by increasing the temperature from 50 to 80°C.

Table 5-5. Relation between particle size and temperature.

Temperature (°C)	Dp (nm)	Variability out of two experiments (nm)
50	51.9	± 2.1
65	49.2	± 2.2
80	46.0	± 1.8

Conditions are: HPO/Asc. Ac., [HPO] = 1.8 mol% to monomer and [SDS] = 10 mol% to monomer

The decrease in particle size with increasing temperature observed could be explained by the fact that higher propagation rate coefficient (k_p)[39] and smaller micelles are obtained at higher temperatures,[28] which could increase the rate of particle nucleation via micellar entry. In addition, higher solubility and mobility of oligoradicals in the water phase are expected when the temperature is increased. These effects combined are known to enhance the generation of particles via homogeneous nucleation, producing smaller particles.[18] Sanghvi et al.[15] also observed the production of smaller particles at higher temperatures, but they attributed this

behavior to a higher flux of radicals formed from the decomposition of KPS at higher temperatures. This does not apply to the results presented here, since the kinetics of HPO/Asc. Ac. decomposition is not a function of the temperature.[19]

Influence of the ionic strength. The influence of increasing ionic strength of the formulation on the average particle size of the latexes obtained is presented in Figure 5-8. The ionic strength was increased by adding NaCl to the formulation. Formulations containing low surfactant concentration presented a higher sensitivity to the increase in the concentration of NaCl. When 2.5 mol% SDS was used the average particle size increased by about 10 nm (from ~46 nm to ~56 nm) by increasing the NaCl concentration from 0 to 0.03 wt%. This result could be attributed to the fact that colloidal systems stabilized by ionic surfactants are known to suffer loss of stability when electrolyte concentration is increased,[40] due to the compression of the electrical double layer and loss of electrostatic repulsion capacity between particles, making them more susceptible to coagulative nucleation or coagulative particle growth.[41] At higher SDS concentrations (10 mol%), the effect of increasing ionic strength was not as important as would be expected. A small increase (less than 5 nm) in particle size was observed for formulations using [HPO] = 7.1 mol% when increasing NaCl concentration, probably due to the large excess of surfactant in the system, minimizing destabilization effects at these conditions.

Increasing electrolyte concentration decreases the CMC, size and aggregation number of SDS micelles,[28] and therefore increase the number of micelles for a fixed surfactant concentration. Thus, increasing electrolyte concentration can potentially increase the number of particles nucleated. Full et al.[42] observed a decrease in particle size in the microemulsion polymerization of Sty with increasing the concentration of electrolytes (KBr, KCl or K_2SO_4), using DTAB (CMC = 0.015 mol/L, pure water)[43] or DTAC as surfactants. Dunn and Said[44] studied the effect of increasing electrolyte (KCl) concentration on the emulsion polymerization of Sty and noticed a

decrease in particle size when using potassium decanoate as surfactant (which has high CMC, 0.1 mol/L, pure water)[45] and an increase in particle size when using potassium octadecanoate as surfactant (which has low CMC, 0.0004 mol/L, pure water). The latter study indicates that the change in the micellization properties with increasing electrolyte concentration is less significant for surfactants which have low values of CMC, and is in agreement with our results since SDS is a low CMC surfactant (0.0082 mol/L, pure water).[46]
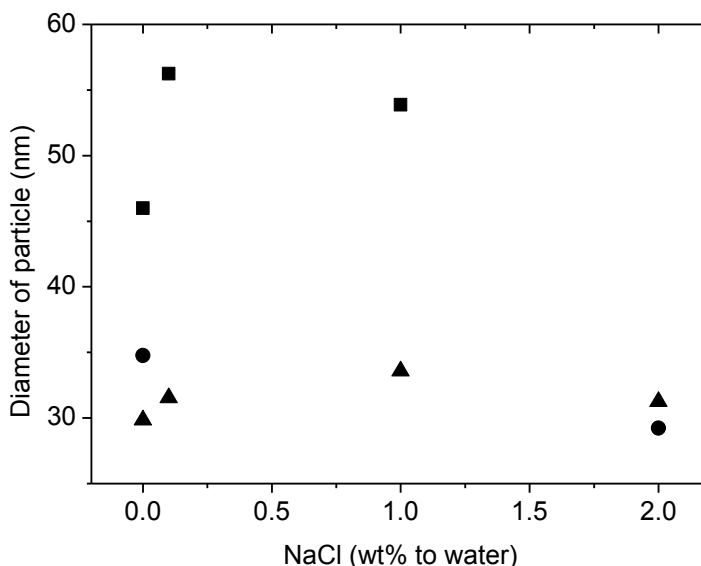
Figure 5-8. Influence of the ionic strength on the average diameter of PS particles. Conditions: (■) [HPO] = 1.8 mol% and [SDS] = 2.5 mol%;(●) [HPO] = 1.8 mol% and [SDS] = 10 mol%; (▲) [HPO] = 7.1 mol% and [SDS] = 10 mol%.

Effect of monomer composition. In order to study the effect of the monomer composition on the results obtained for styrene polymerizations, MMA was used as an example of a more water soluble monomer. Figure 5-9 presents the average particle sizes obtained at different conditions using both Sty and MMA.
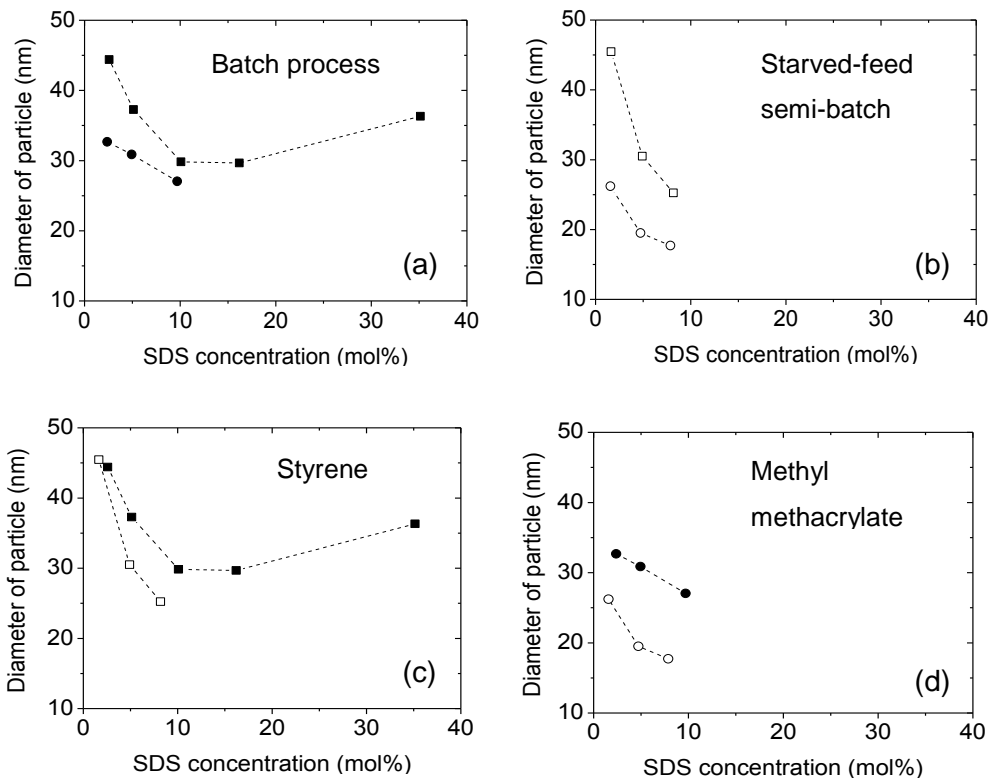
Figure 5-9. Effect of monomer composition and process type on the latex particle size: (square) Sty; (circle) MMA; (solid symbols) batch process; (hollow symbols) starved-feed semi-batch process. Conditions: [HPO] = 7.1 mol% (batch process); [KPS] = 0.18 mol% (semi-batch process).

As shown, independent of the technique used (starved-feed or high flux of free radicals batch process), smaller particle sizes were obtained with MMA compared to styrene at the same surfactant level. The difference in the results of average particle sizes can be attributed to the difference in interfacial tension monomer/water observed for these two monomers, as presented in Table 5-6. This difference in interfacial tension monomer/water observed for styrene and MMA plays a significant role in the emulsion stability. Lower interfacial tension emulsions require less surfactant to stabilize the same surface area. Therefore, MMA emulsions are able to produce smaller particles.[47] To some extent, the smaller particle size can also be attributed to an

increased importance of homogeneous nucleation with MMA as compared to styrene, because of its higher water solubility.[18, 33, 48, 49] The particles nucleated via homogeneous nucleation are likely to be smaller than those nucleated through micellar nucleation, in addition the monomer concentration inside the micelle is likely to be higher, improving the chances of particle growth, as discussed by He and co workers,[48, 49] in their study on the production of small PMMA-PS particles.

Table 5-6. Oil-water interfacial tension of monomers at room temperature (25°C).

Monomer	mN/m	Deviation of 10 measurements
Styrene	25.89	0.06
Methyl methacrylate	10.24	0.22

5.5 Conclusions

Modified (micro)emulsion polymerization approaches were investigated for the production of enhanced polymer to surfactant ratio nano-latexes. The influence of parameters such as SDS concentration, initiator (APS, KPS and HPO/Asc. Ac.) concentration, temperature of polymerization, ionic strength and polymer content in the formulations were studied and discussed. It was shown that by increasing the flux of free radicals, it is possible to decrease average particle size in (micro)emulsion polymerization for the same concentration of surfactant (SDS). The use of high concentrations of initiators enabled the production of nano-latexes with particle sizes smaller than 50 nm and a polymer to surfactant ratio of 15-20.

At high SDS concentration, increasing ionic strength had a minor effect in particle size of the latexes obtained. With increasing temperature, smaller particle sizes were obtained, however, at 90°C auto polymerization of styrene was observed causing the results to lose efficiency. Starved-

feed process produced smaller particle sizes for the same SDS concentrations; however, the high radical flux batch polymerizations are extremely interesting due to the reduced time required for the process completion compared to starved-feed process. Due to the high reaction rates obtained, high temperatures were observed inside the reaction vessel, although this could be controlled by using lower initial temperatures and pressurized reactors in large scale operations.

When using batch polymerization, the smallest particle size obtained was ~30 nm and 27 nm for styrene and MMA respectively, with a polymer to surfactant ratio of 5. Starved-feed semi-continuous emulsion polymerization developed in Chapter 3 was shown to produce smaller particle size latexes for the same level of surfactant by increasing the initiator concentration. The smallest particle size obtained using this process was 21 nm and 17 nm for styrene and MMA respectively, with a polymer to surfactant ratio of 8.

In terms of the overall project objective, this Chapter have shown an alternative methodology to produce the small particles with significant efficiency in terms of latex concentration, particle size and surfactant concentration. This methodology was used with success to the production of the small particles population in Chapter 6. In addition, the results presented here showed that MMA could be used as an alternative monomer to produce smaller particles compared to styrene for the same surfactant concentration. Even though this strategy was not fully explored in this project because it was out of the scope, this topic is proposed for future developments in Chapter 8.

References

1. Pavel, F. M. *Journal of Dispersion Science and Technology* **2004***, 1,* 1-16.

2. Chow, P. Y.; Gan, L. M. *Advances in Polymer Science* **2005**, 257-298.

3. Sanghvi, P.; Devi, S. *Int. J. Polym. Mater.* **2005***, 4,* 293-303.

4. Gupta, A. K.; Wells, S. *IEEE Trans Nanobioscience* **2004***, 1,* 66-73.

5. Reddy, K. R.; Sin, B. C.; Yoo, C. H.; Sohn, D.; Lee, Y. *J. Colloid Interface Sci.* **2009***, 2,* 160-165.

6. Moraes, R. P.; Hutchinson, R. A.; McKenna, T. F. L. *J. Polym Sci. Part A: Polym. Chem.* **2010**, 48.

7. Norakankorn, C.; Pan, Q.; Rempel, G. L.; Kiatkamjornwong, S. *J. Appl. Polym. Sci.* **2010***, 3,* 1291-1298.

8. Chen, W.; Liu, X.; Liu, Y.; Bang, Y.; Kim, H. *Colloids Surf. , A* **2010***, 1-3,* 145-150.

9. Smeets, N. M. B.; Moraes, R. P.; Wood, J. A.; McKenna, T. F. L. *Langmuir* **2011***, 2,* 575-581.

10. Pepels, M. P. F.; Holdsworth, C. I.; Pascual, S.; Monteiro, M. J. *Macromolecules (Washington, DC, U. S.)* **2010***, 18,* 7565-7576.

11. Antonietti, M.; Landfester, K. *Prog.Polym.Sci.* **2002***, 4,* 689-757.

12. Guo, J. S.; El-Aasser, M. S.; Vanderhoff, J. W. *J. Polym. Sci. A Polym. Chem.* **1989***, 2,* 691-710.

13. Guo, J. S.; Sudol, E. D.; Vanderhoff, J. W.; El-Aasser, M. S. *J. Polym. Sci. , Part A: Polym. Chem.* **1992***, 5,* 691-702.

14. Puig, J. E.; Perez-Luna, V. H.; Perez-Gonzalez, M.; Macias, E. R.; Rodriguez, B. E.; Kaler, E. W. *Colloid Polym. Sci.* **1993***, 2,* 114-123.

15. Sanghvi, P. G.; Pokhriyal, N. K.; Devi, S. *Polym. Int.* **2002***, 8,* 721-728.

16. Chen, J.; Qiao, J.; Zhang, Z.; Zhang, Q. *Polym. Bull. (Heidelberg, Ger.)* , No pp. yet given.

17. Hu, X.; Zhang, J.; Yang, W. *Polymer* **2009***, 1,* 141-147.

18. Pusch, J.; van Herk, A. M. *Macromolecules* **2005***, 16,* 6939-6945.

19. Boutti, S.; Zafra, R. D.; Graillat, C.; McKenna, T. F. *Macromol. Chem. Phys.* **2005**, *14,* 1355-1372.

20. Chai, X. -.; Hou, Q. X.; Schork, F. J. *J. Appl. Polym. Sci.* **2006**, *3,* 1296-1301.

21. Lane, W. H. *Ind. Eng. Chem. , Anal. Ed.* **1946**, 295-296.

22. Vijayendran, B. R. *J. Appl. Polym. Sci.* **1979**, *3,* 733-742.

23. Guo, J. S.; El-Aasser, M. S.; Sudol, E. D.; Yue, H. J.; Vanderhoff, J. W. *J. Colloid Interface Sci.* **1990**, *1,* 175-184.

24. Santos, A. F.; Lima, E. L.; Pinto, J. C.; Graillat, C.; McKenna, T. *J. Appl. Polym. Sci.* **2003**, *5,* 1213-1226.

25. Okubo, M.; Fujimura, M.; Mori, T. *Colloid Polym. Sci.* **1991**, *2,* 121-123.

26. Santos, A. M.; Vindevoghel, P.; Graillat, C.; Guyot, A.; Guillot, J. *J.Polym.Sci., Part A: Polym.Chem.* **1996**, *7,* 1271-1281.

27. Schneider, M.; Graillat, C.; Boutti, S.; McKenna, T. F. *Polym.Bull.(Berlin, Ger.)* **2001**, *3-4,* 269-275.

28. Mazer, N. A.; Carey, M. C.; Benedek, G. B. The size, shape and thermodynamics of sodium dodecyl sulfate (SDS) micelles using quasielastic light scattering spectroscopy. In *Micellization, Solubilization, and Microemulsions;* Mittal, K. L., Ed.; Plenum Press: New York and London, 1976; pp 359-381.

29. Esposito, M.; Sayer, C.; Hermes de Araujo, P. H. *Macromol. React. Eng.* **2010**, *11-12,* 682-690.

30. Hutchinson, R. A. Free-radical polymerization: Homogenenous. In *Handbook of polymer reaction engineering;* Meyer, T., Keurentjes, J., Eds.; Wiley-VCH: Weinheim, 2005.

31. Chern, C. *Principles and applications of emulsion polymerization;* Wiley: Hoboken, N.J., 2008.

32. De La Cal, J.; Leiza, J. R.; Asua, J. M.; Butte, A.; Storti, G.; Morbidelli, M. Emulsion Polymerization. In *Handbook of Polymer Reaction Engineering;* Meyer, T., Keurentjes, J., Eds.; Wiley-VCH: Weinheim, 2005; Vol. 1.

33. Gilbert, R. G. *Emulsion Polymerization, a mechanistic approach;* Academic Press: London, 1995.

34. Jonsson, B.; Lidman, B.; Holmberg, K.; Kronberg, B. *Surfactants and polymers in aqueous solution;* John Wiley & Sons: New York, 1998.

35. Shah, S. S.; Jamroz, N. U.; Sharif, Q. M. *Colloids Surf. , A* **2001***, 1-3,* 199-206.

36. Winsor, P. A. *Solvent properties of amphiphilic compounds.* Butterworths Scientific Publications: London, 1954.

37. Rodrigues, C.; Kunieda, H. Phase Behavior and Microstructure of Liquid Crystals in Mixed Surfactant Systems. In *Mixed surfactant systems.* Abe, M., Scamehorn, J. F., Eds.; Marcel Dekker: New York, 2005.

38. Alany, R. G.; El Marghraby, G. M.; Krauel-Goellner, K.; Graf, A. Microemulsion Systems and Their Potential as Drug Carriers. In *Microemulsions properties and applications;* Fanun, M., Ed.; Taylor & Francis: Boca Raton, Fla., 2008.

39. Brandrup, J.; Immergut, E. H.; Grulke, E. A. *Polymer Handbook;* John Wiley&Sons: New York, 2003.

40. Fortuny, M.; Graillat, C.; McKenna, T. F. *Ind. Eng. Chem. Res.* **2004***, 23,* 7210-7219.

41. Lovell, P. A.; El-Aasser, M. S. In *Emulsion Polymerization and Emulsion Polymers.* John Wiley & Sons: Chichester, 1997.

42. Full, A. P.; Kaler, E. W.; Arellano, J.; Puig, J. E. *Macromolecules* **1996***, 8,* 2764-2775.

43. Schulz, P. C.; Morini, M. A.; Minardi, R. M.; Puig, J. E. *Colloid Polym. Sci.* **1995***, 10,* 959-966.

44. Dunn, A. S.; Said, Z. F. M. *Polymer* **1982**, *8,* 1172-1176.

45. Maa, Y. F.; Chen, S. H. *J. Colloid Interface Sci.* **1987**, *2,* 437-442.

46. Bales, B. L.; Messina, L.; Vidal, A.; Peric, M.; Nascimento, O. R. *J Phys Chem B* **1998**, *50,* 10347-10358.

47. Cosgrove, T.; Knovel. *Colloid science principles, methods and applications.* Blackwell Pub.: Oxford, 2005.

48. He, G.; Pan, Q. *Macromol.Rapid Commun.* **2004**, *17,* 1545-1548.

49. He, G.; Pan, Q.; Rempel, G. L. *Macromol.Rapid Commun.* **2003**, *9,* 585-588.

Chapter 6

Large mode and unseeded approach production of bimodal latex – Re-nucleation *in situ* of the small particles population

6.1 Abstract

High solids content low viscosity bimodal PS latexes with overall particle distribution <200 nm were obtained using two modified (micro)emulsion polymerization approaches. As a first step, large particles latex was produced with a concentration of 52.7 wt% solids content. The second family of particles was produced by addition of surfactant followed by either starved-feed microemulsion polymerization or using single addition of the monomer and initiator. Both methods led to the production of small particles in the range of 10-30 nm in the presence of the large particles. Bimodal latexes with 60 wt% solids content were produced with viscosity of 490 mPa•s at 20 s^{-1}.
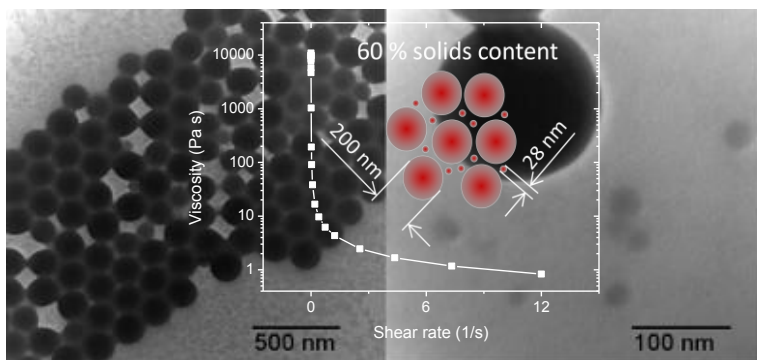
6.2 Introduction

High solids content (HSC) latexes generally refer to products in which the polymer content is equal to or higher than 60 wt% in a continuous aqueous phase. These products are useful for a number of economic and application-related reasons.[1-3] As discussed in Chapters 1 and 2, a considerable fraction of the worldwide latex production is applied as paper coating[4] and for this application the average particle size of the latex should be smaller than 200 nm. Such commodity products require high speed application and low viscosity to allow even film formation.

Our objective is to increase solids content from what is currently possible for paper coating applications from ~50 wt% to ~60 wt%. Therefore, the challenge while increasing the solids content of this type of latex product is to keep viscosity levels as low as possible.

A proven method to increase solids content while maintaining low viscosity is to create a latex with a bimodal particle size distribution (PSD)[5-9] such that, simply speaking, the small particles fit in the spaces between the big particles. Since, as was discussed in Chapters 1 and 2, the thickness of the EDL is independent of particle size, as particle size decreases (increasing ratio of particle surface area to volume), the maximum packing fraction of a latex in terms of solids content decreases[2] because the stabilization layer takes up relatively more space. The literature shows different results of HSC latexes for different ranges of PSD. For instance, Boutti et al.[10] obtained solids content of 77 wt% and viscosity lower than 1500 mPa•s at 20 s^{-1} in the production of a bimodal latex with particle sizes of 1109 and 210 nm. Schneider et al.[11] obtained 73 wt% solids content with viscosity of 820 mPa•s at 20 s^{-1} for a bimodal latex with particles of 900 and 75 nm. However, Mariz et al.[3] showed that it is very difficult to obtain such values when working with small latex products. In their work, they were able to make bimodal latexes of poly(MMA/BA/MAA) with 65 wt% solids content with particles of 270 and 60 nm and viscosity of 500 mPa•s at 20 s^{-1}.

For better rheological properties, the ratio of the effective diameter of large to small particles (Dp_L/Dp_S) should be larger than 6.5 and the volume fraction of the large mode (ϕ_L) should represent about 80% of the total dispersed phase.[5, 9, 12, 13] Therefore, in order to achieve the lowest possible viscosity, the second population of particles should be smaller than 30 nm.

In this Chapter, we develop a methodology to first produce the base latex that will compose the population of large particles. This latex corresponds to a commercially available paper coating product, being monodisperse of about 50 wt% SC and having average particle size of 195 nm. Then we further concentrate this latex to about 60 wt% by creating a second population of small particle size, using the methodologies developed in Chapters 3 and 5.

The innovative aspect related to adapting this renucleation approach to our product, apart from the challenge of implementing this approach to significant smaller particle sizes, is that the objective in our case is to nucleate the extremely small (< 30 nm) family of particles and keep them as small as possible, being the renucleation the final step in the process, with no further concentration and growth of any of the families of particles.

6.3 Experimental

Materials. Styrene (99+%), hydrogen peroxide (HPO, 30 wt% solution in water) and ascorbic acid (Asc. Ac., 97+%) from Sigma-Aldrich, sodium dodecyl sulfate (SDS, 99+%) from MP Biomedical, Disponil FES77 (33.1 wt% solution in water) from Cognis and sodium chloride (NaCl, 95%) from Fisher Scientific, were used as received. Reactions were carried out in jacketed glass reactors, 1.5 L and 250 mL, equipped with anchor and radial blade impellers respectively, temperature controller and condenser. Deionized water (Millipore – Synergy Ultrapure) was used in all manipulations. All reactions began with an N_2 purge for 30 minutes prior to start-up and were maintained a blanket of N_2 during the entire process.

Synthesis of large particle population. Polystyrene (PS) seed latex containing particles of 38 nm in diameter were produced using the procedure described in Chapter 3 and in Moraes et al.[14] to a solids content of 33.5 wt%. 4.1 g of this mixture was further polymerized by semi-continuous emulsion polymerization at 90°C to a final volume of 1 L, a solids content of 52.7 wt% and an average particle size of 195 nm with low polydispersity index (PdI), smaller than 0.050. Details of this recipe are reported in Table 6-1.

Table 6-1. Recipe for the synthesis 1 L, 52.7 wt% solids content large particles latex.

| Components | Reactor heel (g) | Semi-continuous addition | | | | | | Initiator solution (g) (3.5h) |
| | | Preemulsion (g) | | | | | | |
		0.5h	1h	1.5h	2h	2.5h	3h	
seeds[a]	4.1	-	-	-	-	-	-	-
water	100.0	43.6	52.0	52.6	51.7	52.2	52.2	40.0
FES77[b]	-	19.7	7.4	6.2	7.4	6.7	6.3	-
styrene	-	86.6	86.6	86.6	86.6	86.6	86.6	-
HPO[c]	-	0.14	0.14	0.14	0.14	0.14	0.14	-
Asc. Ac.	-	-	-	-	-	-	-	0.52

[a] Corresponds to the mass of 33.5 wt% solids content seed latex with average particle size of 38 nm, produced according to a process described earlier in Chapter 3 and in Moraes et al. 2010[14]; [b] Corresponds to the mass of 33.1 wt% surfactant solution as provided by supplier; [c] Corresponds to the mass of 30 wt% HPO solution as provided by supplier.

The preemulsion (PE) semi-continuous addition lasted 3 hours, divided into 6 fractions of 0.5 hours. More information regarding development of the production process of the large mode can be found in Appendix C. We chose to present this information in the appendix because it is non-essential for the discussion of the results in this Chapter. This process used a constant styrene addition rate and a variable surfactant addition rate in order to maintain surfactant coverage of approximately 45%, assuming specific surface area coverage of 1 nm^2 per molecule of FES77, as reported for surfactants with similar structure.[15] The initiator system was the redox pair HPO/Asc. Ac., using a mass ratio of 1:2,[16] and HPO concentration of 0.05 wt% to monomer mass. The HPO was added as part of the PE continuous addition. The Asc. Ac. was solubilized in 40 g of H$_2$O and added continuously over 3.5 hours. This methodology for producing the so-called "large particles" latex showed good reproducibility.

In situ generation of small particles population. The small particles, ranging from 10-30 nm in diameter, were synthesized in the presence of the large particles using two modified procedures, starved-feed semi-continuous microemulsion (developed in Chapter 3) polymerization and monomer+initiator shot (developed in Chapter 5), as described below. The fraction of the large particles latex used for this final step is specified in the recipes presented in Table 6-2. Both methods led to similar results and were reproducible. In order to minimize the addition of water and achieve high-solids content, the SDS was added to the reactor in powder form. This "dry SDS shot" step was done slowly with the reactor at room temperature to avoid water evaporation and stirred to provide sufficient latex mixing. Non-uniform mixing and localized accumulation of SDS could lead to coagulation of the latex particles by both water absorption (excessive concentration) and local increase of the ionic strength of the dispersion leading to stability problems. In addition, 0.03 wt% NaCl (relative to water) was added to decrease the latex viscosity, as discussed below.

Table 6-2. Recipes for nucleation of small particles population

Component/location		Starved-feed	Monomer + initiator shot
		Mass (g)	
reactor heel	Large particles latex[a]	200	
	SDS[b]	4.78	
	Asc. Ac.[b]	0.057	2.65
posterior addition	Styrene	34.22	
	HPO[c]	0.034	1.59

[a] Large particles latex as described in experimental part, mass corresponds to the latex at 52.7 wt%; [b] "Dry shot" at room temperature and under mixing; [c] Corresponds to the mass of 30 wt% HPO solution as provided by supplier.

Starved-feed approach. The initiator system was used in the same proportion as for the growth of the large particles (0.05 wt% to monomer), with the difference that the Asc. Ac. was added to the reactor as a "dry shot" with the SDS. The reactor temperature was increased to 80°C, then the mass of styrene (Table 6-2) was added over a 2 h period. The HPO mass was diluted in 5 g of H_2O and added over a 2.5 h period.

Monomer + initiator shot approach. The same initiator system was used, however at a higher concentration, 4.6 wt% HPO relative to styrene (Table 6-2). The Asc. Ac. was added as a "dry shot" with the SDS. The reactor temperature was increased to 60°C, at which point the mass of styrene was added at once followed by the mass of HPO. The reactor jacket was kept at 60°C during the reaction (30 minutes), even though the temperature inside the reactor increased at the beginning, as will be reported in the results and discussion session.

Characterization. The latexes' conversion was followed by gravimetry. Particle sizes were measured by dynamic light scattering (DLS), Malvern Zeta-Sizer Nano ZS, and transmission electron microscopy (TEM), in a Philips CM20 operated at 80 KeV. Reactor temperature data was recorded using datalogging thermometer (Sper Scientific, model 800005) coupled to a computer. Rheology profiles of the latexes were obtained in a Viscotech by Reologica Instruments rheometer in the constant rate mode, in the shear rate range from 0.001 to 10 s^{-1}, using a concentric cylinder set up at room temperature.

6.4 Results and Discussion

Large particle population. The evolution of latex parameters during the synthesis of the large particles latex is shown in Figure 6-1 (a). One third of the total number of particles (Np) required was introduced to the reactor as the 38 nm seeds, and the other two thirds were nucleated within the first 0.5 hours of PE addition. After nucleation, the total NP in the reactor was kept reasonably constant during the growth of the seeds and concentration of the latex up to 52.7 wt%. The evolution of PSD during the growth of the large particles latex is shown in Figure 6-1 (b). The narrow PSD is reflected in the low values of PdI obtained from the DLS measurements, in the order of 0.030 for the final sample.

Attempts to further increase the concentration of the large mode monomodal latex failed; the highest solids content obtained before latex coagulation was 53.9 wt%.
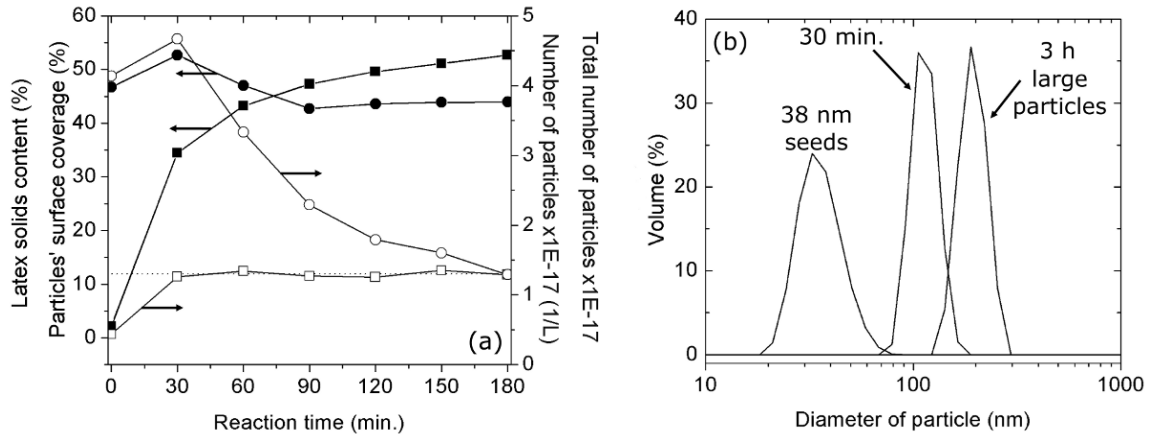
Figure 6-1. (a) Evolution of latex parameters with polymerization time: [■] latex solids content, [●] particles' surface coverage by surfactants, [□] number of particles per liter of latex, [○] total number of particles in the reactor, [····] targeted number of particles, and (b) PSD of large particles during the growth of the large particles.

Bimodal latexes. The recipes in Table 6-2 were designed to achieve final solids content of 60 wt%. Both methods used to synthesize the small particles population in the presence of the large particles led to similar results. The starved-feed microemulsion polymerization requires less initiator and more time. The monomer + initiator shot approach requires less time; however, the initiator concentration is considerably higher and the heat removal is a concern. The extremely fast reaction releases considerable thermal energy, as shown in Figure 6-2. It can be seen that there is a sharp increase of about 25°C over a 4 minute period. While this type of temperature profile can be controlled at the laboratory scale, this option is less feasible at large scales since the heat removal capacity decreases as the reactor size increases. However, it is possible that this issue can be overcome by using lower initial temperature and pressurized reactors, since the mass of monomer to be polymerized is relatively not very large compared to the mass of latex.

The bimodal latexes were examined via TEM, as presented in Figure 6-3. DLS was also used; however, the instrument did not detect the small population. This is not unexpected as it is well known (more information about this topic can be found in Appendix D) that large particles can

mask the smaller ones in DLS analyses.[17] For both approaches, DLS records particle size distributions very similar to that of the starting large particle population ($\pm$ 2-3 nm for starved feed, $\pm$ 2-8 for monomer + initiator shot), with low PdI. Even using TEM (Figure 6-3), visualization of the small particles is difficult due to the lack of contrast observed. As shown in the images, the large particles are very monodisperse around 200 nm, and the small particles are as small as 10 nm. These images, plus a simple mass balance proves that small particles are created in the second step of each approach. If no small particles were nucleated, the diameter of the large particles would grow by 22-25 nm with the monomer added, which they clearly do not do.
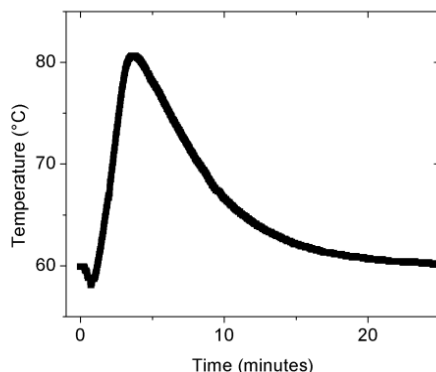
Figure 6-2. Evolution of reactor temperature with reaction time during the synthesis of the small particles using monomer + initiator shot modified (micro)emulsion polymerization.

As shown in the rheological profile in Figure 6-4, these 60 wt% bimodal latexes with final ratio of surfactant to polymer of 6.6 wt% have viscosity of 490 mPa•s at 20 s^{-1}. The rheological profiles of the large particles latex, at low (6 x10^{-3} mol•L^{-1}) and high ionic strength (I)[3] (1.1 x10^{-2} mol•L^{-1}), are also shown in Figure 6-4 for reference. As expected, the increased I decreased the thickness of the EDL and thus decreased the viscosity of the large particles latex. As can be seen

---

[3] The latexes ionic strengths were calculated using the IUPAC recommendations.[19] It should be noted that it neglected Asc. Ac. partial ionization and free surfactant molecules in the water phase.

in Figure 6-4, increasing the solids content from 52.7 to 60 wt% with the second population of small particles did not increase viscosity significantly.
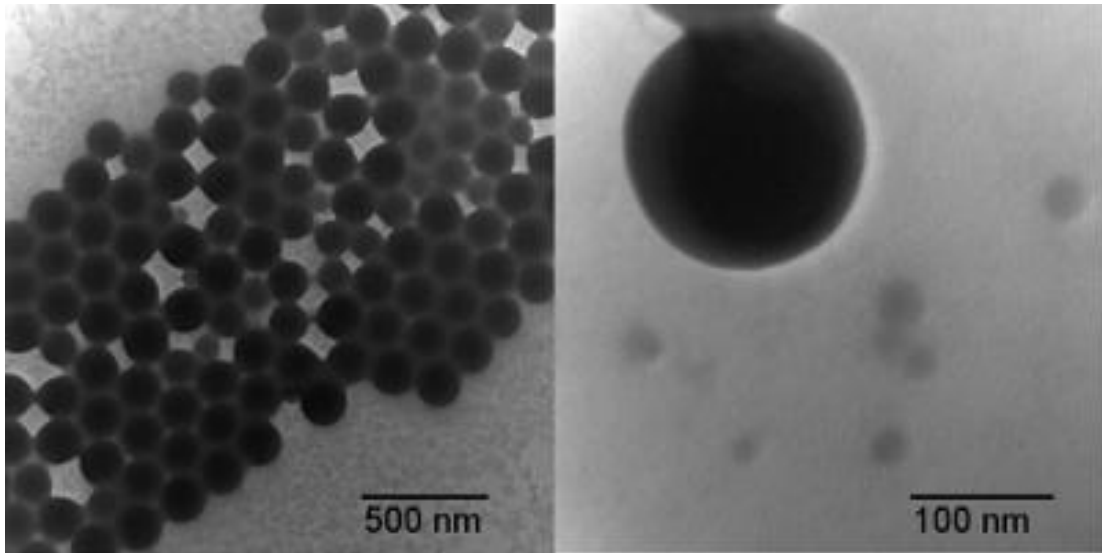
Figure 6-3. TEM characterizations of bimodal latexes
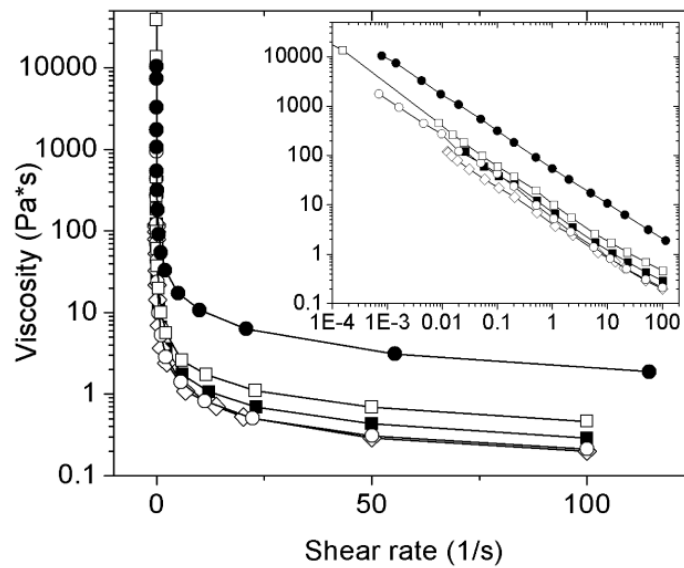
Figure 6-4. Rheological profiles of the latexes obtained: [◊] 52.7 % large particles - I = 1.1 x10^{-2} mol•L^{-1}, [○] 60 % bimodal - I = 1.1 x10^{-2} mol•L^{-1}, [■] 52.7 % large particles - I = 6 x10^{-3} mol•L^{-1}, [□] 53.9 % monomodal, [●] 62.2 % bimodal - I = 1.1 x10^{-2} mol•L^{-1} (solids content on a w/w basis)

Attempts to bring the bimodal latex to 65 wt% were unsuccessful using both methods, with coagulation occurring. The highest solids content obtained was 62.2 wt% using the starved-feed approach, the rheological profile of which is also shown in Figure 6-4. A significant increase in the latex viscosity was observed, an indication that the latex concentration was very close to the maximum packing fraction[13] such that any additional increase in volume fraction decreases colloidal stability due to the crowding effect.[18]

The EDL thickness was calculated using Equation 6 (Chapter 2), and found to be $\delta = 3.9$ nm and 2.9 nm for the low (6 x10^{-3} mol•L^{-1}) and high ionic strengths (1.1 x10^{-2} mol•L^{-1}) respectively. Thus, the maximum solids content of a particular ideal bimodal system can be estimated (adopting $\delta = 3$ nm for sake of simplicity). Assuming that the large ($_L$) and small ($_S$) particles are perfectly monomodal hard spheres of 200 nm and 28 nm respectively, the relative volume fraction occupied by the EDL of each population, is calculated by:

$$\left(\frac{V_\delta}{V_p}\right) = \frac{(r_p + \delta)^3 - r_p^{\ 3}}{(r_p + \delta)^3} \tag{14}$$

where r_p and $(r_p+\delta)$ are the particle radius and effective radius (including EDL), respectively.

Even though the thickness of the EDL is only 3 nm, it occupies 44% of the volume taken up by the small (28 nm) particles, while for the large (200 nm) particles the volume fraction taken by the EDL is 8.5%. Using Greenwood et al.'s approach,[5] assuming random loose packing ($\phi_{rlp} = 0.589$) for the large particles and simple cubic packing ($\phi_{scp} = 0.524$) for the small particles in the voids, we have a maximum bimodal packing fraction (ϕ_{max}, v/v) of this specific latex as

$$\phi_{max} = 0.589 * \left[1 - \left(\frac{V_\delta}{V_p}\right)_L\right] + (1 - 0.589) * 0.524 * \left[1 - \left(\frac{V_\delta}{V_p}\right)_S\right] \tag{15}$$

and a theoretical optimal volume fraction of the large particles (ϕ_L) of

$$\phi_L = \frac{0.589 * \left[1 - \left(\frac{V_\delta}{V_p} \right)_L \right]}{\phi_{max}} \tag{16}$$

For this specific sample calculation, these equations yield ϕ_{max}=0.659 and ϕ_L=0.818 respectively. Converting the value of 0.659 (v/v) to (w/w) one finds 0.672, assuming density of PS = 1.04 g•cm^{-3} and density of latex = 1.02 g•cm^{-3}. However, at this solids loading, the average distance between particles will be close to zero and viscosity would be virtually infinite.

These calculations illustrate the limitations faced in terms of maximum solids content achievable as the particle sizes are decreased. For instance, applying the same calculations (assuming δ = 3 nm) to a latex with slightly higher particle sizes, as in the case of Mariz et al.,[3] in which the large and small particles were approximately 280 nm and 70 nm, the maximum bimodal packing fraction obtained was 0.721 (v/v), 0.735 (w/w). A theoretical increase of approximately 6.3 % on a weight basis is achieved by increasing the diameter of the large particles by 80 nm. In the same manner, considerable larger particles of 1109 and 210 nm as the ones obtained by Boutti et al.[7] would lead to ϕ_{max} = 0.777 (v/v), 0.792 (w/w).

It should be reinforced that these calculations assume perfectly monodisperse small and large particles, and in reality one normally obtains a PSD around the average particle sizes. Moreover, the higher the ratio of Dp_L/Dp_S the higher the value of ϕ_{max} that can be achieved, as Pishvaei et al.[9] pointed out. However, in this specific case of latex with extremely small particles, such as the current work, there is a physical limitation to further decreasing the size of the small particles population. The differences in the ϕ_{max} and the corresponding ϕ_L as a function of particle size and δ for a fixed ratio Dp_L/Dp_S are illustrated in Figure 6-5.
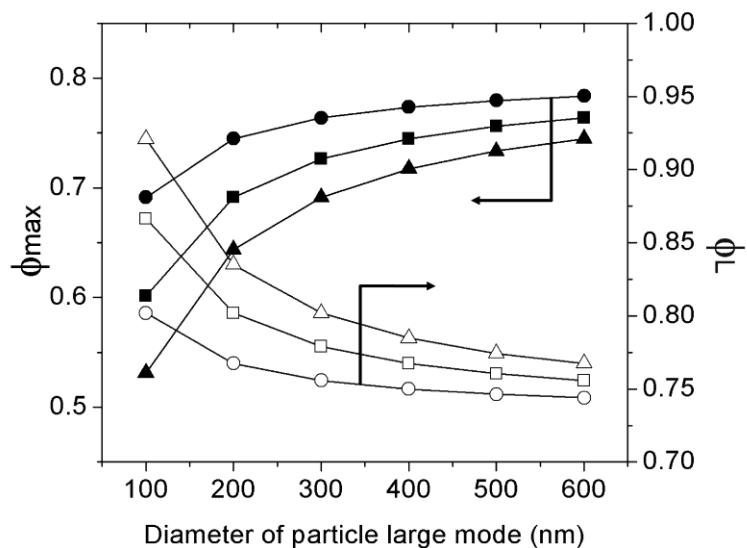
Figure 6-5. Maximum theoretical bimodal packing fraction (v/v) according to Equation (15) (solid symbols) and the correspondent optimal volume fraction of the large mode according to Equation (16) (open symbols) as a function of large mode particle size and EDL thickness, assuming $Dp_L/Dp_S=7$; EDL thickness: circle = 1 nm, square = 2 nm, triangle = 3 nm.

Decreasing δ (increasing I) increases the achievable value of ϕ_{max}; however, there is a practical limit, as additional salt decreases colloidal stability and increases the chances of coagulation.[18] Therefore care should be taken when working with the ionic strength of the latex to avoid destabilization of the system.

6.5 Conclusions

Bimodal PS latexes containing 60 wt% and particle sizes of 200 nm were obtained with low viscosity, 490 mPa•s at 20 s^{-1}. The second population of particles, 10-30 nm, were produced in the presence of the large particles using two different procedures (described in Chapters 3 and 5) based on the concept of modified (micro)emulsion polymerization approaches. As the maximum theoretical weight fraction of solids achievable decreases with decreasing particle size, due to the

increasing volume fraction occupied by the stabilizing EDL, this achievement of 60-62 wt% solids is close to the maximum possible. Further developments could be possibly made to these results in terms of reducing the surfactant concentration for the renucleation step as well as by using a more hydrophilic monomer such as MMA instead of styrene. These steps were suggested in Chapter 8 for future outlook of this work.

References

1. Guyot, A.; Chu, F.; Schneider, M.; Graillat, C.; McKenna, T. F. *Prog.Polym.Sci.* **2002**, *8,* 1573-1615.

2. Ai, Z.; Deng, R.; Zhou, Q.; Liao, S.; Zhang, H. *Adv. Colloid Interface Sci.* **2010**, *1,* 45-59.

3. Mariz, I. d. F. A.; de la Cal, J. C.; Leiza, J. R. *Polymer* **2010**, *18,* 4044-4052.

4. Schmidt-Thummes, J.; Schwarzenbach, E.; Lee, D. I. Applications in the Paper Industry. In *Polymer dispersions and their industrial applications;* Urban, D., Takamura, K., Eds.; Wiley-VCH: Weinheim, 2002.

5. Greenwood, R.; Luckham, P. F.; Gregory, T. *J. Colloid Interface Sci.* **1997**, *1,* 11-21.

6. Greenwood, R.; Luckham, P. F.; Gregory, T. *Colloids Surf. , A* **1998**, *1-3,* 139-147.

7. Boutti, S.; Graillat, C.; McKenna, T. F. *Polymer* **2005**, *4,* 1211-1222.

8. Boutti, S.; Graillat, C.; McKenna, T. F. *Polymer* **2005**, *4,* 1223-1234.

9. Pishvaei, M.; Graillat, C.; Cassagnau, P.; McKenna, T. F. *Chem. Eng. Sci.* **2006**, *17,* 5768-5780.

10. Boutti, S.; Graillat, C.; McKenna, T. F. *Polymer* **2005**, *4,* 1189-1210.

11. Schneider, M.; Graillat, C.; Guyot, A.; Betremieux, I.; McKenna, T. F. *J Appl Polym Sci* **2002**, *10,* 1935-1948.

12. Sudduth, R. D. *J. Appl. Polym. Sci.* **1993***, 1,* 37-55.

13. Schneider, M.; Claverie, J.; Graillat, C.; McKenna, T. F. *J Appl Polym Sci* **2002***, 10,* 1878-1896.

14. Moraes, R. P.; Hutchinson, R. A.; McKenna, T. F. L. *J. Polym Sci. Part A: Polym. Chem.* **2010**, 48.

15. Heredia, M. F. Modélisation de Procédés de Synthèse de Latex Multipopulés, LCPP-CNRS/CPE, Lyon, France, 1992.

16. Boutti, S.; Zafra, R. D.; Graillat, C.; McKenna, T. F. *Macromol. Chem. Phys.* **2005***, 14,* 1355-1372.

17. Schneider, M.; McKenna, T. F. *Part.Part.Syst.Charact.* **2002***, 1,* 28-37.

18. Chern, C. *Principles and applications of emulsion polymerization;* Wiley: Hoboken, N.J., 2008.

19. McNaught, A. D.; Wilkinson, A.,; Jenkins, A. D.; International Union of Pure and Applied Chemistry. *IUPAC compendium of chemical terminology the gold book.* International Union of Pure and Applied Chemistry: [Research Triangle Park, N.C.], 2006.

Chapter 7

Bimodal latex using seeded approach- cross-linking of the small particles and competitive growth of the large particles population

7.1 Abstract

An innovative process for the production of bimodal latexes with particles smaller than 200 nm containing ~57 wt% solids content and viscosities <1400 mPa•s at 20 s^{-1} is presented. The ratio of large to small diameter of particles (Dp_L/Dp_S) was maintained in the range of 3.9-5.7 and the volume fraction of small particles between 11-26% to enable a high packing fraction with low viscosity. The particle size distribution was controlled using highly cross-linked small particles to reduce monomer uptake and thus minimize their growth during latex concentration, enabling an independent control over the rate at which the different populations of particles grow during the synthesis. Because of the volumetric growth rate ratio between the large and the small population of particles of approximately 25.4, the small particles were considered to behave as pseudo inert nano-fillers. Due to the particle size constraint (Dp_L < 200 nm) the solids content was limited by the challenging task of producing highly cross-linked latexes with extremely small particle size (< 25 nm) and acceptable concentrations.
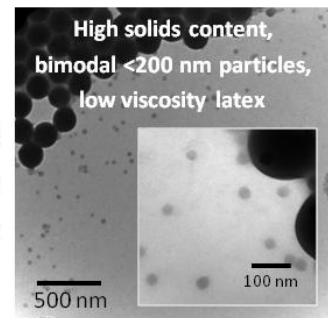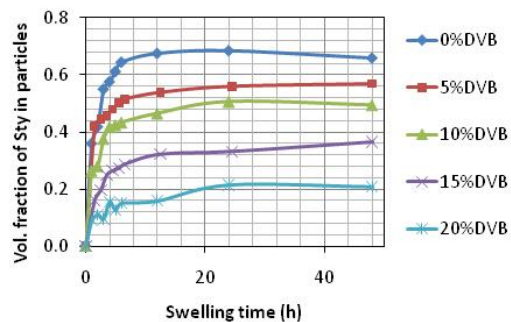
Highly cross-linked particles as pseudo inert nanofillers

7.2 Introduction

Paper coating formulations demand about 23% of the global emulsion polymer market,[1] which is estimated at 7 - 20 million tons, with an annual growth rate of 3.6%.[1-3] In the case of latex dispersions for paper coating formulations, small particle sizes are desired to promote higher binder efficiency, improve high-speed blade runnability, dry pick strength and gloss results.[4]

With respect to latex production, as particle size decreases (increasing ratio of particle surface area to volume), the maximum packing fraction of a latex in terms of solids content decreases because the stabilization layer takes up relatively more space, as has been extensively discussed in Chapters 1, 2 and 6. This limitation underlines the reason why, in order to satisfy the requirement of low viscosity for the high speed machines used in the application process, these products are industrially produced at concentrations of about 50 wt% solids content.[1]

Increasing the solid content of such commodity products at a relatively low cost, e.g. to approximately 60%, while keeping viscosity low would be quite useful. These products have strong commercial importance for economic reasons such as lower costs for storage and transportation, higher productivity per unit volume, as well as better application performance such as shorter drying time and improved film properties.[5-7] The production of bimodal latexes enable the achievement of higher solids content while keeping viscosity low, due to the increase in the maximum packing fraction of the dispersion by the inclusion of small particles to fill the gaps (void spaces) of the large particles, as illustrated in Figure 7-1. The theoretical increase in the maximum packing fraction was demonstrated by Equation 15 in Chapter 6.

As discussed in Chapter 6, in order to achieve high solids content while keeping viscosity low, one has to control the particle sizes and the volume fraction of each population adequately. For highest values of maximum packing fraction, the critical diameter radio (Dp_L/Dp_S) that permits small particles to fit into the interstitial pores between large particles is 6.46.[8] Thus, the size of the small family of particles in the preparation of HSC bimodal latexes for paper coating applications should to be < 30 nm.

In this Chapter, we use the methodology developed in Chapter 3 to produce this small family of particles. These particles were then cross-linked in order to avoid their swelling and growth during the production of the bimodal latex. The concentration of monomer inside these particles,

already naturally lower compared to large particles due to their extremely small size (refer to Figure 2-6) should be further reduced by introducing physical cross-links. The lower monomer concentration reduces the ratio of volumetric growth compared to the large particles which will, in principle, give us some control over the PSD.
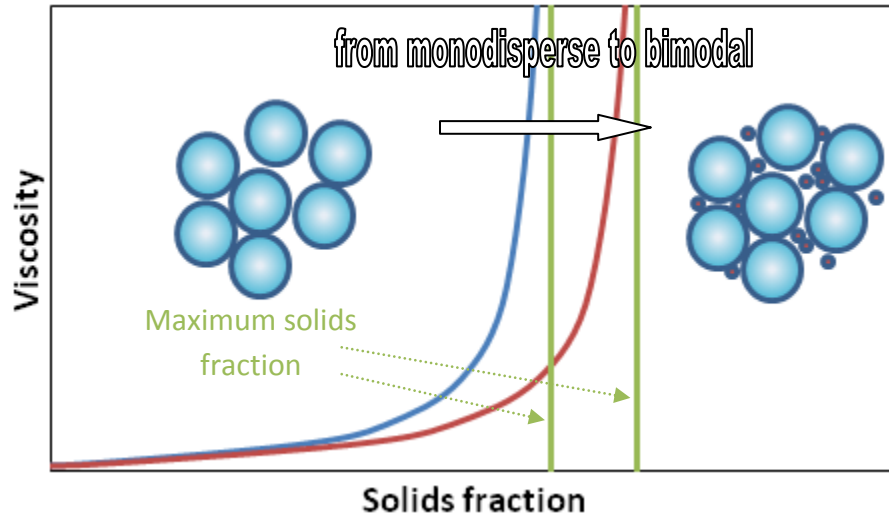
Figure 7-1. Illustrative scheme on the principle for increasing solids content while keeping viscosity low in polymer dispersions.

The objective was to study the potential of using the cross-linked particles in an innovative approach to control the PSD during the production of HSC/LV bimodal latexes. In contrast to Chapter 6, the use of cross-linked particles allows a reverse order of nucleation, generating and growing the larger family of particles in the presence of the small family, as an advanced application of these highly cross-linked particles as pseudo (inert) nanofillers. This Chapter will describe the production and characterization of the small-cross-linked particles, estimate the relative growth rate of cross-linked and non-cross-linked particles, and describe the procedure to produce a high solids content bimodal latex using the cross-linked particles as pseudo (inert) nanofillers.

140

7.3 Experimental

Materials. Styrene (Sty, ≥99%) and acrylic acid (AA, 99%), divinylbenzene (DVB, Technical grade 80.2%, being 19% ethylvinylbenzene (EVB)), hydrogen peroxide (HPO, 30 wt% solution in water) and ascorbic acid (Asc. Ac., 97+%) from Sigma-Aldrich, sodium persulfate (NaPS, 98+%) from Acros, sodium chloride (NaCl, 95%), tetrahydrofuran (THF, Certified) from Fisher Scientific, sodium dodecyl sulphate (SDS, solid powder 99% grade) from MP Biomedicals and Disponil FES77 (33.1 wt% solution in water) from Cognis were used as received. All water was deionized using a Millipore - Synergy Ultrapure Water System.

7.3.1 Small particles polymerizations and the effect of degree of cross-linking

Experiments were carried out to study the effect of cross-linking on the latex particle size and swelling equilibrium. DVB was used as cross-linking agent at levels that varied from 0-20 mol% of the monomer mixture. Polymerizations were carried out in a 1-L jacketed glass reactor equipped with a reflux condenser, nitrogen inlet, anchor stirrer and valve at the bottom for sampling. All polymerizations were carried out at 80°C. The methodology is identical to the procedures described in Chapter 3, the main difference consisting of adding DVB to the monomer mass. The DVB molar fraction was varied from 0-20 mol%, assuming the mass of EVB as part of the Sty mass. Appendix E shows a sample calculation concerning the mass of DVB required in each formulation according to the desired overall molar fraction of DVB. In addition, the DVB mass was fed to the reactor using three different strategies: (i) uniformly distributed over the entire semi-batch monomer feeding (*Stage 1*) and the monomer shot at the end (*Stage 2*); (ii) concentrated in *Stage 1*, with pure Sty added at *Stage 2*; and (iii) concentrated in *Stage 2*, with pure Sty added during *Stage 1*. The initial formulations (reactor heel) are provided in Table 3-2, with a total initial mass of 750 g before semi-continuous addition of monomer.

Table 7-1. Initial formulations for the synthesis of cross-linked Sty/DVB small particles latexes.

Components	wt%
Monomer mixture*	0.5
SDS	3-5
NaPS	0.1
DI water	94.4-96.4

*Styrene + variable mass fraction of DVB

The water, surfactant and monomer mixture was added to the reactor under nitrogen atmosphere, and left under agitation while the temperature was raised using a controlled temperature water bath. The required mass of initiator was dissolved in a small aliquot of water (25 mL) and the initiator solution was added to the reactor when temperature reached 80°C. At this moment the reaction was considered started. A small nitrogen flux was used throughout the entire experiment. For *Stage 1* reactions, additional monomer mixture (160 g) was fed into the reactor using an infusion pump at a rate of approximately 0.5 ml/min (total of 5.5 hours addition). These formulations have a final solids content of about 20%. For higher solids content *Stage 2* experiments, one extra monomer mixture aliquot (variable mass, for a 30 wt% SC latex an additional 160 g is required) was added to the reactor. The monomer shot was made 7.5 minutes after the end of *Stage 1*. One hour after the monomer shot, the temperature was raised to 85°C and kept constant for 30 minutes as an attempt to minimize residual monomer. Samples were withdrawn every 30 minutes, beginning 7.5 minutes after the start of the reaction, for conversion and particle size determinations.

Characterizations. The degree of swelling of the latex particles was determined by diluting one small drop of latex in approximately 15 mL of a solution of SDS at critical micellar concentration (2.36 g/L) and adding 10 drops of styrene (visible excess with phase separation) to

the flask and closing with a cap to avoid losses due to evaporation. Magnetic stirring, at extremely low rates to avoid emulsification, was used to assist the diffusion of monomer to the particles. Aliquots of these systems were taken below the level of oil-water phase separation at specific times and transferred to a glass cuvette for particle size determination. The measurement setup for the Malvern equipment was set to automatic to increase precision (in this mode the equipment defines how many measurements and runs have to be performed for a particular sample). After the measurement the aliquot was carefully returned to the flask and closed with a cap. The entire procedure was carried out at room temperature (25°C).

Soxhlet extractions of polymer samples were performed to determine the gel content of the cross-linked polymers. Latex samples were dried, and then the polymer powder was fused together using small aliquots of THF. The polymer sample was then left to dry in the fume hood overnight. The cellulose extraction thimbles (25 mm x 80 mm) used were purchased from Whatman, and were soaked in THF for 1 hour then air dried in the fume hood overnight. The masses of the cellulose thimble and the polymer sample were determined. The soxhlet extractions were performed for 24 hours in an oil bath with magnetic agitation at ~80°C using THF as a reflux solvent under nitrogen atmosphere (for safety reasons), changing the THF for a new aliquot every eight hours. After 24 hours of extraction, the cellulose thimble was left to dry in the fume hood overnight and its new mass (thimble + polymer gel, if any) was measured. The gel content was calculated by the ratio of the mass of gel retained in the cellulose thimble to the mass of original polymer sample.

Differential scanning calorimetry (DSC) of polymer samples were performed in a DSC-Q-100 TA Instruments in the temperature range of 50-170°C and a heating rate of 10°C/min. The values of T_g were obtained from the third scanning cycle of the samples. The specific surface area (SSA) of polymer samples were determined using BET[9] technique in an Autosorb-1C by Quantachrome

143

Corp. The samples were out gassed at 20°C overnight and then a 5-point BET was done in liquid nitrogen. Nitrogen was used as analysis gas. This characterization was kindly performed at the Royal Military College in Kingston, Ontario by an experienced instrument manager.

7.3.2 Synthesis of bimodal latexes using a mixture of cross-linked particles and non-cross-linked seeds in the reactor heel

This experiment had as objective the production of bimodal latexes with the particle size distribution being controlled by the competitive growth of the different families of particles. A mixture of cross-linked particles and non-cross-linked polymer seeds were added to the reactor heel, and a mixture of monomer and surfactant was then fed. Starting with a small latex particles with 15 mol% DVB, diameter of 38.05 nm (Z-average, PdI = 0.021) and with 30.6 wt% SC and a large seed latex with 51 wt% SC, diameter of 78.83 nm (Z-average, PdI =0.029) (formulation and procedure to prepare this latex seed provided in Appendix F), the number of particles (Np) of each family required to obtain a bimodal latex with 60 wt% solids was calculated. The objective was to obtain a latex with a volume fraction of small particles of 0.15. The number of small particles (Np_s) was calculated based on the total volume of particles required to fulfil the volume fraction of the small particles in the final bimodal latex, assuming that these particles would grow in diameter by 15% (final average diameter of 43.75 nm). This calculation resulted in a Np_s of 2.05×10^{18} particles required, which in turn corresponds to a mass of 208 g of cross-linked latex (144.2 g water, 63.8 g polymer). The same calculation was done to determine the number of large particles (Np_L) and the mass of latex seed required, assuming that the large particles would grow to 150 nm. These calculations yielded $Np_L = 2.89 \times 10^{17}$ and a mass of seed latex of 72 g (34.55 g water, 37.45 g polymer). Finally, it was determined the remaining mass of water and solids (monomer+surfactant) required to bring the entire latex to 60 wt%, using a semi-batch experiment. In addition, the mass of surfactant required to stabilize the growth of surface area of both populations of particles was determined using the same approach described in Chapter 6 and

144

Appendix C. Different from the experiment of large particle growth described in Chapter 6, in this experiment the initiator used was NaPS and the surfactant used during the semi-batch was SDS. Table 6-1 summarizes the information regarding the formulation of this experiment. The experiment was carried out at 70°C under nitrogen atmosphere in a 1-L jacketed glass reactor equipped with a reflux condenser, nitrogen inlet, anchor stirrer and valve at the bottom for sampling. The preemulsions (PE) prepared for semi-continuous addition were fed to the reactor over a period of 3 hours, having their composition independently prepared for each individual hour. Samples were periodically taken for monitoring of the process.

Table 7-2. Recipe for the synthesis 1 L, 60 wt% solids content bimodal latex with cross-linked particles in the reactor heel.

Components	Reactor heel (g)	Preemulsion (g)		
		0.5h	1.5h	2.5h
79 nm seeds[a]	72	-	-	-
38 nm latex[b]	208	-	-	-
NaPS[c]	2.5			
water	29.4	60	60	60
SDS	-	6.9	2.1	1.1
styrene	-	166	166	166

[a] Corresponds to the mass of 51 wt% solids content seed latex, produced according to Appendix F; [b] Corresponds to the mass of 30.6 wt% solids content cross-linked latex; [c] corresponds to 0.5 wt% relative to styrene mass, solubilized in 29.4 g of water.

7.3.3 Synthesis of bimodal latexes using cross-linked particles during the semi-batch feed.

The procedure used to synthesize the population of large particles is identical to that used in Chapter 6. The differences related to the production of the bimodal latexes using the cross-linked particles consist of calculating the number of small particles corresponding to the desired volume fraction, determined using Equation 16 (Chapter 6) to be in the range of 80-85 %. The cross-linked seeds used during these experiments were produced using the methodology described previously in this Chapter, using 5 wt% SDS in the reactor heel.

The cross-linked latex used in this set of experiments contained 15 mol% DVB and 32-33% SC, with 31-34 nm in Dp_S. The Np_s required to fulfill the volume fraction of the small population in the final bimodal latex was calculated to be ~ 3.16×10^{18}, corresponding to a mass of latex of ~194 g (~62 g polymer, ~132 g water). In order to prevent these small particles from growing during the process, their addition was delayed to the end of the feeding period. Obviously, as discussed in Chapter 2, it is not possible to mix two latexes of different concentrations (both lower than 60 wt%) and expect to reach HSC without an evaporation or a concentration step. The specific moment during the synthesis when these seeds were added was defined by calculating the mass of cross-linked seeds latex required to fulfill the volume fraction of the small population in the final bimodal latex, and then replacing a portion of the water used in the PE composition by this amount. The calculation indicated that, it was required to start the cross-linked latex addition at the 1.5h PE. Table 7-3 shows a sample formulation for the experiments carried out for this study.

It was observed that the flow rate of PE addition for the last 3 compositions (PE 2h, 2.5h and 3h) should be 3 times higher, lasting for 10 minutes each, as opposed to 30 minutes as originally defined in Chapter 6. Thus, for this study these PE were denominated 2h', 2.5h' and 3h' to differentiate from previous processes described in this thesis. Several experiments were run in

attempt to produce 60 wt% SC latexes using this approach. However it was verified that, because of the small particles growth, the final latex Dp_L/Dp_s ratio was not ideal and high viscosities or latex coagulation (or both) were observed. The critical point in the experiments was identified to be the final PE addition (last 30 minutes), where the solids content is highest. Therefore an experiment was done and the PE addition was stopped before the addition of the entire 3h' PE, with the exact time defined by visual inspection of the latex aspect in the reactor, to prevent a drastic increase in viscosity or coagulation. These procedures resulted in stable bimodal latexes with approximately 58 wt% SC. NaCl was used in the PE formulations containing cross-linked seeds to compress their EDL thickness and reduce their viscosity, necessary to facilitate pumping of the PE to the reactor.

Table 7-3. Recipe for the synthesis 1 L, 60 wt% solids content bimodal latex, using cross-linked seeds during the semi-batch feed.

Components	Reactor heel (g)	Semi-continuous addition						Initiator solution (g) (3.5h addition)
		Preemulsion (g) (2 hour addition)*						
		0.5h	1h	1.5h	2h'	2.5h'	3h'	
seeds[a]	4.1	-	-	-	-	-	-	-
water	100.0	43.6	52.0	27.2	-	-	-	40.0
Cross-linked latex[b]	-	-	-	37.7	51.7	52.5	52.5	-
NaCl	-	-	-	-	0.02	0.02	0.02	-
FES77[b]	-	19.7	7.4	6.2	7.4	6.7	6.3	-
styrene	-	86.6	86.6	86.6	86.6	86.6	86.6	-
HPO[c]	-	0.14	0.14	0.14	0.14	0.14	0.14	-
Asc. Ac.	-	-	-	-	-	-	-	0.52

[a] Corresponds to the mass of 33.5 wt% solids content seed latex with average particle size of 38 nm, produced according to a process described earlier in Chapter 3 and in Moraes et al. 2010[10]; [b] Corresponds to a 15 mol% DVB in their composition, 32-33 wt% SC and 31-34 nm in Dp; [c] Corresponds to the mass of 33.1 wt% surfactant solution as provided by supplier; [c] Corresponds to the mass of 30 wt% HPO solution as provided by supplier. *Preemulsions 0.5h, 1h and 1.5h have an addition time of 30 minutes each; preemulsions 2h', 2.5h' and 3h' have an addition time of 10 minutes each.

Characterizations. Ultracentrifugation technique was used to isolate the small family of particles by decantation of the large particles. This technique enables the characterization of the small mode in terms of PSD via conventional light scattering (with no interference of the large particles) and relative volume fraction in the bimodal latexes by gravimetry of the supernatant after separation. The procedure was adapted from a previous publication, with some adjustments due to our reduced particles size.[11] The bimodal latex samples were diluted to a solids content of approximately 17 wt% with a SDS/water solution at CMC (2.36 g/L) to eliminate viscosity effects. The centrifugation was done in a Beckman L8-70M ultracentrifuge operated at 36,000 rpm using a SW41Ti rotor (average G force of 160,000; maximum G force 222,000) for 30 minutes (at 4°C). After centrifugation a sample of the supernatant was carefully taken with a Pasteur pipette for particle size and gravimetry analysis.

Particle sizes were measured by dynamic light scattering (DLS), Malvern Zeta-Sizer Nano ZS, and transmission electron microscopy (TEM), in a Philips CM20 operated at 80 KeV. Rheological profiles of the latexes were obtained in a Viscotech by Reologica Instruments rheometer in the stress sweep mode, in the stress range from 1 to 50 Pa, using a parallel plate set up at room temperature. The gap containing the latex sample between the plates was covered with a silicone viscosity standard (12500 cp, Brookfield) to prevent latex evaporation during the analysis.

7.4 Results and discussion

7.4.1 Production and characterization of small cross-linked particles.

Figure 7-2 shows the influence of the DVB molar fraction on the final particle size and polydispersity index for 20 wt% solids content latexes. These latexes were produced using the methodology from starved-feed (micro)emulsion polymerization (*Stage I*) described in Chapter 3, having DVB uniformly distributed over the monomer mixture fed to the reactor. The experiments

were performed in duplicate, except the experiment with 20 mol% DVB, which was performed in triplicate for this study. The final particle size decreased slightly when the DVB concentration was increased from zero (no DVB) to 5 and 10 mol%. This is in agreement with the literature reported on (relatively) low cross-linking density polymer produced in microemulsion polymerization; Antonietti et al.[12] observed a decrease in particle size for PS microemulsion latexes from 19 to 13 nm when 11 mol% cross-link agent was used, keeping all other parameters constant. However, since the differences in particle sizes are < 5 nm for the present experimental conditions, overall the effect of increasing DVB concentration was not very large, even though it led to slight smaller particles at these DVB concentrations.
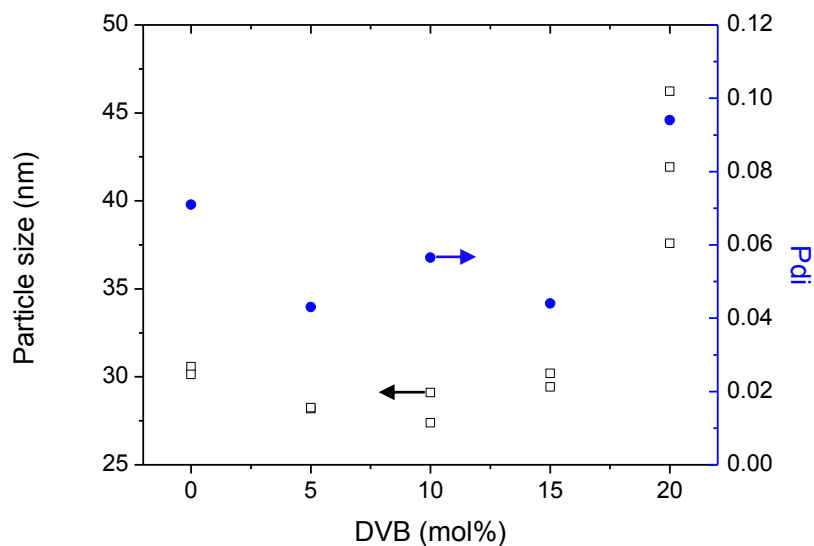
Figure 7-2. Effect of divinylbenzene (DVB) molar fraction on the final particle size of polystyrene latexes. The data points illustrate the reproducibility level of the experiments.

Particle size was observed to be minimal between 5 and 10 mol% DVB in this study, with the experiments with 15 mol % DVB showing a slight increase in final particle size and a significant increase of particle size observed for experiments with 20 mol% DVB. In addition, the variability of the results with 20 mol% DVB increased significantly, as can be seen by the data points

scattering shown for these experiments, which is not surprising as these latexes were shown to have low colloidal stability as discussed in the following pages. The PdI values were relatively low for all conditions, below 0.1, which indicates narrow distributions around the average. The variability observed between the replicates (not shown) was proportional to the variability observed in particle size, being higher for the 20 mol% DVB synthesis.

The high variability in the results observed for the formulations containing 20 mol% DVB is most likely related to the colloidal stability of these latexes. In fact, the particle sizes of the highly cross-linked latexes (≥15 mol% DVB) were observed to increase with time after polymerization. Figure 7-3 presents the particle size fluctuation versus shelf life of latex samples of identical solids content (20 wt%) but different molar fractions of DVB. Increasing the molar fraction of DVB in the latex composition resulted in lower colloidal stability, with the latex containing 15 mol% DVB exhibiting a slower increase in particle size compared to the latex containing 20 mol% DVB. The influence of the level of DVB in the latex composition on the latex stability becomes clear when comparing both cross-linked latexes with the latex containing no DVB. The DVB-free latex was shown to be stable over extremely long periods of time (more than one year now). In addition, the polydispersity indices were observed to increase significantly with time for the latex containing 20 mol% DVB, as opposed to the latex with no DVB which was roughly constant.

Figure 7-4 presents the change in of particle size feed as a function of time for 15 and 20 mol % DVB cross-linked PS latexes produced with DVB uniformly distributed over the monomer mixture, examining the same sets of samples over several days following the reaction. The particles taken at the end of the reaction (higher solids content) were less stable over time than those from the beginning of the semi-batch process (left hand plots), and the 30 wt% SC latex

was less stable than the 20 wt% SC latex. In addition, as presented previously, stability decreases as the molar fraction of DVB in the composition increases from 15 to 20 mol% DVB.
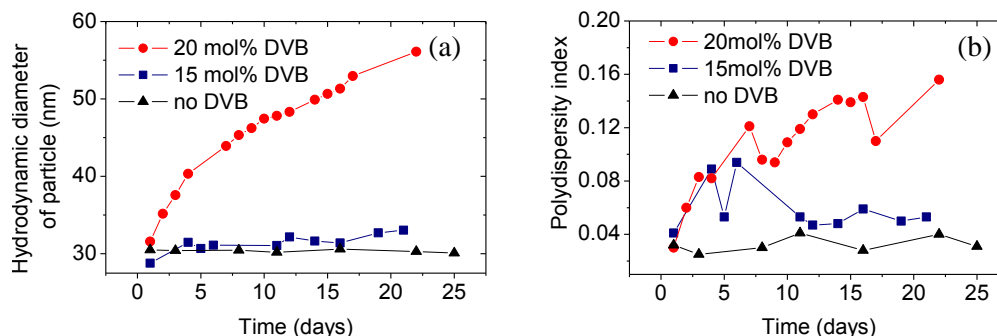
Figure 7-3. Colloidal stability of cross-linked nano-particles – DVB distributed uniformly over the monomer mixture feed: (a) evolution of particle size and polydispersity index with shelf life for final latex samples. 20 % solids content latexes.

The increase in PdI as a function of shelf life indicates that the PSD broadening, suggesting that the cross-linked particles are aggregating due to the lack of stability. Figure 7-5 presents the evolution of PSD with shelf time for a cross-linked nano-particle latex containing 15 mol% DVB. Indeed it is possible to observe the generation of a second peak in the particle size distribution with time suggesting the formation of aggregates of particles. This increase in particle size might be attributed to the fact that the hyper-cross-linked polystyrene particles are extremely hard materials that assume a less amorphous structure, decreasing density and therefore increasing porosity.[13, 14] Several authors[14-17] verified that porous particles of styrene-divinylbenzene can be produced in a controllable manner and that the pores sizes increases with higher DVB molar ratio in the copolymer. In fact, as reported by Ge et al.[18] several peculiar particle morphologies could be obtained depending on the conditions used during the synthesis of these highly cross-linked particles. Similar instability was reported by Kai et al.[16] for highly cross-linked polystyrene microspheres and by Cosyns[19] for latexes composed of several comonomers, including butyl methacrylate, styrene, ethylhexyl acrylate and acrylic acid among others. Even though the latter

polymer particles were not cross-linked, it was observed that the polymer particles had strong roughness at the surface.
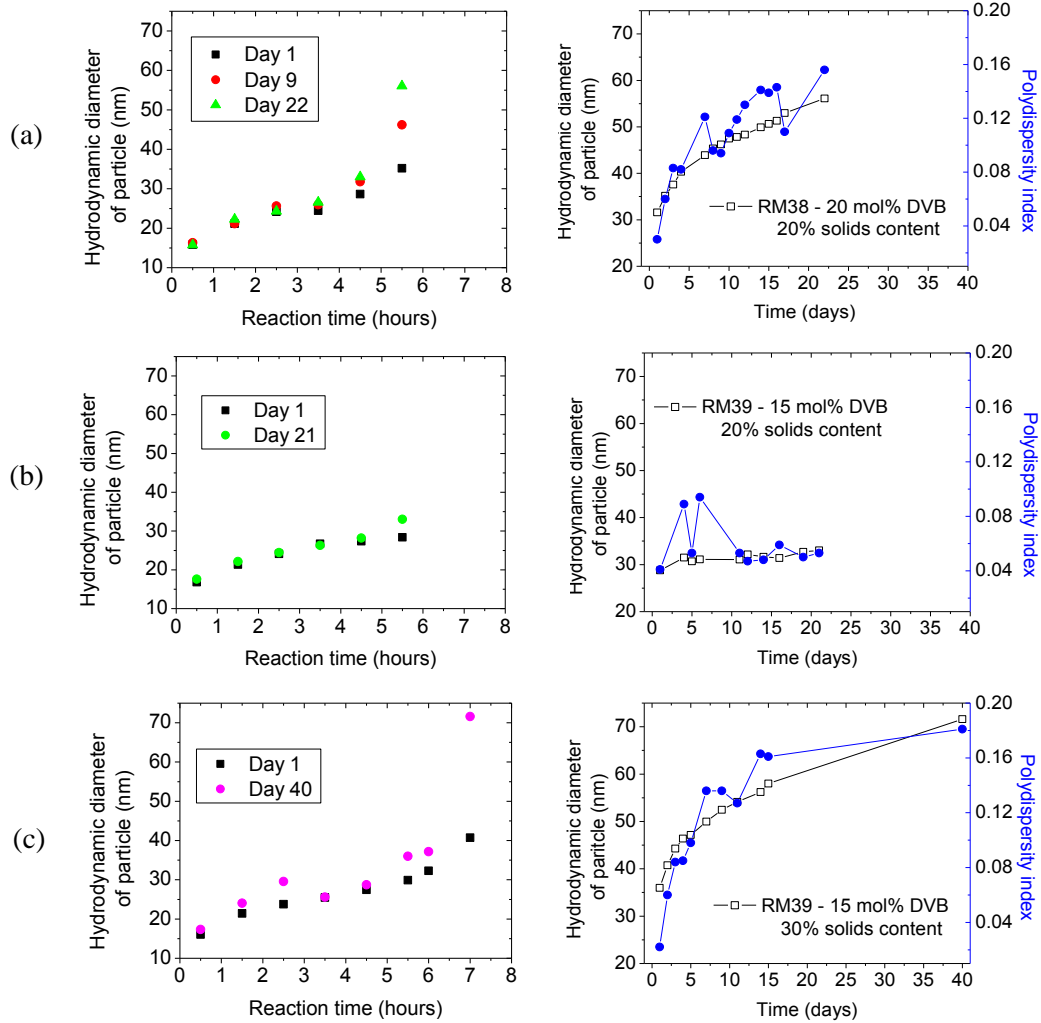
Figure 7-4. Colloidal stability of cross-linked nano-particles – DVB distributed uniformly over the monomer mixture feed. On the left: evolution of particle size with shelf life for intermediate samples taken during the semi-bath latex synthesis. On the right: evolution of particle size and polydispersity index with shelf life for final latex samples. (a) 20 wt% SC latex with 20 mol% DVB on polymer composition, (b) 20 wt% SC latex with 15 mol% DVB on polymer composition, (c) 30 wt% SC latex with 15 mol% DVB on polymer composition

153

In addition, porous cross-linked particle can swell in water, as reported by Yan et al.;[15, 20] the swelling behaviour only became detectable for concentrations higher than 20 wt% DVB (a little less than 20 mol%), achieving a maximum at approximately 50 wt%. The swelling of the particles increases the surface area even more, as well as reduce the surfactant coverage that might lead to the observed aggregation and the overall shift in the PSD with time as observed in Figure 7-5.
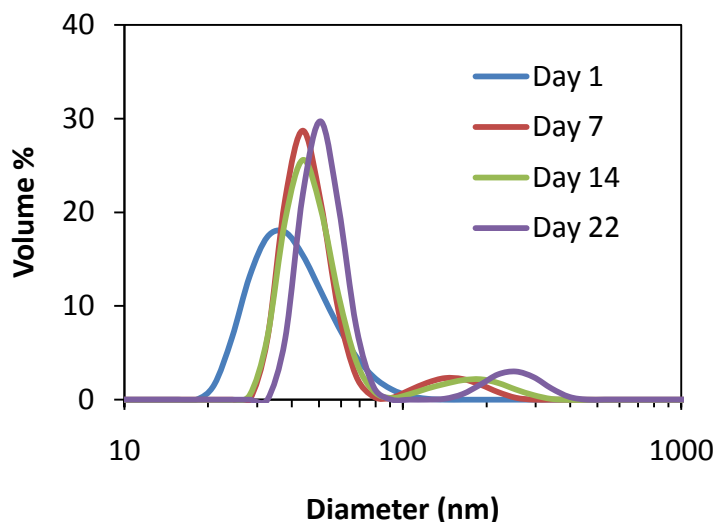
Figure 7-5. Evolution of the particle size distribution of cross-linked nano-particles latex with shelf-time. 15 mol% DVB, uniformly distributed over the semi-batch feed.

Alternative ways in which the DVB is fed to the reactor were studied, keeping the overall concentration the same, at 15 mol% DVB. Figure 7-6 shows that when the DVB was fed at *Stage 2* (final monomer mixture shot), the particles presented a better shelf life colloidal stability. In contrast, when the DVB was fed at *Stage 1* (during the starved-feed addition), the latex particles presented poorer colloidal stability. Having DVB fed evenly distributed during the entire process presented an intermediate stability.

The reason why the latex was more stable when the DVB was fed at *Stage 2* is not clear at this time. As it is likely related to the formation of the porous structure during the polymerization,

BET was performed to quantify the surface area of the material produced by each process. The results are shown in Table 7-4. The surface area obtained for the experiment in which the DVB was added at Stage 1, is almost double the value obtained for the experiment in which the DVB was added at *Stage 2*. Moreover, when DVB was fed at *Stage 2*, the specific surface area (SSA) obtained was in the same order of magnitude of the latex containing no DVB. These results seem to justify the hypothesis that colloidal stability (presented in Figure 7-6) observed for these small particles is related to porosity and surface roughness.
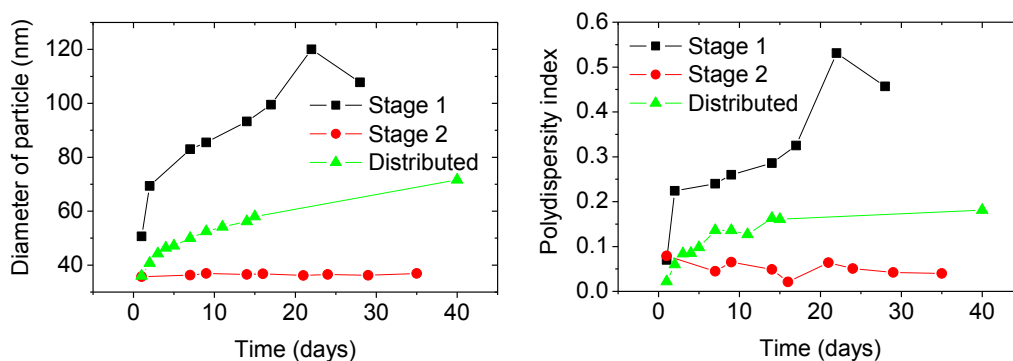
Figure 7-6. Colloidal stability of cross-linked particles – the influence of the DVB feeding procedure. 15 mol% DVB, 30 wt% solids content.

Table 7-4. Specific surface area, glass transition temperature (T_g) and gel content of polymers synthesized under different procedures – effect of DVB feeding strategy.

DVB (mol fraction)	DVB addition	T_g (°C)	SSA [m^2/g]	Gel content* (mass fraction)
0.15	Stage 2	106/138	58.0	0.946 / 0.922
0.15	Stage 1	102	114.9	0.804 / 0.803
0.15	Distributed	105	83.3	0.912 / 0.956
0	-	97	68.0	0.016 / 0.027

*experiments performed in duplicate

To verify the effectiveness of the cross-linking reactions, soxhlet extractions were performed to determine the gel content of the cross-linked polymers and the results are presented in Table 7-4. The higher gel content fractions observed for the experiments in which the DVB was added at *Stage 1* and in a distributed way suggests that a more homogeneous network is formed when compared to the experiment in which the DVB is added at the end of the synthesis, as might be expected. The *Stage 2* addition method likely forms a hard shell of cross-linked polymer, with some linear (non-cross-linked) polymer from the core removed during the extraction process. The gel content of the non-cross-linked PS validated this technique, as expected, no significant gel formation was observed. These results are in agreement with the glass transition temperature (T_g) determined by differential scanning calorimetry (DSC) analysis performed for these materials (Table 7-4), where two transitions were observed for the process in which the DVB was fed at *Stage 2*, in contrast to only one transition observed for the other materials. In addition, the increase in the value of the T_g observed for the experiments polymer containing 15 mol% DVB is in agreement with literature reporting on the physical characterization of cross-liked PS.[21]

Influence of DVB molar fraction on the swelling behaviour of latex particles. In order to examine whether the cross-linked small particles would remain relatively inert during further polymerization, their swelling behaviour was examined. Figure 7-7 and Figure 7-8 present the evolution of Dp/Dp_0 ratio and volume fraction of styrene in the particles versus time for latex particles containing different DVB mol fractions.
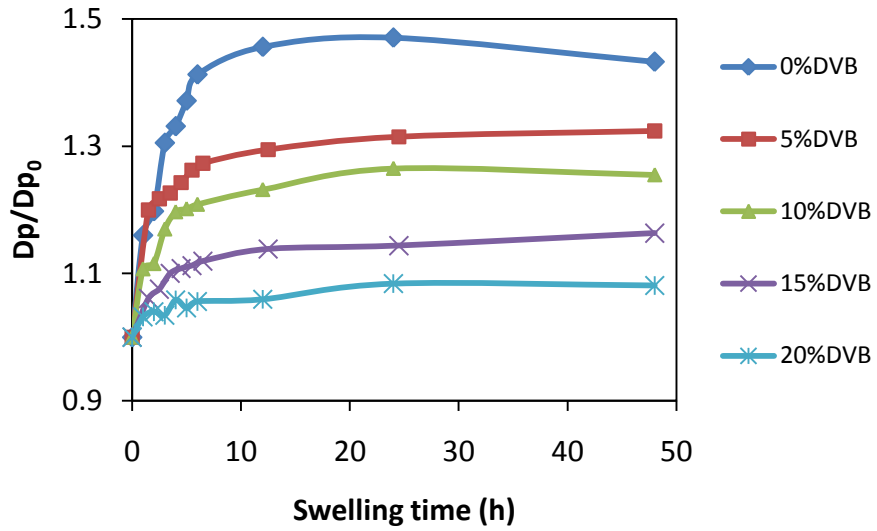
Figure 7-7. Kinetics of swelling of PS particles with styrene in terms of Dp/Dp_0 as a function of DVB mol fraction at room temperature (25°C)
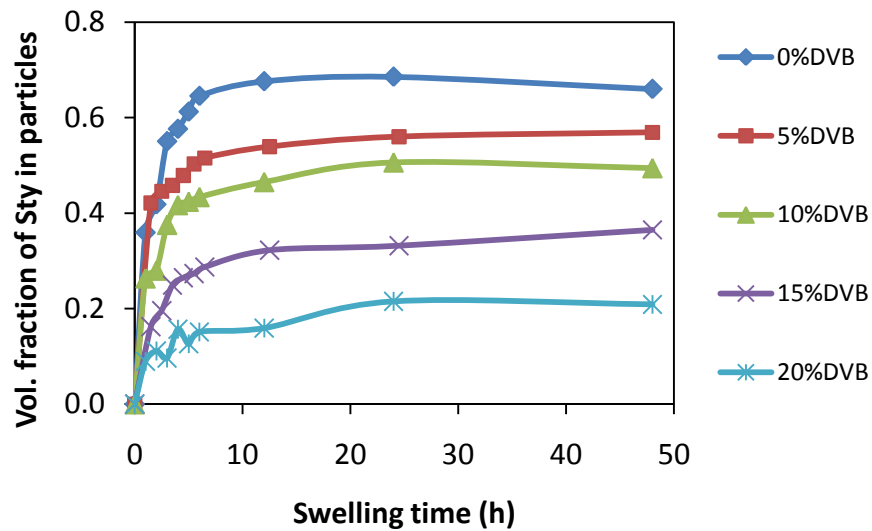
Figure 7-8. Kinetics of swelling of PS particles with styrene in terms of volume fraction of styrene in the particles as a function of DVB mol fraction at room temperature (25°C)

It can be seen that all particles seem to achieve equilibrium of swelling after 12 hours and that, as expected, the degree of swelling is inversely proportional to DVB mol fraction. These results

157

are comparable to the results presented by Kim and Suh[22] who studied the swelling kinetics of polystyrene particles cross-linked with urethane acrylate synthesized in their laboratory. Their results indicated that 6 hours of swelling time was sufficient to reach an equilibrium swelling state at 30°C for most formulations, and that cross-linking reduces significantly the swelling capacity of the polymer particles, in agreement with our results.

Figure 7-9 presents the equilibrium degree of swelling of PS latex particles with styrene as a function of DVB mol fraction in the polymer composition. The ratio Dp/Dp_0 was observed to decrease from 1.4 to 1.1 with increasing the mol fraction of DVB in the copolymer from 0 to 20 mol%. The volume fraction of styrene inside the non-cross-linked polymer particles was 0.66, which corresponds to a concentration of 5.7 mol/L. This result is in agreement with the studies reported by Nomura et al.[23] who reported an equilibrium styrene concentration in the range of 5-6 mol/L inside polystyrene particles. The agreement validates the experimental methodology used in this work. In addition, several authors (for instance see references in Abdollahi and Hemmati[24]) use the value of 5.5 mol/L; as was discussed in Chapter 2, this value is known to vary with particle size and level of surfactant (interface tension). Therefore, when reporting the value of equilibrium concentration of monomer swelling in polymer particles, the parameters of particle size and interfacial tension (and temperature) should be reported as well. The value of interfacial tension is rather difficult to measure and the value of surface tension is often used instead. In our samples this value was approximately 40 mN/m. At 20 mol % DVB the volume fraction of styrene inside the particles was 0.21 which corresponds to a concentration of 1.8 mol/L. Thus, monomer concentration is reduced by a factor of three with the increase of DVB concentration in the copolymer. These results are in agreement with the analysis of swelling behaviour of poly(Sty-co-DVB) done by Errede,[25] as was mentioned in Chapter 2, Errede reported a critical

158

cross-link density (above which the uptake of organic liquids by the cross-linked network is zero) of 22 mol % DVB.
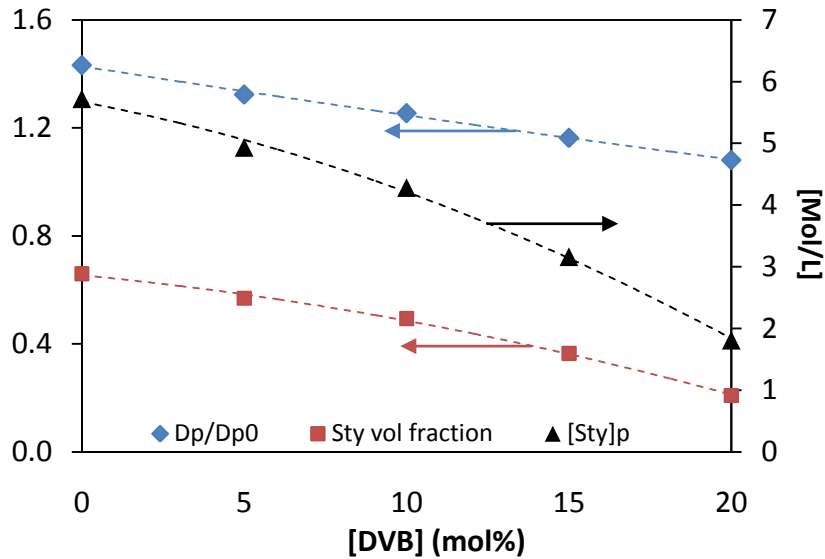
Figure 7-9. Equilibrium degree of swelling of PS particles with styrene as a function of DVB mol fraction.

The swelling studies presented above were for the polymer latexes synthesized by having DVB being fed uniformly distributed over the entire process. Figure 7-10 presents the swelling kinetics of the cross-linked PS particles for the other feeding methodologies utilized. The results indicate that the swelling properties of these particles are not sensitive to the DVB addition procedure.

7.4.2 Competitive parallel growth of cross-linked and non-cross-linked particles.

The initial concept was to nucleate the large particles population in the presence of the cross-linked small particles. However, due to the small target particle size (~200 nm) and the limiting mass of water available to prepare these latexes, the concentration of particles inside the reactor during the nucleation step leads to a value of solids content higher than can be supported and

extremely high viscosities (gels) were observed inside the reactor. Thus, the production of unseeded bimodal latex using the reverse order nucleation approach was not successful at these particle size constraints. In addition, because of the growth of the smaller cross-linked particles and the limitations in minimum size achievable for the cross-linked particles, the ratio of Dp_L/Dp_S cannot be maintained at optimal values. In Chapter 8 presents further discussion about the production of bimodal latexes using this innovative approach.
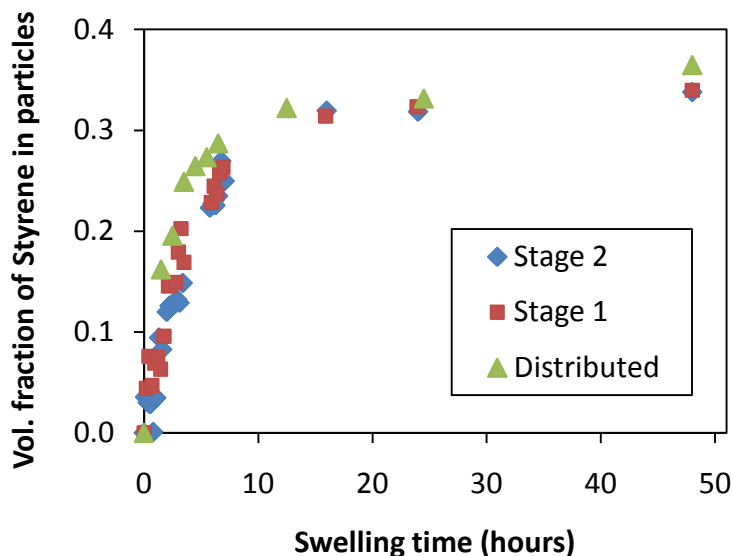
Figure 7-10. Kinetics of swelling of 15 mol% DVB-co-Sty particles with styrene, plotting volume fraction of styrene in the particles at room temperature (25°C) for the three different DVB feeding procedures described in the text.

Thus, the next concept was to start with a mixture of cross-linked seeds and non-cross-linked seeds in the reactor heel and examine their competitive growth under the same reaction conditions; as described above, it is expected that cross-linked particles should grow at a significantly slower rate due to their reduced equilibrium monomer concentration in the particles. A mixture of the two latexes was prepared in the reactor heel and a controlled semi-batch polymerization reaction was carried out to concentrate the latex and monitor the growth of the

individual population of particles. The synthesis started from particles that were 38 nm and 79 nm for the cross-linked and the non-cross-linked populations respectively.

As described in the experimental section, the number of particles of each population (Np_L= 2.89×10^{17} and $Np_S = 2.05 \times 10^{18}$) was calculated to yield a final 1 litre bimodal latex with 60% solids content. However, high viscosities were encountered and the experiment was stopped at a solids content of approximately 52 wt%. As described below, the high viscosity is attributed to the lower than expected value of Dp_L/Dp_s (and thus increasing viscosity at a lower solids level) because the small particles grew more than estimated. The experiment was run for 1 hour and 45 minutes out of the 3 hours originally programmed of semi-batch feeding, with a duplicate experiment yielding similar results.

Despite the failure to reach 60 wt% solids, the experiment provides a means to estimate the relative rates of polymerization inside each population of particles. Figure 7-11 presents the overall conversion profile and the increase in solids content of this experiment and Figure 7-12 presents the particle size distributions, determined by dynamic light scattering (DLS), of the original cross-linked particles and non-cross-linked seeds as well as from samples taken during the semi-batch reaction. The solids content increased from 31 to 52 wt% in the feeding period with the instantaneous conversion close to 100%, indicating that no accumulation of monomer took place. Figure 7-12 shows that a bimodal PSD was observed for all samples (except the 1.5 h sample which presented a "shoulder" relative to the small particles in a monomodal PSD). Moreover, the large particles distribution was observed to shift towards larger values of particle size during the course of the synthesis, while the small mode distribution remained relatively constant or grew at a much slower rate.

161
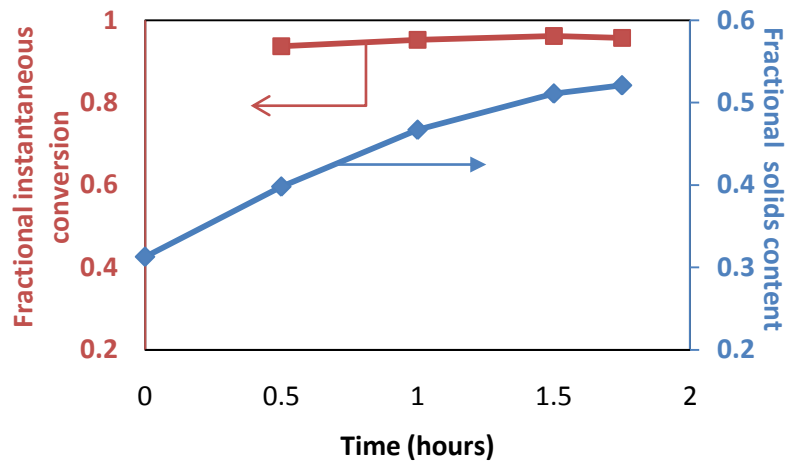
Figure 7-11. Evolution of instantaneous conversion and solids content during the competitive parallel growth of cross-linked and non-cross-linked particles.
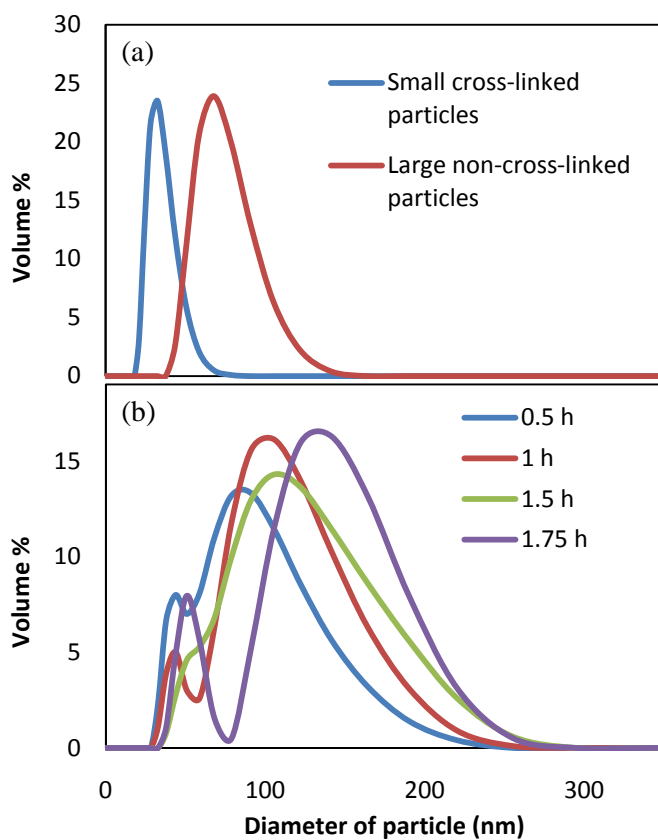
Figure 7-12. Particle size distributions relative to (a) the initial latexes and (b) samples during the competitive parallel growth of cross-linked and non-cross-linked particles.

DLS is not a reliable technique when it comes to bimodal latexes, as was shown in Appendix D and in Chapter 6. In this case, the large initial fraction of small particles and the relatively small difference in initial size of the large and small particles enabled the equipment to identify and process both families of particle sizes. Transmission electron microscopy (TEM) analyses were also performed to verify the bimodal PSD. Figure 7-13, Figure 7-14 and Figure 7-15 present some representative images from the TEM analysis performed on samples retrieved at 0.5 hour, 1 hour, and 1.75 hour respectively.
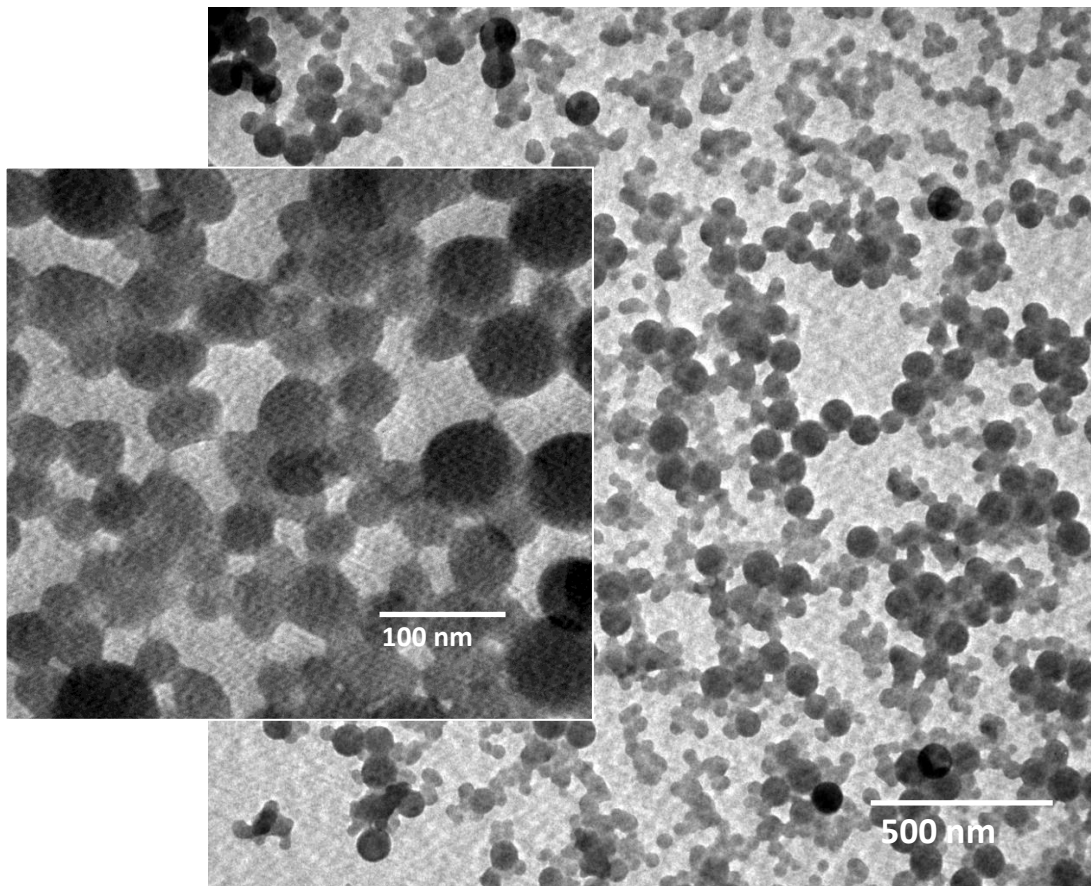
Figure 7-13. TEM images of the competitive parallel growth of cross-linked and non-cross-linked particles. Sample 0.5 h.

The TEM images confirmed the bimodality of the latex and also that the large particles grow at a faster rate than the small particles. A more thorough statistical analysis of the TEM analysis was performed for the final sample of the latex, measuring all particles using available image analysis software (ImageJ). The PSD and the volume fraction contribution from each family of particles to the overall bimodal latex were estimated from a sample size of approximately 100 particles, as is presented in Figure 7-16. The PSD obtained using the TEM images agrees with the PSD obtained via DLS (Figure 7-12). It should be pointed out that this analysis of the TEM images is not meant to be accurate statistically but rather to provide qualitative support to confirm the results from DLS.
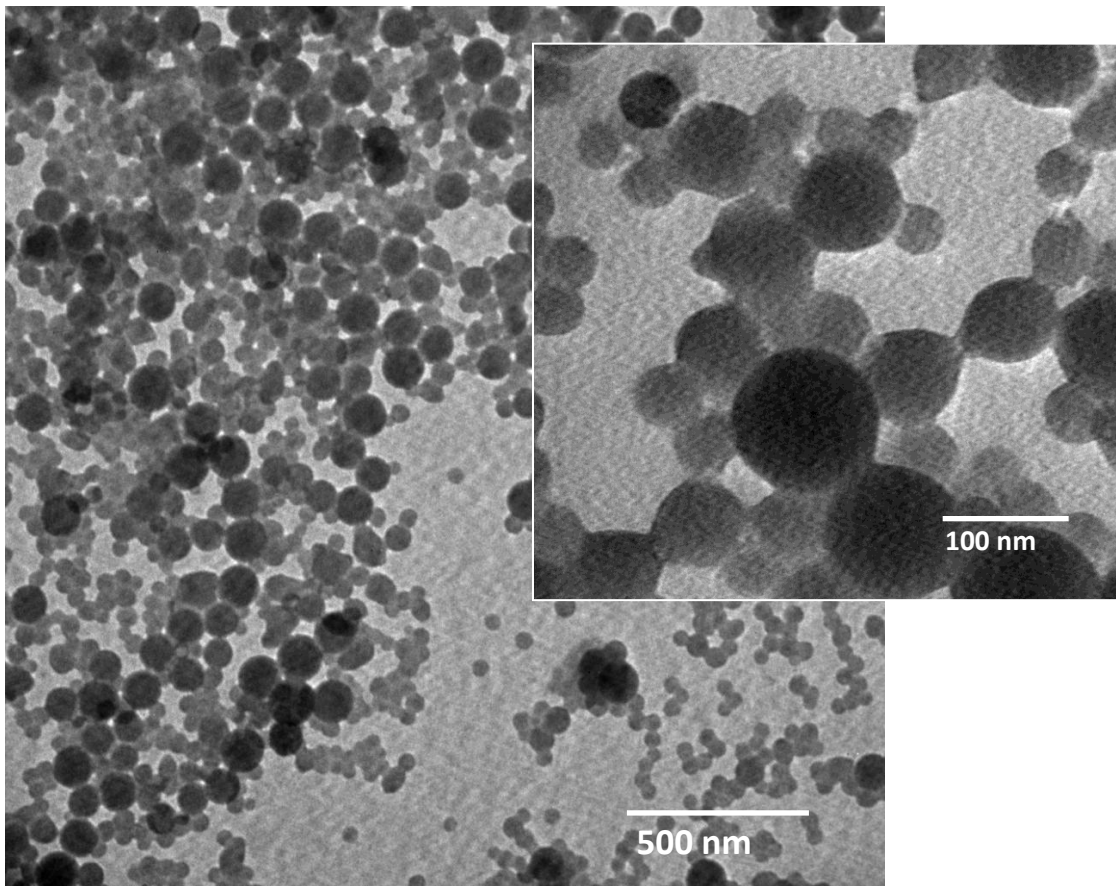
Figure 7-14. TEM images of the competitive parallel growth of cross-linked and non-cross-linked particles. Sample 1 h.

A kinetic analysis of the growth of the individual families of particles was conducted. Figure 7-17 presents the parallel evolution of average particle sizes obtained from the TEM images. Figure 7-18 presents the evolution of the particles' average volumetric growth during the process. The large particles were observed to grow in a rate of 25.37 times faster than the small cross-linked particles.
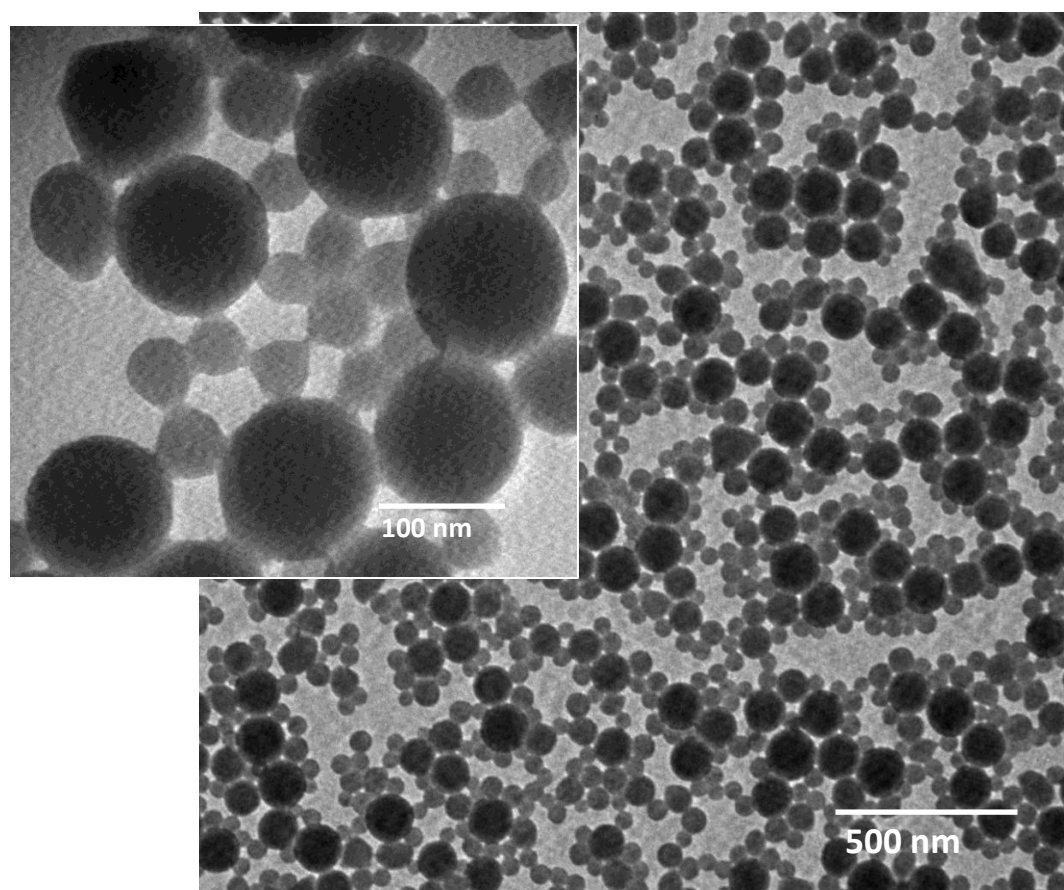

Figure 7-15. TEM images of the competitive parallel growth of cross-linked and non-cross-linked particles. Sample 1 hour and 45 minutes.
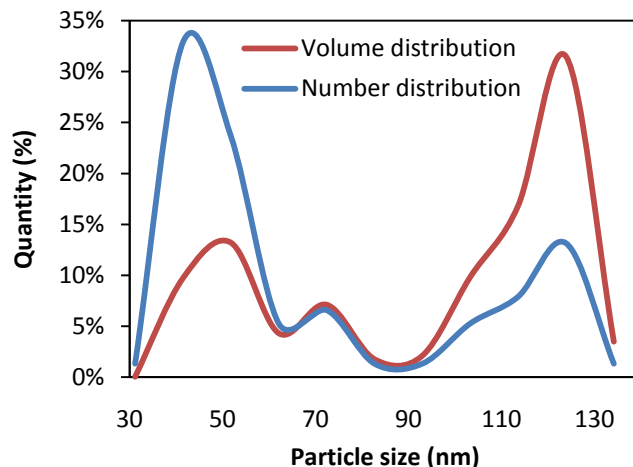
Figure 7-16. Particle size distribution obtained from statistical analysis of TEM images. Final latex from competitive parallel growth experiment.

$$\frac{\Delta Vp_i}{\Delta t} = \frac{R_{p_i}}{Np_i} = k_p [M]_{p_i} \frac{\bar{n}_i}{N_A} \tag{17}$$

The volumetric growth rate (Rp_V) of the particles is related to the rate of polymerization inside them, according to Equation 17, where the subscript *i* corresponds to the small or large particles population. Assuming constant Np during the process for both families, the volumetric growth of the individual family of particles can then be related to the product $[M]_{pi} \cdot \bar{n}$, since the propagation rate coefficient of Sty at 70°C ($k_p = 392.4$ L/mol•s)[26] and N_A are constants.

The difference in monomer concentration inside the small and large particles was determined from the equilibrium swelling measurements as $[M]_{pS} = 3.33/5.72[M]_{pL} = 0.58[M]_{pL}$ and plays a significant role to this difference in Rp_V. Moreover, as discussed in Chapter 2, smaller particles already swell less than large particles naturally due to their increased surface energy, possibly providing an even lower monomer concentration inside the small particles.
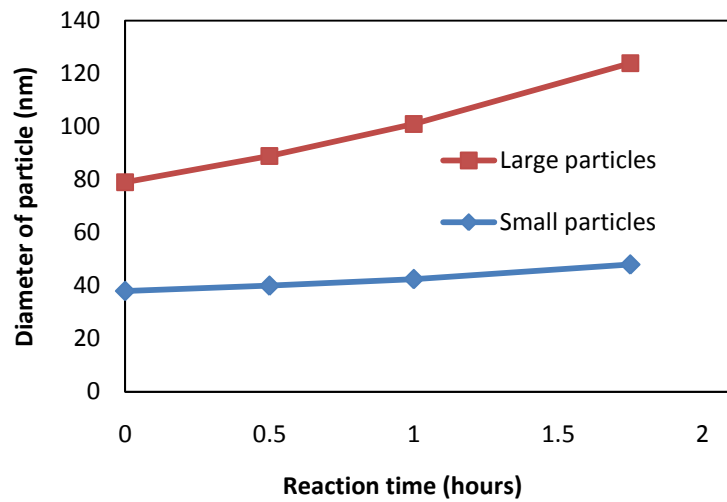
Figure 7-17. Evolution of average diameter of particle during the competitive parallel growth of cross-linked (small) and non-cross-linked (large) particles.
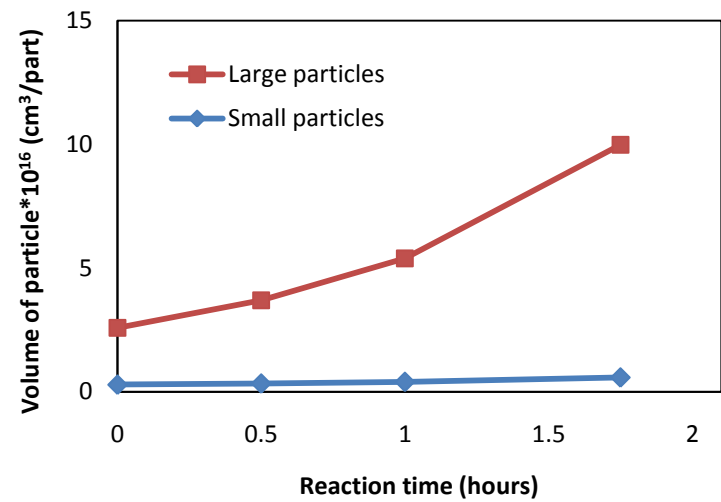
Figure 7-18. Evolution of average volume of particle during the competitive parallel growth of cross-linked (small) and non-cross-linked (large) particles.

167

Another parameter that is believed to play a role in the difference of Rp between the large and small population of particles is the average number of radicals per particle ($\bar{n}$). As mentioned in Chapter 2, smaller particles normally present smaller values of $\bar{n}$ than larger particles, which would further increase the difference in R_p inside each mode of particles in the bimodal latex. The values of $\bar{n}$ can be estimated using Equation 17, assuming a concentration of Sty in the particles and adjusting the units of volumetric growth to molar rate of monomer conversion using density of polystyrene[27, 28] of 1.05 g/cm^3 and Sty molar mass of 104.16 g/mol. For these estimate calculations, we assumed saturated conditions of monomer concentration, $[M]_{pL}$ = 5.72 mol/L and $[M]_{pS}$ = 3.33 mol/L. As was shown in Figure 7-11, the system was operated at starved-feed conditions, therefore the monomer concentration inside the particles are likely to be lower than the equilibrium concentration. As shown in Figure 7-19, the calculated values of $\bar{n}$ inside the large and small particles increase during the process from 0.14 to 0.50, and from 5.5 to 15 respectively. These values were expected considering the high instantaneous conversion of the system leading to a gel effect in the large particles; and the high exit and termination rates expected inside the small particles. Mariz et al.[29] presented an analysis of the competitive growth ratio between large and small particles aiming the production of bimodal latexes with small particle sizes. Their study did not use cross-linked particles, however the authors reported a volumetric growth rate ratio (Rp_{vL}/Rp_{vS}) of 21.36. They justified this difference in rate of polymerization between the large and small particles to be a function of $\bar{n}$ solely. They considered larger than the particles presented in our work and because of that, the authors neglected the difference in $[M]_p$ between the large and small particles. As mentioned earlier, the Rp_{vL}/Rp_{vS} obtained in our experiments was 25.37, and the difference is a consequence of a reduced monomer concentration inside the small cross-linked particles.
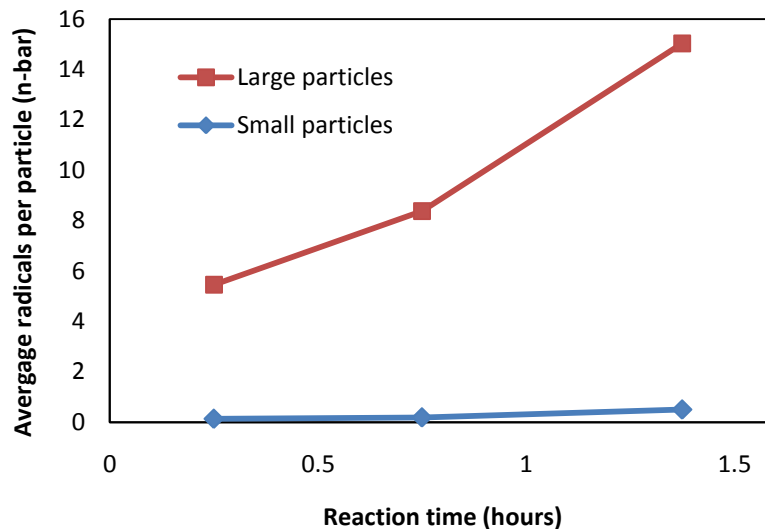
Figure 7-19. Evolution of the average number of radicals per particle in the cross-linked (small) and non-cross-linked (large) particles during the competitive parallel growth experiment.

7.4.3 Addition of cross-linked particles during the semi-batch growth of the large particles.

Experiments were performed in which the cross-linked particles were added during the semi-batch polymerization process, as an attempt to minimize their growth during the concentration of the bimodal latex and obtain a higher final value of Dp_L/Dp_s, and therefore achieve higher solids content at low viscosities. As discussed in the experimental session, due to the small (but significant) growth of the small particles during the process the maximum solids content obtained that respected the viscosity constraints was ~58 wt%.

Table 7-5 presents the results of the characterization of the final latexes obtained using this methodology in terms of average diameter of particle and polydispersity index obtained by DLS and solids content. In addition, it presents the volume fraction and the average diameter of the small cross-linked particles mode after separation by ultracentrifugation. The particle size of the bimodal samples ($Dp_{Bimodal}$) obtained by DLS was observed to be monomodal in the range of 170-190 nm with low polydispersity indices; as the instrument was unable to detect the second mode

169

of small particles present. However, TEM analysis has shown these latexes to be highly bimodal (see Figure 7-20, Figure 7-21, Figure 7-22 and Figure 7-23), indicating once again the low reliability of the DLS technique for bimodal latexes under these circumstances.

Table 7-5. Characterization of the bimodal latexes obtained by addition of the cross-linked particles during the semi-batch polymerization process.

Latex	Overall latex				Small mode			
	$Dp_{Bimodal}$ (nm)[a]	PdI (-)[a]	SC (%)	η @ 20 s^{-1} (mPa•s)	ϕ_s (vol%)[b]	Dp_s (nm)[a,b]	PdI (-)[a,b]	Dp_s (nm)[c]
RM119	176.1	0.016	57.4	1540	26.6	62.9	0.123	43.8
RM121B	165.3	0.051	58.6	NA	NA	NA	NA	NA
RM121B2	172.6	0.075	57.8	NA	22.7	60.4	0.137	44.3
RM122	194.8	0.002	56.8	1390	11.9	69.8	0.183	NA
RM122A	196.2	0.011	56.6	1050	11.5	68.0	0.196	34.4
RM123	196.4	0.056	58.4	1710	17.6	65.2	0.154	35.6

[a] obtained using DLS technique; [b] ultracentrifuge separated samples; [c] obtained using TEM images; NA = non-available.

The experiments presented in Table 7-5 were performed using slightly different formulations. Experiments RM119, RM121B and RM121B2 had their formulation exactly as presented in Table 7-3, stopping the semi-batch feeding at approximately half of the final PE addition. Experiments RM122, RM122A and RM123, had the cross-linked particles latex portion of the PE 1.5h composition replaced by water, as an attempt to compensate for the growth of the small particles to their final volume fraction. These experiments enabled the addition of the entire formulation (total 3h' PE addition).
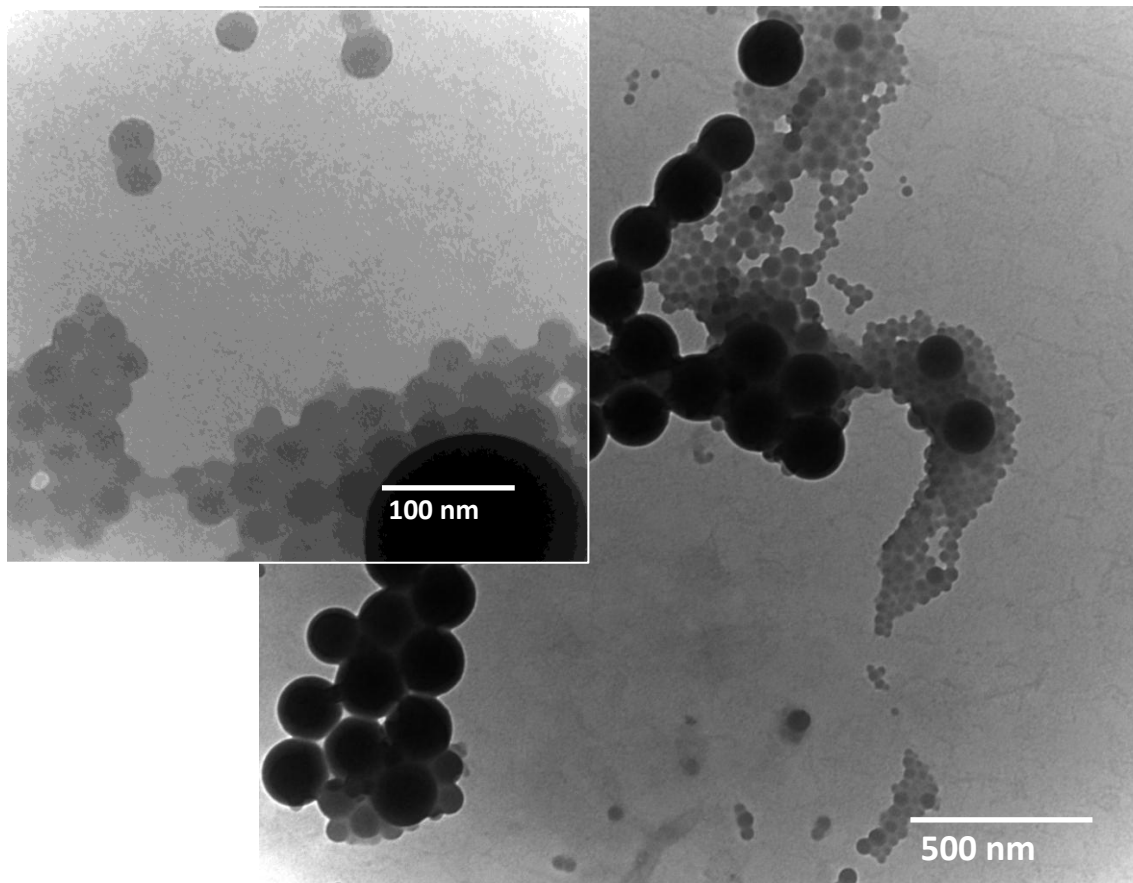
Figure 7-20. Transmission electron microscopy of final bimodal latex obtained using addition of cross-linked particles during the semi-batch feed. Latex RM119

The bimodal latexes were submitted to ultracentrifugation to separate the large and the small mode and enable the characterization of the small particles alone. As shown in Table 7-5, the average diameter of the small particles at the end of the process was in the range of 60-70 nm, which if true, indicates significant growth during the process, since the original size of the cross-linked particles was 31-34 nm. This analysis could be overestimating their growth, since the ultracentrifugation technique may leave in solution a fraction of (smaller) large particles, as the large values of PdI in Table 7-5 suggest. This was confirmed by the measurement of the small particles using the TEM images, which provided a smaller estimate of the average particle size (34-44 nm), as also summarized in Table 7-5. The overestimation of the results from the

ultracentrifugation could also be reflected in the values of volume fractions observed for the samples examined, however, the volume fraction of the small particles was found to be in the range of 11-26% and falls relatively close to the target value of ~15%. The high values of PdI was expected as the cross-linked particles were added in a semi-batch feed and the particles added earlier to the reactor would grow more than the particles added at the end of the process. In addition the TEM images confirm the relatively wider distribution of particle size observed in the TEM images. However, as mentioned again, the ultracentrifugation separation could have contributed to these high values of PdI due to an accumulation of some residual large particles in the supernatant as this methodology was reported to have a high degree of uncertainty.[11]
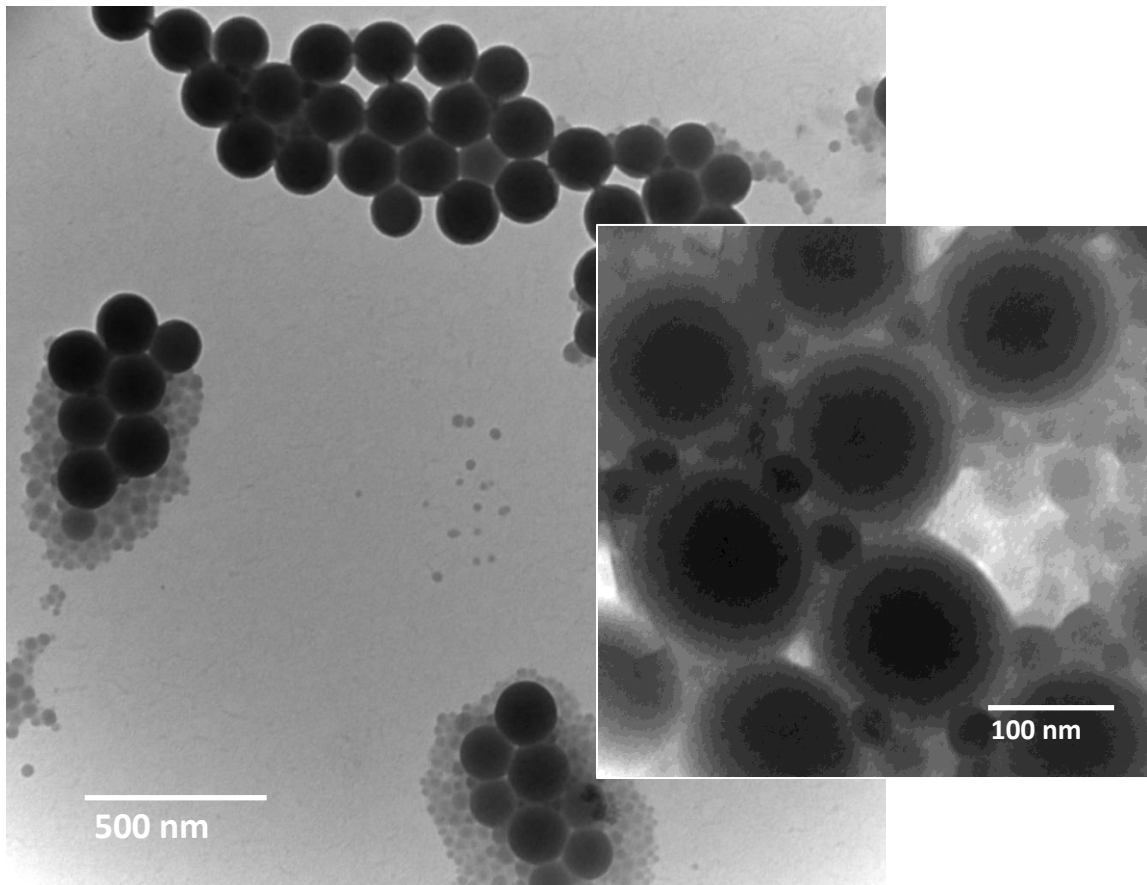
Figure 7-21. Transmission electron microscopy of final bimodal latex obtained using addition of cross-linked particles during the semi-batch feed. Latex RM121B2

The fact that DLS was not able to identify the small particles population in some of these cases enabled the monitoring of the growth of the large family of particles. Figure 7-24 shows the evolution of average diameter and number of large particles during the semi-batch process. In the case of RM122, the experimental results overlap with the simulations using Equation C-7 in Appendix C, and is an evidence that the number of particles of the large mode was successfully stabilized and kept constant during their growth. In the case of RM121B, the small mode was not detected by the DLS instrument; however the overall average PSD was noticed to suffer a small decrease by the presence of the small particles, as would be mostly expected, showing a deviation of the experimental results from the simulated Dp and Np.

Figure 7-22. Transmission electron microscopy of final bimodal latex obtained using addition of cross-linked particles during the semi-batch feed. Latex RM122A
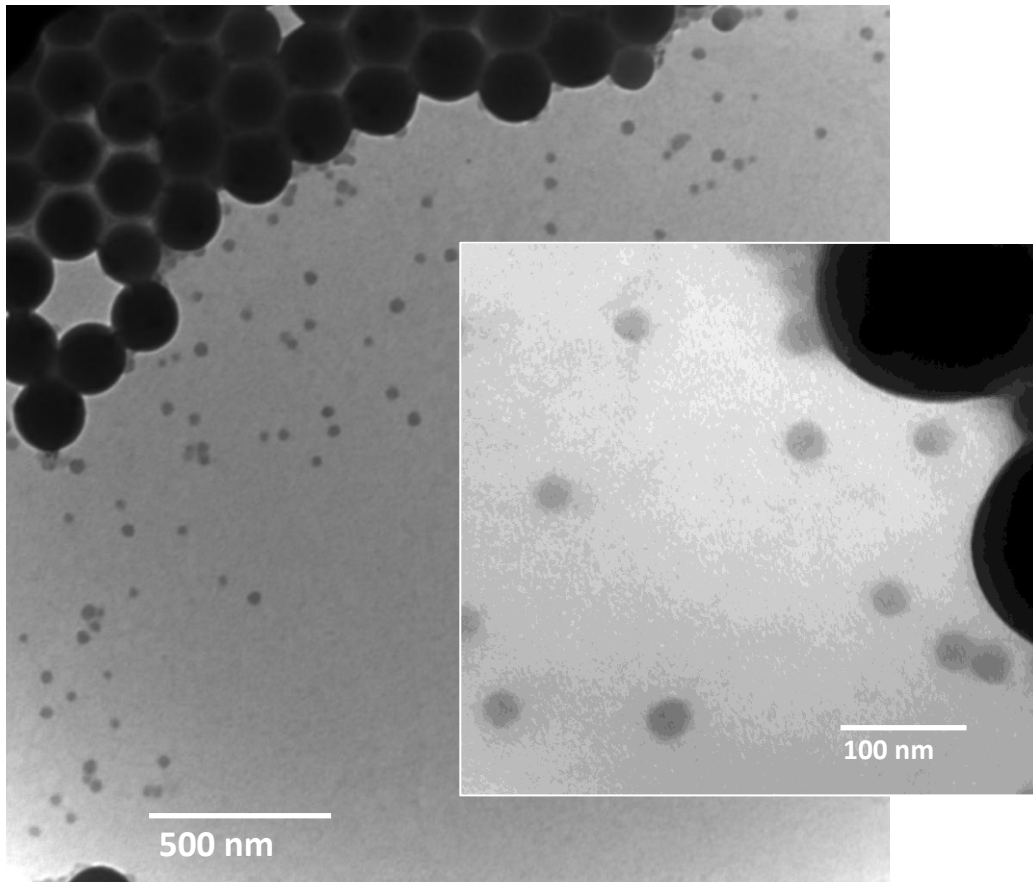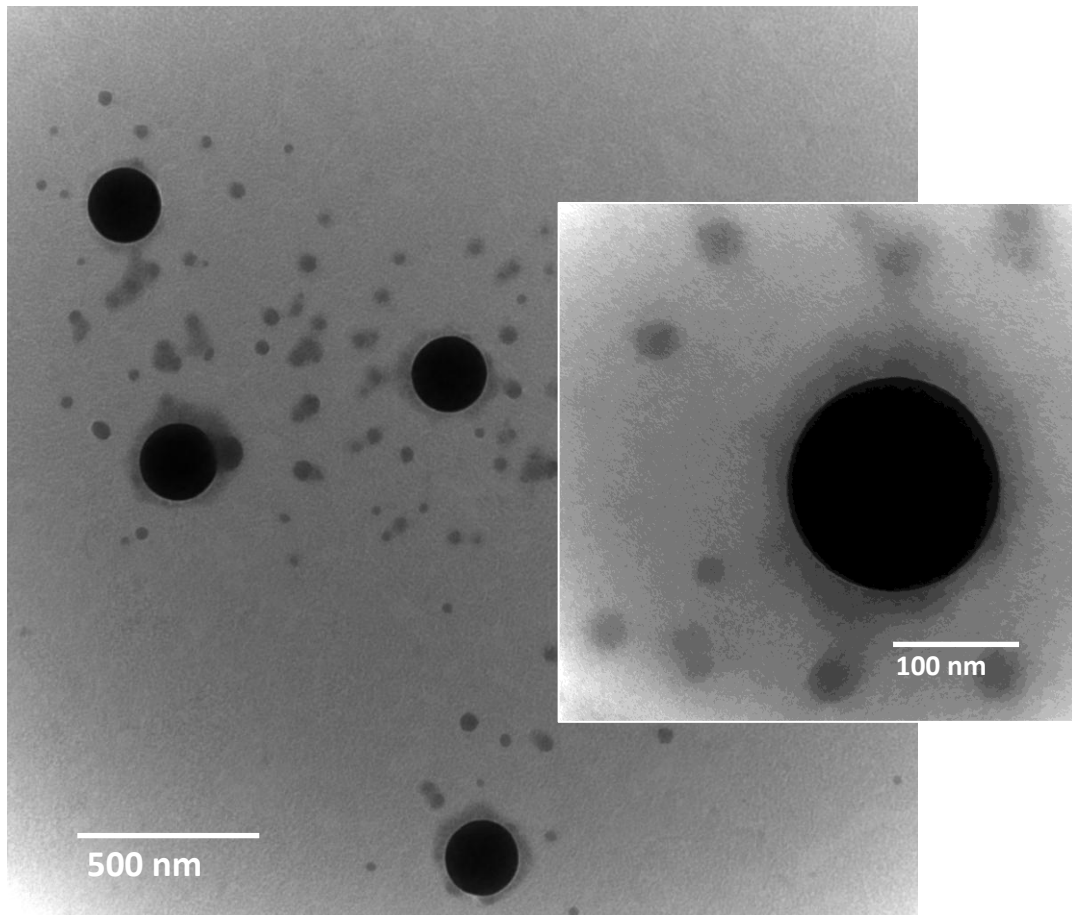
Figure 7-23. Transmission electron microscopy of final bimodal latex obtained using addition of cross-linked particles during the semi-batch feed. Latex RM123

No significant coagulation was observed at the end of these experiments and the latex was stable over a long period of time (several months so far). The rheology profiles of the bimodal latexes are presented in Figure 7-25. A number of latexes had their viscosity values observed to be in the range of specification or very close to it (1200 mPa•s at 20 s^{-1}) as can be seen in Table 7-5. Depending on the latex viscosity, the rheology measurement was able to cover a specific range of shear rate; the lower the viscosity of the latex, the wider the range of shear rate available. From the experiments presented in this section, RM121B2 presented higher viscosity values and

their rheology profile is only available for shear rates < 10 s^{-1}. The other latexes presented lower viscosity and their rheological profile are available at shear rates > 20 s^{-1}, enabling their comparison to the target specification. The rheological measurements are an indication that these experiments are operating very close to their maximum packing fraction as a small increment of solids content (i.e. from RM122A to RM119 and RM123) led to a significant increase in viscosity.
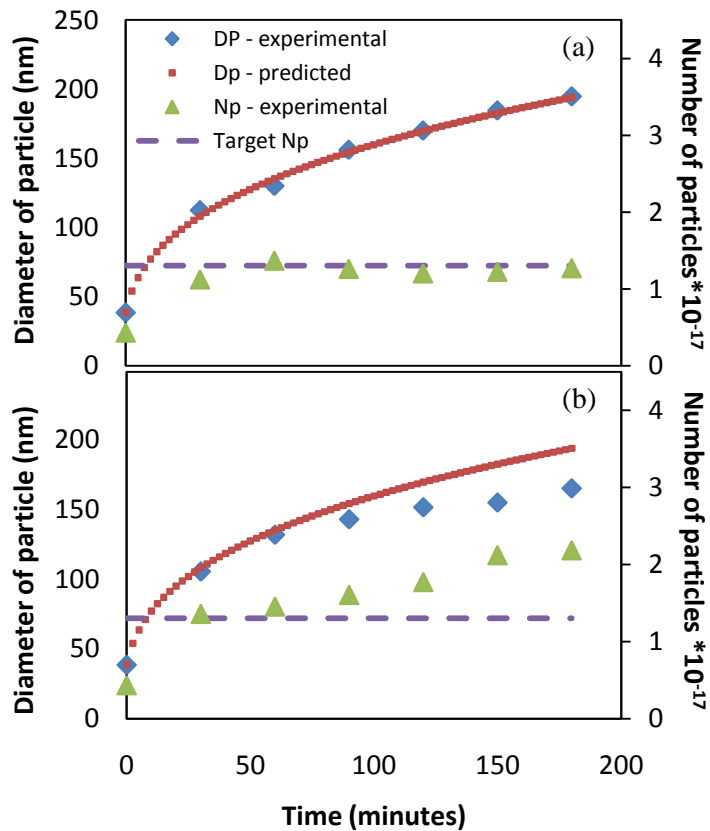
Figure 7-24. Evolution of diameter and number of particles during process of adding cross-linked seeds during the semi-batch feed. (a) Experiment RM122; (b) Experiment RM121B.

The main reason why the level of solids content achieved using this process is lower than the renucleation process presented in Chapter 6 is the smaller Dp_L/Dp_S ratio of the final latexes. From the values of Dp reported in Table 7-5, the Dp_L/Dp_S ratio values of these latexes range from ~4.0

to ~5.6 as estimated from the values of Dp_S measured using TEM images, and are lower than the value of ~6.7 the latexes produced in Chapter 6. As was discussed in Chapters 2 and 6, the target value of of Dp_L/Dp_S ratio is >6.5. The main difficulty of achieving higher solids content for this process is to produce stable highly cross-linked particles in an acceptable solids content concentration (30 wt%) with particle size smaller than 25 nm.
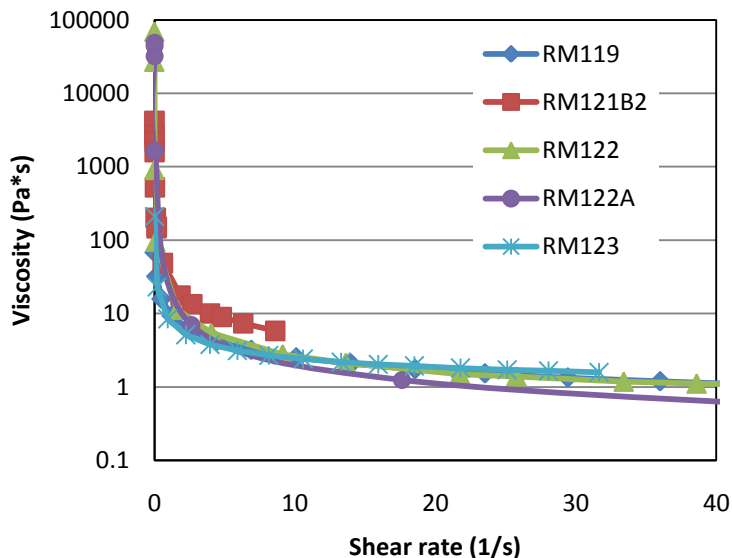

Figure 7-25. Rheological profile of final bimodal latex obtained using addition of cross-linked particles during the semi-batch feed.

7.5 Conclusions

High solids content/low viscosity bimodal polystyrene latexes with overall particle size smaller than 200 nm were obtained using highly cross-linked nanoparticles as pseudo inert nanofillers. The small cross-linked particles suffered from a lack of stability when working at high molar fractions of DVB in the formulation due to the formation of porous polymer particles. A core-shell approach was successfully used to minimize the formation of the pore structures and enabled the production of stable nanoparticles with 15 mol% DVB and 30 wt% solids content of ~40 nm in diameter. The monomer concentration inside these nano-particles were successfully

reduced due to the cross-linking effect and the ratio of volumetric growth rates between the large and small particles populations were estimated to be of approximately 25.4, indicating that the large particles grew 25 times faster than the small ones.

Bimodal latexes with 57 wt% solids content and viscosities <1400 mPa•s at 20 s^{-1} were obtained by introducing the small cross-linked particles during the regular semi-batch polymerization process used to grow the large particles presented in Chapter 6. The final Dp_L/Dp_S was observed to be in the range of 3.9-5.7, which is lower than the optimum, limiting therefore the further concentration of the latexes. The major challenge faced in this process to enable the achievement of more concentrated latexes was the production of stable highly cross-linked particles with extremely small particle size and acceptable solids content concentration.

References

1. Schmidt-Thummes, J.; Schwarzenbach, E.; Lee, D. I. Applications in the Paper Industry. In *Polymer dispersions and their industrial applications;* Urban, D., Takamura, K., Eds.; Wiley-VCH: Weinheim, 2002.

2. De La Cal, J.; Leiza, J. R.; Asua, J. M.; Butte, A.; Storti, G.; Morbidelli, M. Emulsion Polymerization. In *Handbook of Polymer Reaction Engineering;* Meyer, T., Keurentjes, J., Eds.; Wiley-VCH: Weinheim, 2005; Vol. 1.

3.   *http://www.chemanager-online.com/en/topics/chemicals-distribution/surfing-global-megatrends* (accessed 03/07, 2011).

4. Dodgson, D. V. Surfactants and emulsion polymerization: an industrial perspective. In *Surfactants in Polymers, Coatings, Inks and Adhesives;* Karsa, D. R., Ed.; Blackwell Publishing & CRC Press LLC: Boca Raton, 2003.

5. Guyot, A.; Chu, F.; Schneider, M.; Graillat, C.; McKenna, T. F. *Prog.Polym.Sci.* **2002***, 8,* 1573-1615.

6. Ai, Z.; Deng, R.; Zhou, Q.; Liao, S.; Zhang, H. *Adv. Colloid Interface Sci.* **2010***, 1,* 45-59.

7. Mariz, I. d. F. A.; Millichamp, I. S.; de la Cal, J. C.; Leiza, J. R. *Prog. Org. Coat.* **2010***, 3,* 225-233.

8. Greenwood, R.; Luckham, P. F.; Gregory, T. *J. Colloid Interface Sci.* **1997***, 1,* 11-21.

9. Brunauer, S.; Emmett, P. H.; Teller, E. *J. Am. Chem. Soc.* **1938**, 309-319.

10. Moraes, R. P.; Hutchinson, R. A.; McKenna, T. F. L. *J. Polym Sci. Part A: Polym. Chem.* **2010**, 48.

11. Chu, F.; Graillat, C.; Guillot, J.; Guyot, A. *Colloid Polym. Sci.* **1997***, 10,* 986-991.

12. Antonietti, M.; Basten, R.; Lohmann, S. *Macromol. Chem. Phys.* **1995***, 2,* 441-466.

13. Shen, S.; Zhang, X.; Fan, L. *Mater. Lett.* **2008***, 16,* 2392-2395.

14. Macintyre, F. S.; Sherrington, D. C.; Tetley, L. *Macromolecules* **2006***, 16,* 5381-5384.

15. Yan, J.; Wang, X.; Chen, J. *J Appl Polym Sci* **2000***, 4,* 536-544.

16. Kai, J.; Chen, S.; Peng, D.; Liu, R. *Pet. Sci.* **2008***, 4,* 375-378.

17. Esquivel, O.; Trevino, M. E.; Saade, H.; Puig, J. E.; Mendizabal, E.; Lopez, R. G. *Polym. Bull. (Heidelberg, Ger.)* , No pp. yet given.

18. Ge, X.; Wang, M.; Wang, H.; Yuan, Q.; Ge, X.; Liu, H.; Tang, T. *Langmuir* **2010***, 3,* 1635-1641.

19. Cosyns, A. Synthese de Latex Multipopules a Haut Taux de Solide Pour des Primaires Anticorrosion, Universite Claude Bernard Lyon 1, France, 2005.

20. Yan, J.; Xu, R.; Yan, J. *J. Appl. Polym. Sci.* **1989***, 1,* 45-54.

21. Glans, J. H.; Turner, D. T. *Polymer* **1981***, 11,* 1540-1543.

22. Kim, J.; Suh, K. *Polymer* **2000***, 16,* 6181-6188.

23. Nomura, M.; Yamamoto, K.; Horie, I.; Fujita, K.; Harada, M. *J Appl Polym Sci* **1982***, 7,* 2483-2501.

24. Abdollahi, M.; Hemmati, M. *J. Appl. Polym. Sci.* **2009***, 2,* 1055-1063.

25. Errede, L. A. *J Appl Polym Sci* **1986***, 6,* 1749-1761.

26. Brandrup, J.; Immergut, E. H.; Grulke, E. A. *Polymer Handbook;* John Wiley&Sons: New York, 2003.

27. Krevelen, D. W. v.; Hoftyzer, P. J. *Properties of polymers: correlations with chemical structure.* Elsevier Pub. Co.: Amsterdam; New York, 1972.

28. Mark, H. F. Encyclopedia of polymer science and technology. In Wiley-Interscience: Hoboken, N.J., 2007; Vol. 13.

29. Mariz, I. d. F. A.; de la Cal, J. C.; Leiza, J. R. *Polymer* **2010***, 18,* 4044-4052.

Chapter 8

Overall conclusion and future outlook

8.1 Overall conclusion

The experimental chapters of this thesis were divided into two main goals: the production of particles as small as possible with as little surfactant as possible (Chapters 3, 4 and 5) and the production of bimodal latexes with controlled particle size distribution to enable the achievement of high solids content-low viscosity latexes (Chapter 6 and 7).

We have shown in Chapter 3 that polystyrene nano-latexes can be obtained by adopting a semi-batch starved-feed modified (micro)emulsion polymerization, with particle size controlled by adjusting the surfactant concentration in the reactor heel. This methodology was used to produce highly monodisperse 20 wt% solids content polymer nano-latexes of 20-70 nm, with polymer to surfactant ratios ranging from 4 to 22. Shot additions of monomer further concentrated these latexes and enabled the production of up to 40% solids content with small particles size and significantly higher polymer to surfactant ratios.

In Chapter 4, the role of cosurfactants (acrylic acid or 1-pentanol) on the stability and polymerization of styrene-SDS oil-in-water microemulsions was investigated. Both cosurfactants were effective in decreasing the interfacial tension between styrene and water and increasing the composition range of stable microemulsion formulations. However, neither cosurfactant led to a significant increase in solids content concentration or a reduced particle size of the polymerized latexes compared to a styrene system without added cosurfactant. The nano-latexes obtained had <10 wt% solids content, polymer to surfactant ratios <1 and particle sizes in the range of 26-33 nm. This study has also shown that the incorporation of acrylic acid into the polymer particle was

more effective when KPS was used as initiator, as opposed to the hydrogen peroxide/ascorbic acid redox pair.

The fast production of relatively high polymer to surfactant ratio nano-latexes was demonstrated in Chapter 5 using a batch polymerization approach with a high flux of radicals to enhance particle nucleation. The smallest particle size obtained was approximately 30 nm and 27 nm for styrene and MMA respectively with 20 wt% solids content latexes and a polymer to surfactant ratio of 5. The high initiator concentration was combined with the starved-feed semi-continuous process developed in Chapter 3 to enable the production of latexes with average sizes of 21 nm and 17 nm for styrene and MMA, respectively, with a polymer to surfactant ratio of 8.

A process to yield a latex which corresponds to a commercially available paper coating formulation, consisting of a ~50 wt% solids content, monodisperse <200 nm particles latex was demonstrated in Chapter 6. In addition, this latex was concentrated via a surfactant shot (utilizing the methodologies developed in Chapters 3 and 5) to generate a second population of 10-30 nm particles in the presence of the larger particles. The final product had an average large-mode particle size of $\leq$200 nm, 60 wt% solids content and viscosities lower than 500 mPa•s at 20 s^{-1}. This innovative approach differs from previous work as it utilizes a "dry shot" of surfactant to nucleate the required population of extremely small particles required as the last concentration step of the process.

In Chapter 7, a second innovative approach, the use of cross-linked latex particles as a pseudo (inert) nanofiller, was developed. The process to produce small cross-linked particles was based on the procedures from Chapter 3 and 5. However, it was not possible to keep the reduced particle sizes when the cross-linking agent was used in the formulations because of the different composition of the polymer. The minimal particle size of highly-cross-linked particles obtained was in the order of 38 nm in 30 wt% solids content latexes.

It was found that when the molar fraction of divinylbenzene is ≥15%, the polymer particles have a porous structure which severely reduced their colloidal stability. Thus, a core-shell approach was developed to improve stability and produce particles with 15 mol% DVB cross-linking agent. These particles were then applied in the production of bimodal particle size distribution latexes. The cross-linking effectively reduced the monomer concentration inside the small particles, leading to a reduced volumetric growth rate relative to larger non-cross-linked seeds by a factor of 25.4. This kinetic study showed that the rates of polymerization inside the distinct population of particles can be manipulated to control the latex particle size distribution in the production of bimodal latexes. The best results were obtained by adding the cross-linked particles towards the end of the feeding period during the semi-batch growth of the large seeds to produce approximately 57 wt% latexes with viscosities <1400 mPa•s at 20 s^{-1}. The slightly lower solids content and higher viscosity observed using this methodology compared to the renucleation approach presented in Chapter 6 is due to a Dp_L/Dp_S of ~4-6, slightly lower than the optimal ratio of >6.5.

The two procedures developed in this thesis both lead to high solids content low viscosity latexes with average particle diameters less than 200 nm, an achievement not previously reported in the open literature.

8.2 Future outlook

The main difficulty experienced in this project was the production of stable highly cross-linked poly(styrene-co-divinylbenzene) particles with extremely small particle size at acceptable solids content, as was discussed in Chapter 7. Although the use of the cross-linked particles to produce bimodal latexes with solids content up to 58 wt% was demonstrated, the Dp_L/Dp_S ratio at the end of the polymerization was higher than optimal. Since the product specifications required

182

the large particles to be smaller than 200 nm, obviously the small particles should have their size reduced to increase Dp_L/Dp_S ratio.

To improve the current results, methods should be developed in any of the following directions: (i) the production of **smaller** highly cross-linked latex particles (for instance using MMA rather than Sty), (ii) the production of stable particles with a **higher cross-linking density** or (iii) the production of more concentrated (**higher solids content**) small cross-linked particles latex, which would allow the further delay for their addition to the reactor. In addition, it would be useful to explore some thermodynamic aspects regarding the swelling of these particles (i.e., looking at the swellability of styrene and butadiene in different polymers) to identify an inexpensive material that undergoes **negligible growth** during the polymerization process. For this purpose, different monomers, surfactants, cross-linking agents and polymerization techniques (including controlled radical polymerization) could be explored. In addition, a comprehensive study to understand and control the main factors associated with the formation of a porous structure in highly cross-linked polymers could be undertaken, with the objective of producing highly cross-linked particles with a smooth surface, and therefore colloidally stable nano-latexes.

The synthesis of inorganic particles could also be investigated in microemulsion systems. The objective of this front should be the creation/identification of routes to synthesize inexpensive materials or the identification of natural inexpensive materials that could be used as nano-fillers.

The reverse order of particles nucleation unseeded approach could be further explored and developed by releasing the particle size constraint of this project. If the overall particle size distribution of the latex could be set at a higher limits (>200 nm), the optimal Dp_L/Dp_S could be achieved taking advantage of the ratio of volumetric growth rate between the large and small populations. This innovative approach could be developed by synthesizing the small cross-linked seeds in the reactor heel and then nucleating and growing the large non-cross-linked particles in

the presence of the small particles until reaching the target Dp_L/Dp_S and solids content to produce concentrated latexes with low viscosity, as proposed in Chapter 1.

In addition, the results obtained in Chapter 6 could be further developed by using MMA as a more hydrophilic monomer to generate smaller particles and decreasing the concentration of surfactant required for the re-nucleation of the small population of particles.

One more aspect that could be explored is the rheological modeling of these concentrated dispersions. More specifically, by preparing individual latexes of several particles sizes with narrow distributions (using the methodologies developed in Chapters 3 and 6), mixing them at appropriate proportions and concentrating them via rotoevaporation, one can produce a series of latexes with different solids content/concentrations with well controlled particle size distributions. By measuring the rheological behaviour of these well defined particle size distribution latexes, one can assess the predictive capability of the rheological model developed by Pishvaei et al. reported in Pishvaei M, Graillat C, McKenna TFL, Cassagnau P. 2007 J. Rheol. 51: 51 – 69. Latexes with different particle size distributions (e.g.; monodisperse with low polydispersity, monodisperse with high polydispersity, multimodal latexes with different Dp_L/Dp_S ratios) could be used to experimentally verify model predictions, and to improve the model's ability to represent the rheological behaviour of real samples.

Appendix A

Swelling of polymer particles

Latex particles can only be swollen by monomer to a limited extent defining a characteristic monomer concentration in the particles, $[M]_p$, even when monomer and polymer are miscible in all proportions in bulk.[1] The explanation is that the decrease in Gibbs energy which results from mixing the polymer and the monomer is counterbalanced by increase in Gibbs surface energy because of the increase of the surface area of the swollen particles. This theory was developed by Morton et al.[2] who deduced an equation relating the equilibrium swelling to particle size and interfacial tension (Equation 8 – section 2.5).

Two methods are now used to predict the monomer concentration in the polymer particles in emulsion homopolymerization: thermodynamic and empirical methods.[3]

The thermodynamic method is based on Equation 8. Given values of the interaction parameter between the monomer and the polymer χ_{mp} and the unswollen diameter of the particle, it can be solved iteratively to yield φ_p. Then, by introducing the value of φ_p into the following equation (Equation A-1), one can get the saturation monomer concentration in the polymer particles. Although this method is referred as thermodynamic, the determination of χ_{mp} is obtained via empirical methods. [3-5]

$$[M]_p = \frac{1 - \varphi_p}{V_m} \tag{A-1}$$

$[M]_p$ can also be determined experimentally, by re-swelling a fully polymerized latex and then centrifuging the monomer out or by deducing the conversion at which all monomer absorbed into

the latex particles from the transition from zero-order to first-order kinetics, which is assumed as the transition from Interval II to Interval III.[6, 7]

The amount of monomer that can be absorbed in the polymer particles is limited and the excess of monomer form droplets. The limiting swelling of the polymer particles is due to the contribution of the surface energy to the total free energy of the system. Because of the interfacial tension, the surface energy increases as particles swell and, at some point, this compensates for the decrease in the free energy due to monomer-polymer mixing. From the values of the maximum swelling for homopolymerization presented in Table A-1 it can be seen that the higher the water solubility of the monomer, the higher the equilibrium swelling. According to this information the equilibrium monomer concentration inside the polymer particle $[M]_p$ for the homopolymerization of styrene is 5.2 mol/L. However some authors[1] consider the $[M]_p$ for styrene as 6 mol/L.

Table A-1. Swelling equilibrium data for homopolymerization. Adapted from De La Cal et al.[8]

Monomer	$\varnothing^P_M$ [a]
Styrene	0.6
N-Butyl methacrylate	0.6
N- Butyl acrylate	0.65
Methyl methacrylate	0.73
Vinyl methacrylate	0.85
Methyl acrylate	0.85

[a] $\varnothing^P_M$ volume fraction of monomer in the polymer particles

References

1. Dunn, A. S. Harkins, Smith-Ewart and Related Theories. In *Emulsion Polymerization and Emulsion Polmyers;* Lovell, P. A., El-Aasser, M. S., Eds.; John Wiley and Sons: 1997.

2. Morton, M.; Kaizerman, S.; Altier, M. W. *J. Colloid Sci.* **1954**, 300-312.

3. Nomura, M.; Tobita, H.; Suzuki, K. *Adv.Polym.Sci.* **2005***, Polymer Particles,* 1-128.

4. Errede, L. A. *Polymer* **1992***, 10,* 2168-2176.

5. Sakar, D.; Sarac, A.; Cankurtaran, O.; Karaman, F. *Polym.Bull.(Heidelberg, Ger.)* **2007***, 1,* 305-312.

6. Harada, M.; Nomura, M.; Kojima, H.; Eguchi, W.; Nagata, S. *J Appl Polym Sci* **1972***, 4,* 811-833.

7. Bartholome, E.; Gerrens, H.; Herbeck, R.; Weitz, H. M. *Z.Elektrochem.Angew.Phys.Chem.* **1956**, 334-46, discussion 346-8.

8. De La Cal, J.; Leiza, J. R.; Asua, J. M.; Butte, A.; Storti, G.; Morbidelli, M. Emulsion Polymerization. In *Handbook of Polymer Reaction Engineering;* Meyer, T., Keurentjes, J., Eds.; Wiley-VCH: Weinheim, 2005; Vol. 1.

Appendix B

Micelles – Thermodynamic and physical aspects

Surfactant is an abbreviation for surface active agent, which literally means active at the surface. In other words, a surfactant is characterized by its tendency to absorb at surfaces and interfaces. The term interface denotes the boundary between any two immiscible phases; the term surface indicates that one of the phases is gas, usually air.

The driving force for a surfactant to adsorb at an interface is to lower the free energy of that phase boundary. The interfacial free energy per unit area represents the amount of work required to expand the interface ($Work \equiv \Delta G = \gamma_i dA$, where γ_i is the interfacial tension between two immiscible liquids when emulsifying agent is present in the system and dA is the increase in the area of contact between the two liquids).[1] The term interfacial tension is often used instead of interfacial free energy per unit area. Thus, the surface tension of water is equivalent to the interfacial free energy per unit area of the boundary between water and the air above it. When the boundary is covered by surfactant molecules, the surface tension (or the amount of work required to expand the interface) is reduced.

The tendency to accumulate at the interfaces is a fundamental property of a surfactant. As surfactant concentration is increased, the surface tension is lowered because of adsorption of surfactant at the surface. The higher the concentration, the larger the adsorption (adsorbed molecules are in equilibrium with bulk dissolved ones) and the lower the surface tension. This surface tension decrease occurs up to a well defined concentration which is called critical micellar

concentration (CMC). Above it, tension remains nearly constant (Figure B-1), which express a constant concentration of molecularly dissolved molecules (unimers[4]).
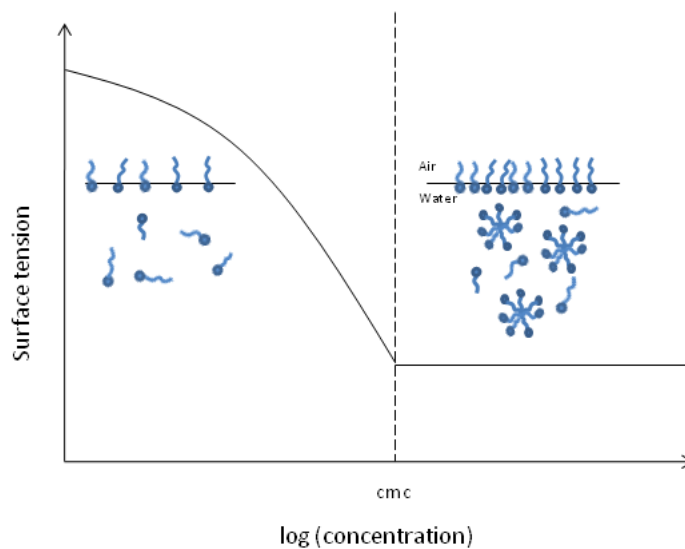
Figure B-1. Surface (air-water) tension as a function of surfactant concentration for an aqueous micellar solution. Schematic structure of the solution is shown below and above the critical micellar concentration (CMC).

Above CMC unimers in solution tend to form aggregates, or so-called micelles. Micelle formation, or micellization, can be viewed as an alternative mechanism to adsorption at the interfaces for removing hydrophobic groups from contact with water, thereby reducing free energy of the system. The micelle formation thermodynamic principle is based on the fact that water does not interact favourably with the hydrophobic groups and there is a driving force for expelling them from the aqueous environment.

The CMC is therefore an important characteristic of the surfactant and is a function of its molecular chemistry. The hydrophobic interactions increases with increasing alkyl chain length of

---

[4] The free or unassociated surfactant is referred to in the literature either as 'monomer' or 'unimer'. In this text we will use 'unimer' and the term 'monomer' will be restricted to the polymer building block.

an alkane or the hydrophobic group of a surfactant. Indeed, the decrease in solubility of an alkane with number of carbons very much parallels the change in CMC. The CMC varies with some other parameters from the chemical structure of the surfactant as well, as for instance, the CMC of non-ionics are much lower than for ionics.[2]

Temperature and co-solutes, such as inorganic salts and low molecular weight organic compounds, the later ones to different extents depending on their polarities, can also affect CMC.[2]

With a good approximation, micelles can in a wide concentration range above the CMC be viewed as microscopic liquid hydrocarbon droplets covered with the polar head groups, which are in interaction with water. It appears that the radius of the micelle core constituted of the alkyl chains is close to the extended length of the alkyl chain, i.e. in the range of 1.5-3.0nm. The reason for this is that as the driving force of micelle formation is the elimination of the contact between the alkyl chains and water. The larger a spherical micelle, the more efficient this is since the volume-to area ratio increases. Decreasing the micelle size always leads to an increased hydrocarbon-water contact. However, if the spherical micelle was made so large that no surfactant molecule could reach from the micelle surface to the centre, one would either have to create a void or some surfactant molecules would lose the contact with the surface. Both alternatives are unsatisfactory.

The micelle size, as expressed by the radius of a spherical aggregate, as well as a related and equally important characteristic of a micelle that is the aggregation number, i.e. the number of surfactant molecules in one micelle, may be obtained from quasi-elastic light scattering spectroscopy (QLS) [this technique is further discussed in Appendix D]. Mazer et al, 1976[3] studied the mean size, shape, aggregation number and polydispersity of SDS micelles as a function of temperature (10-85°C) and NaCl concentration (0.15-0.6 M) for surfactant

concentrations which appreciably exceed the CMC, including a thermodynamic model. It turned out that SDS micelles have a minimum spherical structure with an average diameter of approximately 25 Å, which is quite close to the length of an extended dodecyl sulphate anion (23 Å). In addition, the size of the aggregates and its aggregation number would increase as temperature decreases, concentration of surfactant increases and electrolyte (NaCl) concentration increases, changing as a consequence the shape from spherical to prolate spherocylinders.

Micellar solutions, solubilization and Microemulsion

One of the most important properties of surfactants that is directly related to micelle formation is *solubilization*. Solubilization may be defined as the spontaneous dissolving of hydrophobic solutes (in the same way, reverse micelles dissolve water) by reversible interaction with the micelles of a surfactant in a solvent to form a thermodynamically stable isotropic solution.[4] For non-polar compounds it is probably often appropriate to consider solubilization as a simple partitioning between the micellar nonpolar interior and the aqueous environment in the intermicellar solution. For partly polar solubilizates, this is certainly not a good description since the solubilizate will participate in and influence the surfactant aggregation process. One might therefore consider solubilization of short-chain alcohols for example as a formation of mixed micelles.[5-7]

Solubilization is distinguished from *emulsification* (the dispersion of one liquid phase in another) by the fact that in solubilization the solubilized material is in the same phase as the solubilizing solution and the system is consequently thermodynamically stable. If solubility of a normally-insoluble material is plotted against the concentration of the surfactant solution that is solubilizing it, we find that the solubility is very slight until CMC of the surfactant (in the presence of the solubilizate) is reached at which the solubility increases approximately linearly with concentration of the surfactant, what indicates that solubilization is a micellar phenomenon.[4]

The ability to solubilize in general increases strongly with increasing hydrocarbon chain length of the surfactant.[5] For the same amphiphile, solublilizing power will, naturally, reflect the solubility of the given solubilizate in the hydrocarbon most closely related to the amphiphile tail to some extent. For alkanes, in turn, the extent of swelling depends on the hydrocarbon chain length: Swelling is larger for shorter alkanes.[8, 9]

The solubilization power of a micellar solution can be greatly enhanced by the addition of a cosurfactant.[6, 7] When the swollen micelles reach diameters exceeding 4 or 5 nm, the resulting phase is frequently called a "microemulsion".[6] Nevertheless, the definition of microemulsion is still source for plenty of debate on distinguishing microemulsions from a true micellar solution.[10, 11]

References

1. Prince, L. M. In *Microemulsions, Theory and Practice.* Academic Press, Inc.: New York, 1977.

2. Jonsson, B.; Lidman, B.; Holmberg, K.; Kronberg, B. *Surfactants and polymers in aqueous solution;* John Wiley & Sons: New York, 1998.

3. Mazer, N. A.; Carey, M. C.; Benedek, G. B. The size, shape and thermodynamics of sodium dodecyl sulfate (SDS) micelles using quasielastic light scattering spectroscopy. In *Micellization, Solubilization, and Microemulsions;* Mittal, K. L., Ed.; Plenum Press: New York and London, 1976; pp 359-381.

4. Rosen, M. J. *Surfactants and interfacial phenomena;* Wiley-Interscience: Hoboken, N.J., 2004.

5. Lindman, B.; Wennerstrom, H. *Micelles;* Springer-Verlag: Berlin, 1980.

6. Miller, C. A.; Neogi, P. *Interfacial Phenomena;* Marcel Dekker: New York, 1985.

7. Chevalier, Y.; Zemb, T. *Rep.Prog.Phys.* **1990**, *3,* 279-371.

8. Vold, R. D.; Vold, M. L. *Colloid and Surface Chemistry;* Addison-Wesley Publishing Company: Massachussets, 1983.

9. Hoffmann, H.; Ulbricht, W. *J. Colloid Interface Sci.* **1989**, *2,* 388-405.

10. Leung, R.; Hou, M. J.; Shah, D. O. Microemulsions: Formation; Structure, Properties, and Novel Applications. In *Surfactants in Chemical/Process Engineering;* Wasan, D. T., Ginn, M. E. and Shah, D. O., Eds.; Marcel Dekker: New York, 1988.

11. Prince, L. M. *J. Colloid Interface Sci.* **1975**, *1,* 182-188.

Appendix C

Production of the large mode latex

The production of the latex corresponding the large particles was designed by determining the main target parameter of the final product, the particle size. As mentioned in Chapter 1, the average particle size of the large mode should be smaller than 200 nm (preferably 160 nm). In the initial design we decided to choose a particle size of 195 nm, and depending on the results and time available we would decrease the particle size specifications in a later time.

After determining the particle size, calculations considering the volume fraction the large family of particles should occupy in the bimodal latex (determined using Equation 16) enable one to calculate the average number of particles that should compose the large mode.

It was defined that we would produce the large mode starting from seed latex with particles of about 40 nm in diameter. Thus, if the number of particles that compose the large mode is known, the challenge was to grow the seed particles from 40 nm to 195 nm while maintaining the number of particles constant by assuring to keep the growing particles colloidally stable. By doing that, the final product should have the exact desired particle size (195 nm) and concentration (52% w/w).

In order to control the number of particles during the growth of the particles in a semi-batch emulsion polymerization process, it is evident that the reactor should receive a preemulsion containing monomer, surfactant and initiator. The mass of monomer is easily determined by calculating the difference between the final mass of polymer in the desired latex and the initial mass of polymer in the seeds. The initiator (hydrogen peroxide) was set as 0.05 % (w/w) relative to the monomer mass. Both the monomer and initiator flow rates were designed to be constant during the semi-batch process. The surfactant addition was defined by a mass balance to

determine the growth of the particles during the process and the respective surface area to be stabilized. The mass balance is shown below, where V_p is volume of one particle, N_p is total number of particles per volume, V_R is the volume of the reactor and $\dot{q}$ is the volumetric flow rate of monomer addition, assuming the product $N_p V_R$ constant.

$$\frac{dV_p}{dt} N_p V_R = \dot{q} \tag{C-1}$$

$$\frac{dV_p}{dt} = \frac{\dot{q}}{N_p V_R} \tag{C-2}$$

$$\int_{v_{SEED}}^{v_{p(t)}} dV_p = \frac{\dot{q}}{N_p V_R} \int_0^t dt \tag{C-3}$$
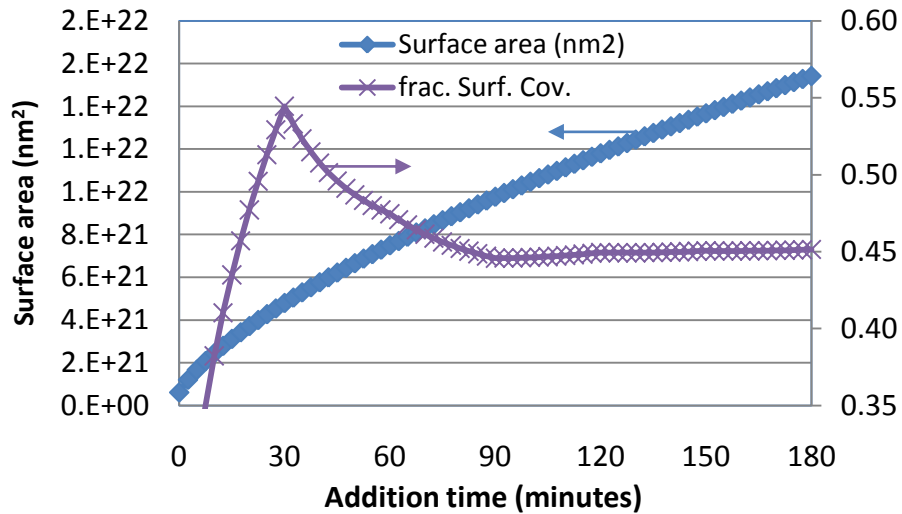
$$V_p(t) - V_{SEED} = \frac{\dot{q}}{N_p V_R} t \tag{C-4}$$

$$V_p(t) = V_{SEED} + \frac{\dot{q}}{N_p V_R} t \tag{C-5}$$

$$\frac{\pi}{6} D^3 = V_{SEED} + \frac{\dot{q}}{N_p V_R} t \tag{C-6}$$

$$D = \sqrt[3]{\frac{\pi}{6} \left(V_{SEED} + \frac{\dot{q}}{N_p V_R} t \right)} \tag{C-7}$$

Equation C-7 provides the profile of surface area generated over the semi-batch emulsion polymerization during the growth of the seeds to form the large mode latex, shown in Figure C-1.

Figure C-1. Surface area generation profile resulting from a mass balance (Equation C-7) describing the growth of the particles during the production of the large family of particles and the surfactant coverage required to keep the particles colloidally stable during the process.

The total reaction time was determined by verifying the maximum theoretical rate of polymerization of the system using Equation 3, applying the values applicable to each reaction conditions. The determining parameter in this process is the reaction temperature, which will define the propagation constant rate. In order to reduce process time, a temperature of 90°C was chosen, having in mind that in industrial processes, the use of pressurized reactors allows the operation at even higher temperatures. The reaction time required assuming maximum reaction rate during the entire process was of about 3 hours.

Several experiments were performed to determine the correct level of surfactant coverage required for the stabilization of the particles during their growth. The non-linear growth of the surface area and the necessity to have a fine control over the surface coverage of the growing particles during the process is the reason why the preemulsion feed was divided into 6 different compositions.

The addition of surfactant in the beginning of the process is higher than at the end. Due to the high mass of surfactant that needed to be added in the first 0.5 hour of reaction, the control over the number of particles was very difficult. Decreasing the surfactant coverage reduced the number of particles in this first phase of the reaction. Increasing the surfactant coverage would nucleate new particles. After a series of experiments, it was concluded that it was more practical to account for the nucleation of new particles in the system by starting with less particles. Finally, a third of the particles are originated from the seed latex and the other two thirds are nucleated in the first 0.5 hour (see Figure 6.1(a)).This process turned out to be highly reproducible and therefore adopted as standard procedure in our project.

Appendix D

Particle size characterization

As particle size distribution is the most important of the system when dealing with HSC/LV latexes, a review of the techniques used for this characterization as well as a comparative analysis is provided in below.

Particle size distribution (PSD) is one of the most important characteristics of a High Solid Content (HSC) latex, as described in the literature review of this project. Nevertheless, it is not so simple to measure this property accurately. In fact, there are a large number of techniques available to measure average particle diameter, however when it comes to determine the entire PSD, the number of efficient techniques is much lower. In addition, not all techniques available are suitable, depending on the range of diameters to be measured, the ratio between the diameter of each population, and the nature of the polymer (i.e. T_g, density, refractive index).

In this appendix we will review briefly the techniques available for PSD and reinforce their advantages and drawbacks due to the importance of this characterization for this work. Recent comprehensive reviews can be suggested as supplementary readings.[1, 2]

Three different categories of techniques can be distinguished for PSD: microscopy, separative techniques and light scattering. All three categories of techniques require important dilution of the sample. Another characteristic is that these analyses have to be done off-line, or in the best case, using sampling loops in real time.

Microscopy

Methods based on microscopy are the most accurate since particles can be seen, measured and counted. Electron microscopy as Transmission Electron Microscopy (TEM) or Scanning Electron

Microscopy (SEM) is the most often used, but Atomic Force Microscopy (AFM) can also provide interesting information concerning surface topology of particles. The limitation in use for microscopy techniques is related to soft (co)polymers. In fact, low T_g (glass transition temperatures) lead to rapid coalescence and filmification, making inadequate or impossible to observe the individual particles and there characteristics. This is not the case for our polymer, since the T_g of polystyrene is 100°C, however, when dealing with (co)polymers of low Tg, this limitation can be overcome by using cryo-fracture technique[2] or by employing some surface treatment, for instance surface cross-linking under UV or by chemical reaction with some markers.

Because of the cost and the time needed for each sample analysis, microscopy cannot be used as a routine analysis to determine PSD, however it can be used as a reference ever since needed.

Light Scattering

Scattering methods are probably the most widely employed means of measuring PSD. They are easy to used, don't require calibration and the measurement is rapid. These methods can be further divided into two forms: Dynamic Light Scattering (DLS) and Static Light Scattering (SLS)

DLS, also known as Photo Correlation Spectroscopy (PCS) or Quasi-Elastic Light scattering (QELS), is based on measuring the movement of particles in a colloidal dispersion as a result of Brownian motion. When a latex sample is illuminated with laser, the intensity of the scattered light measured by a photocorrelator fluctuates with time. As we know, small particles move faster than large one when submitted to Brownian Motion, thus the speed these fluctuations in intensity of the scattered light occur is measured and can used to determine the translational diffusion coefficient D_z, that in turn yields particle diameter according to Stokes-Einstein equation:

$$D_z = \frac{k_B T}{3\pi\eta r_p} \tag{D-1}$$

where k_B is the Boltzmann's constant, T is absolute temperature, η is the viscosity of the sample and r_p is the hydrodynamic particle diameter. The correlation function that relates intensity fluctuations of scattered light with the translational diffusion coefficient requires that the user knows the viscosity and the refractive index of the medium, which is most often water.

According to the Mie theory,[3] the intensity distribution is an oscillatory function of particle diameter. Thus, at a fixed angle, some particle sizes may correspond to a weak detection intensity. In this case, multi-angle DLS can be a helpful solution. It was found that in most cases single angle DLS (usually 90°) fails for the determination of a bi- or trimodal distributions or even latexes with a polydisperse PSD.[1, 2] This is mainly due to the differences in scattering intensities. Indeed, large particles scatter much more light than small ones and are therefore easier to detect. However, single angle detectors placed at wide angles (i.e. 173°) can minimize this effect since large particles scatter light mainly in the forward direction, being possible to counter-balance this way the intensities of small and large particles to enhance detectability. Nonetheless single angle DLS is a very efficient method for daily analysis of particle average diameters of monomodal samples with a limited polydispersity. Schneider and McKenna[2] tested the multi-angle DLS for multimodal PSD and it appeared that this technique provides satisfactory results for particle size measurements, although it is not able to give a reliable estimation of the fraction of each population under the circumstances presented. The main drawback of DLS therefore is the important difference of the scattered intensities as a function of particle diameter when dealing with non-monomodal PSD. It seems to be very difficult to resolve for all populations if they are not present in similar proportions. Especially for our final latex, as we expect to have less than 20% in volume of small particles, being them much smaller than the large ones, what makes them very difficult to detect and the latex is often seem as monomodal.

In the case of SLS (also known as Laser Diffraction), the intensity of light scattered by the particles is measured at different angles at the same time. The particle diameter is determined using the Mie Theory. The basic principle of this theory is that the angular intensity distribution of scattered light is function of the particle size and the polymer refractive index.[3] Thus, in order to apply Mie Theory, the user has to know the refractive index and absorption of the polymer in addition to the refractive index of the medium. The efficiency of static light scattering has also been explored by Schneider and McKenna.[2] The results obtained show good agreement with the reference measurement. The authors concluded that this technique is less satisfactory than multi-angle DLS and separative methods. However a new generation of equipments, SLS coupled with Polarization Intensity Differential Scattering (PIDS) can provide accurate estimates of PSD, especially the regions around the lower size limit of these equipments.[3]

Separative techniques

Separative techniques rely on a separation of different populations of particle sizes prior to their measurement. Thus, the detectors used to determine the particle sizes after separation are similar to those used by light scattering techniques, and therefore present the same drawbacks.

Capillary Hydrodynamic Fractionation (CHDF) is a technique where the particles are separated with respect to their sizes due to a parabolic velocity profile that is developed during a laminar flow inside a column. This separation causes the larger particles to leave the tube first since they move toward the centre of the flow field. A UV detector at the outlet of the tube is used to measure and count the particles. CHDF has being shown to be an efficient technique[1, 2] however it has some limitations that influence its accuracy. It requires precise and frequent calibration to provide reliable measurements. Another point is that CHDF overestimate sizes for some range of particle diameter and provides distributions broader than they really are (determined by TEM images).[2] Another limitation is that the UV detectors require calibration and

201

optical properties of the particles (absorbance) as function of their size. The extinction coefficient used to measure the size is a function of the particle diameter and one can specify just a constant for this parameter. This makes it really difficult to find a value that works for particles that range from small values until large values, what limits the calibration of the detector to not very large ranges of sizes.

Field Flow Fractionation (FFF) is also a separative technique used for PSD determination. The particles are separated according to their size by a cross flow that is used to confine the particles injected in the column. Large particles move toward the wall opposite to the source of the cross flow where the velocity is lower and exit later than small particles. The PSD is measured at the end of the tube by static light scattering at three angles (45°, 90° and 135°) coupled with an UV detector. In comparison to other techniques[2] it has shown an error of about 10% to reference values. Another drawback is that this technique is expensive and not easy to set up, being the operation extremely delicate.

In Disc Centrifuge Photosedimentometry (DCP) particles are separated radially by exploiting the centrifugal force generated by dropping the latex and fluid to a spinning disc. The particles are separated as a function of their mass, size and density. The latex density has to be higher than that of the spin fluid, therefore there are cases that the additional fluid density has to be adapted to the polymer density. In this technique, small particles require high rotation speed and long analysis time (at least 6 h for Dp of 39 nm)[1] and in general it is difficult to detect particles less than 100 nm in diameter. Another drawback is that when working with soft polymers (low T_g), the particles can agglomerate during centrifugation,[2] however it is not applicable to this project. Therefore, this technique is indicated for certain types of material and certain particle size range. It works likewise for analytical ultracentrifuge.[4]

Similarly, Chu et al.[5] proposed a technique that applies centrifugation for the separation of the particles, then the particle size is measured by light scattering and the fraction of each population is determined by gravimetric analysis. This procedure is easy and efficient, and again, is works best for "hard" particles due to coagulation during centrifugation of low Tg polymer particles and relatively large particles.

It is also possible to mention fractional creaming[6, 7] as separative technique. In this method a given concentration of alginate will substantially cream only particles that are larger than a certain critical size, regardless of the nature of the latex. The main drawbacks are the requirement of a calibration curve and the time needed for the determination of the entire distribution (6-8 h for a distribution of 50-1000nm).[6]

References

1. Elizalde, O.; Leal, G. P.; Leiza, J. R. *Part.Part.Syst.Charact.* **2000***, 5-6,* 236-243.

2. Schneider, M.; McKenna, T. F. *Part.Part.Syst.Charact.* **2002***, 1,* 28-37.

3. Xu, R. *Particle characterization: light scattering methods;* Kluwer Academic: New York, 2002.

4. Colfen, H. *Crit.Rev.Opt.Sci.Technol.* **1997***, Materials Characterization and Optical Probes Techniques,* 525-552.

5. Chu, F.; Graillat, C.; Guillot, J.; Guyot, A. *Colloid Polym. Sci.* **1997***, 10,* 986-991.

6. Tauer, K.; Jaeger, W. *Plaste Kautsch.* **1983***, 11,* 612-616.

7. Schmidt, E.; Biddison, P. H. *Rubber Age (N.Y.)* **1960**, 484-490.

Appendix E

Determination of divinylbenzene (DVB) mass required according to the desired molar fraction of cross-linking in the polymer synthesis

Assuming it is desired to produce a polymer with 15 mol% of cross-linking agent (DVB):

In 100 mols

15 mols of DVB = 15*(130.19 g/mol) = 1,952.85 g

85 mols of styrene = 85*(104.15 g/mol) = 8,852.75 g

Total : 10,805.60 g

% mass:

DVB = 18.07%

Sty = 81.93%

Assuming the total monomer mixture mass is 324 g:

In 324 g of monomer mixture:

DVB = 58.55 g

Styrene = 265.45 g

However, DVB solution is 80.2 wt% mixture with isomers, thus:

DVB = 58.55/0.802 = **73 g**

From these 73 g, 19 wt% is ethylvinylbenzene (EVB)

EVB = 13.9 g (*we will assume that this mass will account for the styrene mass*)

So, the mass of styrene:

Styrene = 265.45 – 13.9 = **251.55 g**

Appendix F

Synthesis of 78 nm seed latex

The recipe and the methodology described below were used to prepare a latex of 80 nm particles and 51 wt% solids content.

It consists of a semi-batch process with final volume of 500 mL of latex

Global formulation:

> Styrene = 247.6 g
>
> SDS = 6.2 g (2.5 wt% to monomer)
>
> NaPS = 1.2 g (0.5 wt% to monomer)
>
> H_2O = 245 g

Temperature 75°C

Reactor heel formulation:

> H_2O = 156.5 g (+15 g from initiator)
>
> SDS = 3.1 g
>
> Sty = 58.2 g

Initiator solution:

> NaPS = 1.2 g
>
> H_2O = 15 g

Continuous addition – preemulsion:

H_2O = 73.5 g

SDS = 3.1 g

Sty = 189.4 g

Total mass of preemulsion = 266 g
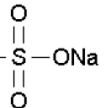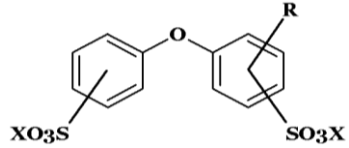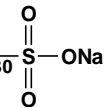
Addition time = 1 h

Mass rate = 4.4 g/ minute

Procedure:

1- Stir reactor heel components during heating up, under nitrogen atmosphere

2- Add initiator solution when reactor reaches 70°C, Reactor heel reacts for 15 minutes.

3- Start continuous addition of preemulsion

4- When continuous addition is over, let the reaction go for another 1 hour to convert residual monomers.

5- Cool down

Appendix G

Specific information on the chemicals and procedures

Table G-1. Physical and Chemical properties of the surfactants used in this work.

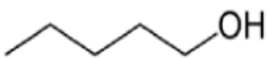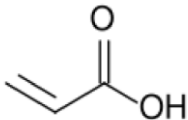| Properties	Surfactants		
	SDS	Dowfax 2A1	Disponil FES77[a]
Formula	$CH_3(CH_2)_{10}CH_2O-S(=O)(=O)-ONa$	R= Branched C_{12}; X= Na	$CH_3(CH_2)_mO(CH_2CH_2O)_{\overline{30}}S(=O)(=O)-ONa$ m= C_{12}-C_{14}
Molar mass (g/mol)	288.38	576	1562
Water solubility @ 25°C (g/L)	150	Infinite	NA
CMC (g/L)*	0.9 [1]	0.07	0.28
CMC (mol/L)*	0.0031 [1]	0.00012	0.00018

Data extracted from the technical sheet provided by the manufacturer when not specified; [a] The molecular structure information was provided in a verbal communication from Dr. Aurelie Mourel at BASF laboratories in Ludwigshafen; * Conditions are 0.1M NaCl @ 25°C. Also available the value for SDS in pure water @ 25°C: 0.0082mol/L or 2.36g/L. [2]

Chemicals

Surfactants. Sodium Dodecyl Sulphate (SDS) solid powder. (Branched) Sodium Dodecyl Diphenyl Oxide Disulfonate (Dowfax 2A1 or Calfax DB-45) solution surfactant with 45.7 wt% actives from Pilot Chemical Company (USA). Disponil FES77 Properties depicted in Table G-1.

Cosurfactants /(and) comonomers. 1-Pentanol (99%, extra pure) from Acros Organics. Acrylic and methacrylic acids from Sigma-Aldrich (both 99% pure). Chemical and physical properties provided in Table G-2.

Table G-2. Physical and Chemical properties of the molecules used as cosurfactants/(and) comonomers in this work.

Properties	Cosurfactants	
	1-Pentanol	**Acrylic acid**
Formula		
Molar mass (g/mol)	88.15	72.06
Boiling point (°C)	138-139	141
Melting point (°C)	-78	13
Water solubility @ 25°C (g/L)	2.7	unlimited
Monomer density (g/cm^3)	N.A.	1.051
Polymer density (g/cm^3)	N.A.	1.22 [3]

Data extracted from the technical sheet provided by the manufacturer when not specified.

Initiator. Potassium persulfate (KPS) from Acros Organics, 99+%, for analysis. Physical and chemical properties of the initiator is provided in Table G-3.

Table G-3. Physical and chemical properties of the initiator used in this work.
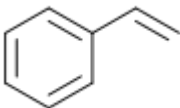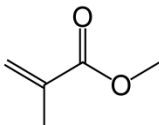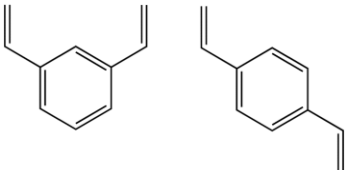
Properties	Initiator
	KPS
Formula	$K^+ \; {}^-O-\overset{\displaystyle O}{\underset{\displaystyle O}{S}}-O-O-\overset{\displaystyle O}{\underset{\displaystyle O}{S}}-O^- \; {}^+K$
$K_d*10^{-5}(s^{-1})$ @ 70°C[a]	4.31 [4]
$t_{1/2}$ (min)[a]	273 [4]
Molar mass (g/mol)	270.32
Water solubility @ 25°C (g/100mL)	4.7

Data extracted from the technical sheet provided by the manufacturer when not specified.
[a] it is also available[5] the K_d (s^{-1}) for APS at 70 and 80°C to be $4.3*10^{-5}$ and $1.6*10^{-4}$ respectively, in addition to the half-lives (min) for the same temperatures to be 264 and 72. Due to their similarity, the difference in the counter-ion in the decomposition rate is negligible, so these values can be used as an estimate for NaPS.

Monomers. Styrene (ReagentPlus, ≥99%) from Sigma-Aldrich. Divinylbenzene (tech., 80%, mixture of isomers) from Sigma-Aldrich. Physical and chemical properties disclosed in Table G-4.

Table G-4. Physical and chemical properties of the monomers used in this work.

Properties	Monomers		
	Styrene	**MMA**	**Divinylbenzene**
Formula			
Molar mass (g/mol)	104.15	100.12	130.2
Density (g/cm^3)	0.903	0.94	0.914
Boiling point (°C)	145	101	195
Melting point (°C)	-30	-48	-69.9--52
Water solubility @ 20°C (mg/L)	310	1500	insoluble
Refractive index	1.5469	1.398[6]	N/A
Homopolymer density (g/cm^3)	1.04-1.065 [67, 8]	1.17-1.20[6]	N/A
Homopolymer glass temperature (°C)	100 [7-9]	105[6]	N/A
Homopolymer refractive index	1.59-1.60 [6, 7]	1.4914[10]	N/A

Data extracted from the technical sheet provided by the manufacturer when not specified.

Methodologies and procedures

Conversion. Gravimetry was employed to determine the conversion of the polymerization. The samples were dried in a forced convection/air-circulation oven at 85°C for 4 hours. Conversion was calculated by the ratio of the solid contents at time t and the theoretical solid content, as calculated for total monomer added. The detailed procedure for conversion analysis can be found below. Samples were withdrawn during the reaction and inhibited with approximately 20 ppm of hydroquinone to stop the reaction. A determined mass of sample was placed in pre-weighted aluminum dish and then placed in a forced convection/air-circulation oven at 85°C overnight in order to remove water and residual monomer.

The solid content was calculated according to equation:

$$SC = \frac{m_{solids}}{m_{latex,samp.}} = \frac{m_{d,dried} - m_{d,empty}}{m_{d,full} - m_{d,empty}} \tag{G-1}$$

where, m_{solids} is the mass of solids in the sample (polymer, surfactant and initiator), $m_{latex,samp.}$ is the mass of latex in the sample, $m_{d.dried}$ is the mass of the dish with dried sample, $m_{d,full}$ is the mass of the dish with the latex sample and $m_{d,empty}$ is the mass of the empty dish.

The polymer content (PC) is calculated according to the following equation:

$$PC = \frac{m_{polymer}}{m_{latex}} = SC - \frac{m_{non\_polymer,form.}}{m_{latex,form.}} \tag{G-2}$$

where, $m_{non\_polymer,form.}$ is the mass of non-polymer solids in the entire formulation (surfactant and initiator) and $m_{latex,form.}$ is the mass of latex in the entire formulation.

The conversions were calculated according to the following equation:

$$Conv. = \frac{PC * m_{latex, form.}}{m_{mon, form.}} \tag{G-3}$$

where $m_{mon, form.}$ is the mass of monomer of the entire formulation. In order to calculate the instantaneous conversion, the $m_{latex, form.}$ and $m_{mon, form.}$ are considered the total mass of monomer and latex in the formulation according to the amount of monomer added up to instant t.

Particle size distribution. Particle size distribution was determined using Dynamic Light Scattering (DLS) in a Malvern Zeta-Sizer Nano-ZS instrument. The size range from this equipment is claimed to be 0.6 nm to 6 μm. Samples were diluted with a water solution of the surfactants at CMC in order to avoid particle coalescence. The Z-Average particle size and Polydispersity Index (PdI) were obtained from a series of 3 measurements with 5 runs, giving in total 15 runs for each sample at 25 °C.

The term polydispersity has multiple meanings that are dependent upon the context of its use. In the area of polymer chemistry, polydispersity is defined as the weight average divided by the number average molecular weight (M_w/M_n), and is used to give the researcher an idea of the breadth or width of the molecular weight distribution. In a similar although not identical sense, polydispersity in the area of light scattering is used to describe the width of the particle size distribution.

In the light scattering area, the term polydispersity is derived from the polydispersity index, a parameter calculated from a Cumulants analysis[11] of the DLS measured intensity autocorrelation function. In the Cumulants analysis, a single particle size is assumed and a single exponential fit is applied to the autocorrelation function. The autocorrelation function, along with the

exponential fitting expression, is shown below, where I is the scattering intensity, t is the initial time, τ is the delay time, A is the amplitude or intercept of the correlation function, B is the baseline, D is the diffusion coefficient, q is the scattering vector, λ_o is the vacuum laser wavelength, $\tilde{n}$ is the medium refractive index, θ is the scattering angle, k_B is the Boltzmann's constant, T is the absolute temperature, η is the viscosity of the medium, and r_p is the hydrodynamic radius.

$$G_2(\tau) = \langle I(t) \cdot I(t+\tau) \rangle = A[1 + B\exp(-2\Gamma\tau)] \tag{G-4}$$

$$\Gamma = Dq^2 \tag{G-5}$$

$$q = \frac{4\pi\tilde{n}}{\lambda_o} \sin\frac{\theta}{2} \tag{G-6}$$

$$D_z = \frac{k_B T}{3\pi\eta r_p} \tag{G-7}$$

In the Cumulants approach, the exponential fitting expression is expanded to account for polydispersity or peak broadening effects, as shown below.

$$G_2(\tau) = A[1 + B\exp(-2\Gamma\tau + \mu_2\tau^2)] \tag{G-8}$$

The expression is then linearized and the data fit to the form shown below, where the D subscript notation is used to indicate diameter. The 1st Cumulant or moment (a_1) is used to calculate the intensity weighted Z average mean size and the 2nd moment (a_2) is used to calculate a parameter defined as the polydispersity index (PdI).

$$y(\tau) = \frac{1}{2}\ln[G_2(\tau) - A] \cong \frac{1}{2}\ln AB - \langle\Gamma\rangle\tau + \frac{\mu_2}{2}\tau^2 = a_o - a_1 + a_2\tau^2 \tag{G-9}$$

$$B = \frac{\exp(2a_o)}{A} \tag{G-10}$$

$$Z_D = \frac{1}{a_1}\frac{k_B T}{3\pi\eta}\left[\frac{4\pi n}{\lambda_o}\sin\left(\frac{\theta}{2}\right)\right]^2 \tag{G-11}$$

$$PdI = \frac{2a_2}{a_1^{\,2}} \tag{G-12}$$

It is important to note here, that the Cumulants analysis algorithm **does not** yield a distribution – it gives only the intensity weighted Z average and the polydispersity index. If one were to *assume* a single size population following a Gaussian distribution, then the polydispersity index would be related to the standard deviation (σ) of the hypothetical Gaussian distribution in the fashion shown below.

$$Pdi = \frac{\sigma^2}{Z_D^{\,2}} \tag{G-13}$$

Using the above expression, polydispersity can then be defined in the following terms.

Polydispersity Index (PdI) = Relative variance

Polydispersity (Pd) = Standard deviation or width[φ]

%Polydispersity (%Pd) = Coefficient of variation[Ŧ] = (PdI)^{½} x 100

φ Also known as the absolute polydispersity

Ŧ Also called the relative polydispersity

According to Malvern Nanosizer user manual, the cumulants analysis gives a good description of the size that is comparable with other methods of analysis for spherical, reasonably narrow monomodal samples, i.e. with polydispersity below a value of 0.1. For samples with a slightly increased width, the Z-average size and polydispersity will give values that can be used for comparative purposes. For broader distributions, where the polydispersity is over 0.5, it is unwise

to rely on the Z-average mean, and a distribution analysis should be used to determine the peak positions.[12]

Number of particles. The number of particles (Np) is calculated from the average diameter of particle (Dp), conversion (Conv.) and the mass of monomer added to the reactor (M_{mon}), using the formula:

$$Np = \frac{V_{pol.}}{V_{part.}} = \frac{\dfrac{M_{mon}}{d} \times Conv.}{\dfrac{\pi}{6} \cdot Dp^3 1E10^{-21}} \tag{G-14}$$

where $V_{pol.}$ is the volume of polymer and $V_{part.}$ is the average volume of a single particle, d is the polymer density (g/cm^3) and 1×10^{-21} is the unit treatment for $nm^3 => cm^3$, so the units of Dp (given in nm) and density are compatible. If one desire to express this information as concentration of particles, it is just necessary to divide by the volume of latex in litres.

References

1. Williams, R.; Phillips, J.; Mysels, K. *Transactions of the Faraday Society* **1955**, 728-737.

2. Bales, B. L.; Messina, L.; Vidal, A.; Peric, M.; Nascimento, O. R. *J Phys Chem B* **1998***, 50,* 10347-10358.

3. Kholodovych, V.; Welsh, W. J. Densities of amorphous and crystalline polymers. In *Physical Properties of Polymers Handbook;* Mark, J. E., Ed.; AIP Press: Woodbury, NY, 1996.

4. Santos, A. M.; Vindevoghel, P.; Graillat, C.; Guyot, A.; Guillot, J. *J.Polym.Sci., Part A: Polym.Chem.* **1996***, 7,* 1271-1281.

5. Schneider, M.; Graillat, C.; Boutti, S.; McKenna, T. F. *Polym.Bull.(Berlin, Ger.)* **2001***, 3-4,* 269-275.

6. Brandrup, J.; Immergut, E. H.; Grulke, E. A. *Polymer Handbook;* John Wiley&Sons: New York, 2003.

7. Krevelen, D. W. v.; Hoftyzer, P. J. *Properties of polymers: correlations with chemical structure.* Elsevier Pub. Co.: Amsterdam; New York, 1972.

8. Mark, H. F. Encyclopedia of polymer science and technology. In Wiley-Interscience: Hoboken, N.J., 2007; Vol. 13.

9. Plazek, D. J.; Ngai, K. L. The glass temperature. In *Physical properties of polymers handbook;* Mark, J. E., Ed.; Springer: New York, 2007.

10. Kasarova, S. N.; Sultanova, N. G.; Ivanov, C. D.; Nikolov, I. D. *Opt. Mater. (Amsterdam, Neth.)* **2007***, 11,* 1481-1490.

11. Xu, M.; Choi, Y. S.; Kim, Y. K.; Wang, K. H.; Chung, I. J. *Polymer* **2003***, 20,* 6387-6395.

12. Malvern Instruments *zetasizer nano user manual;* Malvern Instruments: United Kingdom, 2007.